FINAL REPORT

Validation of Biotechnology for Quantifying the Abundance and Activity of Vinyl-chloride Oxidizers in Contaminated Groundwater

ESTCP Project ER-201425

FEBRUARY 2019

Timothy Mattes
The University of Iowa

ESTCP

Page Intentionally Left Blank

Page Intentionally Left Blank

REPORT DOCUMENTATION PAGE

1. REPORT DATE *(DD-MM-YYYY)* February 2019	2. REPORT TYPE ESTCP Final Report	3. DATES COVERED *(From - To)* 7/1/2014 - 7/1/2019

4. TITLE AND SUBTITLE	
Validation of Biotechnology for Quantifying the Abundance and Activity of Vinyl-Chloride Oxidizers in Contaminated Groundwater	**5a. CONTRACT NUMBER** 14-C-0036
	5b. GRANT NUMBER
	5c. PROGRAM ELEMENT NUMBER

6. AUTHOR(S)	
Timothy Mattes	**5d. PROJECT NUMBER** ER-201425
	5e. TASK NUMBER
	5f. WORK UNIT NUMBER

7. PERFORMING ORGANIZATION NAME(S) AND ADDRESS(ES)	8. PERFORMING ORGANIZATION REPORT
The University of Iowa Controller and Asst. VP Business Office, 4 Jessup Hall, Iowa City, IA 52242	ER-201425

9. SPONSORING / MONITORING AGENCY NAME(S) AND ADDRESS(ES)	10. SPONSOR/MONITOR'S ACRONYM(S)
Environmental Security Technology Technology Certification Program (ESTCP) 4800 Mark Center Drive Suite 16F16 Alexandria, VA 22350-3605	ESTCP
	11. SPONSOR/MONITOR'S REPORT NUMBER(S) ER-201425

12. DISTRIBUTION / AVAILABILITY STATEMENT
DISTRIBUTION A. Approved for public release: distribution unlimited.

13. SUPPLEMENTARY NOTES

14. ABSTRACT

The objective of this project was to demonstrate and validate quantitative, real-time PCR (qPCR) technologies for enumerating the abundance and functionality of vinyl chloride (VC)-oxidizing bacteria (i.e. etheneotrophs) at several VC-contaminated sites. The qPCR technology targets the functional genes known to be involved in the aerobic VC and ethene biodegradation pathways of etheneotrophs. We collected over 100 distinct groundwater samples from 6 different contaminated DoD sites, extracted nucleic acids and performed qPCR estimation of gene and transcript abundance from etheneotrophs, methanotrophs and anaerobic VC-dechlorinators. These genes were present in 99% and expressed in 59% of the samples. Etheneotroph functional genes (etnC and etnE) and VC reductive dehalogenase genes (bvcA and vcrA) were strongly related to VC concentrations ($p < 0.001$). We also used cryogenic soil coring to collect 134 high-resolution samples from a contaminated aquifer and investigated the spatial relationships between same set of VC biodegradation genes. Functional genes for etheneotrophs, methanotrophs, and anaerobic VC dechlorinators coexisted in 48% of soil samples, most of which appeared anaerobic. Both the groundwater and aquifer sediment sampling campaigns indicated that aerobic etheneotrophs could play a significant role in VC biodegradation in aquifers that have little dissolved oxygen.

15. SUBJECT TERMS

Vinyl chloride, Etheneotrophs, Methanotrophs, Anaerobic VC-Dechlorinator, Bulk VC attenuation rate, qPCR, Monitored Natural Attenuation, Groundwater, Cryogenic coring, Aquifer sediments

16. SECURITY CLASSIFICATION OF:			17. LIMITATION	18. NUMBER OF PAGES	19a. NAME OF RESPONSIBLE PERSON Timothy Mattes
a. REPORT UNCLASS	**b. ABSTRACT** UNCLASS	**c. THIS PAGE** UNCLASS	UNCLASS	224	**19b. TELEPHONE NUMBER** *(include area code)* 319-335-5065

Standard Form 298 (Rev. 8-98)

Page Intentionally Left Blank

FINAL REPORT
Project: ER-201425

TABLE OF CONTENTS

TABLE OF CONTENTS (Continued)

LIST OF FIGURES

LIST OF FIGURES

v

LIST OF FIGURES

LIST OF FIGURES

LIST OF FIGURES

LIST OF TABLES

ACRONYMS AND ABBREVIATIONS

AkMO   Alkene monooxygenase

BSA   Bovine Serum Albumin

cDCE   *cis*-1,2-Dichloroethene
cDNA   Complementary DNA
C_t Threshold cycle

DNA   Deoxyribonucleic acid
dsDNA   Double stranded DNA
DO   Dissolved oxygen
DoD   Department of Defense

EaCoMT   Epoxyalkane:Coenzyme M transferase
EPA   Environmental Protection Agency
EZVI   Emulsified zero-valent iron

FISH   Fluorescence *in situ* hybridization

IFC   integrated fluidic circuit
ISCO   in situ chemical oxidation

LOD   Level of detection
LOQ   Level of quantification

MCL   Maximum contaminant level
MCRD   Marine corps recruit depot
MNA   Monitored natural attenuation
mRNA   Messenger RNA

NTC   No template control

ORP   Oxidation-reduction potential

PCE   Tetrachloroethene
PCR   Polymerase chain reaction
pMMO   Particulate methane monooxygenase

qPCR   Quantitative PCR
QA/QC   Quality assurance/quality control

RNA   Ribonucleic acid
RT-qPCR   Reverse transcription quantitative PCR

SDIMO   Soluble di-iron monooxygenase alpha subunit
SERDP   Strategic Environmental Research and Development Program
sMMO   Soluble methane monooxygenase

TCE   Trichloroethene
TeCA   Tetrachloroethane

VC   Vinyl Chloride (monochloroethene)

ABSTRACT

INTRODUCTION & OBJECTIVES

Vinyl chloride (VC) plumes are present at many Department of Defense (DoD) sites, and there are significant costs associated with their cleanup. Microbial VC oxidation could be occurring at many of these contaminated sites and contribute significantly to VC natural attenuation. However, there are few options available to site managers for documenting these aerobic processes. The overall objective of this project was to demonstrate and validate quantitative, real-time PCR (qPCR) and reverse transcription technologies for enumerating the abundance and functionality of two major groups of VC-oxidizing bacteria (the etheneotrophs and methanotrophs) at several VC-contaminated sites. A biological data set that describes how the abundance and functionality of VC-oxidizing bacteria change both spatially and temporally within six different VC plumes was developed, which included associated geochemical parameters and contaminant concentrations in the groundwater. This demonstration is expected to show that application of environmental molecular diagnostic tools such as qPCR during long-term monitoring of contaminated groundwater will yield useful and cost-effective information for site managers who are interested in better understanding and documenting aerobic VC natural attenuation processes.

TECHNOLOGY DESCRIPTION

The qPCR technology, developed under SERDP project ER-1683, yields rapid information concerning presence, abundance, and functionality of VC-oxidizing etheneotrophs. This method employs protocols for DNA and RNA extraction, use of internal nucleic acid controls, and reverse transcription of RNA to complementary DNA (cDNA) so that the qPCR technology can be applied to DNA and RNA extraction from groundwater and aquifer sediment samples. Degenerate oligonucleotide primers that target the functional genes *etnC* and *etnE*, both of which are known to be involved in the aerobic VC and ethene biodegradation pathways of etheneotrophs are used during qPCR. To provide context for interpreting the etheneotroph qPCR results, the technology also includes qPCR analysis for the additional functional genes that may participate in VC biodegradation. This includes the genes *mmoX* and *pmoA*, which target methanotrophic bacteria (potential cometabolic VC-oxidizers) and the genes *bvcA* and *vcrA*, which target VC reductive dehalogenase genes.

DEMONSTRATION RESULTS

During the demonstration we collected over 100 distinct groundwater samples from VC plumes located at 6 different contaminated DoD sites. Both DNA and RNA were extracted from these samples. The resulting DNA and cDNA was subjected to qPCR estimation of *etnC*, *etnE*, *pmoA, mmoX, bvcA*, and *vcrA* gene and transcript abundance. We also measured an array of geochemical parameters from the same groundwater samples during the groundwater sampling campaign A statistical analysis of the gene and transcript data and the contaminant and geochemical parameters was performed. Functional genes from the etheneotrophs, methanotrophs and anaerobic VC-dechlorinators were present in 99% and expressed in 59% of the samples. Etheneotroph functional genes (*etnC* and *etnE*) and VC reductive dehalogenase genes (*bvcA* and *vcrA*) were strongly related to VC concentrations ($p < 0.001$). Methanotroph functional genes (*mmoX* and *pmoA*) were not related to VC concentration ($p > 0.05$). Samples from sites with bulk VC attenuation rates >0.08 year^{-1} contained higher levels of etheneotroph and anaerobic VC-dechlorinator functional genes and transcripts than those with bulk VC attenuation rates <0.004 year^{-1}.

We used cryogenic soil coring to collect 134 high-resolution samples from a chlorinated ethene contaminated aquifer at Parris Island Site 45, characterized aquifer geochemical conditions, and investigated the spatial relationships between functional genes aerobic and anaerobic VC-degrading bacteria and chlorinated ethene concentrations. Functional genes for etheneotrophs (*etnC* and/or *etnE*), methanotrophs (*mmoX* and/or *pmoA*), and anaerobic VC dechlorinators (*bvcA* and/or *vcrA*) coexisted in 48% of soil samples, most of which appeared to be experiencing anaerobic conditions. Etheneotrophs and VC-dechlorinators were correlated to VC concentrations in the lower surficial aquifer ($p<0.05$), while methanotrophs were not related to VC concentrations. Cryogenic soil coring was a powerful tool for capturing high-spatial resolution trends in geochemical and nucleic acid data. Both the groundwater and aquifer sediment sampling campaigns indicated that aerobic etheneotrophs could play a significant role in VC biodegradation in aquifers that have little dissolved oxygen.

IMPLEMENTATION ISSUES

Implementation of qPCR technology for etheneotrophs at chlorinated ethene contaminated sites is already feasible in real-world situations as many long-term groundwater monitoring programs currently prescribe DNA extraction and qPCR analysis for anaerobic chlorinated ethene degrading bacterial biomarkers. However, RNA is not typically used in qPCR practice, as DNA is more readily obtained and easier to work with than RNA. While it may be possible to obtain meaningful relationships between attenuation (or biodegradation rates) and qPCR data obtained with DNA. But DNA is not necessarily a reliable indicator of active biomass, qPCR analysis of RNA may yield stronger correlations with rates than DNA. When using RNA, technology performance is dependent on the efficiency of RNA extraction. We recommend that when RNA is desired, that at least 3L of each groundwater sample should be filtered, if possible, to maximize RNA yields.

EXECUTIVE SUMMARY

INTRODUCTION & OBJECTIVES

Vinyl Chloride (VC) plumes are present at many DoD sites, and there are significant costs associated with their cleanup (e.g., VC plumes are often dilute, and a large volume of VC-contaminated water must be treated). Microbial VC oxidation could be occurring at many of these contaminated sites and contribute significantly to VC natural attenuation. However, there are few options available to site managers for documenting these aerobic processes and the effects they may be having at their site. The overall objective of this project is to demonstrate and validate quantitative, real-time PCR (qPCR) and reverse transcription (RT)-qPCR technologies for enumerating the abundance and expression of key functional genes from two important groups of VC-oxidizing bacteria (the etheneotrophs and methanotrophs) at several VC-contaminated Department of Defense (DoD) sites. Over the course of the project, we built a biological data set that describes how the abundance and functionality of etheneotrophs and methanotrophs change both spatially and temporally at several locations in one or more VC plumes. We analyzed this data set with respect to the bulk rate of VC attenuation observed across plume transects over the same time period. This demonstration has shown that application of environmental molecular diagnostic tools such as qPCR during long-term monitoring of contaminated groundwater yields useful and cost-effective information for site managers interested in better understanding the potential for aerobic natural attenuation of VC at their sites.

TECHNOLOGY DESCRIPTION

Under SERDP project ER-1683, the team developed a qPCR method that yields rapid information concerning presence, abundance, and functionality of VC-oxidizing etheneotrophs. This method employs degenerate oligonucleotide primers that target the functional genes *etnC* and *etnE*, both of which are known to be involved in the aerobic VC and ethene biodegradation pathways of etheneotrophs. The gene *etnC* encodes the alpha subunit of alkene monooxygenase (AkMO). The gene *etnE* encodes the epoxyalkane:coenzyme M transferase (EaCoMT). AkMO converts VC and ethene to epoxide intermediates, while EaCoMT detoxifies and/or transforms these epoxides into compounds that can enter central metabolic pathways. For comparison to etheneotroph functional genes, four additional functional genes are quantified. This includes genes encoding particular and soluble methane monooxygenase alpha subunits in methanotrophs (*pmoA* and *mmoX*, respectively), and genes encoding VC reductive dehalogenases *vcrA* and *bvcA*. Protocols for groundwater sampling, DNA and mRNA extraction, use of internal nucleic acid controls, and subsequent qPCR analysis were developed as part of the technology. This novel technology is innovative because it can now be used to reveal the abundance and functionality of etheneotrophs at VC-contaminated sites. By considering qPCR data alongside geochemical and contaminant data, as well as the site-wide VC attenuation rate, this technology could provide important lines of evidence that aerobic VC biodegradation is a significant contributor to overall VC natural attenuation processes at contaminated sites.

PERFORMANCE ASSESSMENT

For this demonstration we developed 3 qualitative and 11 quantitative performance objectives. The qualitative performance objectives addressed ease of technology, implementation in the field, usefulness of data collected, and regulatory acceptance. Of the 11 quantitative performance objectives, 7 assessed specific qPCR performance metrics. These were time-efficiency, cost-effectiveness, accuracy, precision, reproducibility, comparability of different qPCR primer sets, and sensitivity. The remaining 4 quantitative performance objectives aimed to determine temporal and spatial relationships between qPCR data and geochemical and contaminant parameters (e.g., VC concentrations), and correlations between qPCR data and VC attenuation/ degradation rates.

During the demonstration we collected 95 distinct groundwater samples from VC plumes located at 6 different contaminated DoD sites (including NAS Oceana SWMU 2C and Parris Island Site 45). Both DNA and RNA were extracted from these samples. RNA was concerted to complementary DNA (cDNA) by RT. The resulting DNA and cDNA was subjected to qPCR estimation of *etnC*, *etnE*, *pmoA*, *mmoX*, *bvcA*, and *vcrA* gene and transcript abundance. An array of geochemical and contaminant parameters was also obtained from the same groundwater samples. A statistical analysis was performed to investigate potential spatial and temporal relationships among gene and transcript data and the contaminant and geochemical parameters. The qPCR, geochemical and contaminant data, along with the results of the statistical analyses were used to assess the remaining 4 quantitative performance objectives as follows.

Analysis of temporal relationships in groundwater samples

The first of these 4 performance objectives addressed temporal relationships between functional gene and transcript abundances. The assessment was performed using data from a dilute VC plume located at NAS Oceana. The abundance and expression of functional genes from VC-oxidizing bacteria was low. It was also difficult to obtain enough data points for statistical analysis due to the small size of our gene abundance database. Despite this we observed a significant increase in *mmoX* abundance with time in all three wells. In the case of monitoring well MW25, *mmoX* abundance was also negatively correlated with VC concentration, as would be expected if methanotrophs were controlling the rate of VC attenuation at this site. This indicates that although difficult in dilute VC plumes, it is possible to use the qPCR technology to observe statistically significant temporal relationships between geochemical and contaminant parameters and functional genes, thus we deemed the success criteria met for this performance objective.

Analysis of spatial relationships in groundwater samples

Application of qPCR technology to the 95 groundwater samples from several VC plumes indicated that *etnC*, *etnE*, *pmoA*, *mmoX*, *bvcA*, and *vcrA* were quantified (DNA) in 99% and expressed (cDNA) in 59% of the samples. Statistical analysis (i.e., multi-level modeling) revealed a statistically significant correlation between etheneotroph functional genes and transcripts and VC concentrations (**Figure E1**). VC reductive dehalogenase genes *bvcA* and *vcrA* also displayed statistically significant correlations with VC concentrations. Conversely, there was no relationship between methanotroph functional gene and transcript abundance and VC concentrations (**Figure E1**).

The relationship etheneotroph functional genes and transcripts and VC concentrations can be used to roughly predict that the higher the VC concentration in groundwater, the higher the etheneotroph abundance and activity will be. This was somewhat surprising as areas of higher VC centration also tended to have little or no dissolved oxygen (DO). However, either there was no relationship or negative correlations were observed between etheneotroph functional gene/transcript abundance and DO and ORP measurements. These results are difficult to interpret but suggest that DO and ORP values do not hold any predictive value with respect to etheneotroph abundance or activity in the environment.
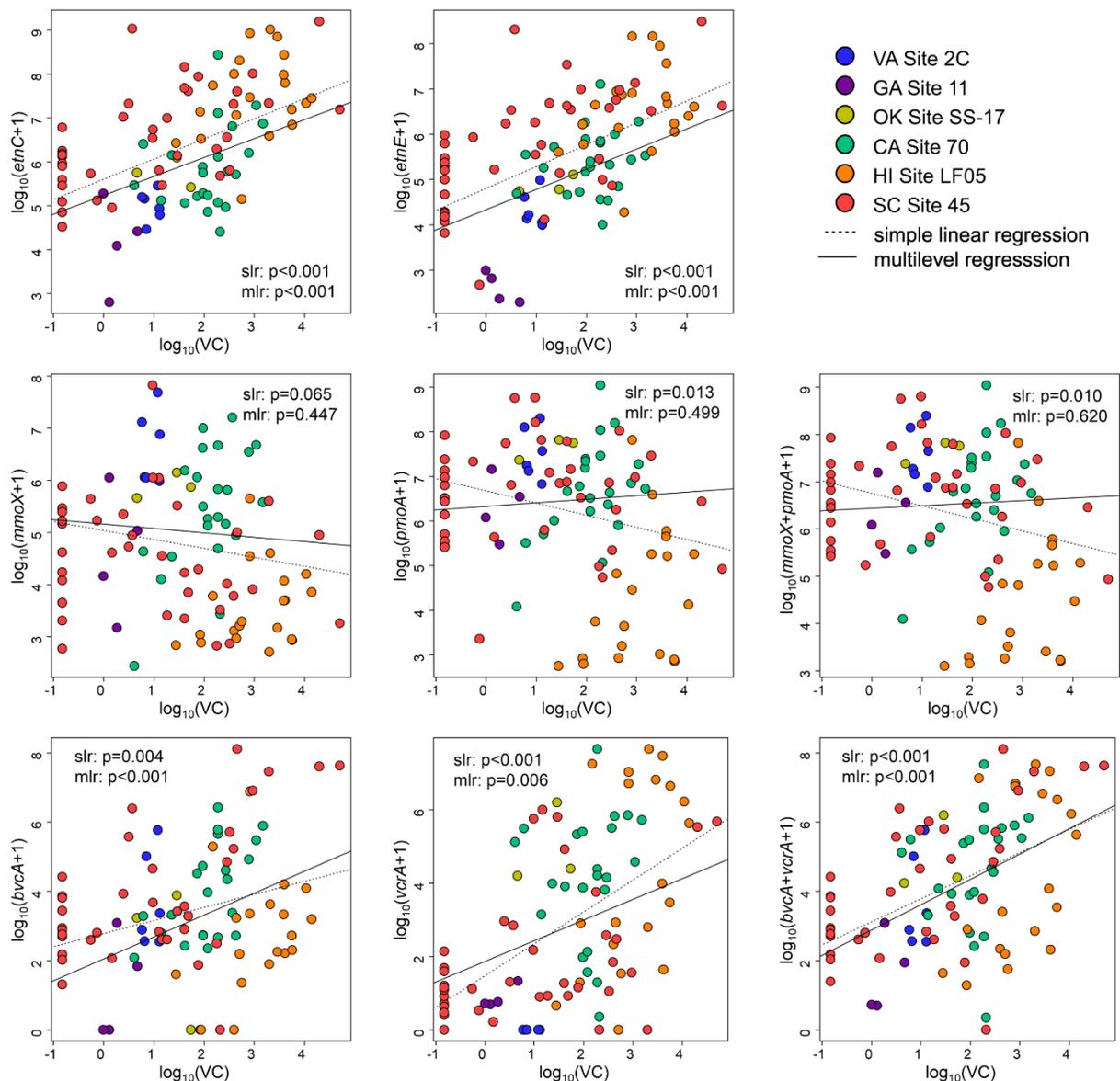
Figure E1. Relationships Among Functional Genes and VC Concentrations as Assessed by Multilevel Regression (mlr, solid line) and Simple Linear Regression (slr, dotted line).

p values for slr and mlr are indicated for each functional gene.

Analysis of spatial relationships in cryo-cores

The simultaneous presence and expression of genes from etheneotrophs and anaerobic VC-dechlorinators in groundwater samples is a novel and important observation that has implications for bioremediation of VC. However, the co-occurrence of aerobic and anaerobic VC-degrading bacteria in the subsurface environment remained inconclusive following our initial assessment of this performance objective. It could be that aquifer material within the influence of monitoring wells contains aerobic and anaerobic microenvironments in close proximity to each other or that mixing of aerobic and anaerobic groundwater zones occurred during sampling. Analysis of aquifer sediment samples was therefore conducted to provide more precise spatial proximity and distribution of aerobic and anaerobic VC-degrading populations. Aquifer sediments were collected from four borehole locations in the northern VC plume at Parris Island site 45 with a cryo-coring procedure. The surficial aquifer at Parris Island site 45 has an upper unit composed of silt and a lower unit composed of silty sand. These are termed the upper surficial aquifer and the lower surficial aquifer (a diagram of the two hydrogeologic units is shown in **Figure E2**)

Initial geochemical results (cDCE, VC, ethene and methane concentrations) for core 1, located near the PCE source zone, are shown in **Figure E2**. The data indicates that dissolved chlorinated ethenes are migrating in both the upper and lower surficial aquifers, and that reductive dechlorination of VC to ethene is also occurring in both regions of the aquifer.
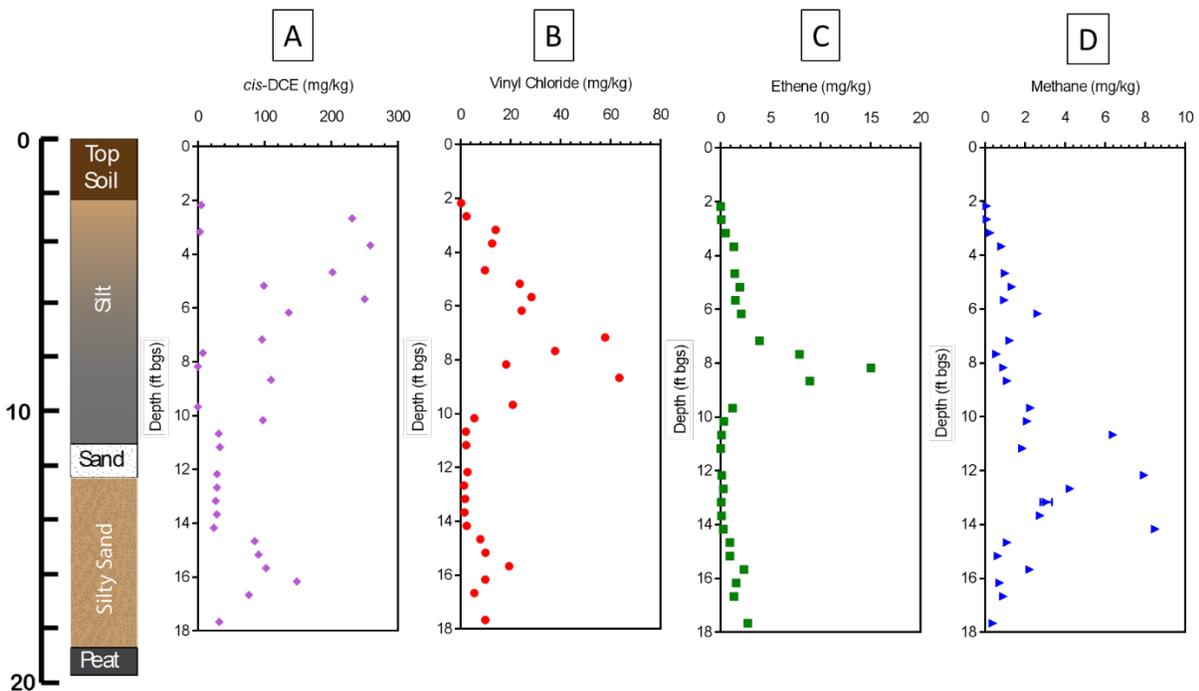
Figure E2. Spatial Resolution of A) cDCE, B) VC, C) Ethene, and D) Methane in Sediment Core 1, Frozen in Place with Liquid Nitrogen, Obtained from Parris Island Site 45. The Graphic on the Left Shows the Soil Characteristics of the Upper (Silt) and Lower (Silty Sand) Surficial Aquifers.

DNA was extracted from relatively small aquifer sediment samples (~0.25 g) (also within the same 1" cryo-core sections) and qPCR was performed for six functional genes (*etnC*, *etnE*, *mmoX*, *pmo*A, *bvcA*, and *vcrA*), as well as total 16S rRNA genes. The results of this analysis for core 1, is shown in **Figure E3** below. The qPCR analysis shows that indeed, functional genes from etheneotrophs and anaerobic VC-dechlorinators coexist within small (~0.25 g) sediment samples as deep as 18 feet below ground surface in this particular sediment core. ***This suggests that there is the potential for essentially simultaneous aerobic and anaerobic VC biodegradation at this site, even at a substantial depth.*** The source of DO at depth is currently unknown and poorly understood. However, as expected, the abundance of etheneotroph and methanotroph functional genes are highest closer to the ground surface, presumably because there is the strongest oxygen gradient here near the shallow groundwater table (~2-3 feet bgs).

Figure E3. Spatial Resolution of A) Total 16S rRNA Genes, B) *etnC* and *etnE* (Etheneotroph Functional Genes), C) *mmoX* and *pmoA* (Methanotroph Functional Genes), and D) *bvcA* and *vcrA* (VC Reductive Dehalogenase Genes) in an Aquifer Sediment Core, Frozen in Place with Liquid Nitrogen, Obtained from Parris Island Site 45. The Graphic on the Left Shows the Soil Characteristics of the Upper (Silt) and Lower (Silty Sand) Surficial Aquifers.

Analysis of relationships between functional genes/transcripts and bulk VC attenuation rates

The positive relationship between VC concentration and etheneotrophs noted in the previous performance objective assessment suggests that there will also be a relationship between etheneotroph and activity and VC degradation rates, as estimated over a plume transect. This is because as the VC plume moves further from the source it will be subject to attenuation processes, such as biodegradation.

Using site data (site maps and monitoring well data) we developed plume transects and plotted VC concentration vs. distance according to the direction of groundwater flow. Using reported hydrogeological data (hydraulic gradient, porosity, hydraulic conductivity) we estimated seepage velocities for the transects so that VC concentration vs. distance plots were expressed as VC concentration vs. travel time. Bulk VC attenuation rates were estimated from these plots by linear regression. However, because of uncertainties in reported values of seepage velocity, hydraulic gradient, porosity, and hydraulic conductivity, we were not confident in the absolute values of the estimated bulk VC attenuations. Therefore, to determine the relationship between functional genes/transcripts and bulk VC attenuation rates, we used a categorical regression approach. Following estimation of the bulk VC attenuation rate over a transect at a site, each site was assigned to one of two categorical rate groups: high attenuation or low attenuation. Sites in the low attenuation group include NSB Kings Bay site 11 and NAS Oceana SWMU 2C, Altus AFB biowalls and Seal Beach Site 70. Sites included in the high attenuation group included Parris Island site 45 (northern and southern plumes) and Joint Base Pearl Harbor Hickam site LF05. For the categorical regression analysis, a multilevel modeling approach was also used to take into account the effect of intercorrelations between samples from the same sites and the same monitoring wells sampled on different dates. Regression analysis was performed to test the hypothesis that functional gene or transcript abundances are different among the different rate groupings (null hypothesis is that there is no difference).

Analysis of relationships between functional genes/transcripts and bulk VC attenuation rates

We found that log transformed etheneotroph functional gene (*etnC* and *etnE*) abundances in high rate group were significantly higher than those in the slow rate group, while no significant difference was found for methanotroph functional genes among different groups **Table E2**. For reference, log transformed *vcrA* abundances were also significantly higher in the high rate group as compared to the low rate group (although *bvcA* was not). The significantly higher abundances of etheneotroph functional genes and anaerobic VC reductive dehalogenase genes in the high rate group (as compared to the low rate group) suggests that VC degradation was categorically faster when there were higher abundances of etheneotrophs and anaerobic VC-degraders together in the same groundwater sample. It is possible that under field conditions, VC may support the growth of etheneotrophs and anaerobic VC degraders, and etheneotrophs and anaerobic VC dechlorinators both contributed significantly to VC degradation in the contaminated groundwater.

Table E2. Average Gene and Transcript Abundances within Slow and High Rate Group Categories as Assessed by Categorical Multilevel Regression.

p values <0.05, which indicate a statistically significant difference between two groups, are in bold.

	Rate category	gene		transcript	
		$\log_{10}(x+1)$	p value	$\log_{10}(x+1)$	p value
etnC	low rate	4.58		4.39	
	high rate	6.49	**0.040**	3.91	0.743
etnE	low rate	3.49		1.35	
	high rate	5.73	**0.036**	3.80	**0.026**
mmoX	low rate	5.61		2.79	
	high rate	4.79	0.454	1.81	0.474
pmoA	low rate	6.93		5.62	
	high rate	6.23	0.593	3.76	0.202
bvcA	low rate	2.41		1.21	
	high rate	3.28	0.389	2.62	0.349
vcrA	low rate	0.45		0.00	
	high rate	3.54	**0.030**	3.96	**0.035**
mmoX+pmoA	low rate	6.96		5.66	
	high rate	6.32	0.605	3.91	0.206
bvcA+vcrA	low rate	2.60		1.12	
	high rate	4.36	**0.024**	4.66	**0.002**

For transcripts, significant differences were observed between *etnE* transcript abundances of the high rate group and slow rate group, suggesting that etheneotrophs were more active at sites where more rapid VC attenuation was observed. The *vcrA* transcript abundance in the high rate group was also significantly higher than the low rate group (**Table E2**).

In summary, the results of correlation analysis between functional gene/transcript abundances and bulk VC attenuation rates suggest that etheneotrophs and anaerobic VC-degraders were more abundant and active at sites with faster bulk VC attenuation rate, and they could be both important factors contributing to VC degradation in groundwater. Therefore, we believe that the results of this performance assessment indicate a success.

Analysis of relationships between etnE abundance and VC biodegradation rates

Because of uncertainties in estimating bulk VC attenuation rates in the field, we sought to look at relationships between *etnE* abundance and actual VC biodegradation rates in aerobic VC-degrading laboratory cultures. This required demonstrating that qPCR for the *etnE* gene can be used as a specific surrogate for active etheneotroph biomass in the enrichment cultures, and that the abundance of *etnE* is correlated to the rate of VC biodegradation. This was demonstrated with pure cultures of VC-assimilating *Nocardioides* strain JS614, grown on VC We also extracted DNA from the cultures after the end of the experiment and measured *etnE* abundance with qPCR. The relationship between the VC biodegradation rate and *etnE* abundance is shown in **Figure E4**. We observed a strong linear relationship (R^2=0.98) between the biomass concentration (as *etnE*) and the maximum VC biodegradation rate by strain JS614.

This data supports the idea that the rate of VC oxidation in these cultures is proportional to etheneotroph functional gene concentration, and that VC oxidation rates can be adequately described by Michaelis-Menton enzyme kinetics when functional gene concentrations are used as the biomass concentration. Thus, the success criteria for performance objective "Determine relationships between etheneotroph functional genes and the VC biodegradation rate in VC-oxidizing laboratory enrichment cultures" appears to be met, at least on a preliminary basis.

We hypothesize that if etheneotrophs are contributing significantly to the rate of VC oxidation in enrichment cultures that we will observe a similar linear relationship between the raw VC biodegradation rate and *etnE* abundance.Subsequently we compared measured aerobic VC-biodegradation rates in VC-oxidizing enrichment cultures from PH and NI (in duplicate) under the same pH and temperature conditions as the JS614 experiments. These data points are included in **Figure E4**. The data indicate that relationships between *etnE* gene abundance and VC biodegradation rate in enrichment cultures are different than that for a pure culture of JS614 even at the same pH and temperature. A possible explanation for the observed differences is active etheneotroph biomass. In other words, there may have been lower active etheneotroph biomass in the PH culture and higher active biomass in the NI culture, as compared to the JS614 culture. Because we only measured DNA in this experiment, we do not know the expression level of *etnE* or the activity of the EtnE product in this case. We also know that the activity of EtnE is variable even among different pure cultures of etheneotrophs (Coleman & Spain, 2003a, Mattes, *et al.*, 2005). Further study of the relationship between *etnE* expression (or transcript per gene ratio) as well as the correlation of *etnC* gene and transcript abundance and VC biodegradation rates is warranted.

Figure E4. Raw VC Depletion Rate vs etnE Concentration in VC-grown Nocardioides sp. Strain JS614 (Black Circles) as Compared to VC-oxidizing Enrichment Cultures from Pearl Harbor (PH; Red Squares) and Naval Air Station North Island (NI; blue triangles).

For the JS614 experiments, six microcosms were prepared with varying amounts of active JS614 biomass. Substrate depletion curves were fit to the Michaelis-Menton kinetic model and the maximum VC biodegradation rae was estimated. DNA was extracted from the microcosms at the end of the experiment, and etnE was quantified by qPCR.

COST ASSESSMENT.

There are two major elements of the cost model for implementing the qPCR technology into existing monitoring plans – sampling cost and qPCR/RT-qPCR costs.The only cost drivers that were considered was the number of samples and replicates required as this will impact the total cost of implementing the technology as part of a long-term monitoring strategy. Typically, we take duplicate samples for DNA and RNA to assess sampling variability.

Overall, our analysis indicates that labor and materials costs for qPCR/RT-qPCR were $530 per monitoring well. This does not include the sampling costs in the field. We estimate that the time required to set-up and take two 1 L filter samples for DNA and two 3L filter samples for RNA was about 2 hours per monitoring well, on average. Although one person could sample wells alone, it was often helpful to have another helping at times. So, to be conservative – 3 hours per well ($90). This brings the total costs per monitoring well to $620.

We do not include the costs for flights, hotel, food, rental car, equipment rental in this analysis. When we were sampling groundwater at Parris Island Site 45, there were additional costs for disposal of investigation derived wastes (IDW) incurred that perhaps should be taken into account as part of the overall cost per monitoring well. The groundwater IDW collection, storage, analysis, and disposal costs for one sampling event in 2015 were $2,800 for 17 monitoring wells (or ~ $165 per monitoring well). However, we were not charged for IDW costs for obtaining samples for any of the other sites when working alongside a contractor. This leads us to conclude that the extra groundwater filtered for qPCR analysis would not likely contribute very much extra to the overall IDW costs that we were forced to incur separately at Parris Island.

IMPLEMENTATION ISSUES

Implementation of qPCR technology for etheneotrophs at chlorinated ethene contaminated sites is already feasible in real-world situations as many long-term groundwater monitoring programs currently prescribe DNA extraction and qPCR analysis for anaerobic chlorinated ethene degrading bacterial biomarkers. However, RNA is not typically used in qPCR practice, as DNA is more readily obtained and easier to work with than RNA. While it may be possible to obtain meaningful relationships between attenuation (or biodegradation rates) and qPCR data obtained with DNA. But DNA is not necessarily a reliable indicator of active biomass, qPCR analysis of RNA may yield stronger correlations with rates than DNA. When using RNA, technology performance is dependent on the efficiency of RNA extraction. We recommend that when RNA is desired, that at least 3L of each groundwater sample should be filtered, if possible, to maximize RNA yields.

Page Intentionally Left Blank

1.0 INTRODUCTION

1.1 BACKGROUND

Contamination of groundwater by the widely used chlorinated solvents tetrachloroethene (PCE) and trichloroethene (TCE) is a pervasive environmental problem at Department of Defense (DoD) installations. In addition, certain DoD installations face groundwater contamination issues with chlorinated ethanes such as 1,1,2,2 tetrachloroethane (TeCA), among other contaminants.

A very popular groundwater clean-up strategy for chlorinated ethenes and ethanes is anaerobic reductive dechlorination. In many cases, injection of electron donor amendments to the contaminated aquifer is sufficient to develop anaerobic conditions conducive to reductive dechlorination of PCE and TCE and TeCA. When the appropriate microorganisms are present, electron donor injection leads to the production of lesser chlorinated daughter products (i.e., *cis*-dichloroethene (cDCE) and vinyl chloride (VC)) and in some cases non-chlorinated products (i.e., ethene and ethane). In some cases, bioaugmentation with cultures containing specialized anaerobic strains can speed up the process of generating the desired end-products of ethene and ethene.

VC is a common daughter product found in contaminated groundwater undergoing reductive dechlorination of chlorinated solvents. VC is most commonly generated in groundwater by reductive dechlorination of cDCE. VC can also be formed by dihaloelimination of 1,1,2-trichloroethane (a daughter product of TeCA dechlorination).

Although *in situ* bioremediation via anaerobic reductive dechlorination is a robust approach for clean-up of chlorinated solvents, VC often accumulates in groundwater at sites where this strategy is employed, under even appropriate field conditions. Therefore, VC plumes are present at many DoD sites. This is problematic from a regulatory standpoint in that VC is a known human carcinogen with a low Environmental Protection Agency (EPA) maximum contaminant level (MCL) of 2 ppb. There are significant costs associated clean-up of VC plumes, primarily because they can resist further reduction to ethene and often evolve into large, dilute plumes. As a result, monitored natural attenuation (MNA) represents an attractive, cost-effective treatment option for VC plumes.

In the context of MNA, VC plumes formed under anaerobic conditions have often migrated (or have the potential to migrate) into zones where sufficient oxygen is present for oxidative degradation processes to become significant. Under this scenario, intrinsic aerobic biodegradation processes could account for the majority of VC mass removal. For instance, the co-migration of methane along with VC into aerobic groundwater could promote the activity of methanotrophic bacteria, which are known to cometabolize VC. Ethene, the by-product of VC reduction, also commonly co-migrates with VC from anaerobic zones. Ethene can stimulate the activity of ethene-assimilating bacteria (i.e. etheneotrophs), which are also known to cometabolize VC while utilizing ethene as a primary substrate. Several etheneotrophic strains are known to switch from a cometabolic VC oxidation mode to a growth-coupled VC oxidation mode. Growth-coupled VC oxidation is especially attractive approach to VC bioremediation because it represents a sustainable process not subject to the toxicity issues and requirements for a primary substrate associated with cometabolic VC processes.

Although methanotrophs have long been known to cometabolize VC, there is a paucity of studies demonstrating the contributions of methanotrophs to cometabolism of VC in the field. Several studies of the potential contribution of etheneotrophs to natural attenuation of VC in the field have recently been published (Begley, *et al.*, 2012, Atashgahi, *et al.*, 2013, Patterson, *et al.*, 2013, Mattes, *et al.*, 2015). These recent small-scale field studies suggest that etheneotrophs could contribute significantly to aerobic natural attenuation of VC plumes.

Despite these scientific advances, the potential contribution of these bacteria to natural attenuation of VC has largely been overlooked by practitioners. The lack of rapid and cost-effective methods for providing lines of evidence for VC oxidation in aquifers could partially explain this. Our SERDP-supported research (Project ER-1683) addressed several of these knowledge and technology gaps. We have developed quantitative PCR (qPCR)(Jin & Mattes, 2010, Jin & Mattes, 2011) and reverse transcription quantitative PCR (RT-qPCR) methods (Mattes, *et al.*, 2015) that could provide rapid, useful and cost-effective information about the abundance and activity of VC-oxidizing etheneotrophs in the context of a long-term MNA strategy. We also adapted existing qPCR methods for methanotrophs for use in RT-qPCR experiments (Mattes, *et al.*, 2015).

Oxidative processes may also be generally perceived as insignificant under the typical geochemical conditions encountered in aquifers contaminated with chlorinated ethenes. However, other recent publications suggest that aerobic VC-oxidizers could be active in regions of the aquifer that are considered anoxic or anaerobic (Gossett, 2010, Fullerton, *et al.*, 2014). Therefore, we are poised to apply our qPCR-based molecular diagnostic tools for VC-oxidizing bacteria to groundwater and aquifer sediment samples to demonstrate that VC oxidation processes are present and active at VC-contaminated sites where geochemical conditions appear favorable for VC oxidation and possibly in areas that may appear favorable for VC oxidation (i.e., in anoxic groundwater zones). This information will assist site managers in documenting the performance of chlorinated ethene bioremediation strategies and obtaining regulatory acceptance for a monitored natural attenuation remedy (enhanced or otherwise) to address VC plumes that often form as a result of anaerobic reductive dechlorination of chlorinated ethenes.

1.2 OBJECTIVE OF THE DEMONSTRATION

A primary objective of the demonstration is to use quantitative, real-time PCR (qPCR) and reverse transcription qPCR (RT-qPCR) technologies to reveal evidence for VC oxidation processes (both potential and active), particularly those involving etheneotrophs, at DoD installations. We are particularly interested in showing that these tools can provide evidence for VC oxidation processes at sites that might be considered "anoxic" or even anaerobic. The data that we gather should ultimately lead to a guidance document for addressing oxidative VC processes at contaminated sites. This protocol would stress that evidence for VC oxidation processes should be considered and gathered at sites where VC plumes are present, and point out the most cost-effective methods for doing so.

Another potential product of this effort is an improved understanding of the contribution of VC oxidation processes to the overall rate of VC degradation at contaminated sites. The subsurface environment is complex and should really not be considered to be either completely aerobic or completely anaerobic. Our initial analyses suggest that functional genes associated with both VC oxidation and VC reduction can be located closely enough so that they are detected in the sample

groundwater sample. Therefore, in order to develop relationships between the rate of VC degradation and the abundance/activity of functional genes involved in VC degradation, we should consider that both aerobic and anaerobic processes contribute to some extent. To what extent will vary according to site specific conditions. In the demonstration plan, we will outline an approach to investigate the contribution of aerobic VC oxidation processes to the rate of overall VC degradation in one or more wells at the Parris Island site. This information will also be included in the guidance document that we will deliver at the conclusion of this project. Finally, we expect that this demonstration will show that application of environmental molecular diagnostic tools such as qPCR during long term monitoring of VC-contaminated groundwater will yield useful and cost-effective information for site managers who are interested in better understanding the potential for natural attenuation of VC.

1.3   REGULATORY DRIVERS

The USEPA MCL for VC in drinking water is 2 µg/L. Although the goal of enhanced bioremediation of chlorinated ethenes is complete conversion into ethene, this is rarely achieved in practice. Generation of VC plumes resulting from incomplete anaerobic reductive dechlorination of the more highly chlorinated ethenes can significantly increase the costs and time of clean-up, particularly if the VC plume is dilute. Therefore, this demonstration seeks to improve the current understanding of the contribution of VC oxidation processes to attenuation of VC plumes, particularly when implementation of MNA is desirable to achieve cleanup goals and site closures. These findings will be detailed in a proposed Guidance Protocol, which is aimed at assisting site managers and regulators to better interpret qPCR/RT-qPCR data for VC-oxidizers as representing a significant component of bioremediation strategies involving VC.

Page Intentionally Left Blank

2.0 TECHNOLOGY

2.1 TECHNOLOGY DESCRIPTION

We have developed a SYBR green-based qPCR method that yields rapid information concerning presence, abundance, and expression of functional genes from aerobic VC-oxidizing microorganisms. This method employs degenerate oligonucleotide primers that target functional genes which are involved in the aerobic VC biodegradation pathway employed by etheneotrophs. The etheneotroph qPCR technology was developed, demonstrated, and validated in our laboratory (Jin & Mattes, 2010, Jin & Mattes, 2011, Mattes*, et al.*, 2015). This technology is innovative because it provides opportunities to explore relationships between the abundance and functionality of aerobic VC-oxidizers at contaminated sites and the concentration of VC, as well VC biodegradation rates.

Etheneotrophs and methanotrophs are two major bacterial groups that could contribute significantly to aerobic VC biodegradation in contaminated groundwater systems. The genes *etnC* and *etnE* and their transcripts are targeted as indicators of the abundance and activity of etheneotrophs. The gene *etnC* encodes the alpha subunit of alkene monooxygenase (AkMO). The gene *etnE* encodes the epoxyalkane:coenzyme M transferase (EaCoMT). AkMO attacks VC and ethene and incorporates oxygen atoms into these compounds to form epoxide intermediates. EaCoMT detoxifies and/or transforms these epoxides into compounds that can enter central metabolic pathways (Mattes*, et al.*, 2010). Methanotrophs, which can cometabolize VC in the presence of methane, are present and likely to be active at most VC-contaminated sites because methane is commonly generated under the same conditions favorable for reductive dechlorination of chlorinated ethenes. Methanotroph functional genes *pmoA* (encodes the particulate methane monooxygenase alpha subunit) and *mmoX* (encodes the soluble methane monooxygenase subunit) and their transcripts are targeted to reveal the abundance and activity of methanotrophs (McDonald*, et al.*, 2008). For comparison purposes, we also include qPCR assays for anaerobic VC reductive dehalogenase genes (*bvcA* and *vcrA*) as these genes could be participating in simultaneous VC removal in groundwater systems alongside those from etheneotrophs and methanotrophs.

2.1.1 DESIGN AND LAYOUT OF TECHNOLOGY COMPONENTS

The qPCR technology for estimating the abundance of functional genes from VC-oxidizing etheneotrophs was developed under SERDP (Project ER-1683). The qPCR technology, subsequent improvements, and applications have been described elsewhere (Jin & Mattes, 2010, Jin & Mattes, 2011, Mattes*, et al.*, 2015). We use published primer sets to amplify methanotroph functional genes and their transcripts (Holmes*, et al.*, 1995, McDonald*, et al.*, 1995, Fuse*, et al.*, 1998, Kolb*, et al.*, 2003). We have recently published an article describing the RT-qPCR method extension with a small field-scale application (Mattes*, et al.*, 2015).

2.1.1.1 *Groundwater sampling, filtering, and preservation*

Because groundwater sampling from pre-existing monitoring wells is routinely performed by field technicians, bacteria (including VC-oxidizers) are therefore collected by sampling groundwater from wells along with other geochemical parameters of interest (e.g. chlorinated ethenes and dissolved gases (ethene and methane)). The sampling equipment include Geopump Peristaltic Pump Series I with easy-load I pump head or low flowrate groundwater sampling.

A YSI Professional Plus handheld multiparameter meter (or similar piece of equipment) was used to measure DO, pH, ORP, and conductivity of the groundwater prior to sampling for other chemical analyses or passed through Sterivex filters to collect groundwater biomass. The probes are inserted into a flow-through cell to facilitate these parameter measurements. The sampling equipment set-up is shown in **Figure 1**. A close-up of the fittings used to connect the Sterivex filter is shown in **Figure 2.**
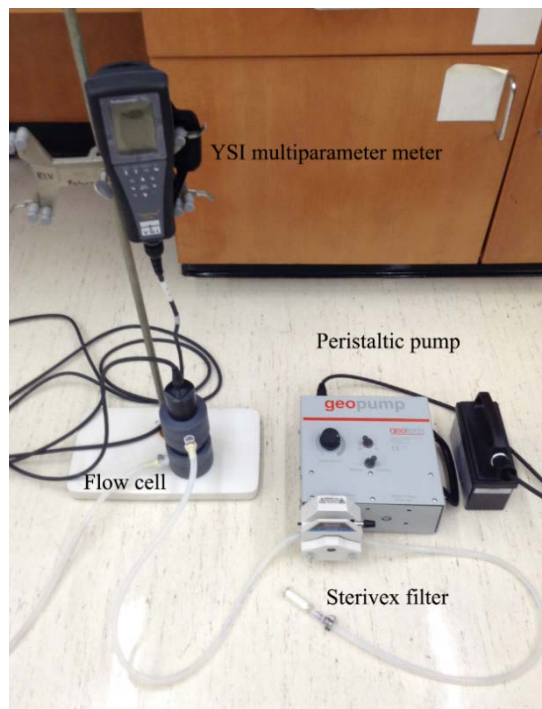
Figure 1. Set-up of Our Groundwater Sampling Equipment

Groundwater sampling follows USEPA 540/S-95/504 low-flow procedures (Puls & Barcelona, 1996). Prior to sampling, monitoring wells are purged at a flow rate <500 mL/min. Groundwater geochemical parameters are recorded in the field as described above. When readings stabilize (i.e. vary <10% within a minute), the flow-through cell is disconnected and groundwater is collected in 40 mL glass vials with Teflon-lined screw caps (VOA vials) and preserved with concentrated hydrochloric acid. VOA vials are placed on ice and shipped to a commercial laboratory for chlorinated ethenes (PCE, TCE, DCEs, VC) analysis using EPA method 8260B and dissolved gases (ethene and methane) using EPA method RSK 175.
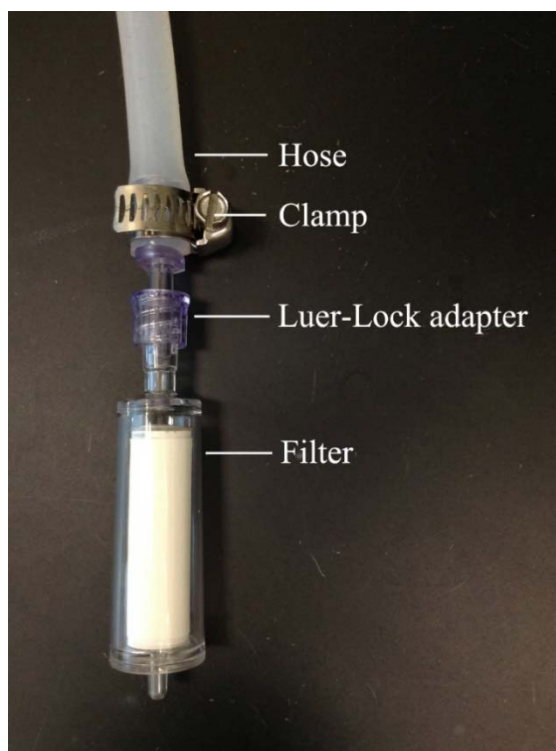
Figure 2. Close-up of the Fitting Used to Connect the Hose to the Sterivex Filter.

After sample collection in VOA vials, microbial biomass samples for replicate DNA and RNA extractions are collected by passing groundwater through Sterivex-GP filters (pore size 0.22 µm, diameter 1.7 cm, Millipore, Germany) (Figure 2). Up to 3 liters groundwater is collected for RNA extraction and up to 1-liter groundwater is collected for DNA extraction. To preserve RNA for laboratory extraction, 3 mL of RNAlater (Ambion, Grand Island, NY) per filter is injected into Sterivex filters with a sterile syringe immediately after sampling. Filters are then placed into sterile 50 mL screw-capped Falcon tubes and shipped on ice by overnight courier to the laboratory. Filters with RNAlater preservation are subjected to RNA extraction immediately upon arrival. Filters for DNA extraction are stored at -80°C prior to extraction.

2.1.1.2 DNA and RNA extraction

Nucleic acid extraction is performed using commercially available DNA and RNA extraction kits. The MoBio PowerWater Sterivex DNA isolation kit and PowerWater RNA isolation kits (now provided by Qiagen) were used in this project, primarily because these kits are commonly used in practice. These kits utilize a mechanical cell lysis procedure (i.e., beadbeating) for releasing nucleic acids. DNA is extracted from filters without opening the filter housing according to the kit instructions. Prior to RNA extraction, the residual RNAlater left in the Sterivex filter is washed out by the buffer "PBS" (8 g/L NaCl, 0.2 g/L KCl, 1.44g/L Na_2HPO_4, 0.24 g/L KH_2PO_4, pH 7.4). After opening the filter cartridge with a PVC pipe cutter, the filter membrane is carefully excised with an autoclaved razorblade, removed with sterile tweezers, inserted into kit-supplied bead tubes, and subjected to RNA extraction according to kit instructions. After extraction, RNase Inhibitor is added to RNA samples to prevent them from degrading. Extracted DNA and RNA is stored at -80°C prior to further analysis.

7

2.1.1.3 Addition of reference nucleic acids (RNA)

Before the cell lysis step in RNA extraction, known amounts of a reference nucleic acid (1 ng) (luciferase mRNA (1 ng) (GenBank accession No. X65316, Promega, Madison, WI) are added to the RNA samples after the lysis step to serve as internal controls for the efficiency of reverse transcription and other RNA losses throughout the remaining steps in the process (such as DNAse I treatment and RNA purification). To achieve this we used mRNA transcribed from the luciferase gene (ref mRNA), as described in a previous study (Johnson, *et al.*, 2005). Using reference mRNA allows us to more accurately estimate transcript abundance following qPCR.

The RNA recovery efficiency (%) is calculated as follows:

$$\% \ recovery = \frac{luciferase \ cDNA \ copies \ after \ qPCR}{total \ luciferase \ mRNA \ added} \times \frac{total \ cDNA \ vol \ after \ R.T.}{cDNA \ vol \ used \ for \ qPCR}$$

$$\times \frac{total \ RNA \ vol \ after \ RNA \ clean \ up}{RNA \ vol \ used \ for \ R.T.} \times 100\%$$

RNA recovery efficiencies are highly variable, ranging from 0.015-17.8% during this project.

Possible reasons for the variability of RNA recovery include:

- Contaminants (e.g. iron oxides) from the original groundwater sample are co-extracted and affect the stability of RNA after cell lysis
- variable reverse-transcription efficiencies from sample to sample.
- The RNA extraction protocol used was highly stringent in terms of removing contaminating DNA. Normally, an on-column DNA digestion step is performed, but in our experience, we have found that the on-column step does not eliminate all contaminating DNA from the RNA sample. To address this, we performed separate in-solution DNA digestion, which required extra time and heat (to the possible detriment of RNA yield). Thus, we have balanced our desire to obtain high quality RNA with the potentially lower yields from a more stringent DNA digestion protocol.

2.1.1.4 Reverse transcription of RNA into cDNA

After extraction, RNA is subjected to DNA removal, RNA clean up, and converted to complementary DNA (cDNA) using the enzyme reverse transcriptase with random hexamer primers. Some RNA extract is kept as a control to test for any remaining DNA contamination in the RNA during qPCR. RNA samples are reversed transcribed into single stranded complementary DNA (cDNA) by SuperScript II Reverse Transcriptase (Invitrogen, Carlsbad, CA) after contaminating DNA removal by DNase I (Biolab, Ipswich, MA) and purification by the RNeasy Mini Kit (Qiagen, Germantown, MD) according to manufacturer's protocol. For example, a 60 μL first strand cDNA synthesis reaction contains 30 μL purified RNA, 10 mM dNTP mix, and 2.25 μg random primers.

2.1.1.5   qPCR standard construction

We use an absolute quantification qPCR approach to estimate the gene copy numbers in the DNA or cDNA sample, which means that each qPCR experiment needs to include a standard curve. A qPCR standard curve establishes a linear relationship between the Ct values and log of input nucleic acid concentration. For our qPCR experiments, we use PCR products amplified from pure cultures as standards. We chose to use PCR products larger than the target amplicon rather than the amplicon cloned into a plasmid because we found in earlier experiments this resulted in improved PCR efficiencies (Jin & Mattes, 2010). Specifically, PCR product amplified from luciferase DNA with primer set ref-STF/R is used as standard for luciferase mRNA qPCR. For *etn*C and *etn*E qPCR, PCR products amplified from JS614 (ATCC AF498452) genomic DNA with RTC-f/r and RTE-f/r are used as standards. For *mmo*X and *pmo*A qPCR, standards are PCR products amplified from *Methylococcus capsulatus* (ATCC 33009) genomic DNA with mmoX-std2f/r and from *Methylocystis* sp. strain Rockwell (ATCC 49242) genomic DNA with pmoA-std1f/r, respectively. For *bvcA* and *vcrA* qPCR, standards were linearized pCR2.1 TOPO-TA vectors containing *bvcA* and *vcrA* gene insertions (Ritalahti, *et al.*, 2006). Primer sets that are used to amplify PCR products for use in standards are shown in **Table 1**. The primers that we use for qPCR are shown in **Table 2**.

2.1.1.6   qPCR analysis of VC biodegradation functional genes and the luciferase reference gene, using both DNA and cDNA templates

Once DNA and RNA have been extracted, ref mRNA added, and RNA reversed transcribed (for RNA samples), and standards prepared, then the samples are subjected to qPCR. Here we aim to estimate the gene and transcript abundances of *etnC, etnE, mmoX, pmoA, bvcA,* and *vcrA*. For cDNA samples, the luciferase reference gene abundance is also quantified to measure the RNA loss during the experiment. DNA and cDNA samples (and DNA standards) are mixed with qPCR reagents (PCR Buffer containing Mg^{2+}, Taq polymerase, DNA building blocks (dNTPs), oligonucleotide primers and SYBR Green dye), samples and calibration standards are loaded onto a plate (either 96 well or 384 well), and placed into an Applied Biosystems real-time PCR instrument. The overall workflow is depicted in **Figure 3.**

Each 20 µL qPCR contains 10 µL Power SYBR Green PCR Master Mix (Invitrogen, Carlsbad, CA) and variable primer and template (DNA and single-stranded cDNA) concentrations (**Table 3**). Bovine serum albumin (100 ng/µL) is added to each reaction to relieve possible PCR inhibition. PCR thermocycler conditions are as follows: 10 min at 95°C, followed by 40 cycles at 95°C (15 s) and 60°C (1 min).
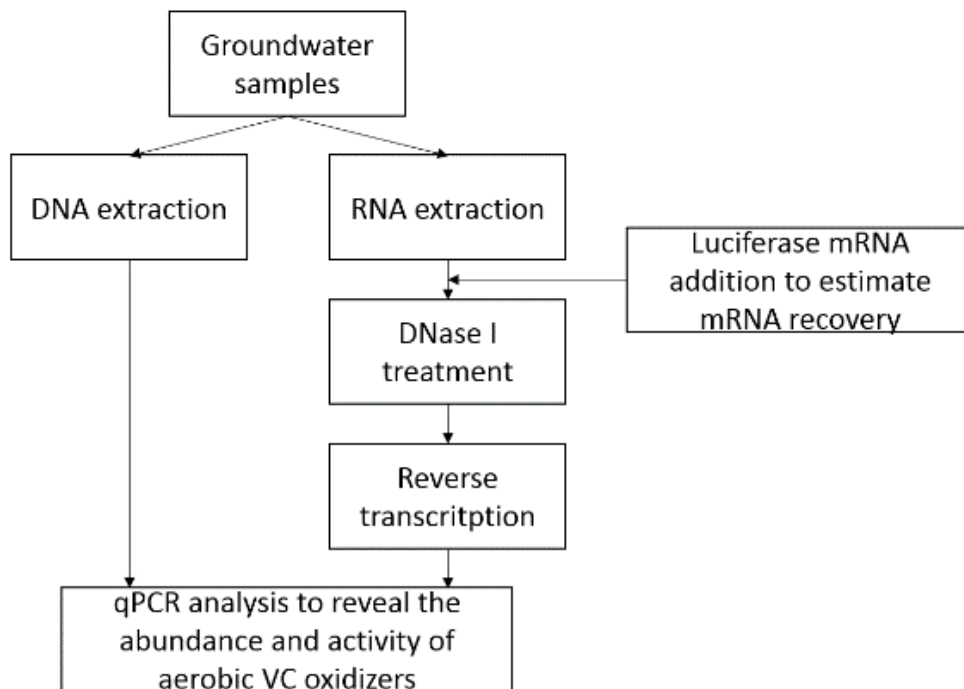
Figure 3.   Overall Schematic Diagram of the Nucleic Acid Extraction and Analysis Workflow.

During real-time PCR, the target genes are amplified and detected by increase in fluorescence as SYBR Green is a non-specific double-stranded DNA (dsDNA) binding dye. For each gene of interest, a range of standard DNA template concentrations must be included to develop a linear relationship between gene copy numbers and the Ct value (threshold cycle, the cycle number required for the generated fluorescence to reach the threshold detection line).

Following the real-time PCR thermocycling program, the temperature is raised incrementally, which will eventually lead to denaturation of the dsDNA PCR products. This is indicated by observing changes in the fluorescence intensity as SYBR Green dissociates from the melting PCR product. The software program produces a "melt curve" where peaks in the curve correspond to the sequence-dependent melting of PCR products as different temperatures. Non-specific amplification products and primer-dimers will impact quantitation since they cannot be distinguished from specific products. Thus, the melt-curve is an important QA/QC step in this process as it is helpful in determining the specificity of amplification. Additional details are provided in Section 2.1.1.8.

Following qPCR and QA/QC steps, Applied Biosystems Sequence Detection System software is used to determine standard calibration curve relationships and estimate gene and transcript abundance in the samples. After carefully accounting for dilutions made throughout the process, the amount of luciferase genes and transcripts quantified is compared to the amount added, and the percent loss is applied as a correction factor when quantifying *etnC*, *etnE*, *mmo*X, *pmoA*, *bvcA*, and *vcrA* gene and transcript abundance. Finally, gene expression is shown in terms of the transcript per gene ratio.

Additional qPCR information, including primer concentrations, template concentrations, qPCR linear range, qPCR efficiency range of the standard curves, and Y-intercepts are recorded in accordance with Minimum Information for Publication of Quantitative Real-Time PCR Experiments (MIQE) guidelines for the purpose of quality control (Bustin, *et al.*, 2009).

Table 1.   Primer Sets Used for the Amplification of Standards.

Note: plasmids were used as standards for bvcA and vcrA.

Target Gene	Primer Name	Sequences	Expected Product Size	Source
luciferase mRNA	ref-STF	5'-CCAGGGATTTCAGTCGATGT-3'	1014 bp	(Liang, *et al.*, 2014)
	ref-STR	5'-TTTTCCGTCATCGTCTTTCC-3'		
*etn*C	JS614-etnCF	5'-GCGATGGAGAATGAGAAGGA-3'	1138 bp	(Jin & Mattes, 2010)
	JS614-etnCR	5'-TCCAGTCACAACCCTCACTG-3'		
*etn*E	CoM-F1L	5'-AACTACCCSAAYCCSCGCTGGTACGAC-3'	891 bp	(Mattes, *et al.*, 2005)
	CoM-R2E	5'-GTCGGCAGTTTCGGTGATCGTGCTCTTGAC-3'		
*mmo*X	mmoX-std2f	5'- AGGCAGTCAAGGACGAAAGG-3'	1123 bp	this study
	mmoX-std2r	5'-ATCTGGCCGTTGTACTCGTG-3'		
*pmo*A	pmoA-std1f	5'-TCGGTCCGTTCAACTCCG-3'	703 bp	this study
	pmoA-std1r	5'-GAATACCAACGGCCCATGAA-3'		

2.1.1.7   *Platforms used for qPCR*

The platforms (96 well and 384 well plate) used for qPCR and their capabilities are described below and illustrated in **Figure 4**. The choice of platform depends on the number of target genes and the number of samples to be processed. Both 96-well plate and 384-well plate qPCR are performed with an ABI 7900 HT Fast Real-Time PCR System.
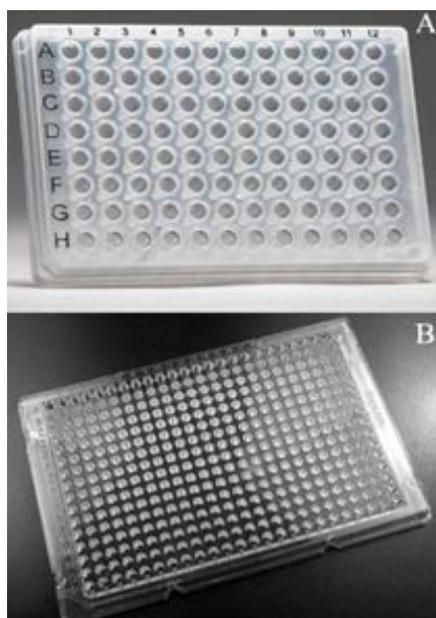
Figure 4.   A) 96-well and B) 384-well qPCR Plates

<u>96-well plate</u>

The 96-well plate (8 rows x 12 columns) is the smallest platform available for qPCR/RT-qPCR. We often use this platform when a small number of samples is being tested. Our 96 well plate qPCR workflow usually includes one set of standards, which comprises 6 dilutions of a known amount of one target gene (with each dilution in triplicate). For each sample, qPCR is usually performed in replicate. For each monitoring well, DNA and RNA samples are usually taken in triplicate. The 96-well plate to accommodate 5 monitoring wells at most for the test of one gene of interest. A No Template Control (NTC) is required for each plate for QA/QC.

<u>384-well plate</u>.

The 384-well plate is similar to the 96-well plate, but is an array of wells 16 rows x 24 columns. A 384-well plate can accommodate DNA, cDNA, and RNA samples from 24 monitoring wells (assuming triplicate filters are taken for DNA and RNA extraction for each monitoring well, respectively) at the same time for the test of one gene of interest. If two genes of interest are analyzed on one plate, nucleic acids from 11 monitoring wells can be included on one 384-well plate.

2.1.1.8 *Calculating genes and/or transcripts per liter of groundwater*

The following equation is used for calculating the gene abundance per liter of groundwater (GW):

$$\frac{genes}{L\,GW} = \frac{genes\,per\,qPCR}{ng\,DNA\,used\,for\,qPCR} \times \frac{ng\,DNA\,after\,extraction}{volume\,of\,groundwater\,sampled}$$

Equation used for transcript abundance calculation per liter of GW:

$$\frac{transcripts}{L\,GW} = \frac{transcripts\,per\,qPCR}{fraction\,RNA\,recovery} \times \frac{cDNA\,volume\,after\,R.T.}{cDNA\,volume\,used\,for\,qPCR}$$
$$\times \frac{RNA\,vol\,after\,RNA\,clean\,up}{RNA\,volume\,used\,for\,R.T.} \times \frac{2\,(factor\,corrected\,for\,single\,strand)}{volume\,of\,groundwater\,sampled}$$

2.1.1.9 *Quality assurance/quality control of nucleic acid extraction and qPCR*

A successful DNA extract is one that contains amplifiable DNA, with concentrations above the Qubit^TM dsDNA HS assay kit detection limit (0.05 ng/µl). An RNA extract is deemed successful if, after reverse transcription and qPCR with the ref-f/r primer set, it yields a luciferase gene PCR product. The integrity of DNA and RNA extracts should always be confirmed prior to conducting qPCR analysis.

The specificity of qPCR primers (RTC-f/r, RTE-f/r, mmoX-536f/898r, pmoA472-A189f/mb661r) should be routinely checked by observing the qPCR product melting curves of each sample. For example, the melting curves of RTE-f/r, mmoX-536f/898r and pmoA472-A189f/mb661r showed similar pattern in groundwater samples as in the standards (Figure 5), which indicates that those primer sets are amplifying their specific targets.

For the RTC-f/r primer set, different groundwater DNA/cDNA samples were found to generate different melting curves, some of which are different from the ones generated by standard DNA. For example, in samples from NAS Oceana and NSB Kings Bay, multiple peaks were observed in PCR product melting curves, indicating possible primer dimer formation or non-specific amplification (**Figure 5**). A clone library was then constructed to investigate the sequences from NAS Oceana and NSB Kings Bay DNA samples amplified with the RTC primer set. In most cases, the peaks seen at low melting temperatures were attributed to primer dimers formation at low template concentrations. Otherwise, the only PCR products identified in RTC primer clone libraries returned BLAST results as being related to soluble di-iron monooxygenase alpha subunit (SDIMO) genes related to the *etnC* gene. SDIMOs are key enzymes in the bacterial oxidation of hydrocarbons. The AkMO and sMMO enzymes targeted here are SDIMOs (Coleman, *et al.*, 2006). Because many SDIMOs can oxidize VC by co-metabolism, the presence of SDIMO also represent the oxidation potential for VC. In contrast, for Parris Island samples, RTC primers generated similar melting curves for both groundwater samples and standards, indicating their good specificity for Parris Island samples at the higher *etnC* concentrations observed there.

If the RTC primer set does not perform well, the MRTC primer set provides another option to amplify *etn*C. MRTC is a mixture of unique, non-degenerate gene-specific primers that based on the database of 38 *etn*C sequences targeting the same priming sites as the RTC primers (Jin & Mattes, 2011)(**Table 2**). The MRTC primer set possibly minimizes the mismatches with template sequences and thus introduces less primer bias than the RTC primer set. Despite this, we chose to utilize the RTC primer set for the samples analyzed in the demonstration for consistency.

Strict quality control procedures are employed to ensure the accuracy of qPCR technology. For each qPCR experiment, one standard curve is included with a dynamic linear range usually between 30 - 3×10^6 or 3×10^7 gene copies per reaction. A linear regression analysis is used to evaluate the linearity of the standard curve and the amplification efficiency.

PCR efficiency (E, %) is calculated based on the slope of standard curve as follows:

$$E = (10^{(-1/\text{slope})} - 1) * 100\%$$

A standard curve is considered to be acceptable when the R^2 of the linear regression is larger than 0.99, and the PCR amplification efficiency is between 90% and 110%.

NTCs should be used with each qPCR primer set on each qPCR plate. This control ensures that cross contamination of samples has been not occurred (at least within the water and reagents used for PCR). In NTCs, the target gene should either be not detected or detected only as primer dimers (as assessed by dissociation curve analysis). RNA sample aliquots (corresponding to each reversed-transcribed sample) should also be included on the same qPCR plate to test for DNA contamination if cDNA samples are to be analyzed. If amplification levels observed in any RNA sample are similar to its corresponding cDNA sample, the cDNA sample should be removed from subsequent analysis.

For DNA and cDNA samples, replicate or triplicate qPCR is performed for the same sample, the Ct difference or standard deviation should be less than 0.3. Samples with target gene abundances that are less than the lower quantification limit (usually 30 gene copies per qPCR reaction) are labeled accordingly. The gene abundance estimation of those samples is considered not as accurate since it is outside the linear range of the standard curve.

For each qPCR, dissociation curves are used to assess amplification specificity. This facilities identification of potential false-positive SYBR green qPCR results. Dissociation curves of samples are compared with standards to rule out non-specific amplification or dimer formation. Agarose gel electrophoresis can be used to confirm the size of PCR product. When necessary, cloning and sequencing should be performed to verify the specificity of PCR products. We recommend that the specificity of qPCR products be verified with clone library analysis prior to embarking on extensive qPCR analysis of samples from each site. According to this analysis, the RTC primers have a tendency to form primer dimers, particularly when the target gene is at low abundance. Primer dimer formation by both the methanotroph functional gene primer sets could occur when target gene abundance is low. Occasional primer dimer formation was noted with Bvc925f/1017r.

2.1.2   Chronological summary of the development of the technology to date

In general, the application of qPCR to track the progress of *in situ* bioremediation strategies has been growing in popularity over the last decade. It is considered a robust technology for estimating gene abundance and expression in environmental samples as indication of microbial bioremediation (Smith & Osborn, 2009). The technique of qPCR has been widely used to quantify the abundance of *Dehalococcoides* sp. and associated functional genes to assess the reductive dehalogenation potential at sites contaminated with chlorinated compounds (Cupples, 2008, Sowers & May, 2013). It has also been applied to monitor the microbial metal reduction (Hwang, *et al.*, 2008, Wang, *et al.*, 2015) and hydrocarbon degradation (Powell, *et al.*, 2006, Biggerstaff, *et al.*, 2007).

The qPCR technology for estimating the abundance of functional genes from VC-oxidizing etheneotrophs was developed by the PI under contract with SERDP (Project ER-1683). There are currently two journal articles that describe the technology and subsequent improvements (Jin & Mattes, 2010, Jin & Mattes, 2011). We use previously published primer sets to amplify methanotroph functional genes and transcripts (Holmes, *et al.*, 1995, McDonald, *et al.*, 1995, Fuse, *et al.*, 1998, Kolb, *et al.*, 2003). The optimization of qPCR conditions and selection of primer sets were performed under SERDP project ER-1683 (Dobson, 2011). We have recently published an article that describes the RT-qPCR method extension with a small field-scale application (Mattes, *et al.*, 2015). Currently, we are performing qPCR analyses on 384 well plates. Overall, we believe that previous efforts with qPCR, along with the publication and funding history of the etheneotrophs qPCR technique indicate that they are sufficiently mature to be used in this demonstration.
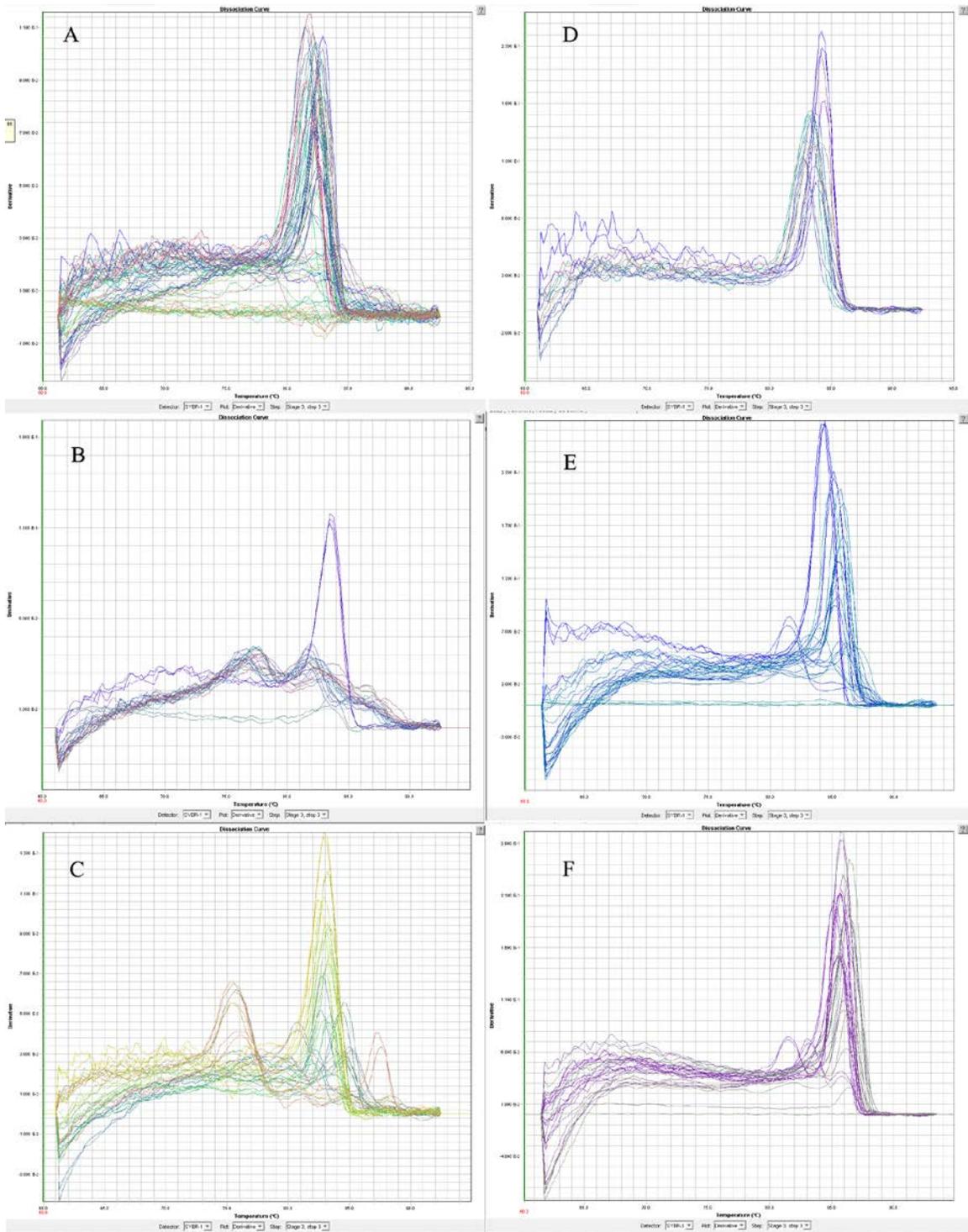
Figure 5.   Melting Curves of Primer Sets A) RTC-f/r Amplifying DNA Samples from MCRD Parris Island, B) RTC-f/r Amplifying DNA Samples from NAS Oceana, C) RTC-f/r Amplifying DNA Samples from NSB Kings Bay, D) RTE-f/r Amplifying DNA Samples from MCRD Parris Island, E) mmoX-536f/898r Amplifying DNA Samples from MCRD Parris Island, and F) pmoA472-A189f/mb661r Amplifying DNA Samples from MCRD Parris Island.

Table 2. Primer Sets Used for qPCR Experiments

Target Gene	Primer Name	Sequences	Expected Product Size	Source
luciferase mRNA	ref-f	5'-TACAACACCCCAACATCTTCGA-3'	150 bp	(Johnson, *et al.*, 2005)
	ref-r	5'-GGAAGTTCACCGGCGTCAT-3'		
*etn*C	RTC-f	5'- ACCCTGGTCGGTGTKSTYTC-3'	106 bp	(Jin & Mattes, 2010)
	RTC-r	5'- TCATGTAMGAGCCGACGAAGTC-3'		
*etn*C	MRTC-f	5'-ACACTCGTCGGCGTTGTTTC-3' 5'-ACCCTGGTCGGTGTGCTCTC-3' 5'-ACGCTGGTCGGTGTTCTTTC-3' 5'-GCTCTGGTCGGCGTTCTTTC-3' 5'-ACTCTGGTCGGCGTTCTTTC-3' 5'-ACCTTGGTTGGTGTGCTTTC-3' 5'-ACCCTGGTCGGTGTGGTCTC-3' 5'-ACCCTGGTCGGCGTGGTCTC-3'	106 bp	(Jin & Mattes, 2011)
	MRTC-r	5'-TCATGTACGAGCCGACGAAGTC-3' 5'-TCATGTAAGAGCCGACGAAGCC-3' 5'-TCATGTAAGAGCCGACGAAGTC-3' 5'-TCATGTAGGAGCCGACGAAGTC-3' 5'-TCATGTAAGAACCGACGAAGTC-3' 5'-TCATGTACGAACCGACGAAGTC-3'		
*etn*E	RTE-f	5'-CAGAAYGGCTGYGACATYATCCA-3'	151 bp	(Jin & Mattes, 2010)
	RTE-r	5'-CSGGYGTRCCCGAGTAGTTWCC-3'		
*mmo*X	mmoX536f	5'-CGCTGTGGAAGGGCATGAAGC G-3'	542 bp	(McDonald, *et al.*, 1995, Fuse, *et al.*, 1998)
	mmoX898r	5'-GCTCGACCTTGAACTTGGAGC C-3'		
*pmo*A	pmoA472-A189f	5'-GGNGACTGGGACTTCTGG-3'	283 bp	(Holmes, *et al.*, 1995, Kolb, *et al.*, 2003)
	pmoA472-mb661r	5'-CCGGMGCAACGTCYTTAC C-3'		
*bvc*A	Bvc925F	5'-AAAAGCACTTGGCTATCAAGGAC-3'	92 bp	(Ritalahti, *et al.*, 2006)
	Bvc1017R	5'-CCAAAAGCACCACCAGGTC-3'		
*vcr*A	Vcr1022F	5'-CGGGCGGATGCACTATTTT-3'	71 bp	(Ritalahti, *et al.*, 2006)
	Vcr1093R	5'-GAATAGTCCGTGCCCTTCCTC-3'		

Table 3. Primer Concentration and Template Mass for qPCR Set Up.

Target Gene	Primer Concentration, μM	Template
luciferase mRNA	0.1	2 ul cDNA
etnC	0.8	10 ng DNA or 2 ul cDNA
etnE	0.8	10 ng DNA or 2 ul cDNA
mmoX	0.3	10 ng DNA or 2 ul cDNA
pmoA	0.3	10 ng DNA or 2ul cDNA
bvcA	0.3	10 ng DNA or 2ul cDNA
vcrA	0.3	10 ng DNA or 2ul cDNA

2.2 PRACTICAL IMPLICATIONS OF THE TECHNOLOGY

Now that qPCR (Jin & Mattes, 2010, Jin & Mattes, 2011) and RT-qPCR methods (Mattes*, et al.*, 2015) for VC-oxidizing bacteria are available, we are poised to further demonstrate the extent and activity of VC oxidation pathways at contaminated sites. ***These powerful new tools for assessing VC oxidation pathways are now available to be added to the molecular diagnostics toolbox for site managers and remediation practitioners.*** Field demonstration of these tools in a variety of different situations (e.g., different VC concentrations, different hydrogeological conditions, natural attenuation vs. biostimulation scenarios) is necessary to establish the relationships between VC-oxidizer functional gene abundance and activity with changes in VC concentration. Although decreases in VC concentrations are observed on the fringes of VC plumes at several sites, there are no published accounts that provide any link between VC concentrations and VC-oxidizing populations measured with molecular tools or otherwise. The data collected and guidance provided as a result of this project is expected to provide site managers the ability to document VC oxidation as a viable pathway responsible for reducing VC concentrations at their site. These crucial lines of evidence could speed up regulatory acceptance of MNA and ultimately reduce lifecycle costs for clean-up.

Remediation activities at Parris Island Site 45 could benefit from application of qPCR/RT-qPCR tools for VC-oxidizers, which is a primary reason why have made it the focus of this demonstration. Remedial investigations have been ongoing at the site, but there is still no formal record of decision (ROD) of the remediation approach. Nevertheless, full-scale bioremediation remedies (including eventually MNA) are expected to be implemented at the site. Direct oxidation of VC is already suspected at the site based on decreasing VC concentrations in downgradient portions of the northern and southern plumes. The timing of this demonstration with remedial activities at site 45 has the strong potential to provide important lines of evidence for VC oxidation processes. This information could also impact remedial outcomes and support regulatory decisions by accelerating approval of a MNA strategy (and maintaining that strategy in good standing during the monitoring phase) for addressing VC contamination. If this information is successfully collected and communicated, this could ultimately lead to lifecycle cost savings for site 45.

Implementing this technology at other locations subsequently holds promise for reduced lifecycle costs for a significant number of remediation projects.

2.3   ADVANTAGES AND LIMITATIONS OF THE TECHNOLOGY

The RT-qPCR/qPCR technology for etheneotrophs and methanotrophs is an innovative and rapid means of revealing the abundance and functionality of the microbial community and provides unique information about the potential for *in situ* microbial aerobic VC oxidation at contaminated sites. This information is useful in evaluating and monitoring the natural attenuation processes and help inform remediation decisions and strategy development. Conventional microcosm studies are laborious, time-consuming and relatively expensive, and in some cases might not represent *in situ* conditions. Contaminant analyses are useful in understanding the contaminant concentration and distribution at the site but could not provide information about the microbial degradation potential at present and in the future.

RT-qPCR technology estimates the gene and transcript abundances in the environment and provides more accurate and valuable information than traditional PCR (and RT-PCR), which is not quantitative. It also goes a step further than typical qPCR approaches as RNA is analyzed, and thus provides a measure of activity as well as abundance. RT-qPCR is more sensitive and precise in detecting the microbial VC-oxidizers in the groundwater than hybridization-based techniques such as fluorescence in situ hybridization (FISH). We have strict QA/QC procedures to ensure the sensitivity and precision of this technology. In our case, the lower limit of quantification (LOQ) is approximately 500 genes per liter of groundwater and 1000 transcripts per liter of groundwater. This level of sensitivity is especially advantageous in investigating the VC oxidizers at low concentrations.

RT-qPCR/qPCR technology is more time efficient compared to conventional microcosm methods. Depending on the sample amount, RT-qPCR/qPCR analysis from a sampling event containing 18 Sterivex filter samples takes 1-2 weeks. This is in contrast to a typical microcosm study, which can take several months to complete.

A potential disadvantage of RT-qPCR is that it only targets the known functional genes and transcripts associated with aerobic VC oxidation. Any as yet undiscovered VC oxidation pathways that are not targeted by the current primer sets are inherently overlooked, which will result in underestimation of VC oxidation potential and activity. For this reason, expanding current primer sets to include novel VC oxidation biomarkers should be considered a possibility in the future. As we cannot predict when new VC oxidation biomarkers will be discovered, we expect that expanded primer sets will be developed by either work funded elsewhere or in additional proposals to SERDP and/or ESTCP.

It is also prudent to constantly evaluate existing primer sets for performance with environmental samples. It is possible that variability in target gene composition and abundance from site to site could lead to variation in RT-qPCR performance. As biomarker gene sequences from the environment are added to the database, revisions to the primer sets could help improve performance. However, it is important to note that the primer sets we employ that target functional genes in etheneotrophs (i.e. *etnC* and *etnE*) utilize the most current complement of genes in the database.

Another limitation of our current approach is that we so far have only analyzed the abundance and activity of VC-oxidizers in groundwater samples. We are assuming that groundwater extracted from a monitoring well provides a representative sample of the microbial population in the aquifer. Monitoring well samples are advantageous in that they are easily collected, and provide a composite sample of the microbial community within the radius of influence of the well. It is likely that the distribution of VC-oxidizers is heterogeneous and that they will be found in regions where VC is present (diffusing from deeper anaerobic regions of the groundwater) and oxygen is also present (diffusing in from the unsaturated zone and rainwater recharge of the aquifer). Groundwater sampling alone could be biased towards microbes that are planktonic or easily detached from surfaces. Neglecting microbial VC-oxidizers attached to the sediment may lead to bias in evaluating the *in-situ* VC oxidation potential. In addition, the spatial variability of VC-oxidizers in the subsurface would provide an improved understanding of VC oxidation potential and could inform site management decisions concerning MNA. Aquifer sediment sampling is grab sampling – it provides a single point snapshot of the microbial community. Sediment sampling is more difficult, more variable, and it requires a large quantity of sediment samples to ensure representative data than groundwater sampling (thus more expensive). To gain an enhanced understanding of the *in situ* microbial VC oxidation potential with respect to attached and planktonic cells, we will obtain sediment samples for qPCR and RT-qPCR analysis as part of this demonstration.

Because we are planning to perform biomolecular analysis on the sediment samples, including extraction and analysis of RNA, a promising method for taking the samples is via cryogenic coring (Johnson*, et al.*, 2013). Cryo-coring is essentially push coring technology adapted so that liquid nitrogen can be injected and freeze the sediment sample in place. Once the core is removed, it can be packed on dry ice and shipped to the laboratory. Flash freezing the sample at about -80C preserves labile RNA in the sample and facilitates RNA extraction and analysis in the laboratory. Additional information regarding the scope of the proposed cryo-coring is provided in Section 5.53.

The primary goal of the cryo-coring campaign will be to reveal the spatial distribution of VC-oxidizing bacteria abundance and activity with depth in the sediment. This will also help explain why VC-oxidizers and VC dechlorinators can be found in the same groundwater sample. The cores could reveal that VC dechlorinators are distributed in very different locations than the VC-oxidizers. Gene and transcript concentrations in the core sediments are expected to vary widely by location. In some locations, the concentrations will likely be much higher than estimated in groundwater, and in some locations the concentrations could be much lower. This will indicate that groundwater samples provide a composite view of the aquifer under the radius of influence of the well. The cryo-cores will only reveal a snapshot of the microbial community distribution over depth in that location. Obtaining several cyro-cores along a VC plume transect will provide an improved understanding of how gene and transcript abundances vary with depth along the plume.

Alternative technologies

In Section 2.1.1.7, we described the different platforms on which we can perform qPCR/RT-qPCR analyses for VC-oxidizers. These included 96 well plates and 384 well plates.

19

The QuantArray is a recently available qPCR platform used by Microbial Insights, Inc. It is specifically designed to target multiple functional genes and taxa associated with anaerobic reductive dechlorination and aerobic cometabolism of chlorinated solvents. The detection and quantification limits (LOD/LOQ) for functional genes on the QuantArray is ~ 5 "cells/mL". This unit essentially indicates 5 "genes/ml groundwater" or 5,000 genes/L groundwater. This is about an order of magnitude less sensitive than standard qPCR methods.

The QuantArray assay is not focused solely on VC oxidation, although the functional genes associated with VC oxidation by etheneotrophs (*etnC* and *etnE*) are included on the array. There are important differences between our qPCR/RT-qPCR technology and the QuantArray. Most importantly, our qPCR primers have been published in the literature and are freely available for use by the bioremediation community (Jin & Mattes, 2010, Jin & Mattes, 2011). The design of our *etnC* and *etnE* qPCR primers is clearly stated in these journal articles. We use degenerate qPCR primers and SYBR Green qPCR chemistry that incorporates QA/QC procedures that will alert us in the event that a false positive result occurs. The primer sets have been rigorously tested in the laboratory and have been validated in an expanding set of field samples. This has greatly minimized the potential for false positive results.

The *etnC* and *etnE* primers and probes used on the QuantArray are proprietary and utilize TaqMan qPCR chemistry. While using TaqMan qPCR chemistry is considered to optimally minimize false positive results (because of the increased specificity of TaqMan primers and probes), this approach is better suited to quantifying the abundance of single genes in environmental samples. If the diversity of functional genes is not considered, this could potentially lad to false negative results. The performance of these primers with environmental samples in comparison to the primers we have developed is currently unknown.

Our qPCR/RT-qPCR technology, which focuses on functional genes associated with VC oxidation, has lower quantification limits than the QuantArray and has been adapted to quantify mRNA transcript abundance. When performed in microliter volumes (96 and 384 well plates), has a LOQ of 500 genes per liter of groundwater and 1000 transcripts per liter of groundwater. Thus, our technology is well-suited to applications where long-term and/or intensive monitoring of VC-oxidizer abundance and activity is desired (e.g. MNA scenarios involving dilute VC plumes). Thus, we believe our technology represents a robust and cost-effective approach to generating lines of evidence for VC biodegradation during the long-term groundwater monitoring phase of a remedial design.

3.0 PERFORMANCE OBJECTIVES

Table 4. Proposed Performance Objectives

Performance Objective	Data requirements	Success criteria	Objective met?
Qualitative Performance Objectives			
On-site sampling, handling and preservation protocols for RT-qPCR methods are easy to implement	Collect information on how well sampling and preservation requirements fit with procedures currently in place.	The procedure is streamlined and straightforward so that a single field technician to collect samples, preserve them and ship them to a laboratory for analysis.	Yes
Regulatory acceptance	Obtain feedback from the regulatory community regarding acceptance of molecular biology tools in making regulatory decisions.	The regulatory community accepts RT-qPCR data as a means of demonstrating biological evidence for natural attenuation or enhanced remediation of VC.	No, the technology was only recently transferred to SiReM and has yet not been used in a regulatory context as a means of demonstrating natural attenuation of VC.
Usefulness	Communicate qPCR and RT-qPCR to RPMs, site managers, scientists and other DoD personnel and obtain feedback whenever possible and via several approaches. This includes presentations at key conferences, publication of data in the peer-reviewed literature, and a guidance document	Demonstrate successful technology transfer.	Yes, qPCR technology for etheneotrophs (etnE) was transferred to SiReM
		Publish peer-reviewed journal articles and present results at conferences that demonstrates the usefulness of the technology.	Yes, so far 3 peer-reviewed journal articles have been published and there have been numerous conference presentations concerning the data generated during this project
		Make RPMs and other DoD personnel aware of the technology by preparing a guidance document.	Yes, a guidance document has been written an dis posted on the ESTCP website

Table 4. Proposed Performance Objectives (Continued)

Performance Objective	Data requirements	Success criteria	Objective met?
Quantitative Performance Objectives			
Time-efficiency	Determine the average amount of time required from sample collection through data analysis.	Time required should be less than the time to obtain similar data using microcosms.	Yes, the requirements for RT-qPCR (about 3-4 weeks for processing 60 samples) is less than that of conventional microcosm testing.
Cost-effectiveness	Determine the unit cost per monitoring well and per gene of interest for RT-qPCR/ qPCR analyses of VC-oxidizer functional genes	The cost should be equal to or less than the cost of analogous microcosm tests.	Yes, the unit cost of RT-qPCR/qPCR technology is less than analogous microcosm tests
Accuracy	Collect DNA and RNA samples in duplicate (or triplicate); evaluate RNA recovery with an internal nucleic acid control; assess no template controls, evaluate amplification efficiency of qPCR standard curves.	no target gene detected in the NTC; amplification efficiency ranges from 90-110%; Luciferase mRNA recovery is >5%;	-Yes, target genes were not detected in the NTC -Yes, amplification efficiency ranges from 90-110% were noted in 91% of the qPCR standard curve experiment. -No, Luciferase mRNA recovery >5% was not achieved. It was unclear why mRNA recovery was less than expected, but we hypothesize that the stringent DNA removal conditions led to increased loss of mRNA during the extraction process.
Precision	Calculate the Ct (the cycle number required to reach the fluorescence threshold) variance from triplicate/replicate qPCRs for one sample; assess the linearity of standard curves.	Ct standard deviation of triplicate qPCRs is < 0.3; R^2 value of standard curve is > 0.99.	-Yes, the Ct standard deviation of triplicate qPCRs < 0.5 was met for more than 90% of the standards and more than 80% of the samples. -Yes, standard curves displayed R^2 value>99%, was met for all qPCR experiments. suggesting great linearity of standard curves.
Reproducibility	Determine the range in functional gene/transcript abundance of duplicate samples and/or the standard deviation in functional gene/transcript abundance in triplicate samples	The range/standard deviation of Ct values from duplicate/triplicate samples should not exceed 0.5 more than 25% of the time.	Yes, for all functional genes, > 90% of standards showed Ct standard deviation less than 0.5, while >80% of samples showed Ct difference less than 0.5 in duplicate qPCRs

Table 4. Proposed Performance Objectives (Continued)

Performance Objective	Data requirements	Success criteria	Objective met?
Comparability of different qPCR primer sets	Using the same DNA extracts, measure duplicate samples using the qPCR primers of two different laboratories and compare results of mean values for gene abundance from each lab (e.g. student's t-test).	qPCR estimates of *etnC* and *etnE* abundance performed by two independent laboratories on the same DNA samples should yield results within the same order of magnitude	Yes, for *etnC* qPCR results were within the same order of magnitude. However, > 10-fold variability between the two labs occurred for *etnE* qPCR. This could be improved by continued standardization of qPCR laboratory practices between the two groups.
Sensitivity	Evaluate the linear dynamic range of the standard curve, particularly the lower end of the curve that dictates the detection and quantification limits of the assay; Assess melting curves to ensure specificity and sensitivity.	The lower limit of the quantification of 500 genes per liter of groundwater and 1000 transcripts per liter of groundwater; melt-curves should indicate the presence of the specific PCR products only.	No, the lower limit of quantification for DNA samples was 900 genes per liter of groundwater and for RNA samples was 10,000 transcripts per liter of groundwater. Although these values do not meet the original success criteria, in both cases we feel that perhaps these success criteria were ambitious, as these quantification limits are very reasonable for qPCR.
Determine temporal trends in the abundance of *etnC, etnE,* and other VC biodegradation functional genes, alongside VC cDCE, and methane concentrations, and field parameters (e.g., DO, ORP, pH, temp). ▪	Temporal qPCR and RT-qPCR data for six functional genes (*etnC, etnE, mmoX, pmoA, bvcA,* and *vcrA*) from groundwater samples; Groundwater geochemical parameters measured by YSI Professional Plus handheld multiparameter meter during field sampling (i.e, DO, ORP, pH, temperature); Methane, VC and cDCE concentration data from groundwater samples.	Temporal trends of gene and transcript abundances were analyzed by the Mann-Kendall test. An increasing or decreasing trend was considered statistically significant if the $p < 0.05$.	Yes, using data from NAS Oceana showed that establishing temporal relationships between VC degradation and functional gene abundance and activity is possible, but was difficult in the dilute VC plume scenario we encountered

Table 4. Proposed Performance Objectives (Continued)

Performance Objective	Data requirements	Success criteria	Objective met?
Determine spatial correlation of VC-biodegradation functional gene/transcript abundance with the following contaminant and geochemical parameters: • VC concentration • Ethene concentration • Methane concentration • DO, ORP • Other chlorinated ethenes (PCE, TCE, cDCE)	• Spatial qPCR and RT-qPCR data (i.e., *etnC, etnE, mmoX, pmoA, bvcA,* and *vcrA*) from groundwater and cryo-core sediment samples • Geochemical parameter data from groundwater and cryo-core sediment samples (i.e., DO, ORP, pH, temperature). • Ethene and methane concentrations from groundwater samples and cryo-core sediment samples • Chlorinated ethenes (PCE, TCE, cDCE, and VC) in groundwater samples and cryo-core sediment samples	In 95 groundwater samples, relationships between VC-biodegradation functional gene/transcript abundance and contaminant and geochemical parameters were determined with: • Spearman's rank correlation test • simple linear regression • multilevel regression. For multilevel regression, each site was considered as level 1, and each monitoring well was considered as level 2. In 124 cryo-core samples, relationships between VC-biodegradation functional gene/ transcript abundance and contaminant and geochemical parameters were determined with: • Spearman's rank correlation test • simple linear regression • censored regression • Correlations were considered statistically significant if the p value of a test is < 0.05.	Yes, multi-level regression analysis revealed statistically significant correlations between etheneotroph functional genes/transcripts and VC concentrations in groundwater samples. Yes, censored regression analysis revealed statistically significant correlations between etheneotroph functional genes and VC concentrations in cryo-core sediment samples.
Determine relationships between VC biodegradation functional genes/transcripts from and bulk VC attenuation rates determined at field sites	• VC concentrations in groundwater • Estimates of groundwater seepage velocity and retardation coefficients from previous site investigations • Estimates of VC attenuation rates over a transect of at least 4 monitoring wells • Spatial qPCR and RT-qPCR data for etheneotroph and methanotroph functional genes (*etnC, etnE, mmoX, pmoA*) from groundwater samples • Spatial qPCR and RT-qPCR data for anaerobic VC dehalogenase genes *bvcA* and *vcrA*	The relationship between spatial bulk VC atenuation rates and functional gene and transcript abundances was investigated with a multilevel categorical regression model. Each site was assigned to a categorical rate group (high rate attenuation or low rate attenuation group) based on estimated bulk VC attenuation rate and other geochemical parameters. The relationship was considered significant if the p value of categorical regression is less than 0.05.	Yes, categorical regression analysis indicated a statistically significant categorical relationship between etheneotroph functional genes and bulk VC attenuation rates. A statistically significant categorical relationship between etnE transcripts and bulk VC attenuation rates was also noted.

Table 4. Proposed Performance Objectives (Continued)

Performance Objective	Data requirements	Success criteria	Objective met?
Determine relationships between functional gene *etnE* and the VC biodegradation rate in VC-oxidizing enrichment cultures in the laboratory	• VC substrate depletion data from laboratory microcosms and pure VC-oxidizing bacterial cultures • qPCR data for etheneotroph functional gene (*etnE*)	VC substrate depletion data was fitted to Michaelis-Menton enzyme kinetics to determine maximum substrate depletion rates and half-saturation coefficients. *etnE* abundances were correlated to raw VC depletion rates. *etnE* abundances were considered predictive of rates if $r^2 > 0.9$.	Yes (preliminary), we observed a strong linear relationship ($R^2 = 0.98$) between the biomass concentration (as *etnE*) and the q_{max} for VC biodegradation by strain JS614

3.1 QUALITATIVE PERFORMANCE OBJECTIVES

3.1.1 On-site sampling, handling and preservation protocols for RT-qPCR/qPCR methods are time-effective and easy to implement

Sample collection is an important component of the process of estimating gene and transcript abundance in environmental samples.

3.1.1.1 Data requirements

Collect information on how well sampling and preservation requirements fit with procedures currently in place. Determine how much time is required to collect the desired number of samples.

3.1.1.2 Success criteria

The procedure should be streamlined and straightforward enough for a single field technician to collect samples, preserve them and ship them to a laboratory for analysis.

3.1.2 RT-qPCR/qPCR technology is accepted by regulators

3.1.2.1 Data requirements

Obtain feedback from the regulatory community regarding acceptance of molecular biology tools in making regulatory decisions

3.1.2.2 Success criteria

The regulatory community accepts RT-qPCR data as a means of demonstrating biological evidence for natural attenuation or enhanced remediation of VC.

3.1.3 RT-qPCR/qPCR technology is useful.

The main goal of this project was to demonstrate that etheneotroph qPCR technology is useful to site managers. This objective is significantly related to technology transfer activities. Site managers and DoD personnel should be made aware of the technology and its potential usefulness in a variety of ways.

3.1.3.1 Data requirements

Communicate qPCR and RT-qPCR to RPMs, site managers, scientists and other DoD personnel and obtain feedback whenever possible and via several approaches. This includes presentations at key conferences, publication of data in the peer-reviewed literature, and a guidance document.

3.1.3.2 Success criteria

Demonstrate successful technology transfer. Publish peer-reviewed journal articles and present results at conferences that demonstrates the usefulness of the technology. Make RPMs aware of the technology by preparing a guidance document.

3.2 QUANTITATIVE PERFORMANCE OBJECTIVES

3.2.1 RT-qPCR/qPCR technology is time efficient

An important advantage of our RT-qPCR technique is that results can be obtained within a relatively short period of time (weeks) and can provide biological data efficiently to the site manager for further decision-making.

3.2.1.1 Data requirements

The time cost for RT-qPCR technology was assessed. Time spent on each step of the process, including groundwater sample collection and shipping, DNA and RNA extraction, reverse transcription and qPCR was assessed after each sampling event and experiment.

3.2.1.2 Success criteria

The objective is considered met if the time requirements for RT-qPCR is less than that of conventional microcosm technique.

3.2.2 RT-qPCR/qPCR technology is cost effective

The cost effectiveness of RT-qPCR depends on not only the cost of the technology but also the amount of information it can provide.

3.2.2.1 Data requirements

We determined the unit cost per monitoring well and per gene of interest for analyses via "Standard" RT-qPCR/qPCR of VC-oxidizer functional genes. This analysis included the groundwater sample collecting cost, the sample shipping cost, the reagent cost, the consumable cost, and instrument running fees.

3.2.2.2 Success criteria

The objective will be considered to be met if the unit cost per analysis is less than analogous microcosm tests.

3.2.3   RT-qPCR/qPCR technology is accurate

The accuracy of RT-qPCR technology refers to the difference between the actual quantities and experimentally measured results. Although it is not possible to know the exact absolute quantity of genes and transcripts in an environmental sample, we aimed to maximize accuracy with strict quality assurance and controls that ensure the data generated is representative of the actual gene/transcript quantity in the sample.

3.2.3.1   Data requirements

First, for each monitoring well, duplicate/triplicate DNA and RNA extractions were performed, and the results were reported as the average of the triplicate (or duplicate) extractions. Secondly, RNA samples need special care because RNA degrades quickly in the environment. We used RNAlater to preserve Sterivex filters before the RNA extraction. Also, RNA loss during extraction and subsequent DNase treatment, reverse transcription, and qPCR was determined using an internal nucleic acid control (luciferase mRNA). Finally, for each qPCR experiment, strict quality control was employed. Bovine Serum Albumin (BSA) was used in qPCR to relieve possible PCR inhibition in the samples. Each qPCR plate include a "no template control" (NTC) to control for cross-contamination. Amplification efficiency was evaluated by preparing standard curves of known amounts of target gene.

The qPCR technology being demonstrated in this project uses a SYBR green chemistry. Because SYBR Green is a non-specific DNA binding dye, there is the potential for non-specific amplification and thus the generation of false positives during analysis. An additional QA/QC approach – melt-curve analysis – was also performed following qPCR analysis. Melt-curve analysis allows us to assess whether non-specific amplification has occurred during qPCR.

3.2.3.2   Success criteria

Luciferase mRNA recovery is >5%; no target gene detected in the NTC; amplification efficiency ranges from 90-110%.

3.2.4   RT-qPCR/qPCR technology is precise

The precision of RT-qPCR technology refers its robustness. Proper laboratory procedures are critical to ensure high precision of RT-qPCR results. Ideally, samples that are intended to be compared with each other should be analyzed in the same qPCR assay (i.e., on the same qPCR plate) and in accordance with Minimum Information for the publication of Quantitative PCR Experiments (MIQE) guidelines {Bustin, 2009 #2}.

3.2.4.1   Data requirements

RT-qPCR and qPCR precision were evaluated by calculating the variance of the cycle number required to reach the fluorescence threshold (Ct) from triplicate/replicate qPCRs for one sample. The standard curve will also be assessed for linearity to ensure the precision.

3.2.4.2   Success criteria

The objective was considered met if the Ct standard deviation of triplicate qPCR reactions is less than 0.3 and the R^2 value of standard curve is higher than 0.99.

3.2.5 RT-qPCR/qPCR technology is reproducible

The reproducibility of qPCR is important to ensure that there is sufficient quantitative confidence with the results. There must not be too much variability from sampling and analysis.

3.2.5.1 Data requirements

Following qPCR analysis of samples, the range of functional gene abundance (duplicate samples) and the standard deviation of functional gene abundance (triplicate samples) will be calculated. The value of the range and/or the standard deviation was reported.

3.2.5.2 Success criteria

The deviation of the cycle threshold (Ct) of duplicate/triplicate samples does not exceed 0.5 more than 25% of the time.

3.2.6 RT-qPCR/qPCR conducted in different labs provides comparable results

Comparability means that the qPCR results are reproducible and similar in quantity in different laboratories when the same DNA samples are analyzed. Comparability is important for successful technology transfer.

3.2.6.1 Data requirements

Using the same DNA extracts, measure duplicate samples using the qPCR primers of two different laboratories and compare results of mean values for gene abundance from each lab (e.g. student's t-test). DNA samples, originally extracted at the SiReM laboratory, were subjected to qPCR analysis targeting *etnC* and *etnE*. This analysis was performed with DNA samples three different sites to account for potential site-to-site variability in primer performance. The DNA samples were subsequently sent to the Mattes laboratory at the University of Iowa, subjected to the same qPCR analysis, and the results were compared.

3.2.6.2 Success criteria

qPCR estimates of *etnC* and *etnE* abundance performed by two independent laboratories on the same DNA samples should yield results within the same order of magnitude.

3.2.7 RT-qPCR/qPCR technology is sensitive

This qPCR technology should be sensitive enough to detect relatively low copy numbers of gene/transcripts from DNA/cDNA samples. Sensitivity is important in dilute VC plumes, for example, where gene and transcript abundance could be much lower than in more concentrated plumes

3.2.7.1 Data requirements

The sensitivity of RT-qPCR/qPCR technology will be assessed by evaluating the linear dynamic range of the standard curve, and in particular the lower end of the curve that dictates the detection and quantification limits of the assay. Melting curve analysis will also be performed. This is a function that a real-time PCR instrument provides when running a SYBR Green qPCR assay.

When using SYBR green, a non-specific double-stranded DNA binding dye, PCR products are detected by an increase in fluorescence. After PCR, the instrument gradually raises the temperature of the reaction. Eventually, the PCR product will denature and release the SYBR green dye. These melt curves are useful for assessing the specificity and sensitivity. Melt-curve peaks, which indicate the melting temperature of the PCR product, are also a more sensitive means of detecting PCR products than agarose gel electrophoresis and staining with SYBR green or Ethidium bromide. This is important in environmental samples where the target gene concentration could be low.

3.2.7.2 *Success criteria*

The objective will be considered to be met if the lower limit of the quantification of 500 genes per liter of groundwater (0.5 genes per mL) and 1000 transcripts per liter of groundwater (1 transcript per ml). Melt-curves will indicate the presence of PCR products at these concentrations, and also the presence of genes or transcripts even if they are below the quantification limit.

3.2.8 Determine how qPCR/RT-qPCR data correlates with temporal variation in VC concentration and other geochemical parameters

The temporal pattern of aerobic VC-oxidizers in contaminated groundwater, as estimated by qPCR, will help predict the future natural attenuation potential and evaluate the long-term effect of remedial methods. The variation of the abundance and activity of etheneotroph and methanotroph functional genes/transcripts over time was also investigated with respect to the temporal changes in VC concentrations and other geochemical parameters. We hope to identify the geochemical parameter that could affect the etheneotroph and methanotroph at site, which information would be useful in optimizing the conditions for natural attenuation.

We will also analyze the temporal functional gene and transcript data for correlations with other chloroethenes (PCE, TCE, and cDCE) methane, ethene, and DO concentrations as well as ORP values.

3.2.8.1 *Data requirements*

Currently, the NAS Oceana data set is the most extensive temporal data set of functional gene and transcript abundance from VC-oxidizing bacteria. Additional details concerning the experimental plan are described in Section 5.1 Conceptual Experimental Design.

Samples from three selected NAS Oceana, VA SWMU 2C monitoring wells (MW05, MW19 and MW25) over a six years' time-course from 2008 to 2014, were analyzed for the abundance of functional genes associated with etheneotrophs (*etn*C, *etn*E), methanotrophs (*mmo*X, *pmo*A)*, and anaerobic VC reductive dehalogenase genes (*bvcA* and *vcrA*). RNA samples from the three monitoring wells were analyzed for the abundances of *etn*C, *etn*E, *mmo*X, *pmo*A, *vcrA* and *bvcA* transcripts in 2012, 2013 and 2014. VC and other chlorinated ethene concentration data as well as annual geochemical data (including DO) was obtained from NAS Oceana site investigation reports and provided by a consultant (CH2M).

Groundwater geochemical parameters were measured by YSI Professional Plus handheld multiparameter meter during field sampling (i.e., DO, ORP, pH, temperature). Groundwater methane, VC and cDCE concentration data were also obtained for the analysis. The temporal trend of gene and transcript abundances was analyzed by the Mann-Kendall test.

3.2.8.2   Success criteria

A statistically significant increasing or decreasing temporal trend if the p value of the Mann-Kendall test is less than 0.05. The temporal correlation between VC concentrations and functional gene abundances was investigated by the Kendall rank correlation test. The correlation is considered statistically significant if the p value of the test is less than 0.05.

3.2.9   Determine how qPCR/RT-qPCR data correlates with spatial variations in VC concentration and other geochemical parameters

Determining spatial relationships between VC degrading microorganisms (as estimated by the suite of 6 functional genes) with respect to biogeochemical conditions at contaminated sites can provide important information about the relative roles of different types of VC-degrading bacteria in different portions of the VC plume.

One such relationship that could be revealed is the relative contribution of cometabolic and growth-supporting VC oxidation at a site. For instance, if VC oxidation process is primarily cometabolic then we would not expect there to be a statistical relationship between VC-oxidizer functional gene abundance (a surrogate for cell densities identified by qPCR) and VC concentrations. There could instead be a relationship between VC-oxidizer abundance and the concentration of the primary growth substrate (i.e. methane and/or ethene, assuming electron acceptor and nutrients are not limiting growth). However, if the VC (or VC breakdown product resulting from cometabolism) is toxic to certain VC-oxidizing microbes (such as methanotrophs) then an inverse relationship between VC concentration and VC-oxidizer abundance would be expected.

On the other hand, if the VC oxidation process is growth supporting, then we would expect to observe a positive relationship between VC-oxidizer abundance (etheneotrophs) and VC concentrations. A positive relationship could also exist between VC concentrations and VC-oxidizer abundance if the VC is being reduced to ethene by VC dechlorinators nearby. This would provide a source of ethene as a primary growth substrate for etheneotrophs (again this assumes that nothing else is limiting in the aquifer).

Spatial correlations between VC-degrader functional gene and transcript abundance were tested with additional biogeochemical parameters such as the concentration of the other chloroethenes (PCE, TCE, and DCEs), methane, and ethene, and field-measured parameters (DO, ORP, temp, and pH). For instance, we do not expect that methanotroph functional gene and transcript abundance will positively correlate with VC, but rather with methane and DO levels.

3.2.9.1   Data requirements

Spatial qPCR and RT-qPCR data (i.e., *etnC, etnE, mmoX, pmoA, bvcA,* and *vcrA*) were collected from groundwater and cryo-core sediment samples (qPCR data only) at different locations within a VC plume to provide an overall distribution map of the abundance and activity of aerobic VC-oxidizers.

Geochemical data including DO, ORP, pH and temperature were measured the same time when groundwater samples are taken for microbial analyses with YSI Professional Plus handheld multiparameter meter in groundwater. We also attempted to measure DO, ORP, and pH in the cryo-core sediment samples.

Chlorinated ethenes (PCE, TCE, cDCE, and VC), ethene and methane concentrations were measured in groundwater samples and cryo-core sediment samples

3.2.9.2   Success criteria

In 95 groundwater samples, relationships between VC-biodegradation functional gene/transcript abundance and contaminant and geochemical parameters were determined with:

- Spearman's rank correlation test
- simple linear regression
- multilevel regression. For multilevel regression, each site was considered as level 1, and each monitoring well was considered as level 2.

In 124 cryo-core samples, relationships between VC-biodegradation functional gene/transcript abundance and contaminant and geochemical parameters were determined with:

- Spearman's rank correlation test
- simple linear regression
- censored regression
- Correlations were considered statistically significant if the p value of a test is < 0.05.

3.2.10   Determine relationships between qPCR/RT-qPCR data and estimated bulk VC attenuation

Gene/transcript abundance data generated by qPCR/RT-qPCR indicates the microbial VC oxidation potential and activity in the groundwater. It is important to relate the microbial data with the VC degradation rate to provide lines of evidence that microbes are playing a role in removing VC from the groundwater (e.g. during MNA). Developing relationships between functional gene abundance and/or transcript abundance and the VC degradation rate would help site managers make bioremediation strategy decisions based on molecular data.

Several processes could contribute to the overall VC degradation rate in groundwater (both real and apparent). Simple dilution of the VC plume could lead to drops in VC concentration in monitoring wells over time that could be perceived as degradation. Dispersion and sorption processes could also play a role, although VC is not considered to be very sorptive. VC is subject to both anaerobic dechlorination and aerobic oxidation in groundwater. A combination of processes likely contributes to the overall VC degradation rate, the ratios of which vary from site to site depending on aquifer composition, groundwater flow rates, and the abundance and activity of VC-degrading bacteria. Our working hypothesis is that at many sites anaerobic dechlorination and aerobic oxidation of VC are the dominant VC degradation processes. We further propose that by estimating the abundance and activity of functional genes associated with both aerobic and anaerobic VC that we will see improved correlations with the VC degradation rate estimating from monitoring well data.

3.2.10.1 Data requirements

Bulk VC attenuation rate estimation. There are two approaches to estimating the bulk VC attenuation rate. It can be estimated in separate monitoring wells over a time period. It can also be estimated along a specific transect that corresponds to the flow of groundwater and movement of the VC plume. We collected data for this objective by estimating rates across plume transects.

The bulk VC attenuation rate along a plume transect was estimated with a first order kinetic model. VC concentration data from at least three (but preferable 4 or more) monitoring wells along the groundwater flow path was used in the analysis. When possible, the VC concentration data was normalized to account for dilution by using the total chloride concentration. Total chloride is the sum of ionic chloride and organic chlorine (expressed as Cl) found in VOC contaminants such as the chloroethenes. We assumed the total chloride concentration remained constant in the groundwater and acts as the conservative tracer to normalize measured VC concentrations (equation 1). Total chloride is the sum of ionic chloride and organic chloride found in VOC contaminants such as the chloroethenes. We also accounted for the the minor effects of VC sorption.

$$C_{B\ corrected} = C_B \left(\frac{T_A}{T_B} \right) \quad (1)$$

Where:

T_A: total chloride concentration at point A

T_B: total chloride concentration at point B (downgradient of point A)

$C_{B\ corrected}$: corrected VC concentration at point B

C_B: measured VC concentration at point B

The VC biodegradation rate constant was then estimated by regression analysis of normalized VC concentrations against travel time along the groundwater flow (equation 2) (Wiedemeier, 1998). This required the use of previously reported seepage velocities and retardation coefficients, when available, to estimate the plume travel time.

$$C_{B\ corrected} = C_A\ e^{-\lambda t}$$

Where:

$C_{B\ corrected}$: corrected VC concentration at point B

C_A: measured VC concentration at point A

λ: first-order biodegrading rate

t: travel time of VC between point A and point B

This approach was also used to determine ethene and methane degradation rates in the VC plume as important relationships between these rates and trends in VC degradation functional gene and transcript abundance could be revealed, though the primary goal was to assess bulk VC attenuation rates.

qPCR/RT-qPCR data. Gene and transcript abundance of functional genes associated with VC degradation were calculated and reported as genes/transcripts per L groundwater. These included aerobic VC degradation genes from methanotrophs and etheneotrophs that have been previously described (i.e. *etnC, etnE, pmoA* and *mmoX*). We also quantified the presence and functionality of anaerobic VC dechlorinators in samples by analyzing their functional genes and transcripts (*vcr*A and *bvc*A) with published primer sets (Krajmalnik-Brown, *et al.*, 2004, Müller, *et al.*, 2004). The costs for these analyses were tracked.

The bulk VC attenuation rate along the groundwater flow path was calculated with data obtained from each distinct sampling event. It is important to monitor the change of VC attenuation rate and the change of functional gene and transcript abundances at the same time, which will help reveal the contributions of aerobic VC degrading microbes during VC degradation.

3.2.10.2   Success criteria

The relationship between spatial bulk VC attenuation rates and functional gene and transcript abundances was investigated with a multilevel categorical regression model.

Because of uncertainties in the quantitative value of bulk VC attenuation rates, each site was assigned to a categorical rate group (high rate attenuation or low rate attenuation group) based on estimated bulk VC attenuation rate and other geochemical parameters.

The relationship was considered significant if the p value of categorical regression is less than 0.05.

3.2.11   Determine relationships between etheneotroph functional genes and the VC biodegradation rate in VC-oxidizing laboratory enrichment cultures

3.2.11.1   Data requirements

VC oxidizing enrichment cultures must be established from one or more groundwater samples collected from sites evaluated during this project. VC depletion curves must be generated in batch experiments and fit to Michaelis-Menton enzyme kinetics to determine maximum substrate depletion rates and half-velocity constants. DNA samples must also be collected from these experiments and total 16S rRNA and etheneotroph functional gene concentration must be quantified by qPCR.

3.2.11.2   Success criteria

Demonstrate that etheneotroph functional genes can serve as a specific measurement of ethneotroph biomass in a mixed culture. Show that the rate of VC oxidation is proportional to etheneotroph functional gene concentration, and that VC oxidation rates can be adequately described by Michaelis-Menton enzyme kinetics when functional gene concentrations are used as the biomass concentration.

Page Intentionally Left Blank

4.0   SITE DESCRIPTIONS

In this demonstration, we focused on the two VC plumes at MCRD Parris Island Site 45. Pertinent information about other sites included in this project (e.g. NAS Oceana SWMU 2C) are described in Section 5.0.

4.1   SITE SELECTION

Early in this demonstration we aimed to identify VC-contaminated DoD sites where the geochemical conditions favor the occurrence of aerobic microbial VC oxidation. The criteria used for the site selection was as follows:

1. The presence of a groundwater VC plume
2. The presence of dissolved oxygen in the contaminated groundwater that can support the VC oxidation (although anoxic and anaerobic sites were also considered)
3. The availability of chlorinated ethene concentration data and other geochemical data from previous site investigations.
4. The presence of substrates that can support the growth of aerobic VC-oxidizers and the co-metabolism of VC oxidation, such as ethene and methane.
5. The absence of other contaminants that may inhibit the growth and activity of aerobic VC oxidizers.
6. An established monitoring well system.
7. The abundance and activity of aerobic VC-oxidizers (etheneotrophs and methanotrophs) based on initial qPCR/RT-qPCR analyses.

Based on the above criteria, we identified MCRD Parris Island Site 45 as the primary site for this demonstration. MCRD Parris Island Site 45 is a chloroethene-contaminated site that contains two VC plumes with concentrations ranging as high as ~50,000 ppb. Field measured DO levels are generally low (<1 mg/L). Previous site investigations have revealed that ethene is present at the µg/L level in many parts of the site, while methane was found in mg/L levels.

According to our initial qPCR results, etheneotroph functional genes were relatively abundant at several locations in the two VC plumes. Interestingly, etheneotrophs were more abundant where VC concentrations were high, indicating the possibility that VC supported the growth of etheneotrophs. Furthermore, Parris Island is interlaced by several tidal creeks. The incoming tidal water moves into the site 45 storm sewer system and could potentially provide extra DO to support VC oxidation. Additional detailed information about MCRD Parris Island Site 45 is provided in the section 4.2, 4.3, and 4.4.

4.2   SITE LOCATION AND HISTORY

MCRD Parris Island is a military training site located along the southern coast of South Carolina, covering approximately 8,047 acres that consist of dry land, salt marshes, saltwater creeks, and ponds (**Figure 6**). Site 45 previously contained a dry-cleaning facility which began operations in the 1950s. In 1988, four above-ground storage tanks were installed along the northern side of the dry-cleaning facility to replace the underground storage system (**Figure 7**).

Sometime in March 1994, an accidental PCE spill occurred at the dry-cleaning facility. One of the above-ground storage tanks was overfilled and unknown amount of PCE was released into the environment, resulting in a groundwater plume (known as northern plume) downgradient from the area of those storage tanks. Multiple smaller chlorinated solvent spills also occurred in 1995 near the storage tanks.

In late 1997, the dry-cleaning facility was moved to a new location nearby and switched to hydrocarbon-based cleaning solvent that contained no chlorinated ethenes. The former dry-cleaning building, storage tanks, and other related structures were demolished and removed from the site in 2001.

Investigations in 2005 and 2006 showed a second groundwater contamination plume of chlorinated solvents (known as the southern plume), which appears to originate from the new dry-cleaning facility. However, based on engineering blueprints, flow testing, and video imaging of sanitary sewers at the site, it is believed that the source of the southern plume is leakage from an abandoned sanitary sewer line in the vicinity of the new dry-cleaning facility (TetraTech, 2012).

Efforts have been made to reduce the contamination in both the groundwater and the storm water system. After the 1994 spill, some contaminated soil was excavated and removed from the site. A pump and treat system was installed in 1998 to provide some hydraulic containment of groundwater contamination, but high concentrations of dissolved iron in the groundwater led to fouling problems and the pumping operations were discontinued in 2000 (USEPA, 2010). Monitoring wells were installed to screen the upper (normally 7-9 ft bgs) and lower (normally 15-16 ft bgs) surficial aquifers and site investigations have been performed to characterize the contaminant distribution. Chlorinated ethene (including PCE, TCE, cDCE and VC) concentrations have been monitored in many of the monitoring wells on a regular basis since 2005.

In 2006, an ESTCP field demonstration study of emulsified zero-valent iron (EZVI) was performed in the DNAPL source area of the north plume and showed significant reductions in mass flux of PCE, TCE, and cDCE with increases in VC and ethene mass flux (Krug, 2010). This led to the installation of the PMW and ML monitoring wells in that area of the plume that are available for sampling in this project. A pilot study of in situ chemical oxidation (ISCO) is being conducted in the southern plume, while an in situ biostimulation and bioaugmentation pilot study is planned for the northern and southern plumes. Subsequent full-scale remediation will be selected based on the pilot studies (Churchill, 2013).
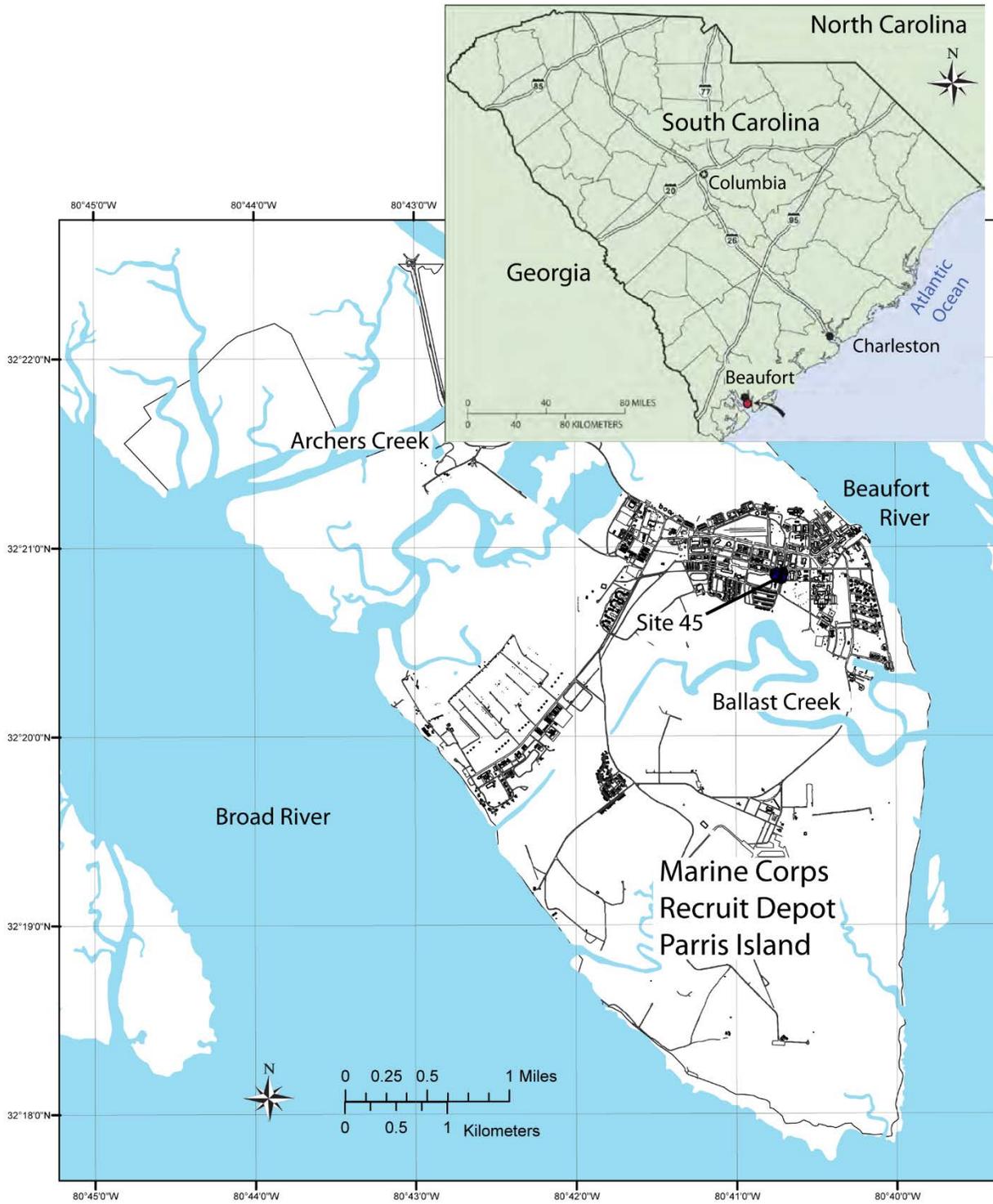
Figure 6.   Location of MCRD Parris Island Site 45 (Vroblesky, 2009).
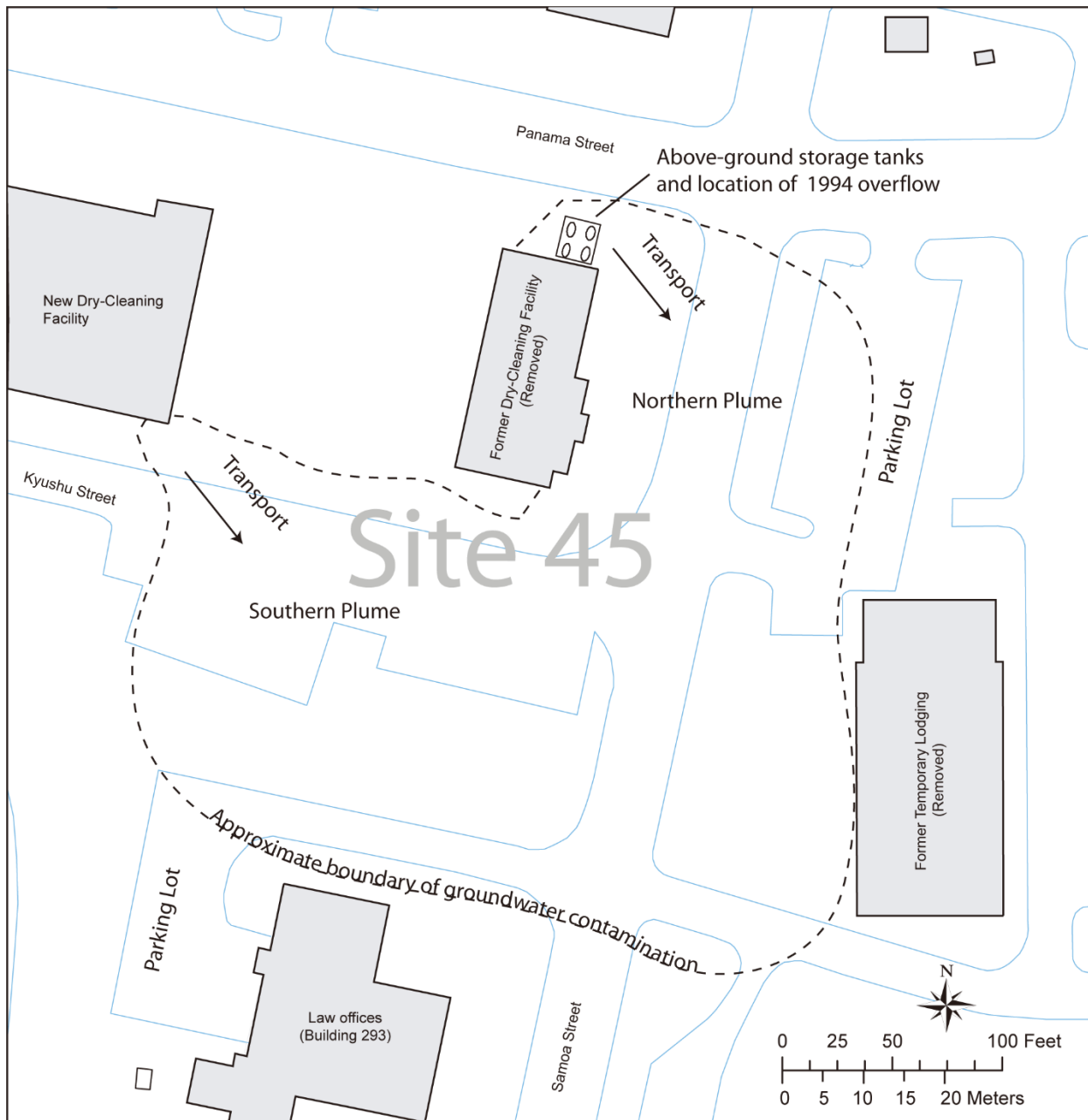
Figure 7.   Location of the Former and Current Dry-cleaning Facility at Site 45, MCRD Parris Island (Vroblesky, 2009).

4.3   SITE GEOLOGY/HYDROGEOLOGY

4.3.1   MCRD Parris Island Site 45 geology

The shallow subsurface lithology of Site 45 consists of a heterogeneous mixture of Pliocene- to Holocene-age sediments of the Pamplico and Waccamaw Formations to a depth of approximately 17 feet, consisting primarily of fine sand and silty sand with a few discontinuous clayey sand seams (Vroblesky, 2009, TetraTech, 2012).

Below the shallow sandy sediments is a thin layer of peat at depths from 17 to 21 feet below ground surface (bgs), which is a complex mixture of sand, silt, and clay with a substantial amount of black to brown organic material. The peat was directly underlain by a 3- to 6-foot-thick clay unit at the depth of 18 to 27 feet bgs. Below the peat and clay layer is the unconsolidated deposits consisting primarily of sand, clayey sand, and silty fine sand with traces of shell fragments. The Miocene-age Hawthorn Formation, a regional confining unit, is expected to directly underlie these deposits, below which is a Floridan aquifer (Vroblesky, 2009, TetraTech, 2012).

4.3.2   MCRD Parris Island Site 45 hydrology

The surficial aquifer underlying Site 45 consists of the sandy Pliocene to Holocene sediments to an average depth of approximately 18 feet. In general, the water table encountered within these heterogeneous sediments is shallow and is typically encountered at a depth of 3 to 4 feet bgs at the site (TetraTech, 2012).

In both northern and southern plumes, the overall groundwater flow direction in the aquifer is from northwest to the south-southwest, where the plumes are intercepted by leaky storm sewers (**Figure 8**). The storm sewer system connects to tidally influenced Ballast Creek, and the tidal cycles could affect the contaminant distribution and degradation in the groundwater near the storm sewers. At low tide, the groundwater levels tend to be higher than water levels in the storm sewers, when contaminants including VC can potentially enters the storm sewer system. At high tide, the water levels in the storm sewers tend to be higher than the groundwater levels and the tidal water could move from the storm sewers to the aquifer at least as far as to Site 45 (Vroblesky, 2009, TetraTech, 2012). The dissolved oxygen brought by the incoming tidal water could potentially support the aerobic VC oxidation.
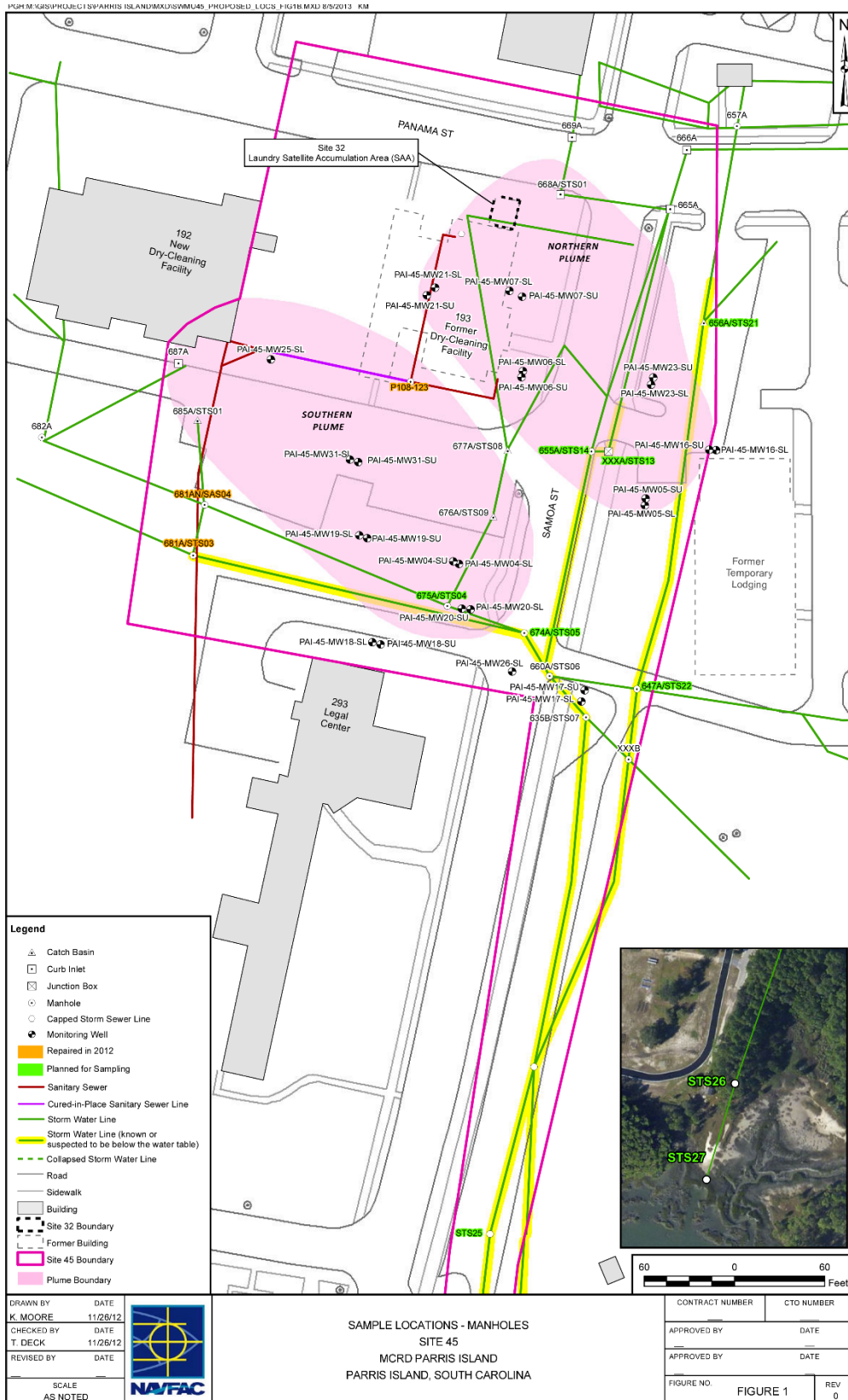
Figure 8. Location of VC Plumes and Storm Sewer System at Site 45 (Churchill, 2013).

4.4   CONTAMINANT DISTRIBUTION

The primary contaminants of concern in the northern and southern plumes at MCRD Parris Island Site 45 are PCE, TCE, cDCE, and VC. VC is generated from incomplete PCE dechlorination as the groundwater migrates southeastward. Site investigations have shown significant decrease in PCE and TCE in the groundwater, with concentrations decreasing from as high as approximately 500-700 ppb to less than 10 ppb or to non-detect levels. VC also decreased, but to a lesser extent than PCE and TCE, while cDCE concentrations remained relatively stable or increased slightly in the groundwater. The relative persistence of VC and cDCE in groundwater is possibly because of the less efficient microbial dechlorination than PCE and TCE. However, the fact that VC and cDCE did not accumulate in the groundwater indicates the occurrence of their degradation possibly through anaerobic dechlorination and/or aerobic oxidation.

The upper and lower surficial aquifers are different in the contaminant distribution, according to a 2012 survey (TetraTech, 2012). At that time, PCE and TCE concentrations were much higher in the lower surficial aquifer, in both the northern and southern plumes. In contrast, VC and cDCE were more abundant in the upper surficial aquifer. The specific contaminant distribution patterns in upper and lower surficial aquifers is possibly because of the different degradation and transportation pathways of different contaminants.

4.5   OTHER SITES USED IN THIS DEMONSTRATION

Although site 45 was the primary site for this demonstration, samples and data from other VC-contaminated sites were crucial for this demonstration. Pertinent information about these sites is provided in Section 5.1 as necessary.

Page Intentionally Left Blank

5.0   TEST DESIGN

5.1   CONCEPTUAL EXPERIMENTAL DESIGN

Molecular tools (i.e. qPCR) for quantifying potential VC-oxidizers in groundwater have been available for some time (for methanotrophs) and since 2010 (for etheneotrophs). More recently, we published an article describing the RT-qPCR method for etheneotrophs and methanotrophs that was developed under SERDP ER-1683 (Mattes*, et al.*, 2015). A field-scale demonstration of RT-qPCR methods described in the literature (for etheneotrophs, in particular) is crucial in establishing relationships between VC concentrations and attenuation rates (and possibly other geochemical parameters) and VC-oxidizer abundance and activity. These relationships will be useful for obtaining lines of evidence for MNA of VC plumes. This could impact remedial outcomes by accelerating regulatory acceptance of MNA for addressing VC plume remediation and eventually reducing overall life-cycle costs for clean-up.

Therefore, the broadest aspect of our conceptual experimental design was to apply qPCR technology for VC-oxidizers to a diverse range of DoD sites where VC plumes are present. We expected this approach to reveal that VC oxidation pathways are potentially relevant at many more sites than currently appreciated. We have indicated several sites containing VC plumes where qPCR for etheneotrophs can be applied over the course of this project: NAS Oceana, VA SWMU 2C, NSB Kings Bay, GA Site 11, MCRD Parris Island, SC Site 45, NWS Seal Beach, and Altus AFB, OK.

We sought to apply our RT-qPCR methods for VC-oxidizers at one or more sites in a more intensive manner in this demonsration. The goal of this phase of the demonstration was to develop statistical relationships between the abundance and activity of VC-oxidizers with VC concentrations and ideally VC attenuation and /or degradation rates, as well as other parameters such as DO, ethene, and methane concentrations. To achieve these goals required determining temporal and spatial distribution of VC-oxidizers in the groundwater (and ideally sediment as well) with respect to VC concentrations and other pertinent geochemical parameters measured in the groundwater. For each qPCR and RT-qPCR experiment, the information about the PCR efficiency, accuracy, precision, and sensitivity was collected for the evaluation of quantitative performance objectives described in Section 3.0.

5.1.1   Sites included in the experimental design

5.1.1.1   NAS Oceana, VA SWMU 2C

This site was selected for investigating long-term temporal trends in the abundance and activity of VC-oxidizers in a dilute VC plume. The abundance and activity of both etheneotrophs and methanotrophs in three monitoring wells (MW05, MW19 and MW25) from 2008 to 2014 was determined with respect to VC concentrations. Despite this and other disadvantages (e.g. lack of ethene concentration data), this data set currently represents the longest time series where we have collected and analyzed DNA and RNA samples for RT-qPCR analysis.

5.1.1.2   NSB Kings Bay, GA site 11.

Groundwater at Site 11 was contaminated primarily by chlorinated volatile organic (i.e. PCE, TCE, DCEs, and VC) and BTEX compounds (benzene). VC concentrations in several monitoring wells at site 11 have exhibited a downward trend over the past ten years and were about 0.5 - 10 µg/L in 2011. The DO and ORP data suggests an anoxic environment in the monitoring wells (DO < 1 mg/L and negative ORP). Ethene data was not available for this site but methane was detected between 0-8 mg/L. In several ways, this VC plume has similar characteristics to the dilute VC plume at NAS Oceana, except that the clean-up remedy at this site included in situ chemical oxidation. We obtained Site 11 DNA samples (2013 sampling event) from monitoring wells USGS-01, 02, 04, 05, 10, 11 and KBA-11A, KBA-11-13A, KBA-11-34 from Frank Loeffler's lab. We also coordinated with Mike Singletary for the collection of additional samples for both DNA and RNA analysis in January 2015.

5.1.1.3   MCRD Parris Island, SC Site 45

This site was selected for exploring both spatial and temporal distribution of aerobic VC-oxidizers in two relatively more concentrated VC plumes. In the first stage of sampling we aim to obtain an overview of the abundance and activity of aerobic VC-oxidizers at the site. The second stage of sampling plan is quarterly sampling over a two-year time course for selected monitoring wells for the investigation of spatial and temporal trend of the abundance and activity of VC oxidizers.

5.1.1.4   NWS Seal Beach Site 70, CA

This site was selected as an alternate site featuring moderately high VC concentrations and evidence of increasingly oxidizing conditions in several portions of the VC plume. This TCE plume has been undergoing enhanced reductive dechlorination for several years (hence the generation of the VC plume). The hydrogeology is fairly complex with the source zone being relatively shallow, with the plume diving down through layers (First sand, second sand, shell horizon and deep sand). Despite the depth of the VC plume, the proximity of this site to the ocean could explain why oxidizing conditions are on the upswing.

5.1.1.5   Joint Base Pearl Harbor/Hickam, HI site LF05

This site was selected because the site features VC concentrations upwards of 1000 ppb or more in portions of the plume. This site thus represents the most concentrated VC plume at a DoD site that we have had the opportunity to apply qPCR/RT-qPCR methods for VC-oxidizers. We were interested in this site mainly for the potential for VC-assimilators to be present and to provide support for correlations between etheneotroph functional genes and VC concentration.

5.1.1.6   Altus AFB, OK

The VC plume at Altus AFB ranges in concentration from 51 – 650 ug/L. As of June 2013, there was also methane present, but apparently very little ethene. Detailed description of the Parris Island site is provided in Section 4.0.

5.2   BASELINE CHARACTERIZATION ACTIVITIES

Baseline characterization activities at most sites involved communicating with NAVFAC personnel, RPMs, their contractors or the literature to acquire groundwater field parameters, chlorinated ethene concentrations and other geochemical data from recent previous site characterization and monitoring events. In some cases, we coordinated with Mike Singletary of NAVFAC to obtain archived DNA samples collected at several sites including Parris Island site 45. This baseline characterization data is presented in Section 5.6.

5.3   DESIGN AND LAYOUT OF TECHNOLOGY COMPONENTS

For each site, the selection of monitoring wells was based on the VC contamination situation and geochemical parameters, which will be provided by site managers. Ideally each site would include groundwater samples from at least three monitoring wells at different locations within the VC plume and from one background well that is away from the VC plume. We also collected data about each qPCR experiment to confirm the accuracy, precision and robustness of this technology during the demonstration.

The sampling equipment included a Geopump Peristaltic Pump Series I with easy-load I pump head or low flowrate groundwater sampling. A YSI Professional Plus handheld multiparameter meter was used to measure DO, pH, ORP, and conductivity of the pumped groundwater before the groundwater passes through the Sterivex filter. The probes were inserted into a flow-through cell to facilitate these parameter measurements. The sampling equipment set-up is shown in **Figure 9**. A close-up of the fittings used to connect the Sterivex filter is shown in **Figure 10**.
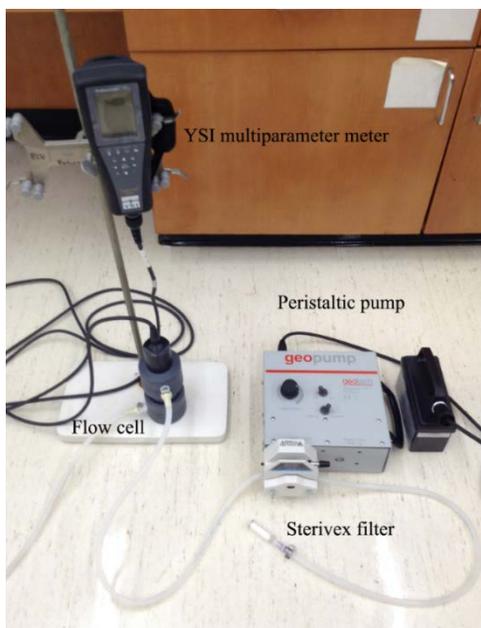
Figure 9.   Groundwater Sampling Equipment Set-up
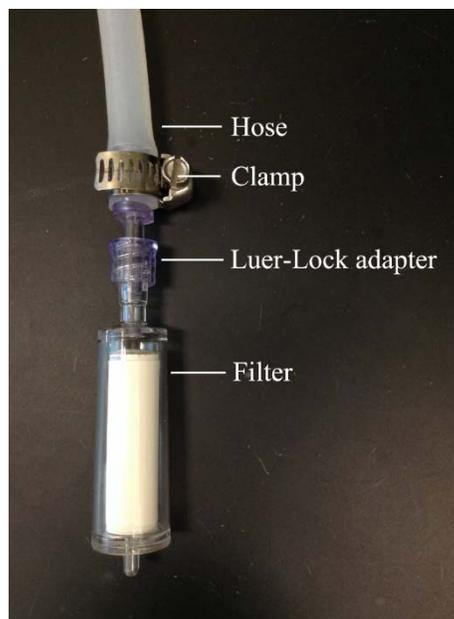
Figure 10. Close-up of the Fitting Used to Connect the Hose to the Sterivex Filter.

Once groundwater samples were collected, they were shipped back to the laboratory for DNA/RNA extraction and qPCR testing as described in Section 2.1.

5.4   FIELD TESTING

Groundwater sampling via low flow purge methods and collection of groundwater biomass onto Sterivex filters are fairly standardized procedures. Thus, no field testing of these components of the technology was necessary other than what was required for our site technicians to become accustomed to operating the equipment. Existing core samples and monitoring well installation records were utilized to determine possible locations for the cryo-cores.

In terms of sampling handling and preservation procedures, we used protocols consistent with those recommended by SERDP ER-1561 (https://www.serdp-estcp.org/Program-Areas/Environmental-Restoration/Contaminated-Groundwater/Monitoring/ER-1561/ER-1561/%28modified%29/06Oct2014). Briefly, we collected groundwater biomass onto sterile Sterivex filters. RNA preservative was added in the field to filters intended for RNA extraction. Filters were immediately placed at 4°C and shipped back to the lab by overnight courier.

When Sterivex filter samples were received in the lab, efforts were to extract RNA immediately and this took priority over Sterivex filters intended for DNA extraction. If Sterivex filter samples for DNA could not be processed immediately, they were stored no longer than 2 weeks at -80°C prior to extraction.

5.5   SAMPLING PLAN AND SAMPLING METHODS

5.5.1   Sampling from diverse VC-contaminated DoD sites

As described in Section 5.1, an objective of this demonstration was to obtain groundwater samples from as many VC-contaminated DoD sites and VC plumes as practical. In most cases (with the exception of Parris Island Site 45) we obtained samples during groundwater sampling events where other geochemical and contaminant data were also collected by another contractor. For each sampling event, monitoring wells were selected when possible based on previous VC concentration and other geochemical parameters (e.g. ethene and methane concentration) as discovered during our baseline characterization activities. In these situations, a cooler containing Sterivex filters, Falcon tubes, syringes, RNAlater solution, and ice packs was shipped to the contractor. Following sampling, Sterivex filters were subsequently stored on ice and shipped back to the Mattes lab via overnight FedEx for DNA and RNA extraction and subsequent qPCR and RT-qPCR analyses.

5.5.1.1   NAS Oceana SWMU 2C

We acquired samples from three monitoring wells (MW05, MW19, MW25) at NAS Oceana SWMU 2C at multiple sampling events between 2008 and 2014 in coordination with Laura Cook from CH2M in Virginia Beach, VA. Samples for both RNA and DNA were collected from these monitoring wells from 2012-2014. All samples coincided with long-term groundwater monitoring activities, yielding a significant amount of geochemical and contaminant data to analyze along with the biological data. The collection of geochemical and molecular data from this site facilitated tracking long-term trends in VC-oxidizer abundance and activity in a dilute VC plume that is undergoing MNA. We discontinued sampling from this site as of the October 2014 event.

5.5.1.2 NSB Kings Bay site 11

Our baseline characterization analyses from this site were performed in collaboration with Frank Loeffler's lab. They had received groundwater samples from a 2013 sampling event and performed qPCR for *Dehalococcoides* 16S and three reductive dehalogenase genes (*tceA, bvcA*, and *vcrA*). The remaining DNA was shared with us and we subsequently performed qPCR for VC-oxidizing bacteria. The initial data led us to obtain groundwater samples in January 2015 in coordination with Mike Singletary (NAVFAC). This was the only sampling event at this site for this project.

5.5.1.3 NWS Seal Beach site 70

Groundwater biomass samples were collected by Mattes lab personnel in July 2015 and December 2015. At this site, the contractor Insight Environmental (IE) was the contractor for long-term groundwater monitoring for VOCs. We negotiated with the RPM (Pei-fen Tamashiro) in coordination with IE staff to obtain groundwater samples without disrupting their activities. The executed monitoring well sampling plan for the July 2015 and December 2015 events is shown in **Table 5**. Site 70 is a particularly complex site, with several biobarriers installed. The July 2015 samples were selected based on available VC and DO data discovered during baseline characterization activities. We attempted to collect samples such that the source zone was represented, and some wells located upgradient of the second sand biobarrier were also represented. This led to our additional wells (PMW01A and B, and PMW13A and B) being sampled in Dec. 2015, which provided a transect of the VC plume over a considerable distance at the site.

We attempted to collect samples such that the source zone was represented, and some wells locates upgradient of the second sand biobarrier were also represented. This led to our additional wells (PMW01A and B, and PMW13A and B) being sampled in Dec. 2015, which provided a transect of the VC plume over a considerable distance at the site.

Table 5.   Executed Sampling Plan for Seal Beach Site 70

	Location	Well depth, ft	VC 2015 Jul	2015 Jul	2015 Dec
Source area treatment grid	MW-70-27	25.5 - 35.5	400		
	MW-70-28	50.3 - 60.3	2000		
	MW-70-28 - Dup	50.3 - 60.3	2000		
	MW-70-PMW01A	25 - 35	39		X
	MW-70-PMW01B	45 - 55	1300		X
Source area biobarrier	IW-70-SAB06	65 - 80	1.2		
	MW-70-PMW03A	70 - 80	0.99		
	MW-70-PMW03B	90 - 100	110		
First sand biobarrier 1	IW-70-FSB118	60-105	3.4		
	IW-70-FSB108	60 - 105	1.7		
	MW-70-38	80 - 100	95	X	X
	MW-70-PMW04A	70 - 80	98		
	MW-70-PMW04B	90 - 100	130		
	MW-70-PMW04B - DUP	90 - 100	130		
	MW-70-PMW05A	70 - 80	97	X	X
	MW-70-PMW05B	90 - 100	330		
	MW-70-PMW06A	69.5 - 79.5	1100	X	X
	MW-70-PMW06B	91 - 101	7.8		

Table 5. Executed Sampling Plan for Seal Beach Site 70 (Continued)

	Location	Well depth, ft	VC 2015 Jul	2015 Jul	2015 Dec
Shell horizon biobarrier 1	IW-70-SHB113	105 - 130	280		
	MW-70-PMW09	120 - 130	0.28		
	MW-70-PMW09 - DUP	120 - 130	0.27		
	MW-70-PMW10	120 - 130	190	X	X
First sand biobarrier 2	IW-70-FSB216	65 - 100	0.2		
	MW-70-PMW07A	65 - 75	1.5		
	MW-70-PMW07B	85 - 95	170		
	MW-70-PMW08A	65 - 75	96		
	MW-70-PMW08B	85 - 95	370	X	X
Shell horizon biobarrier 3	MW-70-PMW11A	85 - 95	65		
	MW-70-PMW11B	115 - 125	20		
	MW-70-PMW12A	85 - 95	23	X	X
	MW-70-PMW12B	115 - 125	290	X	X
Second sand biobarrier	IW-70-SSB119	125 - 165	0.2		
	MW-70-14	160 - 170	6.2	X	X
	MW-70-49	125 - 165	0.4		
	MW-70-PMW13A	125 - 135	200		X
	MW-70-PMW13A-DUP	125 - 135	240		
	MW-70-PMW13B	145 -155	15		X
	MW-70-PMW14A	128 - 138	120	X	X
	MW-70-PMW14B	149 - 159	120	X	X

5.5.1.4 *Joint Base Pearl Harbor/Hickam site LF05*

Baseline characterization with qPCR was conducted with archived 2014 DNA samples obtained from Microbial Insights, Inc. in coordination with Mike Singletary (NAVFAC). After these baseline activities showed promising data, we contracted with Environmental Science International, Inc. (ESI) to collect filter samples from groundwater monitoring wells (FS-MW-01, FS-MW-02, TS-MW-13, TS-MW17, and TS-MW-20) on a portion of Hickam Field Site LF05 in September 2015, December 2015, March 2016, and September 2016. All of these wells are located in the immediate vicinity of the bioreactor remediation system installed at the site. The sample collection was performed concurrently with scheduled groundwater monitoring and sampling events at the site that are already contracted by the Department of the Navy (DoN) to be performed by ESI. These 5 wells were the only ones being sampled during these events. Thus, under this contract we expect to obtain Sterivex filter samples from 5 monitoring events and have access to the VOC and geochemical data that is concurrently collected by ESI.

As part of the DoN sampling program, the annual groundwater sampling of 21 wells at Site LF05 occurred in March 2016. For the March 2016 sampling event, the following wells were sampled: TS-MW-18, MW40, MW42, MW52, MW53, and MW64. These wells, which are different than the wells samples in 2015, were chosen to cover two VC plume transects. Supplemental sampling of 5 wells at Site LF05 (FS-MW-01, FS-MW-02, TS-MW-13, TS-MW17, and TS-MW-20) occurred in September 2016.

5.5.1.5 Altus AFB biowalls

In accordance with ESTCP ER-210429 (PI Travis McGuire, GSI Environmental) groundwater samples were collected at Altus AFB in early May 2015. This project is assessing the effectiveness of existing biowalls to remove TCE from the groundwater. Groundwater monitoring data indicates that VC was accumulating in several of the wells downgradient of the well. Historically these wells were slightly aerobic, thus there was the possibility that VC-oxidizers are present and active in this area of the aquifer and could be contributing to natural attenuation of VC. We coordinated with Travis to obtain filters for DNA and RNA analysis from 3 wells BB04D, BC07D, BE09D, all of which are downgradient of the 3 different biowalls and contain 20-100 ug/L VC (the upgradient wells did not generally contain VC). In addition, GSI Environmental obtained QuantArray analyses. This facilitated a comparison of the results of our qPCR analyses with those of the QuantArray.

5.5.1.6 Naval Air Station North Island (NAS NI) Site 9

We first obtained groundwater from this site rather late in the project (June 2017) so it was not included in the original experimental design. This was the result of communications with Michael Pound, the RPM at NAS NI and Neal Durant at Geosyntec. The chlorinated ethene plume at Site 9 is moving towards and underneath San Diego Bay. VC has been noted in several of the monitoring wells on the site. This site is somewhat unique in that there is a saltwater/fresh water interface, raising the possibility that there are etheneotrophs present that could degrade VC under saline conditions. This is poorly understood in general.

5.5.2 Groundwater sampling at Parris Island Site 45

Parris Island site was the primary site of interest for this demonstration. DNA from 2013, 2014, and 2015 sampling events at this site was shared with us by Microbial Insights in coordination with Mike Singletary at NAVFAC for use in baseline characterization activities. Initial qPCR results indicated that etheneotrophs and methanotrophs were relatively more abundant at this site than any of the DoD sites we have tested previously. We also observed an interesting pattern for etheneotroph functional genes, which were more abundant in the monitoring wells where VC concentrations were also relatively higher. Therefore, the Parris Island site was selected for a more detailed investigation of spatial and temporal patterns in VC-oxidizer abundance and activity with respect to VC contamination and geochemical parameters.

Groundwater was sampled by Mattes lab personnel with a Geopump Peristaltic Pump Series I with easy-load I pump head for low flowrate groundwater sampling following the instruction of USEPA/540/S-95/504 low-flow purge procedures (USEPA, 1996). Geochemical properties of the groundwater including DO, ORP, pH and conductivity was monitored at the same time by a YSI Professional Plus handheld multiparameter meter with a flow-through cell for the probes After DO, ORP, pH and conductivity readings are stable, up to 3 liters of groundwater was passed through the Sterivex-GP 0.22 µm membrane filter cartridges. For filters for RNA analysis, 3 ml of RNAlater was passed through the filter following sampling by a sterile syringe. Sterivex filters were then placed in sterile Falcon tubes and immediately stored on ice (about 4ºC). Filters were handled and shipped to the lab as described in Section 2.1.1.1. Upon receipt in the lab, DNA and RNA was extracted as described in Section 2.1.1.2.

According to **Figure 11** there are at least 57 distinct monitoring wells at site 45, located in northern and southern plumes. The ML and PMW wells are located in the "source zone" of northern plume, they are high in VC concentrations (1000-10000 µg/L in 2015). According to the 2015 data, VC concentrations in northern plume is 10~100 µg/L.

Wells sampled in October 2015 are depicted in **Figure 11** and listed in **Table 6**.
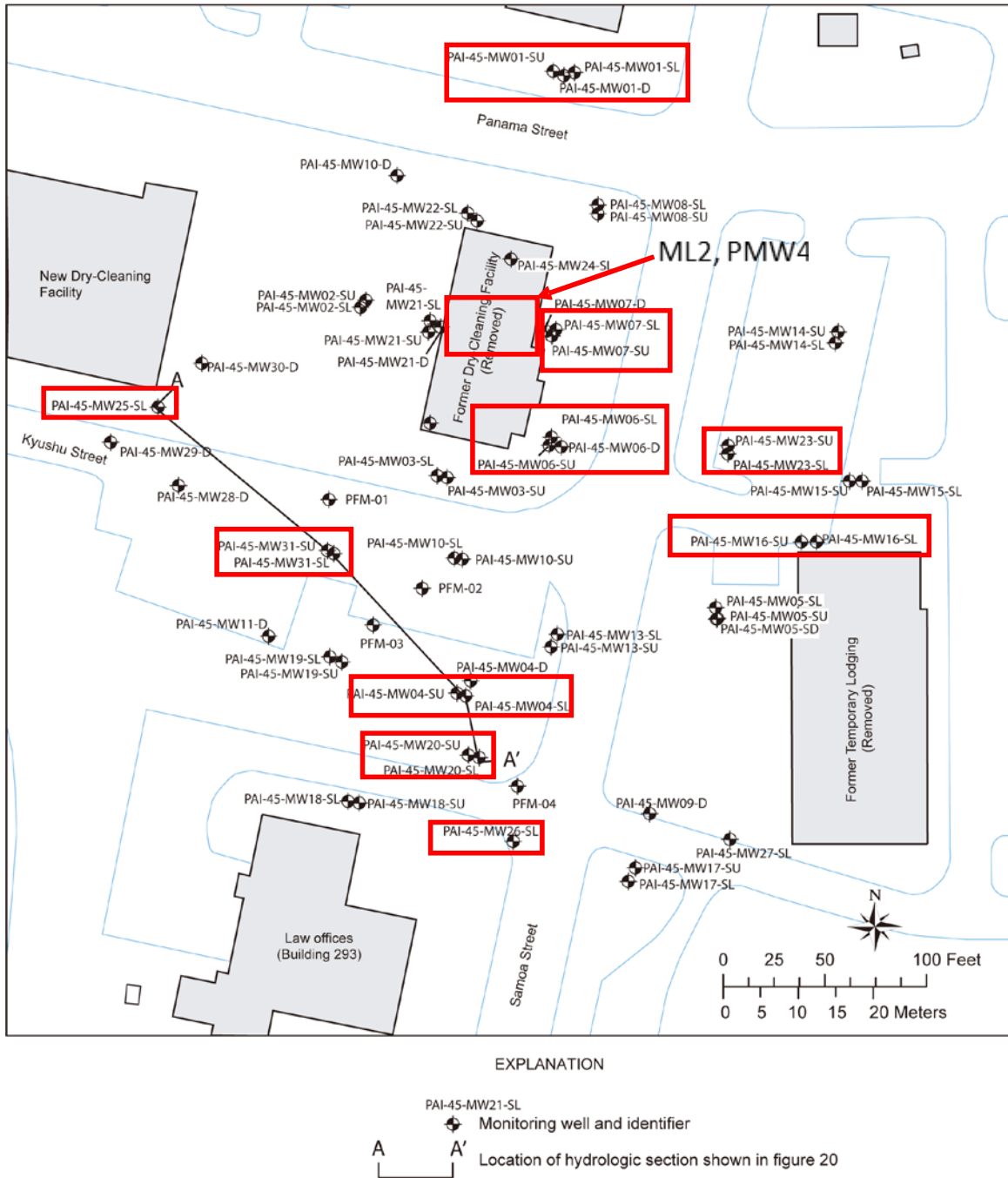
Figure 11. Monitoring Well Locations at Parris Island (red boxes).

Table 6. Parris Island Groundwater Sampling Plan Worksheet (as executed)

	Monitoring well	Oct. 2015	June 2016
Background	PAI-45-MW01-SL/SU	●	●
	PAI-45-MW02-SL/SU	▪	▪
Northern plume source zone	ML-1	▪	▪
	ML-2	●	●
	ML-3	▪	▪
	ML-4	▪	▪
	ML-5	▪	▪
	ML-6	▪	▪
	ML-7	▪	▪
	PMW-1	▪	▪
	PMW-2	▪	▪
	PMW-3	▪	▪
	PMW-4	●	●
	PMW-5	▪	▪
	PMW-6	▪	▪
Northern plume	PAI-45-MW05-SL/SU	▪	▪
	PAI-45-MW06-SL/SU	●	●
	PAI-45-MW07-SL/SU	●	●
	PAI-45-MW08-SL/SU	▪	▪
	PAI-45-MW14-SL/SU	▪	▪
	PAI-45-MW15-SL/SU	▪	▪
	PAI-45-MW16-SL/SU	●	●
	PAI-45-MW21-SL/SU	▪	▪
	PAI-45-MW22-SL/SU	▪	▪
	PAI-45-MW23-SL/SU	●	●
Southern plume	PAI-45-MW03-SL/SU	▪	▪
	PAI-45-MW04-SL/SU	●	●
	PAI-45-MW10-SL/SU	▪	▪
	PAI-45-MW13-SL/SU	▪	▪
	PAI-45-MW17-SL/SU	▪	▪
	PAI-45-MW18-SL/SU	▪	▪
	PAI-45-MW19-SL/SU	▪	▪
	PAI-45-MW20-SL/SU	●	●
	PAI-45-MW25-SL	●	●
	PAI-45-MW26-SL	●	●
	PAI-45-MW27-SL/SU	▪	▪
	PAI-45-MW31-SL/SU	●	●

5.5.3   Aquifer sediment sampling at Parris Island site 45

The spatial distribution and temporal activity of VC-oxidizers are not necessarily uniform in the aquifer. There might be "hot spots and hot moments" of VC oxidation in certain parts of the plume that would be missed by cursory groundwater sampling efforts from monitoring wells. Improved understanding of the spatial variations in VC-oxidizers would be helpful for site managers seeking to collect lines of evidence for VC oxidation. Additional helpful delineation of the spatial distribution can be achieved by analysis of sediment core samples. In light of recent preliminary data from this project, the spatial proximity of VC-oxidizers to VC dechlorinators (i.e. certain *Dehalococcoides)* could provide useful information to site managers. For instance, this information could facilitate decision-making about sampling for MNA or possibly targeting amendments for enhanced MNA. The cryogenic core collection technology (Johnson*, et al.*, 2013) is promising with respect to collecting samples that allow us to determine the abundance and activity of VC-oxidizers in the subsurface, since RNA will be preserved under the cryogenic conditions.

We completed the cryo-core sampling event in June 2016. Four boreholes were sampled at the site along a transect in the northern chlorinated ethene plume (**Figure 12**). Soil cores were collected from the site using a hollow-stem auger and drill rig modified for cryogenic freezing with liquid nitrogen, as previously described (Kiaalhosseini*, et al.*, 2016). Frozen sediment cores were collected in lifts of approximately 4 ft until the rig advanced to a maximum depth of 20 ft bgs, which encompassed the entire vertical extent of the surficial aquifer. Each lift was returned to the surface and sectioned. Briefly, the top soil (0-2 ft bgs) from each core was discarded. Starting at the top of each lift, a one-inch long section was cut off with a miter saw, creating a sample "puck". The following five-inch section was also cut. This pattern was repeated for the length of each lift, resulting in approximately 35 "puck" samples per borehole. Some of the lifts had incomplete recovery, resulting in slightly fewer samples than anticipated. A total of 124 samples were collected. The sections were covered in aluminum foil, sealed in zip lock bags, packed in dry ice, shipped overnight to the laboratory, and then stored at -80C until analyzed. No appreciable thawing was noted during sampling or shipment. An example protocol, providing additional detail related to cryo-genic coring is provided in Appendix B. The core sampling event coincided with groundwater sampling for qPCR, VOC and geochemical parameter analysis.
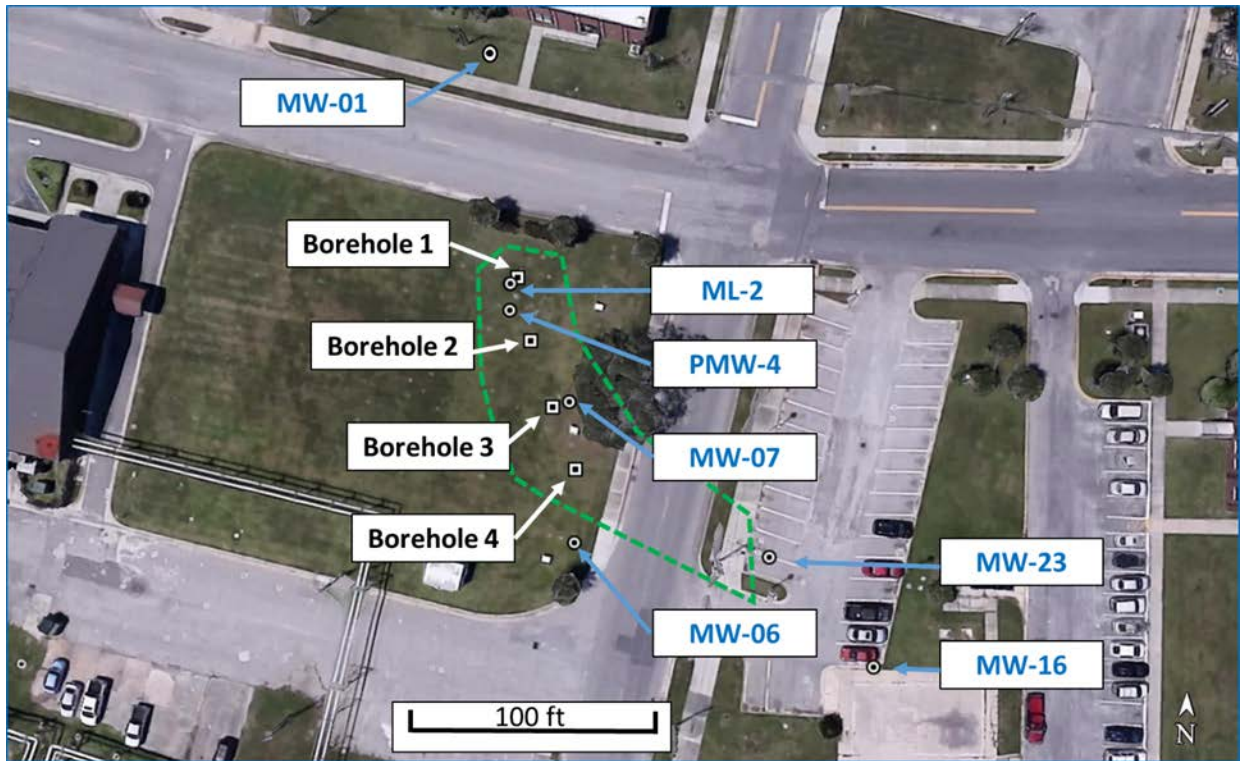
Figure 12. Cryogenic Core Sampling Locations at Parris Island site 45.

There were four boreholes, approximately 20 feet in depth along a transect that attempted to follow the direction of the northern VC plume.

5.5.4 Geochemical parameter data collection

For all groundwater samples that we subjected to the qPCR and RT-qPCR analysis, geochemical data was also collected either by UIowa personnel or a contractor. This included field measured parameters (i.e. DO, ORP, pH, and temperature), chlorinated ethene concentrations (including VC), chloride, ethene concentrations, and methane concentrations. For the sites where groundwater samples are collected by the field technicians, we coordinated with site managers to obtain the geochemical data for the same sampling event. As a result of different sampling plans and contracts, parameters such as chloride, ethene, and methane were not consistently measured in all groundwater samples.

Groundwater sampling at Parris Island and the geochemical parameter measurement were carried out by Mattes lab personnel. For each sampling event, a Geopump Peristaltic Pump Series I with easy-load I pump head for low flowrate groundwater sampling was used to deliver groundwater to pass through Sterivex filters (USEPA, 1996). Before the groundwater passes the Sterivex filters, it was passed through a flow cell where an YSI Professional Plus handheld multiparameter meter monitored DO, ORP, pH, temperature and conductivity. The Geopump Peristaltic Pump and YSI Professional Plus handheld multiparameter meter was calibrated before each sampling event.

Groundwater for chlorinated ethenes, ethene and methane analysis was collected in glass vials with Teflon septa following USEPA methods (USEPA, 2004) at the same time when Sterivex filter samples are taken. The date, time and location of each groundwater sample was recorded. Groundwater samples were subsequently sent to an analytical laboratory for PCE, TCE, cDCE, tDCE, 1,1-DCE, VC, ethene, methane, and chloride concentration measurement. Analyses were conducted by GEL laboratories, LLC (2040 Savage Road, Charleston, SC 29407). Investigation derived waste (IDW) was handled and disposed of by contract with Ensafe, Inc., the firm which is developing the remedial design at this site.

A summary of the types of samples that were collected is shown in Table 7.

Table 7.   Total Number and Types of Samples to Be Collected

Component	Matrix	Number of samples	Analyte	Location
Technology performance sampling at various DoD sites	Groundwater	4-6 per monitoring point	Functional genes and transcripts from VC-degrading bacteria	Selected monitoring wells
Technology performance sampling at Parris Island phase I	Groundwater	4 per monitoring point	Functional genes and transcripts from VC-degrading bacteria	Selected monitoring wells (Table 6)
	Groundwater	1 per monitoring point	PCE, TCE, DCEs, VC, ethene, methane	Selected monitoring wells (Table 6)
	Groundwater: Field measurement	1 per monitoring point	dissolved O_2, ORP, pH, conductivity, temperature	Selected monitoring wells (Table 6)
Technology performance sampling at Parris Island phase II	Groundwater	4 per monitoring point, quarterly/ semi-annually	Functional genes and transcripts from VC-degrading bacteria	Selected monitoring wells (Table 6)
	Groundwater	1 per monitoring point, quarterly/ semi-annually	PCE, TCE, DCEs, VC, ethene, methane	Selected monitoring wells (Table 6)
	Groundwater: Field measurement	1 per monitoring point	dissolved O_2, ORP, pH, conductivity, temperature	Selected monitoring wells (Table 6)
	Aquifer sediment samples	124 frozen "pucks"	Functional genes from VC-degrading bacteria	Multiple boreholes (4) along plume transect sampled with depth (See Figure 12)
			PCE, TCE, DCEs, VC, ethene, ethane, acetylene, methane, DO, NO_3^-, Fe^{2+}, Total Fe, SO_4^{2-}, ORP, pH, TOC, Cl^-	

5.5.5 Calibration of Analytical Equipment

Before each sampling event, the Geopump Peristaltic Pump Series I with easy-load I pump head was calibrated for flow rate using a cylinder and a timer. The DO probe, pH probe, ORP probe and conductivity probe of the YSI Professional Plus handheld multiparameter meter was calibrated daily according to manufacturer's instruction.

5.5.6 Quality Assurance Sampling

For each monitoring well, at least four Sterivex filter samples were collected, two for DNA analysis and two for RNA analysis. If time and resources were available, three DNA and three RNA were collected. The qPCR results from the replicate extracts were averaged to ensure accuracy. Each Sterivex filter was packed separately. All solutions, bottles, syringes, and Falcon tubes used for sampling were provided in a sterile condition. After sampling, the Sterivex filter was placed in a sterile screw capped Falcon tube to ensure no cross-contamination occurred during the sample transportation process. During the DNA and RNA extraction process, all solutions and tubes used were free from DNA and RNA contamination. Proper procedures were used to prevent cross contamination of sample (discussed in Section 5.5.7). For each VOC sampling event, one trip blank was included.

5.5.7 Decontamination Procedures

Following sampling, all used gloves and other consumables were collected and disposed of properly to avoid contamination. Equipment was rinsed and stored after use. IDW was collected, documented, and disposed of in coordination with the site managers, and the contractor Ensafe, Inc.

5.5.8 Sample Documentation

Data sheets were used to record sample and data collected from each monitoring well, including the sampling site, date, time, location, field measurements (water level, temperature, DO, pH, ORP, and conductivity) and the samples taken for geochemical data and microbial analyses.

For each filter sample collected, information about the sampling date, time, location, and the volume of groundwater passed through the filter was written on the side of the Falcon tube that holds the filter. The sample information was also tabulated in a notebook.

5.6 SAMPLING RESULTS

5.6.1 Data required

A variety of data, including microbial data and geochemical data, was required to assess the performance objectives described in Section 3.0. Examples of the data we collected is as follows:

1. qPCR and RT-qPCR data for etheneotroph and methanotroph functional genes (*etnC, etnE, mmoX, pmoA*) from groundwater samples and cryo-core sediment samples (qPCR data for cryo-cores only)

2. qPCR and RT-qPCR data for functional genes involved in anaerobic VC degradation pathways (*bvcA* and *vcrA*) from selected groundwater samples and cryo-core sediment samples (qPCR data for cryo-cores only)

3. Groundwater field parameters, as measured by YSI Professional Plus handheld multi parameter meter during field sampling event, including DO, ORP, pH, temperature, and conductivity.

4. Geochemical parameter data of substrates that can stimulate VC co-metabolism from groundwater samples, including ethene and methane.

5. Chlorinated ethene data from groundwater samples, including PCE, TCE, DCEs, and VC.

5.6.2   Analytical methods

A summary of the analytical methods used is shown in **Table 8.**

Table 8.   Analytical Methods for Sample Analysis from Groundwater and Aquifer Sediment Samples

Matrix	Analyte	Method	Container	Preservative	Holding Time
Groundwater	Functional genes from VC degrading bacteria	qPCR	Sterivex filter - Falcon tube	Shipped on ice	1 day
	mRNA transcripts from VC degrading bacteria	RT-qPCR	Sterivex filter-Falcon tube	Preserved in RNAlater and shipped on ice	1 day
	PCE, TCE, DCEs, VC	EPA method	Glass VOA vial	Preserved in ascorbic acid	1 day
	Ethene, ethane, methane	EPA method	Plastic bottle	Preserved with HCl addition	1 day
	Dissolved O_2	YSI Professional Plus handheld multiparameter meter	Field measurement	N/A	N/A
	ORP				
	pH				
	Conductivity				
Aquifer sediment samples	Functional genes from VC degrading bacteria	qPCR	Cores frozen in liquid nitrogen and divided into 1 inch "pucks"	Shipped on dry ice overnight to lab	Kept at -80C until analysis
	PCE, TCE, DCEs, VC	GC-MS			
	Ethene, ethane, acetylene, methane	GC-FID			
	Dissolved O_2	GC-TCD			
	ORP	Oakton double-junction ORP probe			
	pH	EPA method 100.1			
	chloride, nitrate, and sulfate	Ion chromatography			
	Total organic carbon	TOC analyzer			
	Ferrous iron, total iron	Spectrophotometry - Hach methods 8146 (ferrous) and 8008 (total)			
	Total solids	Gravimetric after drying soil at 105C overnight			

5.6.3   NAS Oceana SWMU 2C

The VC plume at NAS Oceana SWMU 2C is relatively dilute (concentration range 2-100 µg/L).

We have been obtaining groundwater samples from this site since 2008 in collaboration with Laura Cook at CH2MHill, the contractor responsible for remediation activities. Most of the samples we have obtained were collected from three different monitoring wells - MW05, MW19, and MW25. **Figure 13** displays the location of these wells within the VC plume. **Figure 14** shows that VC concentrations in the three monitoring wells have been trending downward over an extended period of time – since 1999. In 2004, Oxygen Releasing Compound (ORC) injections were performed in the vicinity of wells MW05 and MW25. ORC socks were placed in wells MW05, MW19, and MW25 in 2012 to further encourage VC oxidation.
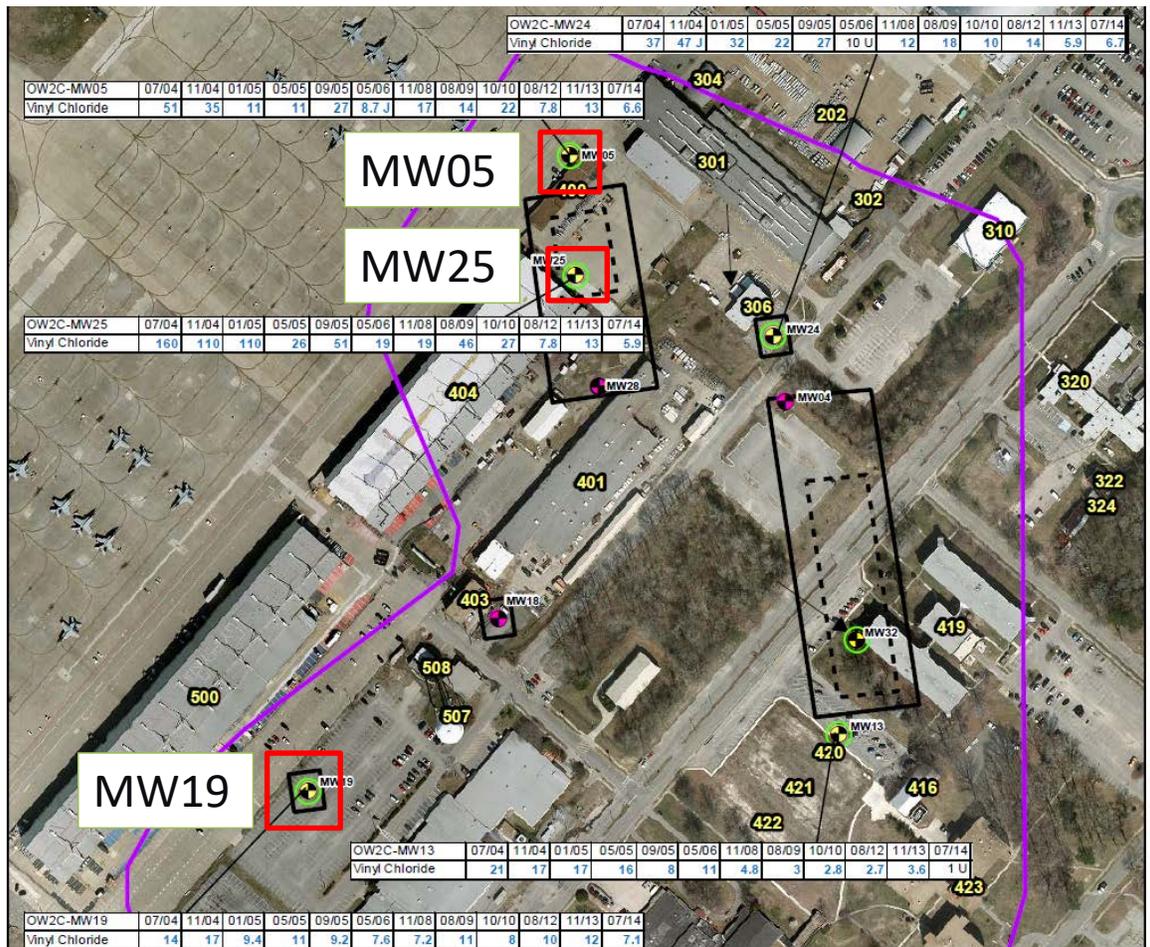
Figure 13. Site Map Showing the Estimated Boundary of the VC Plume (in purple), Location of Monitoring Wells MW05, MW25, and MW19, and VC Concentrations in These Wells Since 2004.

The wells that have a green circle around them have been subjected to Oxygen Releasing Compound (ORC) sock amendments to encourage VC oxidation.

57
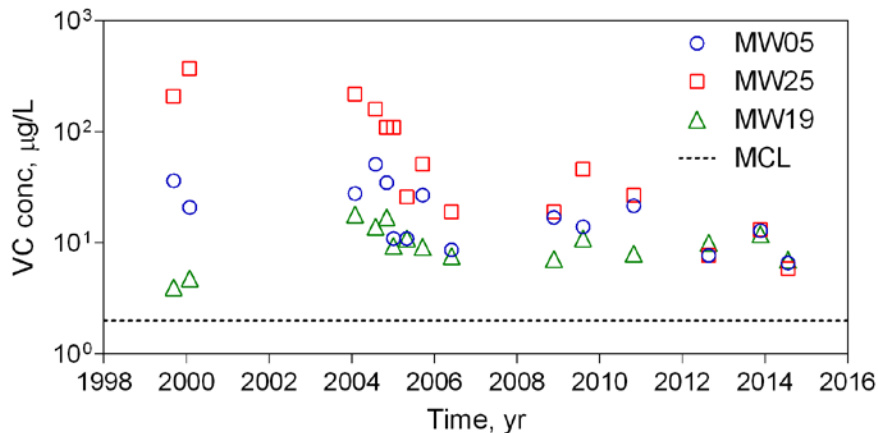
Figure 14. VC Concentrations of MW05, MW25 and MW19 from 1999 to 2014.

The 2 µg/L maximum contaminant level (MCL) is shown with a dotted line.

This site is of interest for this project because long term data collection that has occurred in an area of the VC plume where attempts were made to stimulate VC oxidation. According to DO and ORP values, the groundwater appears to be slightly anoxic (i.e. low DO levels and slightly negative ORP values). Ethene has not been routinely measured in any of the wells studied, although methane has been consistently detected at mg/L levels.

The observed decreases in VC in these monitoring wells with time could be the result of dilution, VC oxidation, and/or VC reduction. However, the extensive concrete paving covering the site indicates that dilution from precipitation infiltration is insignificant, leaving only impacts from upgradient groundwater. Using a simple groundwater flushing model (Wiedemeier, 1999) and estimated site hydrogeological parameters, we found that if advection and dispersion were the only processes affecting VC concentrations, it would require 38.5 years for VC concentrations in MW25 to reach the levels seen in July 2014 (5.6 µg/L) from the baseline levels in July 2004 (160 µg/L). This strongly suggests that VC degradation processes were active in the northern plume during the 2004-2014 time period.

We hypothesized that VC oxidation processes played a role in the observed VC degradation. To test the hypothesis, we conducted a qPCR analysis of temporal and spatial trends in the abundance of functional genes from bacteria known to participate in aerobic cometabolism of VC (methanotrophs and etheneotrophs) as well as reductive dechlorination of VC.

We employed our previously developed a qPCR technique to assess the presence and abundance of etheneotrophs in groundwater (Jin & Mattes, 2010, Jin & Mattes, 2011). This technique targets the functional genes *etnC*, which encodes the alpha subunit of alkene monooxygenase (AkMO), and *etnE*, which encodes the epoxyalkane coenzyme M transferase (EaCoMT) subunit. AkMO and EaCoMT are involved in the ethene and VC biodegradation pathways in several isolates (Coleman & Spain, 2003b, Mattes, *et al.*, 2005, Mattes, *et al.*, 2010). We also utilized qPCR primers available for estimating the abundance of methanotrophs in environmental samples that target the functional genes *pmoA* (Holmes, *et al.*, 1995, Lyew & Guiot, 2003), which encodes the particulate methane monooxygenase (pMMO) alpha subunit and *mmoX* (Fuse, *et al.*, 1998, Lyew & Guiot, 2003), which encodes the soluble methane monooxygenase (sMMO) alpha subunit.

The pMMO and sMMO are well known for their ability to oxidize VC. The sMMO typically displays higher VC oxidation rates. Finally, we estimated the abundance of functional genes known to be involved in reductive dechlorination of VC – the VC dehalogenase genes *bvcA* and *vcrA*. The results of the temporal qPCR study are shown in **Figure 15, Figure 16** and **Table 9.**

Functional genes for both VC oxidation and VC reduction were observed in all three monitoring wells (with the exception of *vcrA*) during the entire monitoring period. However, functional genes for VC reduction were generally very low, except in well MW19.

The presence of the functional genes *etnC*, *etnE*, *mmoX* and *pmoA* clearly indicates the potential for VC oxidation by both etheneotrophs and methanotrophs in and around the three monitoring wells. The relative lack of genes for VC reduction also suggests that VC oxidative processes are dominant in this portion of the aquifer. Methanotroph functional gene abundances were one or more orders of magnitude higher than etheneotroph functional gene abundances. This is consistent with methane concentration measured in the three monitoring wells (794 µg/L in MW05, 446 µg/L in MW19, and 789 µg/L in MW25 of 2012). Unfortunately, long-term groundwater monitoring at this site did not include ethene analysis, which would be helpful in confirming VC reduction as well as documenting a supporting growth substrate for VC oxidation. Because the VC concentrations are relatively low and there is a low abundance of genes involved in VC reduction, this suggests that ethene concentrations are also low in the aquifer.

Figure 15 also shows that etheneotroph functional genes were relatively stable from 2008 to 2014, while there is slight upward trend of methanotroph functional gene abundances. This also seems to be consistent with the available geochemical data along with previous biostimulation of these wells with ORC socks in the past. In other words, a steady supply of methane along with available oxygen (either intrinsic or exogenous) would be expected to lead to growth of methanotrophs over time, assuming nothing else is limiting in the aquifer. The apparently stable etheneotroph population is encouraging and suggests etheneotrophs are making use of available ethene and possibly VC as growth substrates under environmental conditions that are relatively difficult for them.
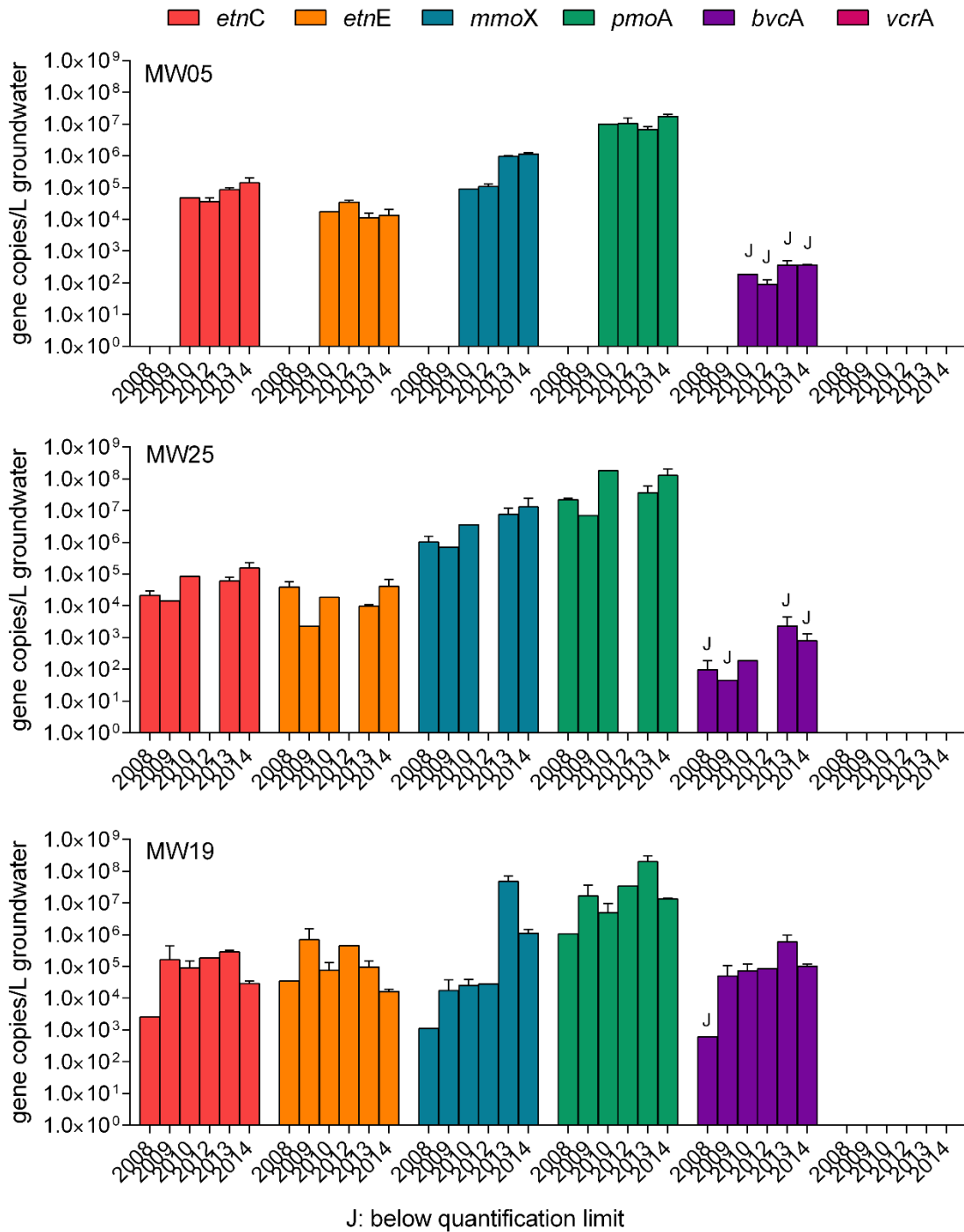
Figure 15. Abundances of etnC, etnE, mmoX, pmoA, bvcA and vcrA in MW05, MW25, and MW19 from 2008 to 2014.

J: estimated, as the result was below our qPCR quantification limit

Table 9. Gene Abundances (etnC, etnE, mmoX, pmoA, and bvcA), Transcript Abundances, and Transcript per Gene Ratios in NAS Oceana Monitoring Wells MW05, MW25, MW19 from 2012 to 2014.

Values reported are the averages of triplicate qPCR measurements.

			MW05			MW25		MW19	
			2012.08	2013.11	2014.07	2013.11	2014.07	2013.11	2014.07
$etnC$	DNA	average	3.55×10^4	8.49×10^4	1.42×10^5	6.19×10^4	1.55×10^5	2.84×10^5	2.88×10^4
		std dev	1.12×10^4	1.52×10^4	5.75×10^4	1.58×10^4	7.10×10^4	3.22×10^4	5.77×10^3
	cDNA	average	1.28×10^3 (J)	5.27×10^2(J)	1.51×10^5(J)	8.52×10^3(J)	9.08×10^3(J)	1.76×10^4	4.72×10^3(J)
		std dev	1.37×10^3	-	2.35×10^5	1.43×10^4	1.57×10^4	5.40×10^3	8.18×10^3
		ratio	0.036	0.0062	1.07	0.14	0.058	0.062	0.16
$etnE$	DNA	average	3.47×10^4	1.11×10^4	1.35×10^4	9.91×10^3	4.10×10^4	9.67×10^4	1.63×10^4
		std dev	4.81×10^3	4.50×10^3	6.83×10^3	8.43×10^2	2.60×10^4	5.47×10^4	3.08×10^3
	cDNA	average	1.30×10^3(J)	1.65×10^3(J)	2.19×10^3(J)	5.28×10^2(J)	1.69×10^3(J)	2.95×10^3(J)	ND
		std dev	1.64×10^3	-	1.95×10^3	9.15×10^2	2.92×10^3	3.38×10^3	-
		ratio	0.037	0.15	0.16	0.053	0.041	0.030	-
$mmoX$	DNA	average	1.06×10^5	9.67×10^4	1.13×10^6	7.51×10^6	1.30×10^7	4.76×10^7	1.11×10^6
		std dev	2.61×10^4	6.70×10^4	1.12×10^5	4.50×10^6	1.16×10^7	2.19×10^7	3.55×10^5
	cDNA	average	1.44×10^3(J)	1.26×10^5	1.15×10^4(J)	1.13×10^4(J)	1.58×10^4(J)	1.69×10^5	1.02×10^5
		std dev	1.84×10^3	-	8.22×10^3	4.05×10^3	4.95×10^3	1.04×10^5	4.55×10^4
		ratio	0.014	0.13	0.010	0.0015	0.0012	0.0036	0.092
$pmoA$	DNA	average	1.03×10^7	6.68×10^6	1.75×10^7	3.66×10^7	1.26×10^8	1.98×10^8	1.31×10^7
		std dev	5.45×10^6	1.71×10^6	2.83×10^6	2.16×10^7	7.88×10^7	1.10×10^8	1.23×10^6
	cDNA	average	4.56×10^5	2.31×10^6	3.31×10^6	1.58×10^4(J)	1.94×10^5	3.63×10^7	6.37×10^6
		std dev	1.16×10^5	-	2.08×10^6	7.66×10^3	4.52×10^4	4.29×10^7	4.00×10^6
		ratio	0.044	0.35	0.19	0.00043	0.0015	0.18	0.49
$bvcA$	DNA	average	8.80×10^1(J)	3.55×10^2(J)	3.65×10^2(J)	2.33×10^3(J)	7.81×10^2(J)	5.90×10^5	1.01×10^5
		std dev	3.39×10^1	1.54×10^2	1.09×10^1	2.14×10^3	5.13×10^2	3.63×10^5	1.45×10^4
	cDNA	average	ND	ND	ND	ND	1.29×10^2(J)	1.71×10^6	3.11×10^6
		std dev	-	-	-	-	2.23×10^2	4.54×10^5	1.03×10^6
		ratio	-	-	-	-	0.16	2.90	30.66

ND: not detected; "-": Not applicable or able to be determined.

J: estimated value; amplification detected but below quantification limit of standard curves

These spatial and temporal trends are important and relevant with respect to the spatial and temporal trends in VC concentration at the site. The apparently increasing trends of *pmoA* and *mmoX* implies an increased potential for VC oxidation, provided there are no other limitations (e.g. oxygen and nutrients). The Mann-Kendall test revealed that the increase in *mmoX* in MW19 was statistically significant ($p < 0.05$). It is possible that the jump in *mmoX* abundance in MW19 in 2013/2014 could be related to the observed drop in VC in that well in 2014. However, additional temporal monitoring data is needed to provide the evidence to support this possibility.

Although qPCR estimation of functional gene abundance can yield spatial and temporal insights that can be useful for assessing the sustainability of bacterial populations involved in VC oxidation, it can only provide information about the metabolic potential for VC oxidation. Molecular diagnostic information that demonstrates the activity of VC-oxidizing bacteria would be relevant to trends in VC concentration with time and provide an additional line of evidence that VC oxidation is a viable and sustained pathway at a contaminated site. We have incorporated procedures to extract RNA from groundwater samples and convert the RNA into complementary DNA (cDNA) via the enzyme reverse transcriptase. Following conversion of RNA to cDNA and incorporation of an internal control nucleic acid to account for the inefficiency of reverse transcription, transcript abundance of target functional genes is estimated by qPCR.

We have tracked *etnC*, *etnE*, *mmoX*, *pmoA,* and *bvcA* transcript abundance in NAS Oceana groundwater samples since 2012 (**Figure 16**). This has revealed that VC oxidizers (etheneotrophs and methanotrophs) and VC reducers are active in the aquifer. Overall, the RT-qPCR data suggest that the methanotrophs are most active group of VC-degraders. This is consistent with the geochemical conditions at the site – methane is relatively abundant, while VC (and presumably ethene) concentrations are much lower. Oxygen has been provided exogenously at times with ORC socks. In other words, the environmental conditions at this site appear to be more conducive for growth and activity of methanotrophs.

The spatial and temporal trends of transcript abundance support the trends in the qPCR data. Although there is not enough information to determine statistical trends, the sustained level *mmoX* transcript abundance in MW19 supports the statically significant upward trend in *mmoX* shown in **Figure 15**. The data shown in **Figure 16** is also relevant with respect to VC concentrations. While qPCR estimated cell densities are informative, RT-qPCR estimated transcript abundance provides another level of information that strengthens the relationship between microbial activity and its effect on VC concentrations. In other words, some percentage of these transcripts are very likely to be translated into active protein, which in the case of EtnC, MmoX and PmoA, are key subunits of monooxygenase enzymes that attack and degrade VC directly.
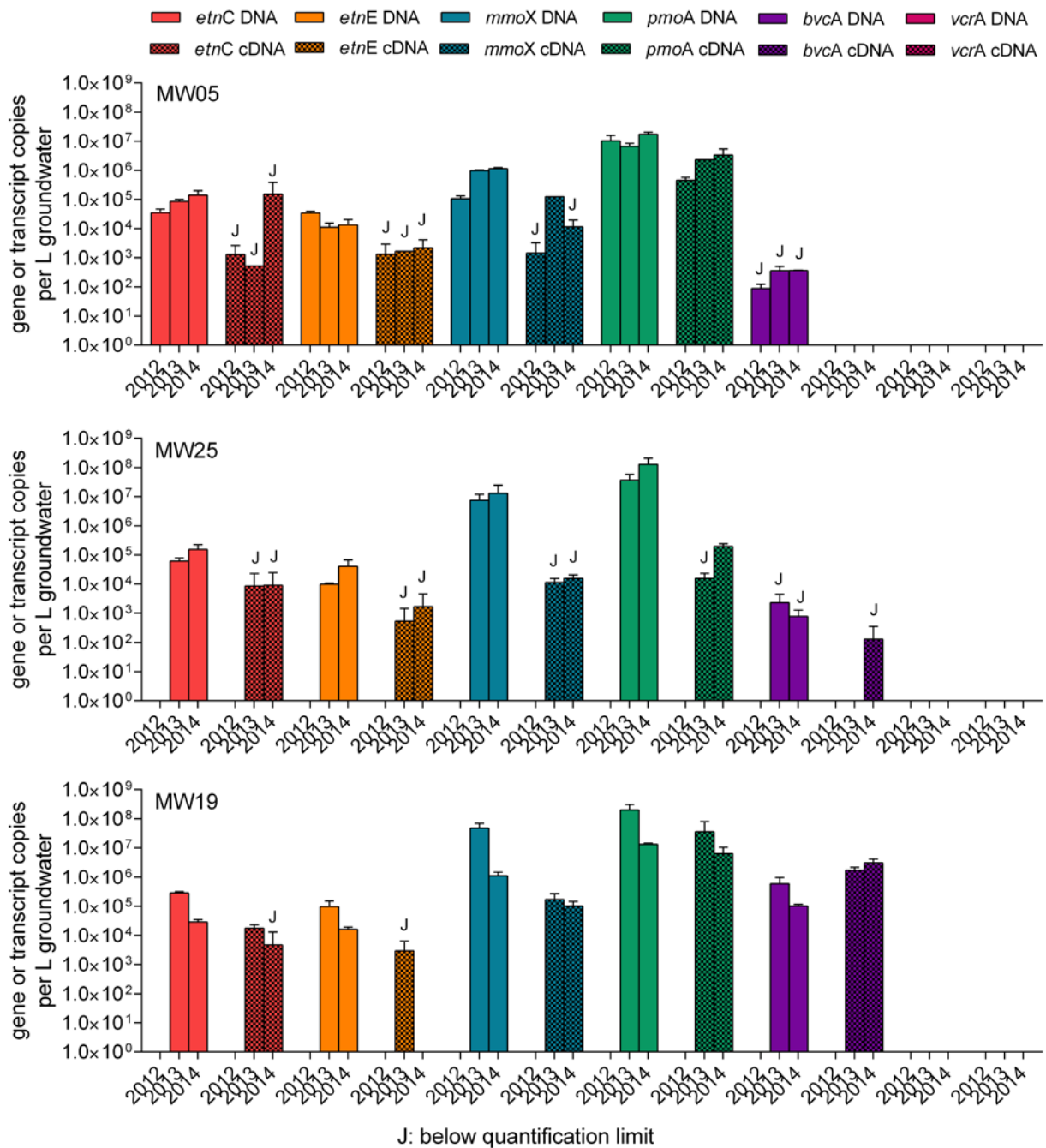
Figure 16. Abundance of etnC, etnE, mmoX, pmoA, and bvcA Genes and Transcripts in Wells MW05, MW19, and MW25 from 2012 to 2014.

Data points labeled with "J" indicate estimated values as amplification was detected but the result was below our qPCR quantification limits.

5.6.4   NSB Kings Bay, SC Site 11 sampling results

Groundwater at Site 11 has been contaminated primarily by chlorinated volatile organic (i.e. PCE, TCE, DCEs, and VC) and BTEX compounds (benzene). VC concentrations in several monitoring wells at site 11 have exhibited a downward trend over the past ten years and were about 0.5 - 10 µg/L in 2011. The DO and ORP data suggests an anoxic environment in the monitoring wells (DO < 1 mg/L and negative ORP). Ethene data was not available for this site but methane was detected at the level of 0-8 mg/L. In several ways, this VC plume has similar characteristics to the dilute VC plume at NAS Oceana, except that the clean-up remedy at this site included in situ chemical oxidation. **Figure 17** shows the shrinking trend of the VC plume at Kings Bay Site 11 and the locations of eight monitoring wells where groundwater was sampled in 2013.

We obtained Site 11 DNA samples (2013 sampling event) from monitoring wells USGS-01, 02, 04, 05, 10, 11 and KBA-11A, KBA-11-13A, KBA-11-34 from Frank Loeffler's lab. We coordinated with Mike Singletary for the collection of additional samples for both DNA and RNA analysis in January 2015.

Figure 18 shows the abundances of *etnC*, *etnE*, *mmoX* and *pmoA* in the 2013 groundwater samples. These results indicate the potential for aerobic VC oxidation by both etheneotrophs and methanotrophs in these wells. So far, in the limited amount of VC-contaminated sites we have studied, we have observed the presence of VC oxidation potential. Methanotroph functional genes (especially *pmo*A) were relatively higher than etheneotroph functional genes. This observation, which is similar to that made in the NAS Oceana VC plume, is consistent with the relative abundance of methane in those wells. The abundance of *etnE* was lower at site 11 than we observed at NAS Oceana, although the *etnC* levels appeared higher.

An interesting finding at Kings Bay Site 11 is that *Dehalococcoides* 16S and reductive dehalogenase genes (*vcrA* and *tceA*) were identified in several of the same DNA samples (data provided by Frank Loeffler's lab). The coexistence of aerobic and anaerobic VC degraders in several wells (USGS-01, 02, KBA-11-13A and KBA-11-34) has not been previously observed. There could be several explanations for this observation. First of all, the wells could be screened over a large enough vertical interval such that groundwater is drawn from both aerobic (i.e. near the groundwater table) and deeper anaerobic zones. Another possibility is the coexistence of aerobic and anaerobic microzones within much closer proximity to each other within the aquifer. The spatial relationships between anaerobic VC dechlorinators and aerobic VC oxidizers could significantly impact decision-making and MNA sampling strategies at a site. One approach to determining the spatial relationships between VC oxidizers and dechlorinators (and their associated activity) would be to perform qPCR/RT-qPCR in core samples. This idea will be discussed in more detail later in this document, as the value of analyzing core samples is a separate action item to be addressed.
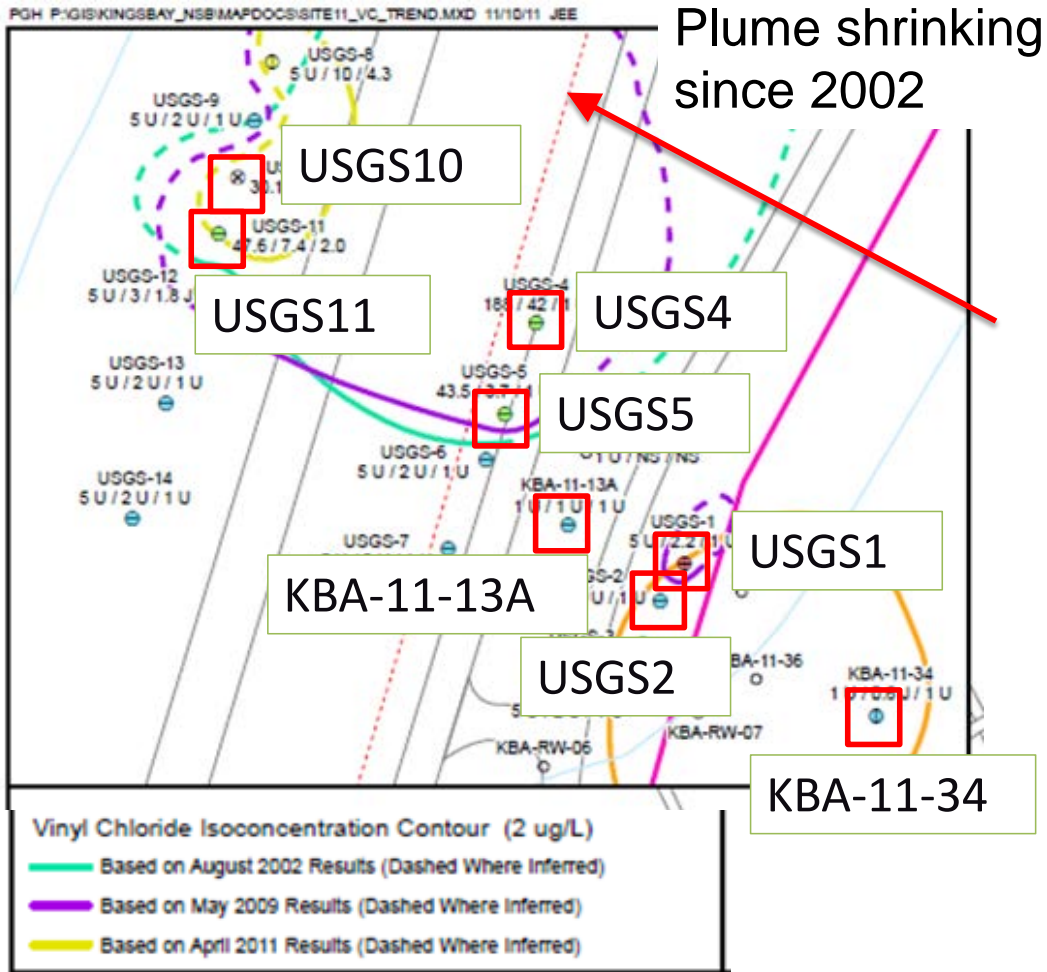
Figure 17. Site Map Showing the Location of Monitoring Wells KBA-11-34, USGS1, USGS2, KBA-11-13A, USGS5, USGS4, USGS11, USGS10, and VC Isoconcentration Contours (2 µg/L) in 2002 (green line), 2009 (purple line) and 2011 (yellow line).

The red arrow indicates the groundwater flow direction.
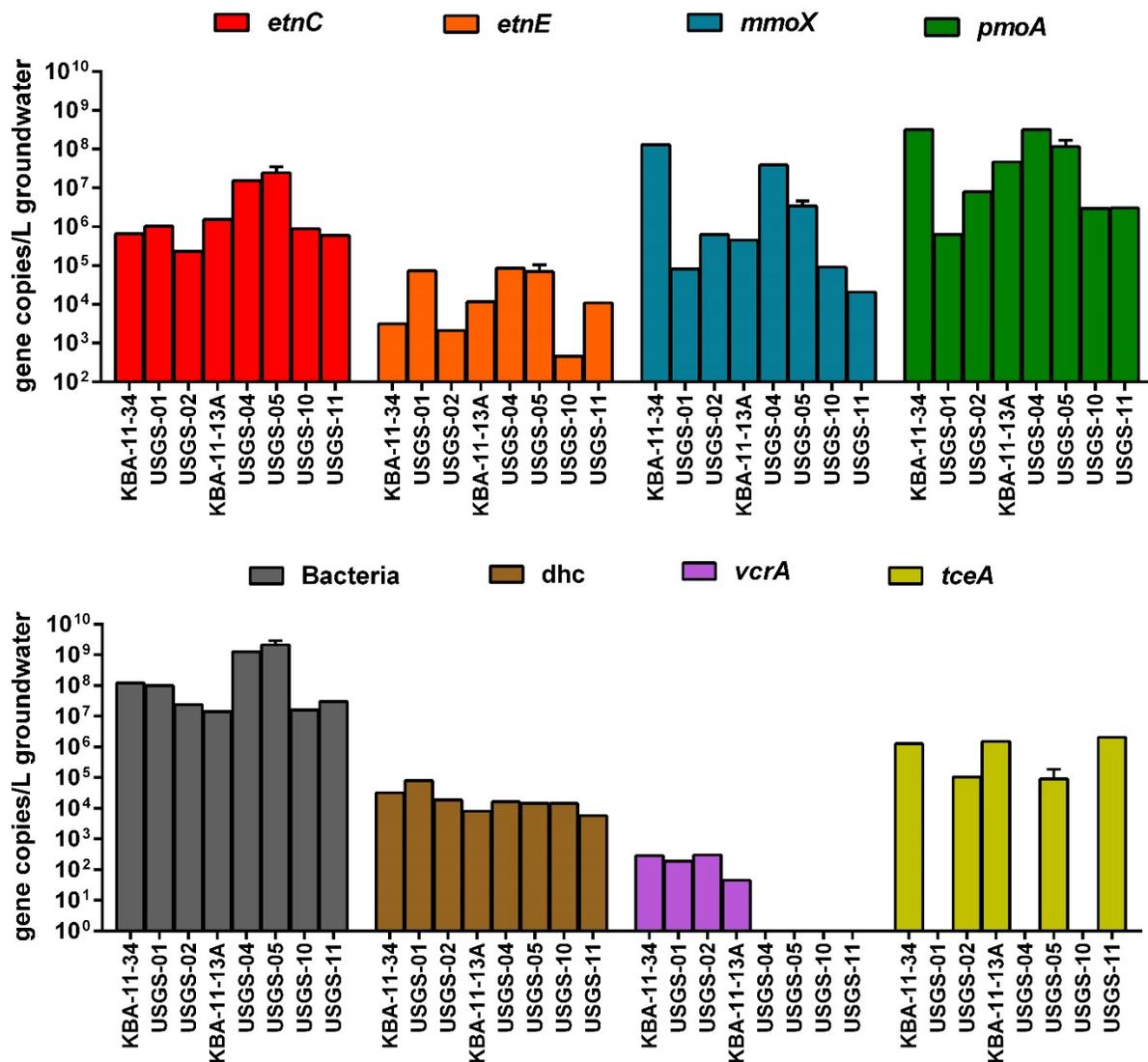
Figure 18. Abundances of *etnC, etnE, mmoX,* and *pmoA* in NSB Kings Bay Site 11 Wells KBA-11-34, USGS1, USGS2, KBA-11-13A, USGS4, USGS5, USGS10, USGS1 from a 2013 Sampling Event.

The abundance of total bacterial 16S rRNA genes, Dehalococcoides specific 16S rRNA genes, vcrA, and tceA in those same wells is also shown (this data was provided by Frank Loffler's laboratory). Wells are arranged left to right in accordance to the groundwater flow direction.

Groundwater samples were collected from a subset of wells (KBA 11-34, USGS4, USGS5, and USGS 10) from site 11 in January 2015 for preliminary analysis of VC-oxidizer abundance and activity. As shown in Figure 17, these wells were selected to cover areas where VC still exists (USGS 10), where VC was present in the last 5 years (USGS 4 and 5) and where VC had been degraded some time ago (KBA 11-34). Estimates of *etnC, etnE, mmoX* and *pmoA* abundance, in comparison to those made from the 2013 sampling event, are shown in Figure 15. The apparent trend for all VC oxidation functional genes is downward in all wells. This is likely related to the fact that this VC plume has been shrinking fairly rapidly since 2002 (i.e. the geochemical conditions are not favorable for an increasing abundance of VC oxidizers).

RT-qPCR analysis (**Figure 20**) of *etnC*, *etnE*, *mmoX*, *pmoA, bvcA,* and *vcrA* gene and transcript abundance indicates low activity of VC-oxidizers and VC-reducers. Overall, the preliminary analysis of VC-oxidizer gene and transcript abundance at site 11 in 2015 (including a comparison of gene abundances in 2013 and 2015; **Figure 19**) suggests that the geochemical conditions are not favorable for sustaining the abundance and activity of VC-oxidizers. A plausible explanation for these observations is that the VC plume is nearly extinguished as this site. Oxygen could also be limiting. No further analyses were performed at this site.
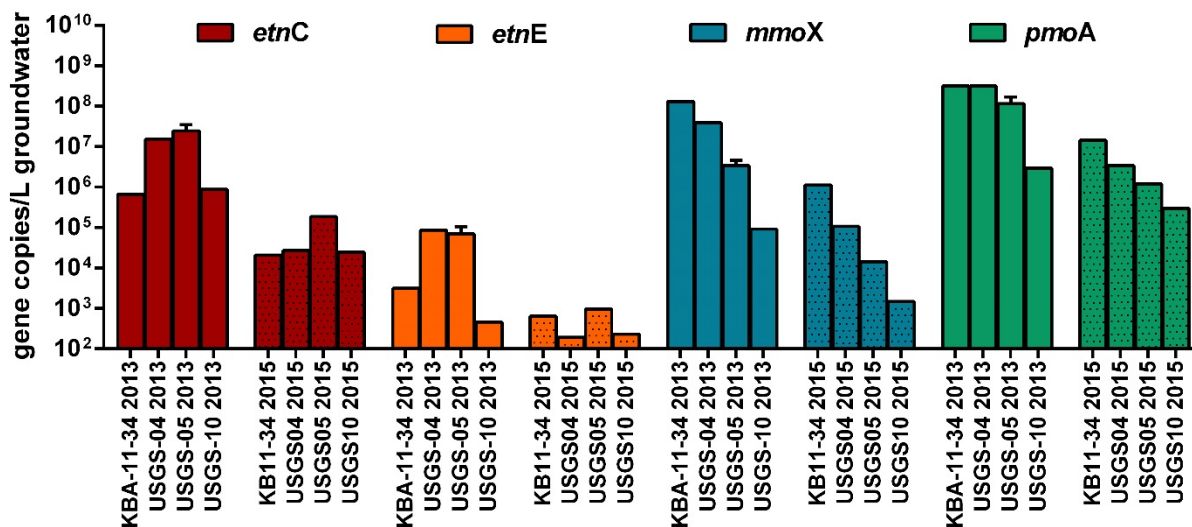
Figure 19. Abundances of *etnC, etnE, mmoX,* and *pmoA* in NSB Kings Bay Site 11 Wells KBA-11-34, USGS4, USGS5, and USGS10 from a January 2015 Sampling Event in Comparison to the Same Wells Sampled in 2013.

These results suggest that the overall populations of VC-oxidizers are in decline.
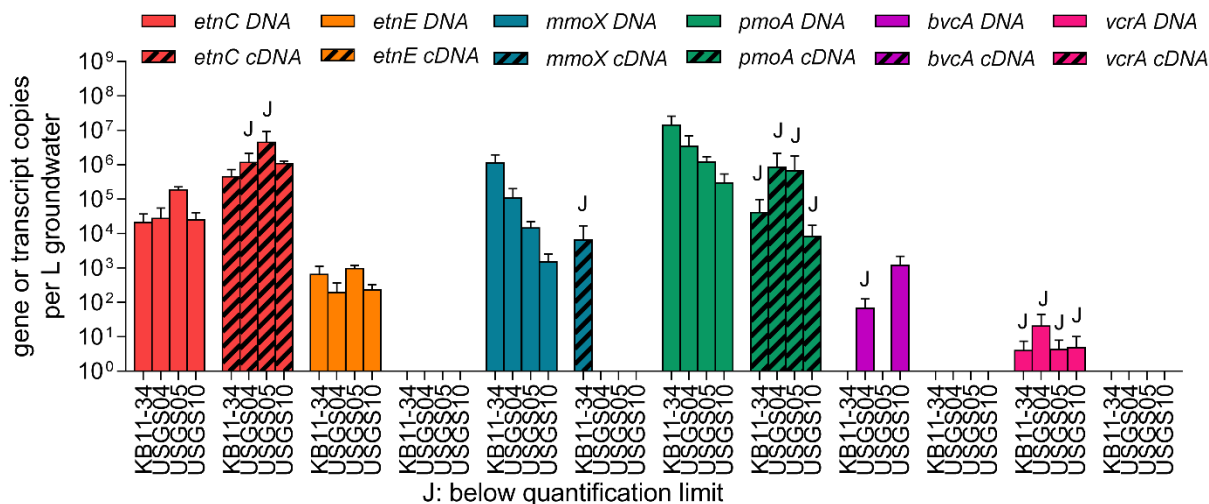
Figure 20. Abundances of *etnC, etnE, mmoX, pmoA, bvcA* and *vcrA* genes (DNA) and transcripts (cDNA) in NSB Kings Bay site 11 wells KBA-11-34, USGS4, USGS5, and USGS10 from a January 2015 sampling event.

These results suggest that the relative activity of VC-oxidizers is low at this site. Data points labeled with "J" indicate estimated values as amplification was detected but the result was below our qPCR quantification limits.

5.6.5 Altus AFB biowalls sampling results

Remediation of a TCE plume at Altus AFB was implemented via mulch biowalls. The performance of these biowalls was the subject of another ESTCP project (ER-201429), led by GSI Environmental. In collaboration with GSI, we obtained Sterivex filter samples from three wells – BC07D, BE09D, and BB04D in April 2015. In general, it appears that VC is produced within the biowalls and moves downgradient until it attenuates. After subsequently reviewing site data, a transect of 4 wells was chosen (**Figure 21**) which demonstrated a decline in VC concentration with distance (**Figure 22**). Abundance estimates for VC biodegradation genes and transcripts were made, as shown in **Figure 23**.
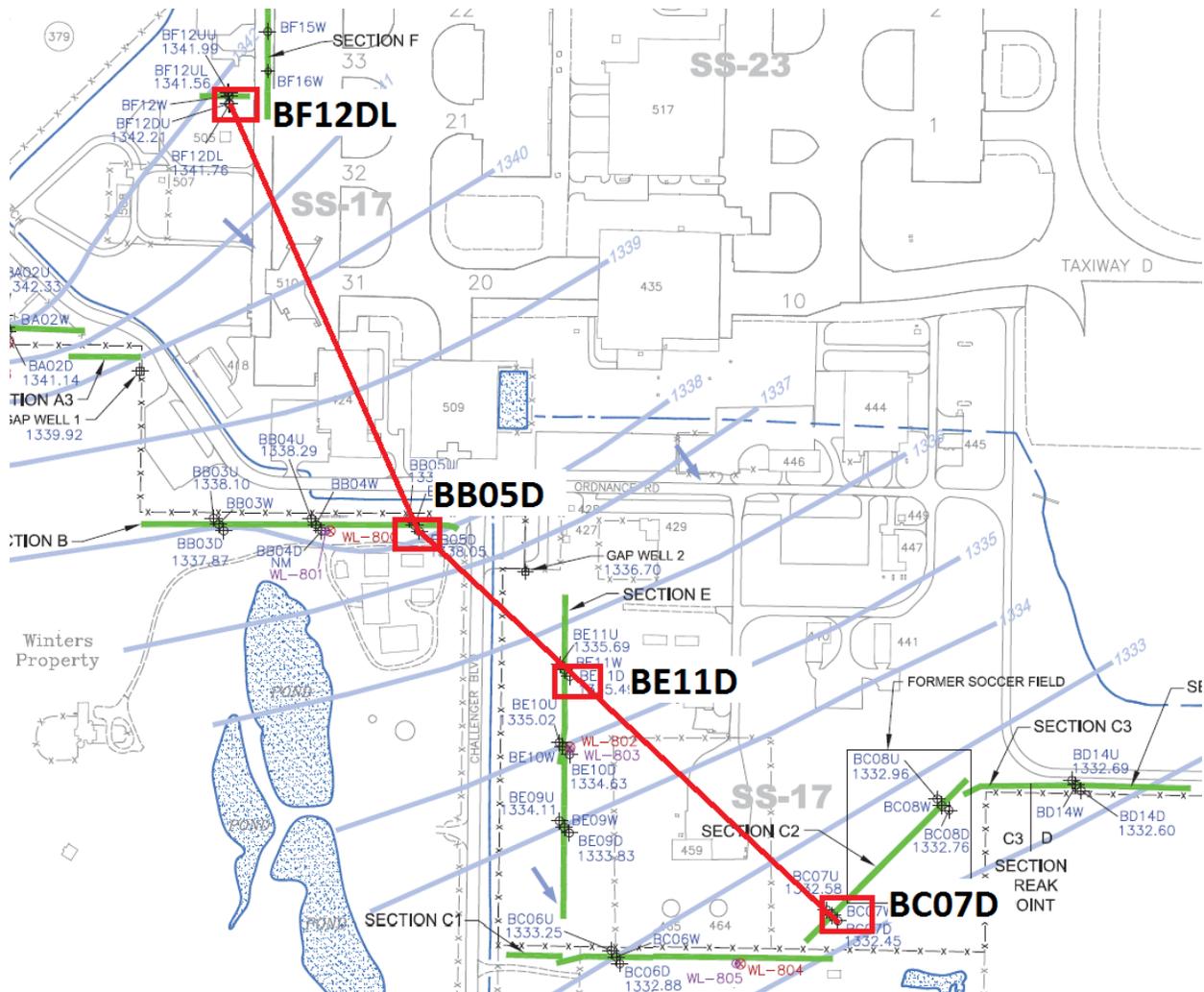
Figure 21. Site Map Depicting the Biowalls and Sets of 3 Monitoring Wells that Transect Biowall Sections (Upgradient of Wall, Wall, Downgradient of Wall)
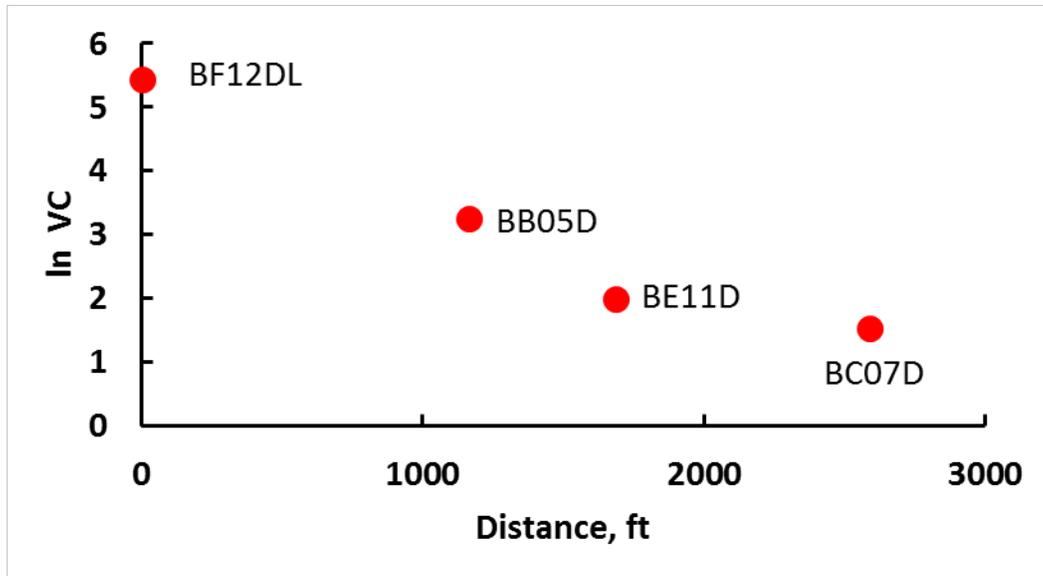
Figure 22. VC Concentration (ln-transformed) vs. Distance for the 4 well VC Plume Transect at Altus AFB Biowall Plume.

These values will be used to estimate bulk VC attenuation rates for the performance assessment. Data from April 2015 sampling event.
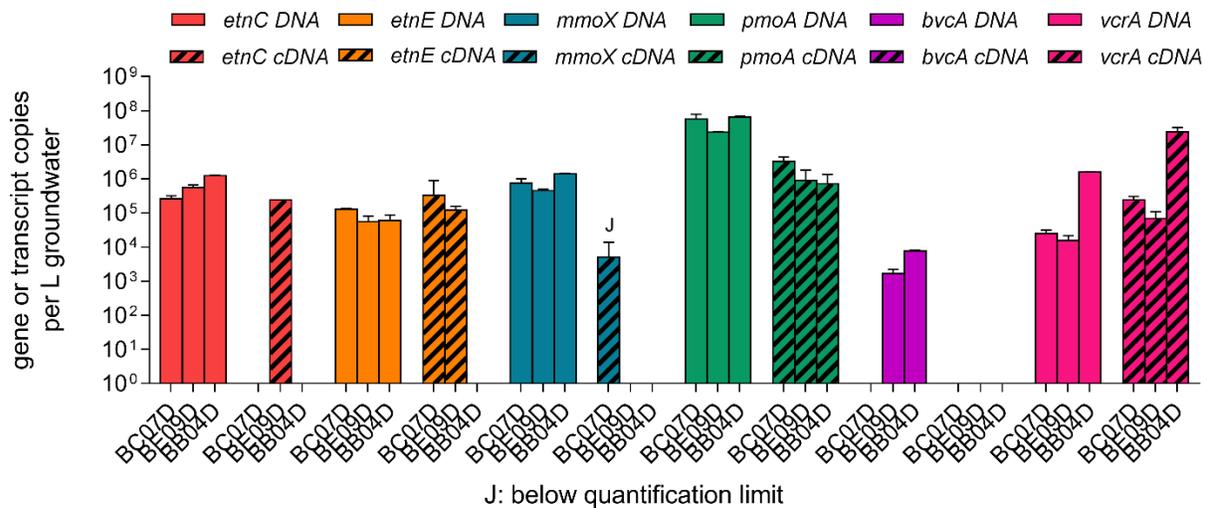
Figure 23. Abundance of *etnC, etnE, mmoX, pmoA, bvcA* and *vcrA* (Genes and Transcripts) in the Altus AFB Biowall VC Plume.

Groundwater from 3 monitoring wells was sampled in May 2015. Data points labeled with "J" indicate estimated values as amplification was detected but the result was below our qPCR quantification limits.

5.6.6   NWS Seal Beach Site 70 sampling results

VC concentrations at Seal Beach site 70 are moderately higher (up to 2,000 µg/L in the source zone area). The plume is also quite a bit larger and longer than at any of the other sites. An overview of the plume is shown in **Figure 24**. Sampling events were conducted by University of Iowa personnel in July 2015 (10 monitoring wells) and December 2015 (13 monitoring wells). VOC and geochemical parameters were measured by a Navy contractor (ECC-INSIGHT LLC).

Figure 24. Illustration of the VC Plume at Seal Beach Site 70.

Monitoring wells that were sampled during the July 2015 and December 2015 events are shown, along with a plume transect. The source area is at the top of the figure in the vicinity of wells PMW01A/B.

Five wells (PMW01B, PMW06A, PMW08B, PMW12B, and PMW14A) were selected for the VC plume transect based on their location as well as their depth - the plume dives to relatively deep depths (**Table 10**). A graph of VC vs. distance shows that VC decreases along the plume transect (**Figure 25**).

Table 10. Information Concerning the Five Wells at Seal Beach Site 70 Used for the VC Plume Transect, Including Treatment Zone Location, Well Screen Interval, VC Concentration and Distance from the Source Area.

Treatment Zone	Well	well screen interval, ft	Vinyl Chloride conc, ug/L	distance, ft
Source area treatment grid	MW-70-PMW01B	45 - 55	1300	0
First sand biobarrier 1	MW-70-PMW06A	69.5 - 79.5	1100	627.8261
First sand biobarrier 2	MW-70-PMW08B	85 - 95	370	1149.565
Shell horizon biobarrier 3	MW-70-PMW12B	115 - 125	290	1979.13
Second sand biobarrier	MW-70-PMW14A	128 - 138	120	2280
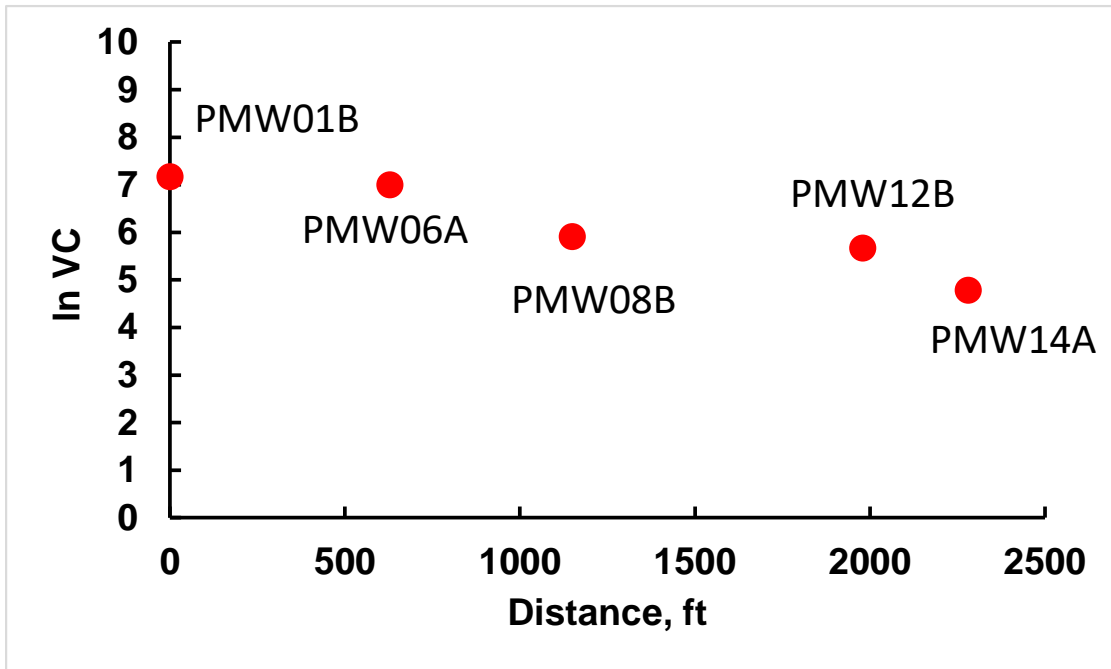
Figure 25. ln VC Concentration vs. Distance for the 5 Well VC Plume Transect at Seal Beach Site 70.

These values will be used to estimate bulk VC attenuation rates for the performance assessment. Data from July 2015 sampling event.

Abundance of *etnC, etnE, mmoX*, *pmoA, bvcA, and vcrA* genes and transcripts from all sampled monitoring wells are shown in **Figures 26-29**. In July 2015, functional gene abundance from VC-oxidizers decreased with distance from the source. VC reductive dehalogenase genes (bvcA and vcrA) were generally a few orders of magnitude less abundant that the genes for VC oxidation.

However, these trends in functional gene abundance were offset by relatively low activity of VC-oxidizers across the plume. VC reductive dehalogenase genes, despite their relatively low abundance, showed pockets of relatively high activity (wells MW70-38, PMW06A, PMW10, and PMW08B).
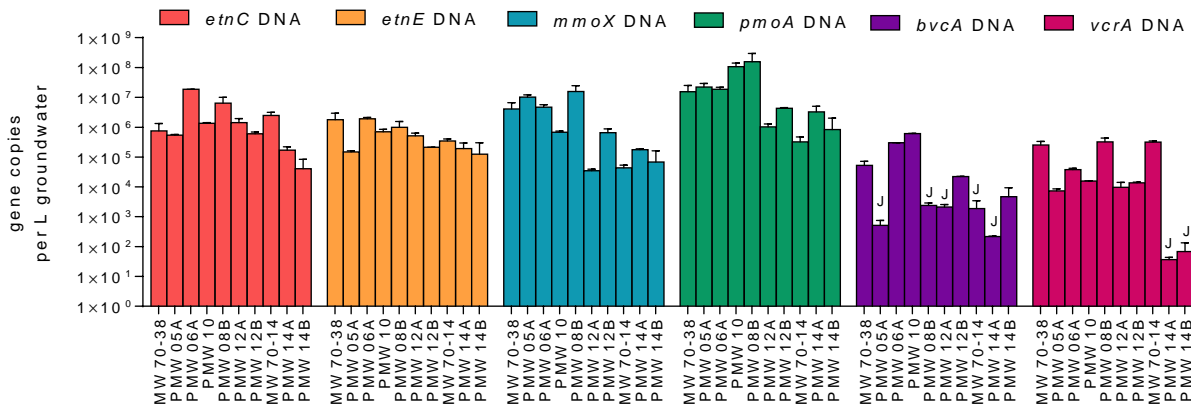
Figure 26. Abundance of *etnC, etnE, mmoX, pmoA, bvcA,* and *vcrA* in the VC Plume at NWS Seal Beach Site 70.

Groundwater from 10 monitoring wells was sampled in July 2015. Data points labeled with "J" indicate estimated values as amplification was detected but the result was below our qPCR quantification limits.
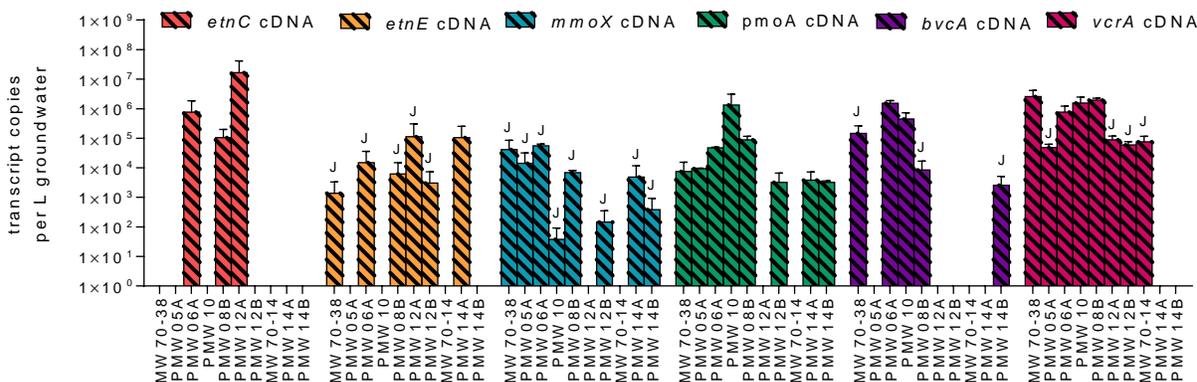
Figure 27. Abundance of *etnC, etnE, mmoX, pmoA, bvcA*, and *vcrA* Transcripts in the VC Plume at NWS Seal Beach Site 70.

Groundwater from 10 monitoring wells was sampled in July 2015. Data points labeled with "J" indicate estimated values as amplification was detected but the result was below our qPCR quantification limits.

In December 2015, we obtained additional samples from the source zone (PMW01A/B) where VC concentrations were higher, and from well PMW13A, which is upgradient from the second sand biobarrier and could exhibit more aerobic activity than wells downgradient of the biobarriers (this was a suggestion from Arun Gavaskar). Interestingly, VC-oxidizing etheneotroph activity and VC reductive dehalogenase activity was higher in the source zone wells This is yet another observation

73

of apparently concurrent VC oxidation (by etheneotrophs) and VC reduction processes occurring in the same groundwater sample from an area of relatively high VC concentrations and low DO levels. VC oxidizer abundance and activity was also elevated in well PMW13A (**Fig. 26 and 27**) – this highlights the spatial variability of biological processes over the extent of the VC plume.
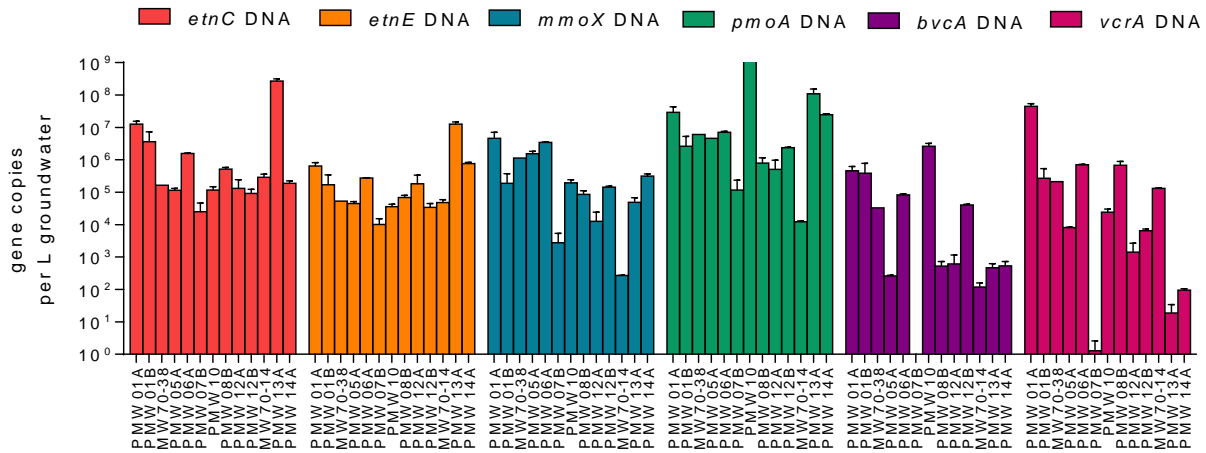
Figure 28. Abundance of *etnC, etnE, mmoX, pmoA, bvcA,* and *vcrA* in the VC Plume at NWS Seal Beach Site 70.

Groundwater from 13 monitoring wells was sampled in December 2015. Data points labeled with "J" indicate estimated values as amplification was detected but the result was below our qPCR quantification limits.
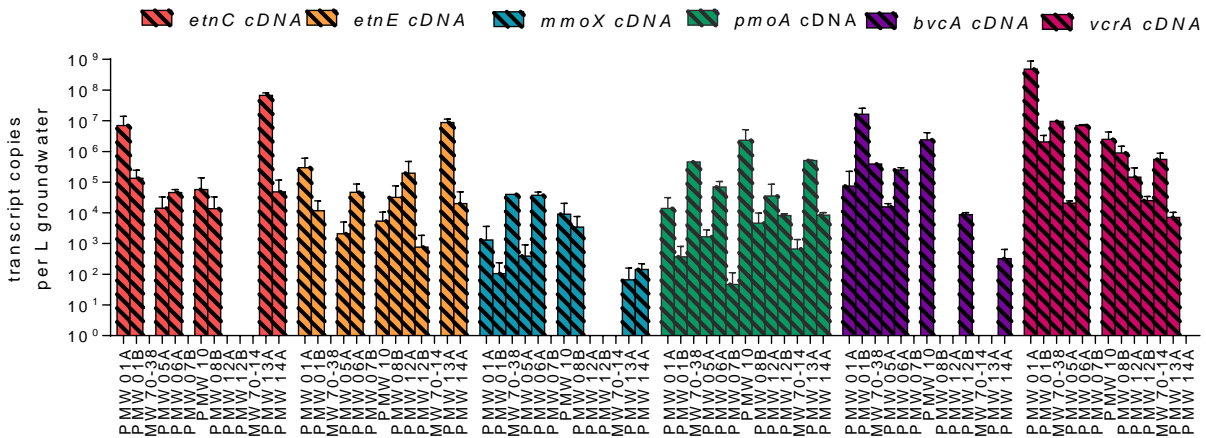
Figure 29. Abundance of *etnC, etnE, mmoX, pmoA, bvcA,* and *vcrA* Transcripts in the VC Plume at NWS Seal Beach Site 70.

Groundwater from 13 monitoring wells was sampled in December 2015. Data points labeled with "J" indicate estimated values as amplification was detected but the result was below our qPCR quantification limits.

74

5.6.7   Site LF05, Joint Base Pearl Harbor Hickam sampling results

This site came to our attention through further discussions with Mike Singletary (NAVFAC Southeast). It immediately became a site of interest primarily because high VC concentrations were observed in several monitoring wells. A site map of the well arrangement in 2014 is shown in **Figure 30**. Groundwater samples from a quarterly event in 2014 had been sent to Microbial Insights for qPCR analysis of *bvcA, vcrA*, and total *Dehalococcoides* 16S genes. We obtained this DNA and also performed qPCR for *etnC, etnE, mmoX* and *pmoA*. The qPCR results – which show that etheneotrophs are dominant in many of the wells - are shown in **Figure 31.**
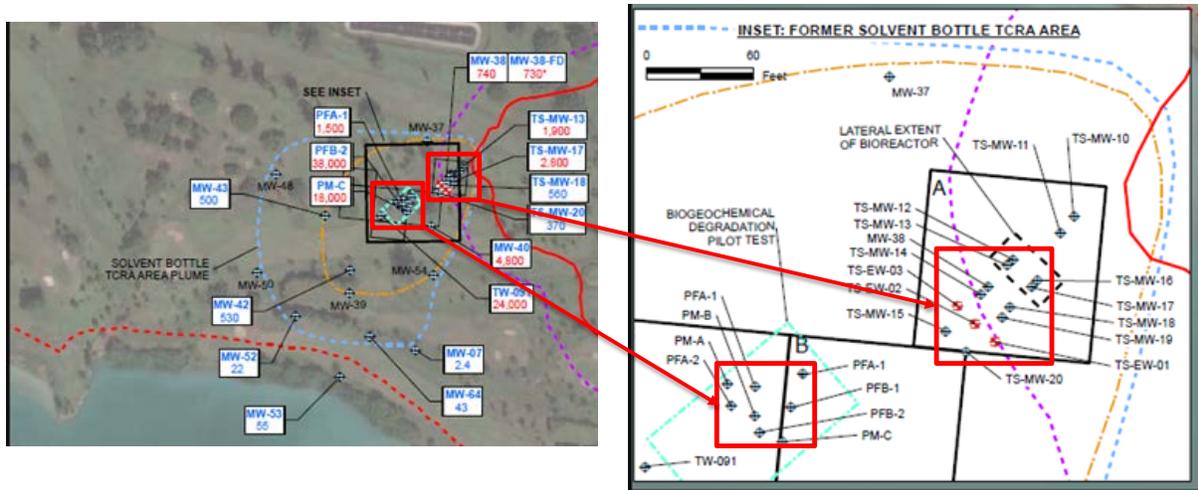
Figure 30. Map of Site LF05 in 2014.

Samples from wells PFB-2, PM-C, TS-MW17, MW38, and MW40 were obtained from Microbial Insights in collaboration with Mike Singletary (NAVFC).

*: qPCR data collected by Microbial Insight Inc
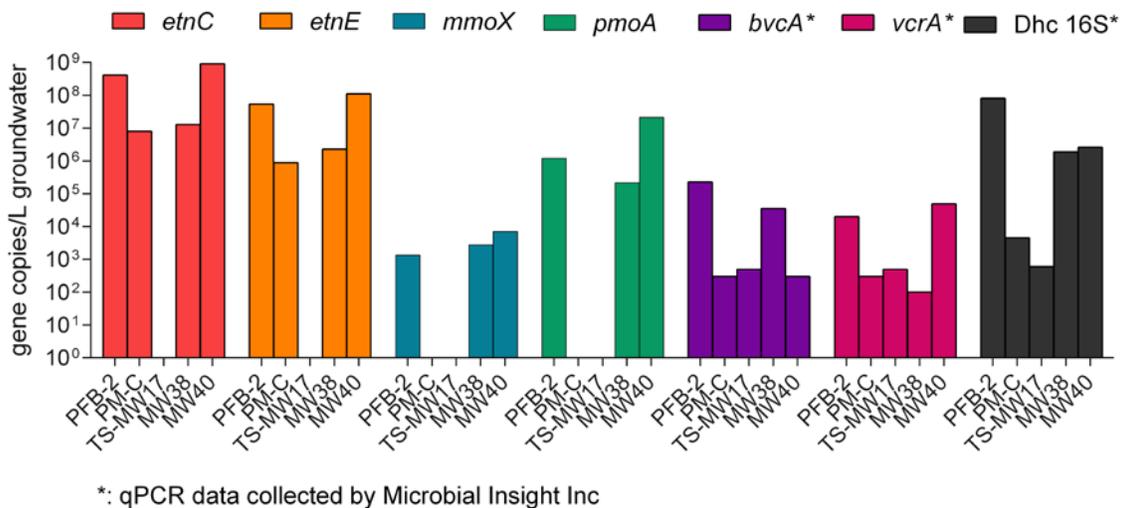
Figure 31. Abundance of *etnC, etnE, mmoX, pmoA, bvcA, vcrA*, and total Dehalococcoides 16S Genes (Dhc 16S) from the 2014 Sampling Event.

Note that bvcA, vcrA, and Dhc 16S were measured by Microbial Insights, Inc.

75

Based on the encouraging preliminary results shown in **Figure 31**, we obtained additional samples from site LF05 from 3 sampling events occurring over a 6-month period (September 2015 – March 2016). Additional wells were sampled during the March 2016 event that cover two potential VC plume transects (**Figure 32**). The VC concentration decreases with distance along these two transects (**Figure 33**).
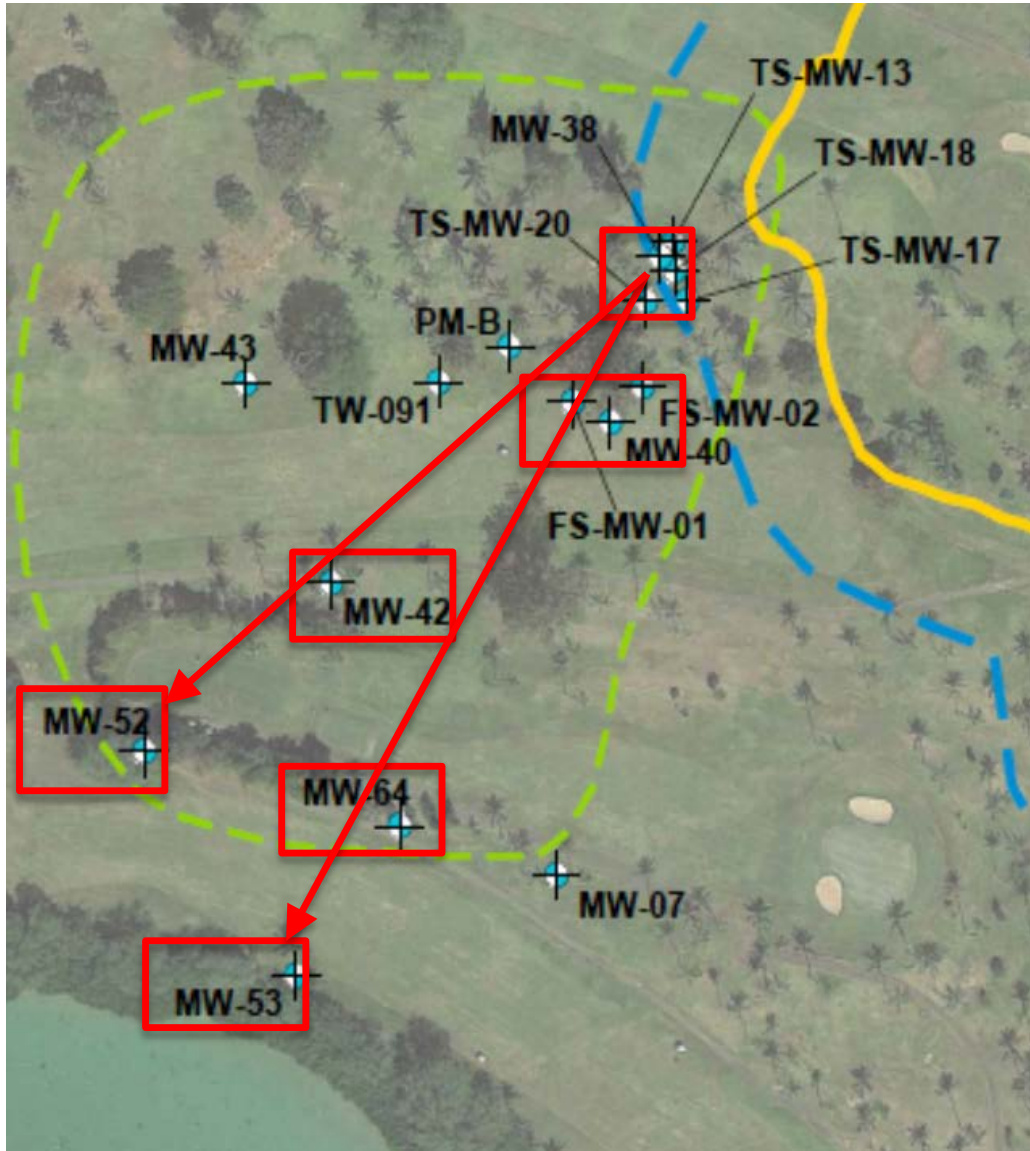
Figure 32. This is a Site Map Depicting the VC Plume Extent at Site LF05 (Green Dashed Line), Locations of the Monitoring Wells TS-MW-18, MW-40, MW-42, MW-52, MW-64, and MW-53 As Well As Two Possible VC Plume Transects Shown by the Red Arrows.
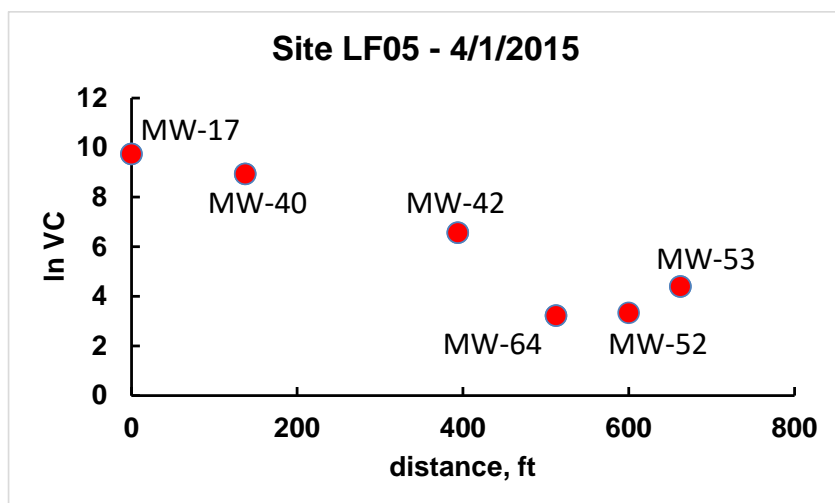
Figure 33. Plot of ln VC Concentration vs. Distance for Six Monitoring Wells Along Two Potential VC Transects at Site LF05.

These values will be used to estimate bulk VC attenuation rates for the performance assessment. VC data from April 2015 sampling event.

Abundance and activity of VC degrading bacterial functional genes for the 3 sampling events are shown in **Figure 34 - Figure 36**. These results reveal that in wells MW01, MW02, MW13, MW17, and MW20, which reside in the areas where the highest VC concentrations were observed, etheneotrophs were highly abundant and active (Sept 2015 and Dec. 2015 sampling events). Methanotrophs were generally much less abundant and active, although *pmoA* gene expression was elevated in Dec. 2015. VC reductive dehalogenase gene expression (*vcrA* in particular) was also elevated in well MW01 (Sept. 2015) and wells MW01, MW13, and MW17 (Dec. 2015). These results are yet again another indication that VC oxidation and VC reduction processes can occur in relatively close proximity to each other (i.e. observed in the same groundwater sample).
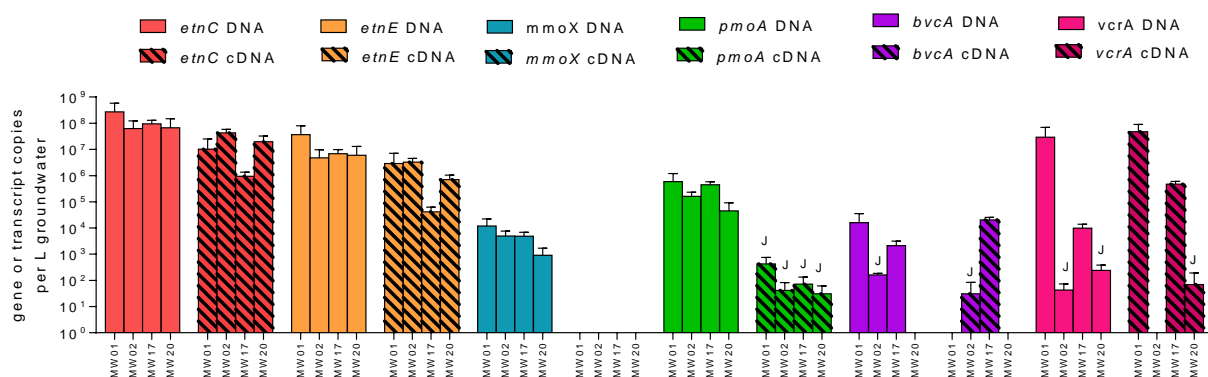
Figure 34. Abundance of *etnC, etnE, mmoX, pmoA, bvcA,* and *vcrA* (Genes and Transcripts) in the VC Plume at Joint Base Pearl Harbor Hickam Site LF05.

Groundwater from 4 monitoring wells was sampled in September 2015. Data points labeled with "J" indicate estimated values as amplification was detected but the result was below our qPCR quantification limits.
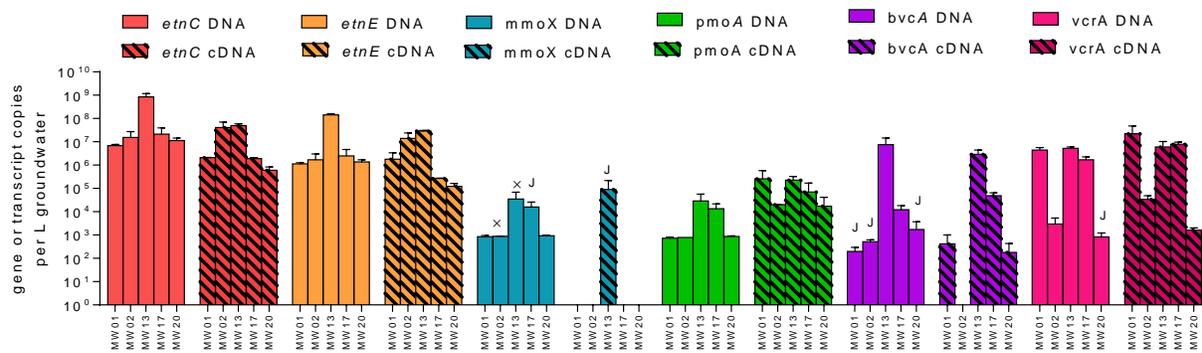
Figure 35. Abundance of *etnC, etnE, mmoX, pmoA, bvcA,* and *vcrA* (Genes and Transcripts) in the VC Plume at Joint Base Pearl Harbor Hickam site LF05.

Groundwater from 5 monitoring wells was sampled in December 2015. Data points labeled with "J" indicate estimated values as amplification was detected but the result was below our qPCR quantification limits. Data points labeled with "×" indicates that the value is likely overestimated because non-specific amplicons and/or primer dimers were detected during QA/QC procedures.

For the March 2016 sampling event we obtained samples across the VC plume transect. This revealed a pattern of decreasing abundance of VC-oxidizers as VC concentrations decreased. VC dechlorinators were restricted to the areas of higher VC concentrations (wells MW18 and MW42) and were not observed further downgradient (Figure 36). VC degrader activity was sporadic along the VC plume. However, possible technical issues (some RNA filters were inadvertently frozen at -80C, which can lead to significant RNA losses) could be masking the true activity.
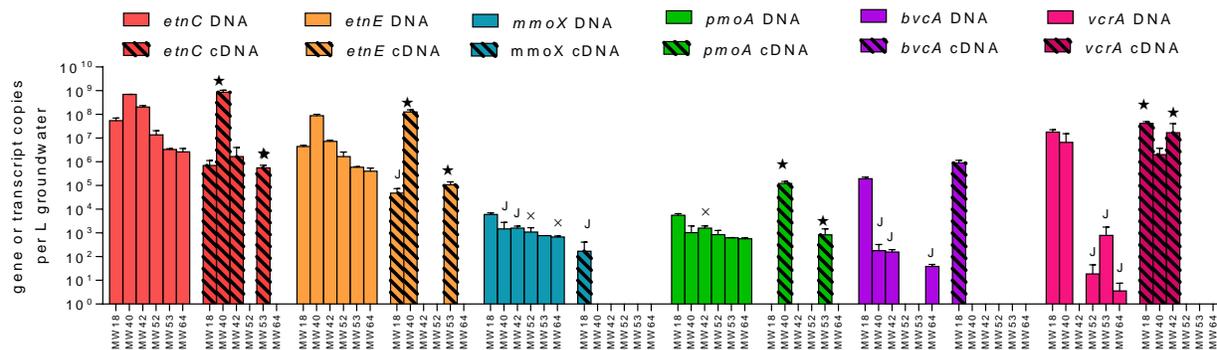
Figure 36. Abundance of *etnC, etnE, mmoX, pmoA, bvcA,* and *vcrA* (Genes and Transcripts) in the VC Plume at Joint Base Pearl Harbor Hickam site LF05.

Groundwater from 6 monitoring wells was sampled in March 2016. Data points labeled with "J" indicate estimated values as amplification was detected but the result was below our qPCR quantification limits. Data points labeled with "×" indicates that the value is likely overestimated because non-specific amplicons and/or primer dimers were detected during QA/QC procedures. Data points labeled with a star indicates that the value is likely overestimated because amplification was observed in the RNA qPCR controls (i.e. there was DNA contaminating the RNA extracts).

Site LF05 Hawaii sampling event in September 2016

We obtained groundwater from five monitoring wells near the source zone (MW01, MW02, MW13, MW17, and MW20) in September 2016 at Site LF05 Hawaii. The abundances of genes and transcripts for etheneotrophs, methanotrophs and VC-dechlorinating populations were analyzed and are presented in **Figure 37** and **Figure 38**.
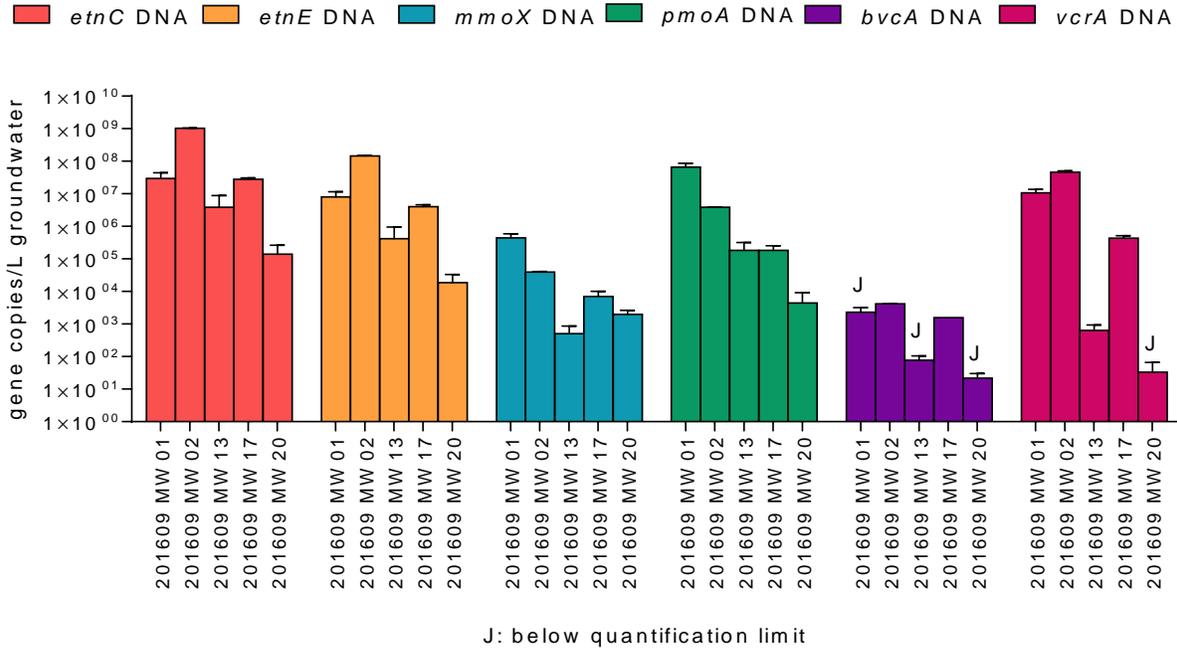
Figure 37. Abundance of *etnC, etnE, mmoX, pmoA, bvcA,* and *vcrA* (genes) in the VC Plume at Joint Base Pearl Harbor Hickam Site LF05.

Groundwater from 5 monitoring wells was sampled in September 2016. Data points labeled with "J" indicate estimated values as amplification was detected but the result was below our qPCR quantification limits.
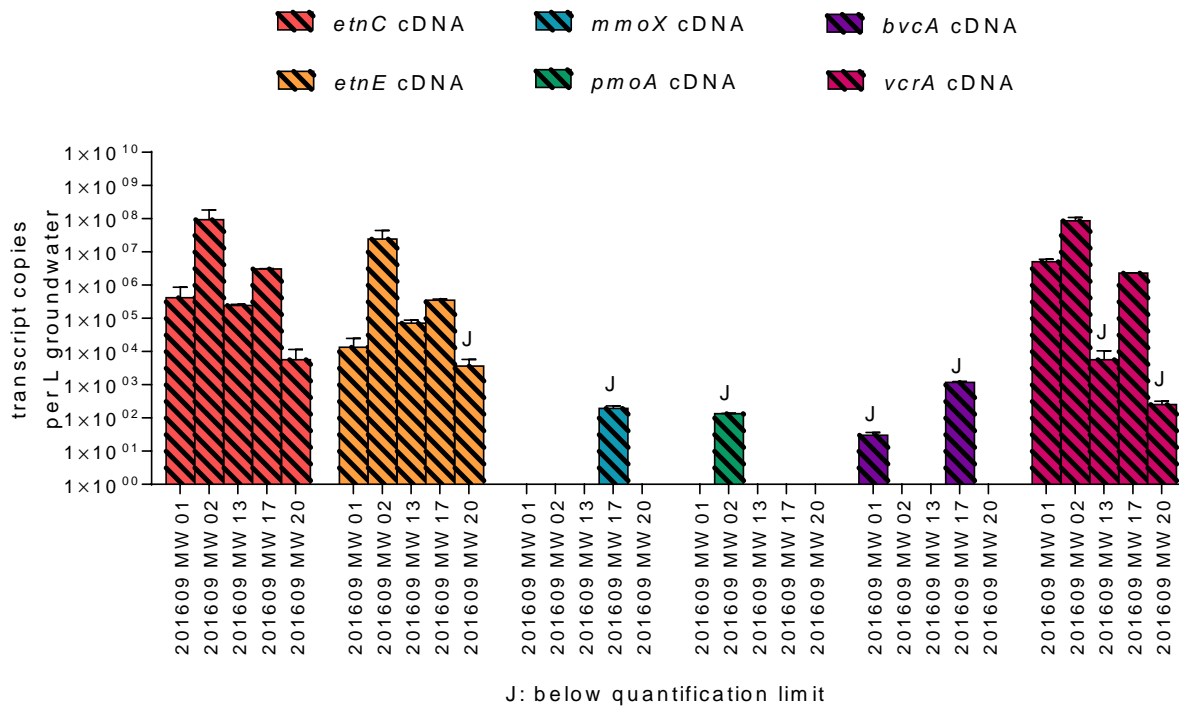
Figure 38. Abundance of *etnC, etnE, mmoX, pmoA, bvcA,* and *vcrA* (transcripts) in the VC Plume at Joint Base Pearl Harbor Hickam Site LF05.

Groundwater from 5 monitoring wells was sampled in September 2016. Data points labeled with "J" indicate estimated values as amplification was detected but the result was below our qPCR quantification limits.

To summarize, the results of September 2016 sampling event suggested that etheneotrophs and *Dehalococcoides* carrying *vcrA* were more abundant and active at Site LF05, while methanotrophs and *Dehalococcoides* carrying *bvcA* were relatively less active. This observation was consistent with previous results from 2015 and 2016 sampling events. This data adds to the dataset we have been developing which shows relationships between functional gene abundance and expression and geochemical parameters.

5.6.8   MCRD Parris Island, SC Site 45 sampling results

5.6.8.1   *Groundwater sampling results*

Monitoring wells are screened off in two sections of the surficial aquifer – in the Upper Surficial Aquifer (7 ft depth), and in the Lower Surficial Aquifer (15 ft depth). Upper surficial aquifer wells are designated with "SU", while lower surficial aquifer are designated with "SL". There are also several multi-level "ML" wells (19.5 ft depth) and performance monitoring wells (PMW; 19 ft depth) that span over the entire surficial aquifer. These were installed during an ESTCP demonstration by Geosyntec (ER-0431).

Two distinct chloroethene plumes exist at Parris Island Site 45 - the northern plume and the southern plume. VC concentrations in these two plumes range from non-detect (at the fringe) to >50,000 µg/L in ML2 in the source zone of the northern plume (measured June 2016). The VC plumes attenuate quite rapidly, possibly because of the presence of several stormwater drains in the flow path of the plumes. According to a previous report, groundwater appears to enter the storm sewers at several locations. These sewers are hydraulically connected to tidally influenced Ballast Creek and this appears to affect the water levels in several of the monitoring wells (Vroblesky, *et al.*, 2009). A site map showing the northern VC plume in the lower surficial aquifer along a transect of several monitoring wells is shown in **Figure 39**. A plot of ln VC concentration vs. distance in the northern plume (**Figure 40**) shows the VC concentration steadily decreases with distance. The yellow lines show the location of the stormwater conduits that intersect the plume. A transect of southern plume monitoring wells is shown in **Figure 53**. Ballast creek water entering the storm sewers around site 45 at high tide can act as a source of dissolved oxygen to the VC plume in several wells, particularly MW20 and MW04 in the southern VC plume

Parris Island site 45 has hosted several pilot scale remediation demonstrations since 2006. Geosyntec performed a demonstration of Emulsified Zero-Valent Nano-Scale Iron Treatment in the northern plume source zone from 2006-2010 (Project ER-0431). EPA performed an In situ Chemical Oxidation pilot scale project in the southern plume from 2013-2014 (Project 640). Finally CH2M performed an emulsified vegetable oil pilot scale injection in the northern plume from late 2014-early 2015 (Project JM13). Groundwater samples collected during pilot studies between 2013 and 2015 were sent to Microbial Insights for molecular biology analysis. In collaboration with Mike Singletary (NAVFAC) we obtained archived DNA samples from these events (six time points - June 2013, April 2014, Nov. 2014, Dec. 2014, Jan. 2015 and Feb 2015). We performed qPCR analysis on these samples with our suite of VC oxidation functional genes from methanotrophs (*pmoA* and *mmoX*) and etheneotrophs (*etnC* and *etnE*), as well as for VC reductive dehalogenase genes *bvcA* and *vcrA*.

The University of Iowa performed its first sampling event in October 2015. We collected field measured groundwater geochemical parameters (temp, pH, DO, ORP) during groundwater sampling. Groundwater samples were also measured for chloroethenes (PCE, TCE, DCEs, and VC), methane, ethene, ethane, and chloride. Sterivex filters samples were taken for DNA and RNA extraction and subsequent qPCR analysis for methanotrophs, etheneotrophs, and VC dechlorinators.
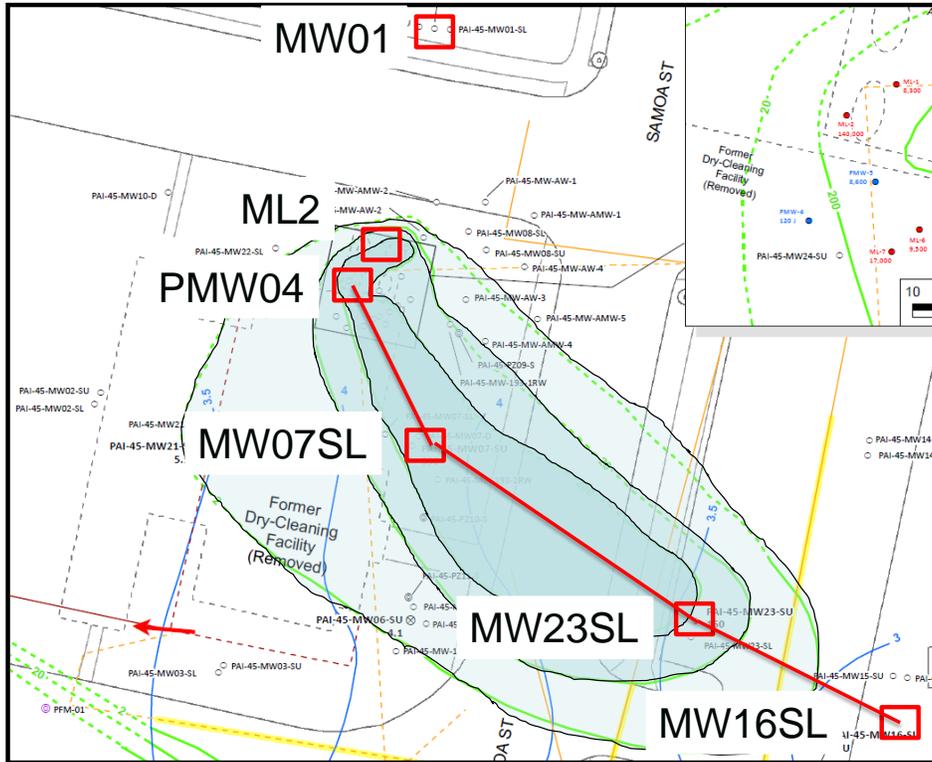
Figure 39. Site Map Showing the Northern VC Plume in the Lower Surficial Aquifer Along with the Location of Monitoring Wells Along a Plume Transect.

Green lines indicate the VC isoconcentration contours in 2012. Each of these wells shown was sampled by University of Iowa personnel in October 2015. The MW01 wells are located upgradient from the source zone and are considered as control wells that will exhibit background functional gene abundances.
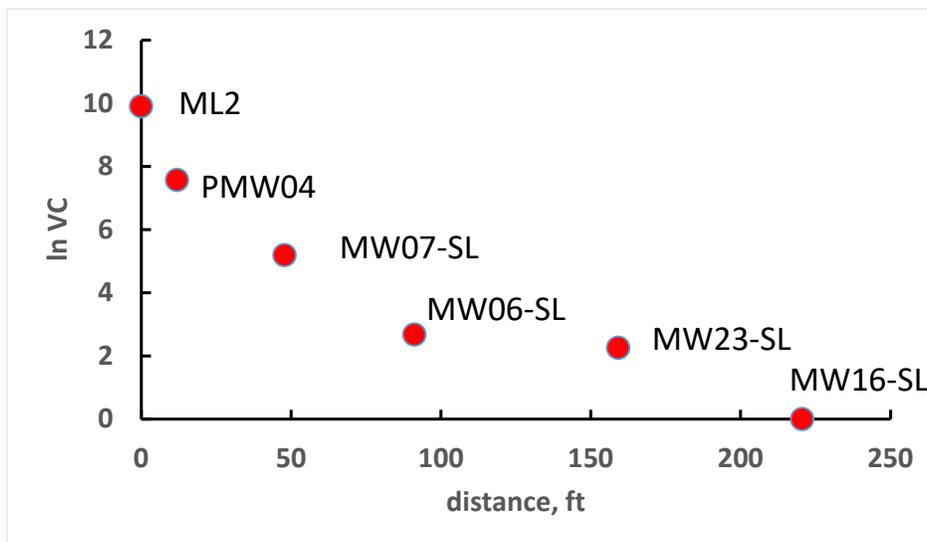
Figure 40. ln VC vs. Distance for a Transect of Parris Island Site 45 Northern Plume Monitoring Wells.

All qPCR data collected from northern plume wells from April 2014-October 2015 is shown in **Figure 41** through **Figure 50**. Inspection of the graphs reveals essentially the same spatial trends in functional gene abundance from the source area out to the plume fringes. These trends are as follows:

1. The abundance of methanotrophs is relatively lower near the source zone and consistently increases towards the VC plume fringe

2. The abundance of VC dechlorinators is higher near the source zone and rapidly decreases as the plume moves away from the source.

3. The abundance of etheneotrophs is relatively higher near the source zone and consistently decreases towards the VC plume fringe

Statistical analyses of these trends will be conducted in Section 6.0 with a subset of this data in order to address performance objectives associated with spatial distribution.

Methanotrophs are known to be susceptible to toxic effects of VC and VC epoxide (Van Hylckama, *et al.*, 1997, Freedman, *et al.*, 2001). It is possible that methanotrophs are more inhibited by VC (and perhaps increased formation of VC epoxide via oxidation) in the high VC concentration portions of the plume than etheneotrophs. TCE and cDCE are also present – methanotrophs are presumably subject to their toxicity as well as the toxicity of fortuitous transformation products (Van Hylckama, *et al.*, 1997) in the subsurface at this site. However, the fringes of the plume where other chloroethenes are dilute or not present, VC contamination is less intense, and DO levels are higher, appear to be a more favorable environment for growth of methanotrophs. This is confirmed in the RT-qPCR data (**Figure 48** and **Figure 50**), which shows relatively low expression of methanotroph functional genes in the majority of the VC plume with expression increasing at the plume fringes.

Anaerobic VC dechlorinators, as expected, prefer the high VC concentration portions of the plume, where there are lower DO values. The activity of VC dechlorinators was confirmed in a few wells where the highest VC concentrations were observed. However, the trend in etheneotroph abundance and activity was the most surprising, with the highest concentrations in the higher VC concentration portions of the plume. ***It is possible that the environmental conditions in this portion of the plume favor the growth of VC-assimilating bacteria.*** Etheneotrophs should be more tolerant to higher VC concentrations than methanotrophs for two primary reasons. First, they already contain an enzyme (encoded by *etnE*) that can detoxify VC epoxide (methanotrophs do not possess this enzyme). The toxicity of cDCE, TCE and their epoxides has not been tested on etheneotrophs. However, their elevated abundance in portions of the VC plume that also contain cDCE and TCE suggests that etheneotrophs are more resistant to chloroethene toxicity than methanotrophs. Second, many etheneotrophs can adapt to VC as a growth substrate. Ethene detections in the northern VC plume are sporadic and the concentrations are low. DO is also low, but etheneotrophs are known degrade VC at very low oxygen tensions well below the limit of detection of field DO meters (Coleman, *et al.*, 2002b, Gossett, 2010). There are several factors at this site that could promote aerobic activity – shallow depth to groundwater, tidally influenced storm sewers at the plume fringe and an abundance of monitoring wells that could serve as oxygen conduits at depth.
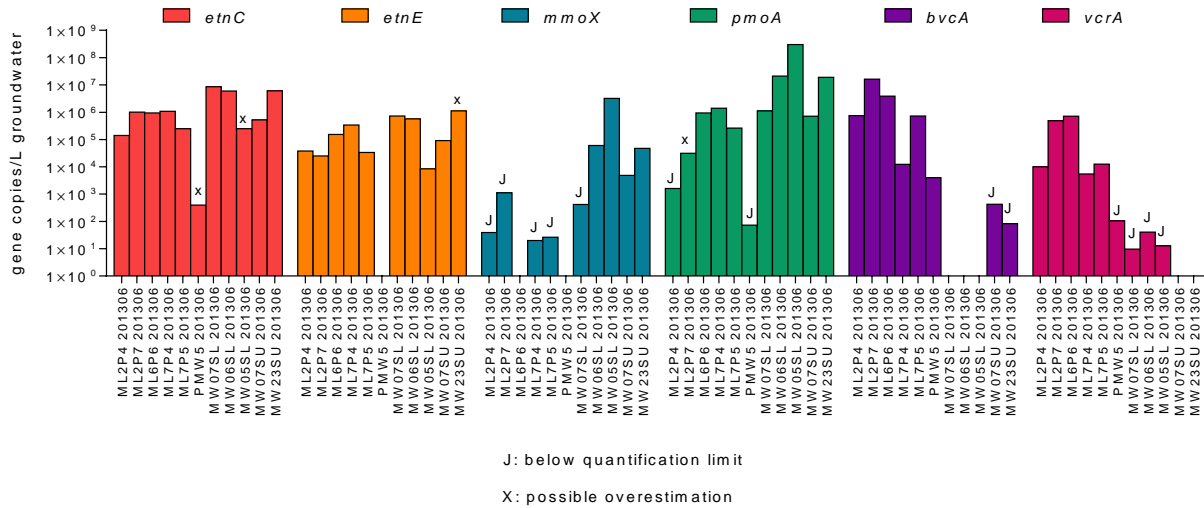
Figure 41. Abundance of *etnC, etnE, mmoX, pmoA, bvcA,* and *vcrA* in Northern VC Plume Monitoring Wells Sampled in June 2013.

The wells sampled are ordered from left to right approximately in the order of higher to lower VC concentrations along the plume. DNA samples were obtained from Microbial Insights, Inc. Data points labeled with "J" indicate estimated values as amplification was detected but the result was below our qPCR quantification limits. Data points labeled with an "×" indicates that the value is likely overestimated because non-specific amplicons and/or primer dimers were detected during QA/QC procedures.
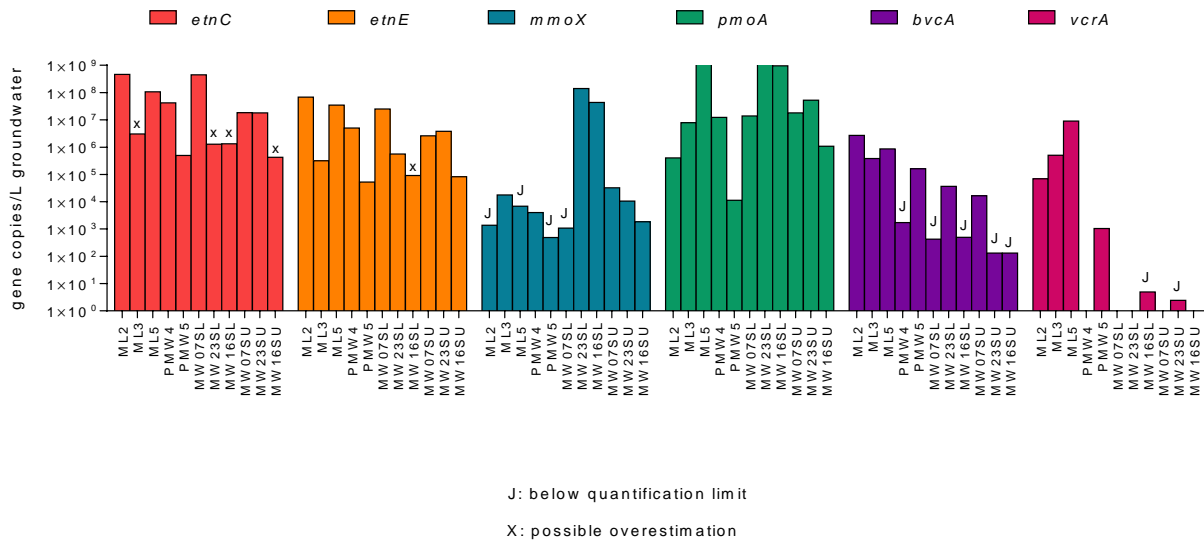
Figure 42. Abundance of *etnC, etnE, mmoX, pmoA, bvcA,* and *vcrA* in the Northern VC Plume Wells Sampled in April 2014.

The wells sampled are ordered from left to right approximately in the order of higher to lower VC concentrations along the plume. DNA samples were obtained from Microbial Insights, Inc. Data points labeled with "J" indicate estimated values as amplification was detected but the result was below our qPCR quantification limits. Data points labeled with an "×" indicates that the value is likely overestimated because non-specific amplicons and/or primer dimers were detected during QA/QC procedures.

84
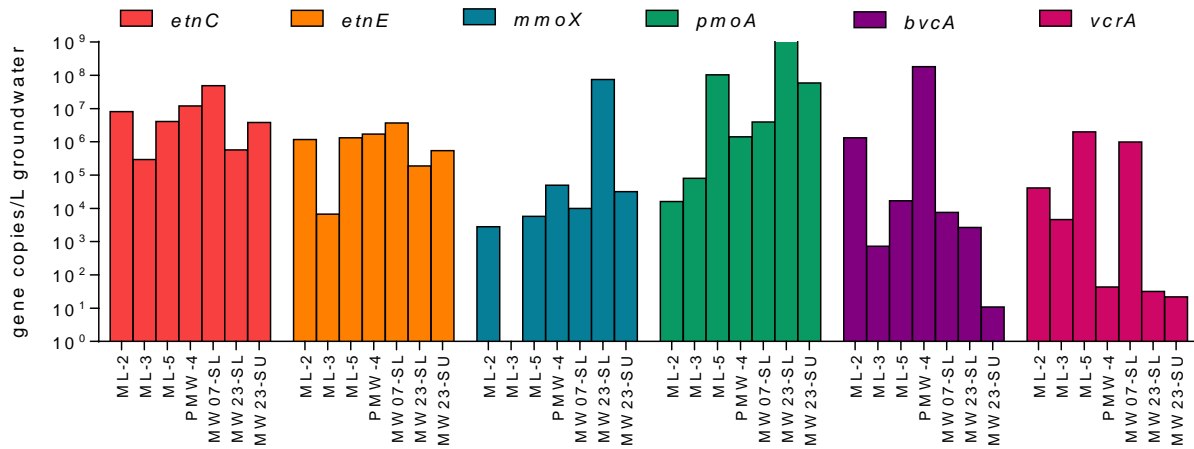
Figure 43. Abundance of *etnC, etnE, mmoX, pmoA, bvcA*, and *vcrA* in Northern VC Plume Monitoring Wells Sampled in November 2014.

The wells sampled are ordered from left to right approximately in the order of higher to lower VC concentrations along the plume. DNA samples were obtained from Microbial Insights, Inc.

74LL 20141218
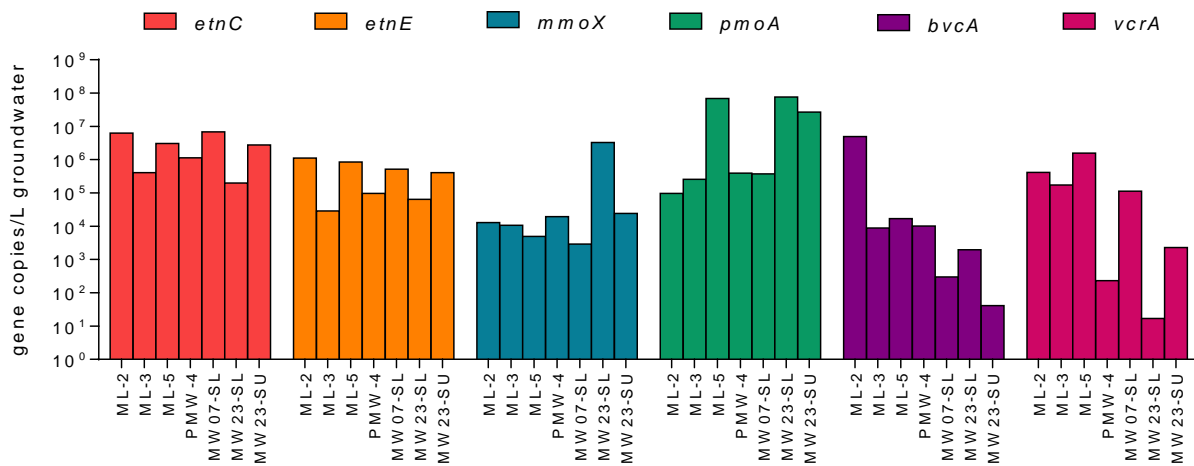
Figure 44. Abundance of *etnC, etnE, mmoX, pmoA, bvcA*, and *vcrA* in Northern VC Plume Monitoring Wells Sampled in December 2014.

The wells sampled are ordered from left to right approximately in the order of higher to lower VC concentrations along the plume. DNA samples were obtained from Microbial Insights, Inc.

39MA 20150115
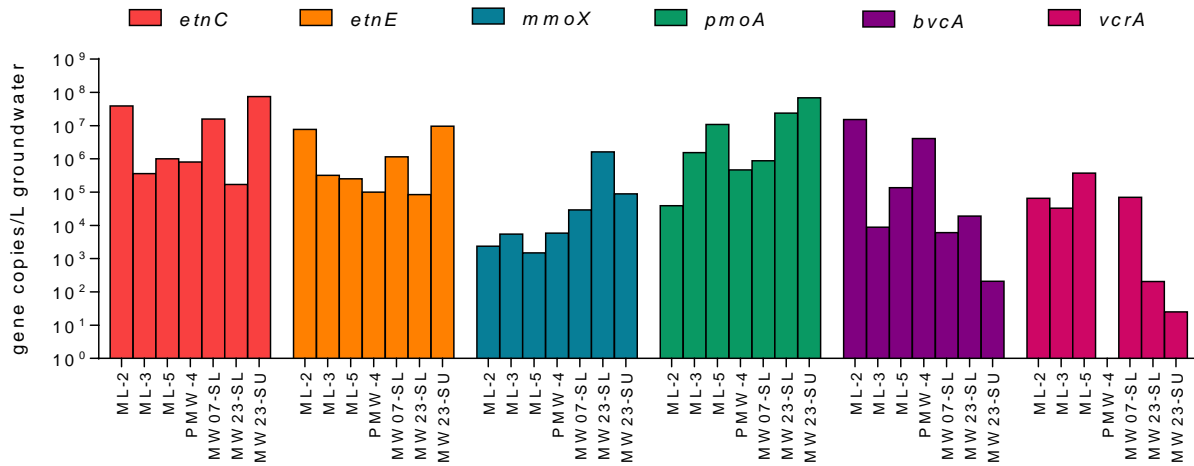
Figure 45. Abundance of *etnC, etnE, mmoX, pmoA, bvcA*, and *vcrA* in Northern VC Plume Monitoring Wells Sampled in January 2015.

The wells sampled are ordered from left to right approximately in the order of higher to lower VC concentrations along the plume. DNA samples were obtained from Microbial Insights, Inc.

62MB 20150225
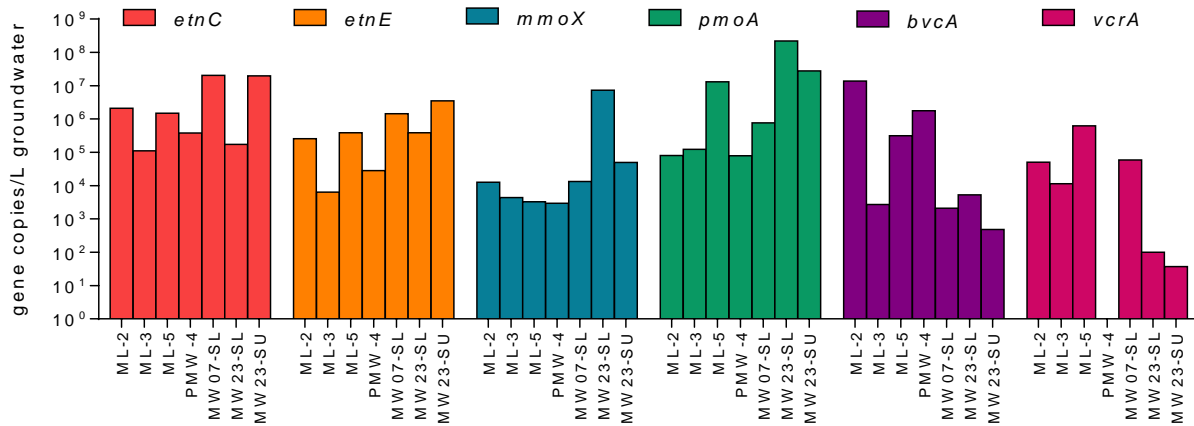
Figure 46. Abundance of *etnC, etnE, mmoX, pmoA, bvcA*, and *vcrA* in Northern VC Plume Monitoring Wells Sampled in February 2015.

The wells sampled are ordered from left to right approximately in the order of higher to lower VC concentrations along the plume. DNA samples were obtained from Microbial Insights, Inc.

86
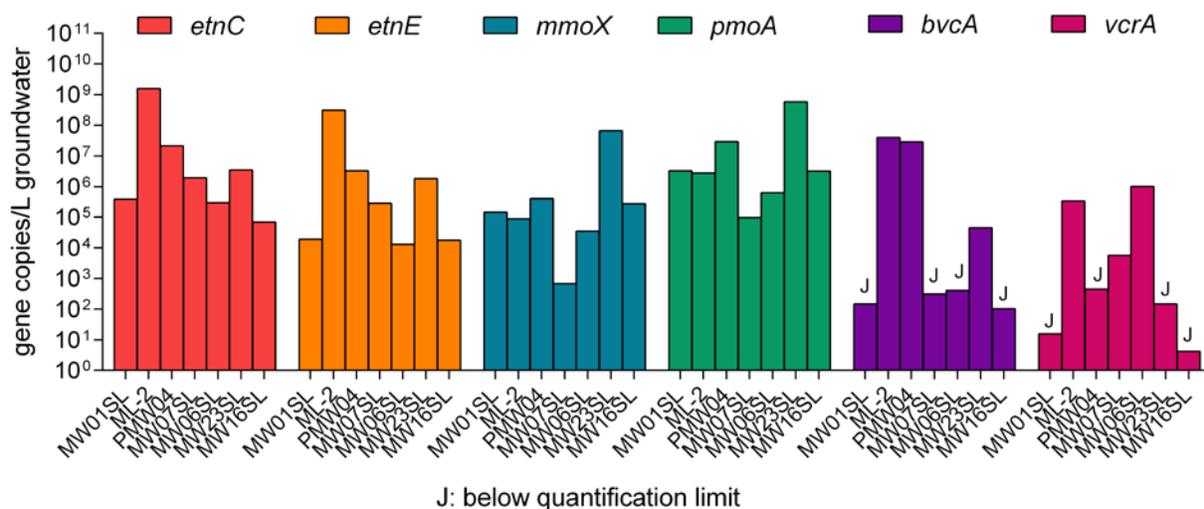
Figure 47. Abundance of *etnC, etnE, mmoX, pmoA, bvcA, and vcrA* in the Northern VC Plume Wells Located in the Lower Surficial Aquifer at Parris Island Site 45.

Groundwater was sampled in October 2015 by University of Iowa personnel. The wells sampled are ordered from left to right approximately in the order of higher to lower VC concentrations along the plume. Data points labeled with "J" indicate estimated values as amplification was detected but the result was below our qPCR quantification limits
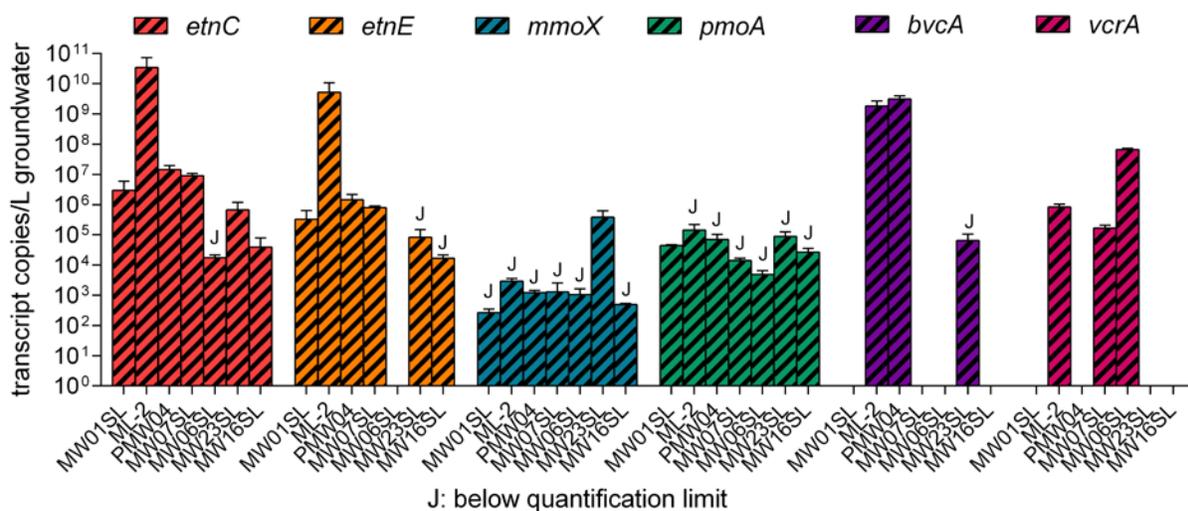
Figure 48. Abundance of *etnC, etnE, mmoX, pmoA, bvcA, and vcrA* Transcripts in the Northern VC Plume Wells Located in the Lower Surficial Aquifer at Parris Island Site 45.

Groundwater was sampled in October 2015 by University of Iowa personnel. The wells sampled are ordered from left to right approximately in the order of higher to lower VC concentrations along the plume. Data points labeled with "J" indicate estimated values as amplification was detected but the result was below our qPCR quantification limits
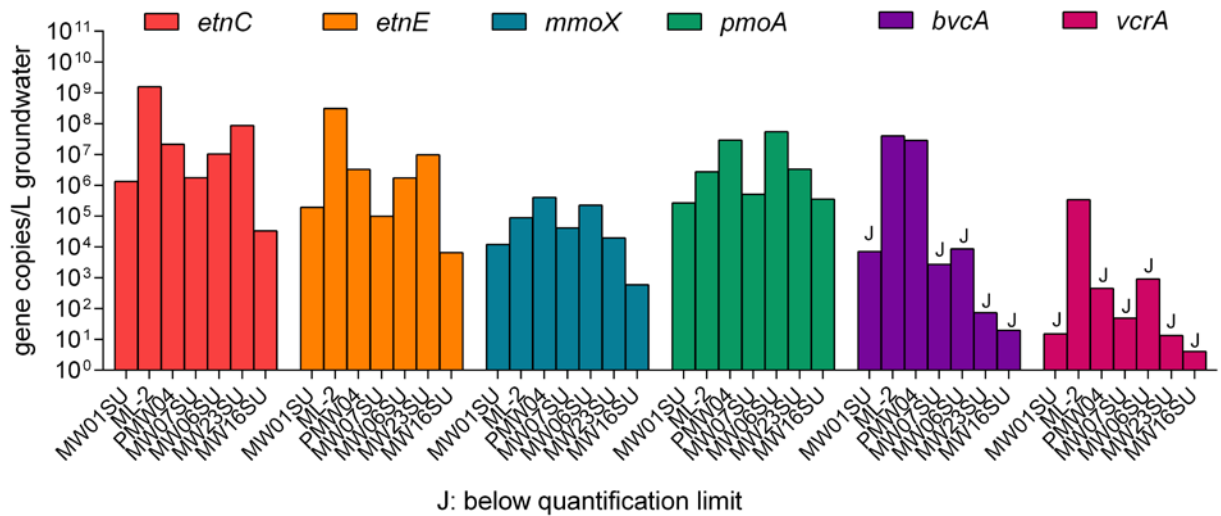
Figure 49. Abundance of *etnC, etnE, mmoX, pmoA, bvcA*, and *vcrA* in the Northern VC Plume Wells Located in the Upper Surficial Aquifer at Parris Island Site 45.

Groundwater was sampled in October 2015 by University of Iowa personnel. The wells sampled are ordered from left to right approximately in the order of higher to lower VC concentrations along the plume. Data points labeled with "J" indicate estimated values as amplification was detected but the result was below our qPCR quantification limits
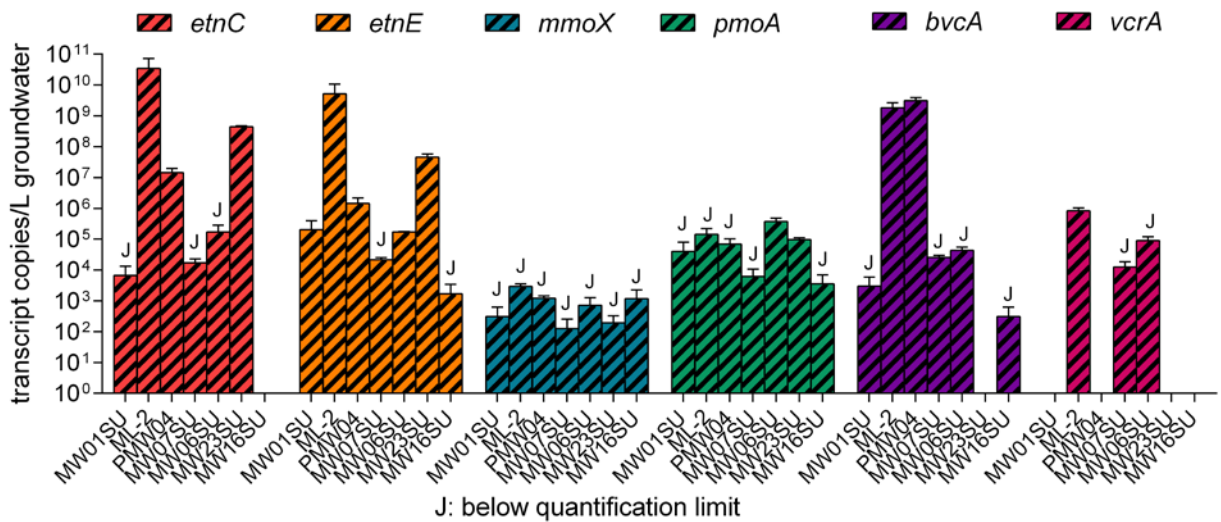
Figure 50. Abundance of *etnC, etnE, mmoX, pmoA, bvcA*, and *vcrA* Transcripts in the Northern VC Plume Wells Located in the Lower Surficial Aquifer at Parris Island site 45.

Groundwater was sampled in October 2015 by University of Iowa personnel. The wells sampled are ordered from left to right approximately in the order of higher to lower VC concentrations along the plume. Data points labeled with "J" indicate estimated values as amplification was detected but the result was below our qPCR quantification limits

Parris Island sampling event July 2016

In July 2016, we collected groundwater samples from the same 20 monitoring wells at Parris Island Site 45 that were also sampled in October 2015. Groundwater samples were analyzed for chlorinated ethenes, volatile gases, chloride, and VC-degrading functional gene and transcript abundances.

PCE and TCE were detected above maximum concentration levels (MCLs) in PMW04, MW07SL, MW25SL, MW31SL, and MW31SU, all of which were within or close to the source zone. Among the three DCE isomers, cis-DCE was primarily formed at Parris Island Site 45 and was detected across the site, while trans-DCE was detected at high level sonly near source zone and 1,1-DCE was only detected in well PMW4. VC was detected in 13 out of 20 monitoring wells, ranging from 0.55 µg/L to 50,400 µg/L. Compared to the October 2015 data, we observed decreases in PCE, increases of TCE and cis-DCE in some monitoring wells near the source zone. VC concentrations were generally lower than in 2015, except for wells ML2, MW23SU, and MW25SL. VC in well MW25SL was not detected in October 2015, but increased to 1170 µg/L in July 2016. The decrease of PCE and corresponding increase of lesser chlorinated ethenes suggested the occurrence of dechlorination and possible migration of chlorinated ethene plumes. Ethene, methane, and ethane were at similar levels as in October 2015.

The abundances of six functional genes (*etnC, etnE, mmoX, pmoA, bvcA, and vcrA*) and their transcripts were quantified in the northern plume wells with qPCR. Functional gene abundance ranges (expressed as gene copies per liter of groundwater) were 1.23×10^5 - 1.44×10^8 (*etnC*), 1.17×10^4 - 3.40×10^7 (*etnE*), 1.79×10^3 - 1.11×10^6 (*mmoX*), 5.51×10^4 - 1.64×10^8 (*pmoA*), $0 - 1.29 \times 10^8$ (*bvcA*), and 0 - 6.38×10^5 (*vcrA*)(**Figure 51**). Transcript abundance ranges (expressed as transcript copies per liter of groundwater) were: 0 - 5.71×10^7 (*etnC*), 0 - 8.41×10^6 (*etnE*), 0 - 2.14×10^4 (*mmoX*), 0 - 2.39×10^5 (*pmoA*), 0 - 4.15×10^8 (*bvcA*), and 0 - 2.95×10^7 (*vcrA*)(**Figure 52**). Abundances of functional genes and transcripts from the July 2016 sampling event varied from the October sampling event. Notably, in MW07SL, significant increases in the abundances of *etnC, etnE* and their transcripts were observed, as well as *bvcA, vcrA* and their transcripts. Methanotroph functional gene abundance (*mmoX* and *pmoA*) increased as well, but their transcript abundances did not. The increase of functional genes and transcripts corresponded to chlorinated ethene concentration decreases in MW07SL (except for TCE).
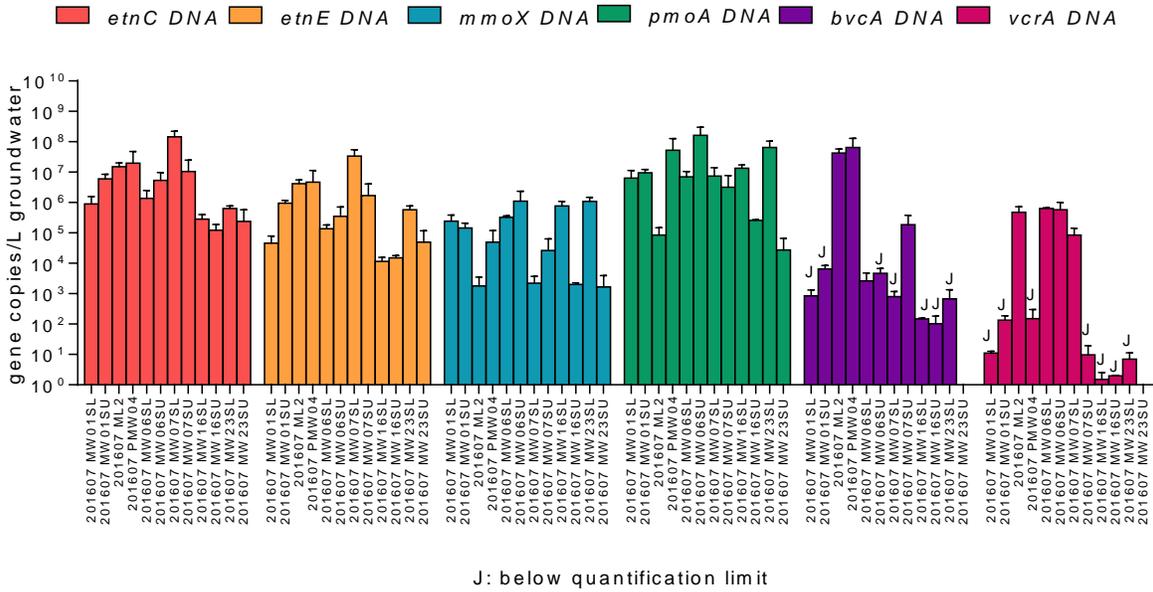
Figure 51. Abundance of *etnC, etnE, mmoX, pmoA, bvcA*, and *vcrA* in the Northern VC Plume Wells Located in the Lower Surficial Aquifer at Parris Island Site 45.

Groundwater was sampled in June 2016 by University of Iowa personnel. The wells sampled are ordered from left to right approximately in the order of higher to lower VC concentrations along the plume. Data points labeled with "J" indicate estimated values as amplification was detected but the result was below our qPCR quantification limits.
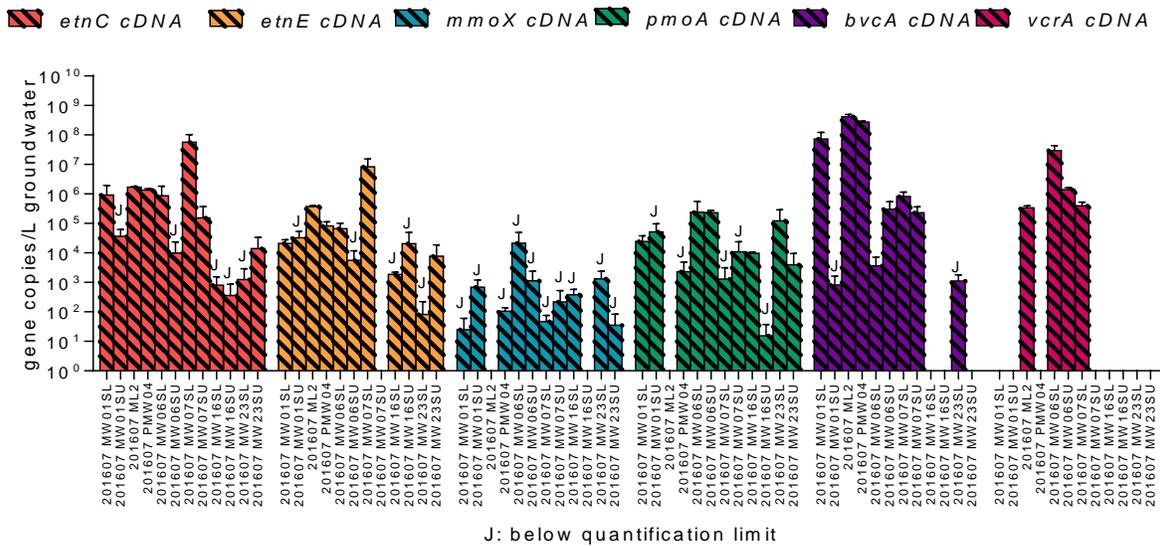
Figure 52. Abundance of *etnC, etnE, mmoX, pmoA, bvcA*, and *vcrA* transcripts in the northern VC plume wells located in the lower surficial aquifer at Parris Island site 45.

Groundwater was sampled in June 2016 by University of Iowa personnel. The wells sampled are ordered from left to right approximately in the order of higher to lower VC concentrations along the plume. Data points labeled with "J" indicate estimated values as amplification was detected but the result was below our qPCR quantification limits.

90

ML2 and PMW4 are two monitoring wells located within the northern plume source zone. From October 2015 to July 2016, PCE and TCE in ML2 decreased from about 10^3 µg/L to non-detectable, while cis-DCE and VC increased from 3.73×10^4 µg/L and 2.01×10^4 µg/L to 8.08×10^4 µg/L and 5.04×10^4 µg/L, respectively. The decrease of PCE and TCE and corresponding accumulation of lesser chlorinated ethenes suggested reductive dechlorination was occurring in ML2. We also found a relatively large decrease in the abundances of etheneotroph functional genes (*etnC* and *etnE*) and their transcripts in ML2 from October 2015 to July 2016. In PMW4, decrease in PCE, VC and increase in TCE, cis-DCE and trans-DCE were observed, suggesting possible dechlorination of higher chlorinated ethenes and degradation of VC. Etheneotroph functional genes (*etnC, etnE*) and their transcripts, as well as *bvcA*, increased in PMW4, suggesting a link with the observed VC concentration decrease in the groundwater.

Figure 53 depicts the lower surficial aquifer of south VC plume and the locations of wells MW25SU, MW31SU, MW04SU, MW20SU, and MW26SU. A plot of ln VC vs. distance is shown in **Figure 54**. The abundance and activity of *etnC*, *etnE*, *mmoX*, *pmoA*, *bvcA and vcrA* in those wells is shown in **Figure 55** to **Figure 59**. Once again, a similar pattern was observed where etheneotrophs were more abundant in portions of the plume where VC concentrations were higher, and decreased where the plume becomes more diluted. Also, methanotroph functional genes displayed a similar pattern where abundances were relatively low where VC concentrations were high, and were relatively more abundant where VC concentrations were lower. Anaerobic VC reductive dehalogenase gene abundance and activity was only seen in the MW31 monitoring wells.
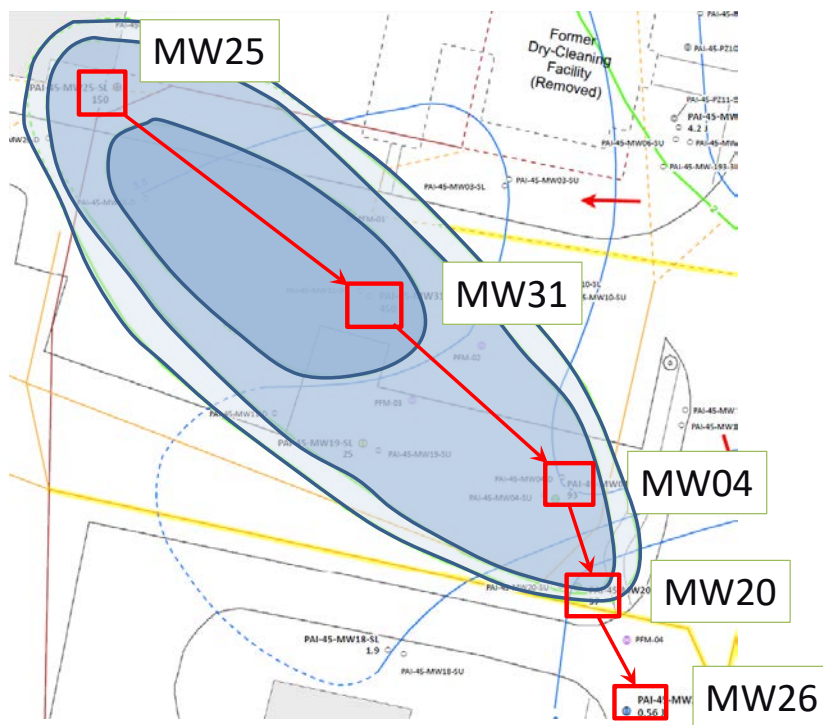
Figure 53. The Southern VC Plume at Parris Island Site 45, Showing the Location of 5 Monitoring Wells MW25, MW31, MW04, MW20, MW26 Along a Plume Transect.

The plume is moving in the general direction of the arrows. Shading indicates the VC isoconcentration contours estimated in 2012.
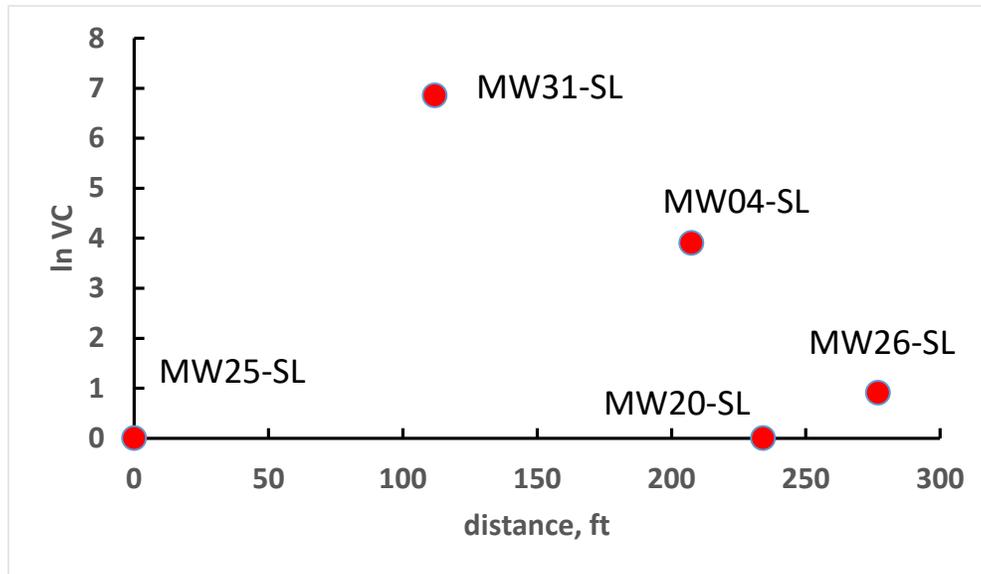
Figure 54. ln VC vs. Distance for a Transect of Southern Plume Monitoring Wells.

VC concentrations were not detected in well MW25-SL due to the presence of permanganate. The rest of the transect shows a clear trend downwards in VC concentration with distance.
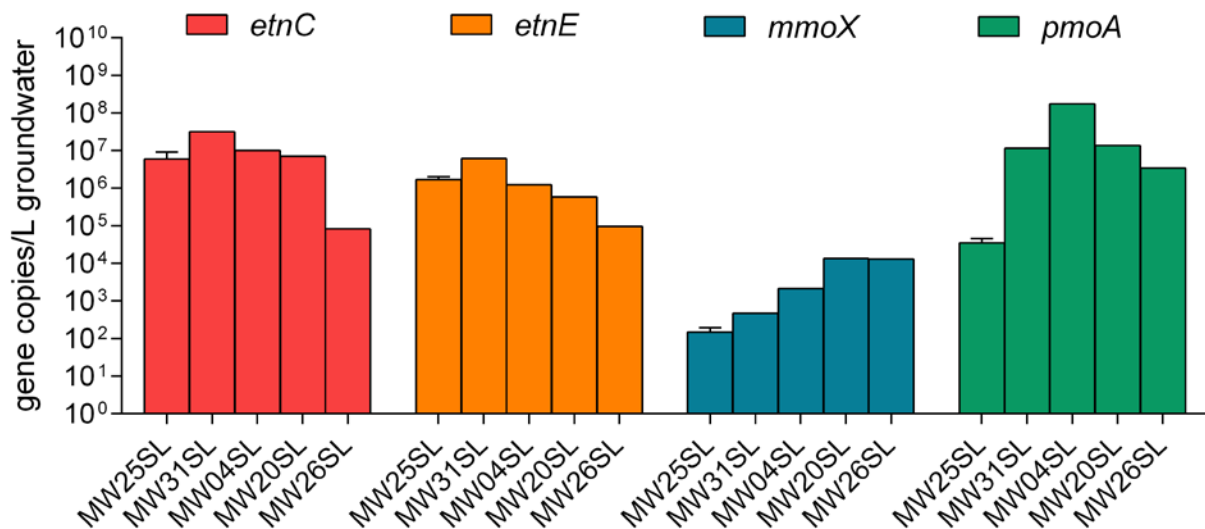
Figure 55. Abundance of *etnC, etnE, mmoX and pmoA* in southern VC plume in the lower surficial aquifer along a transect that includes wells MW25SL, MW31SL, MW04SL, MW20SL, and MW26SL.

Groundwater was sampled June 2013.
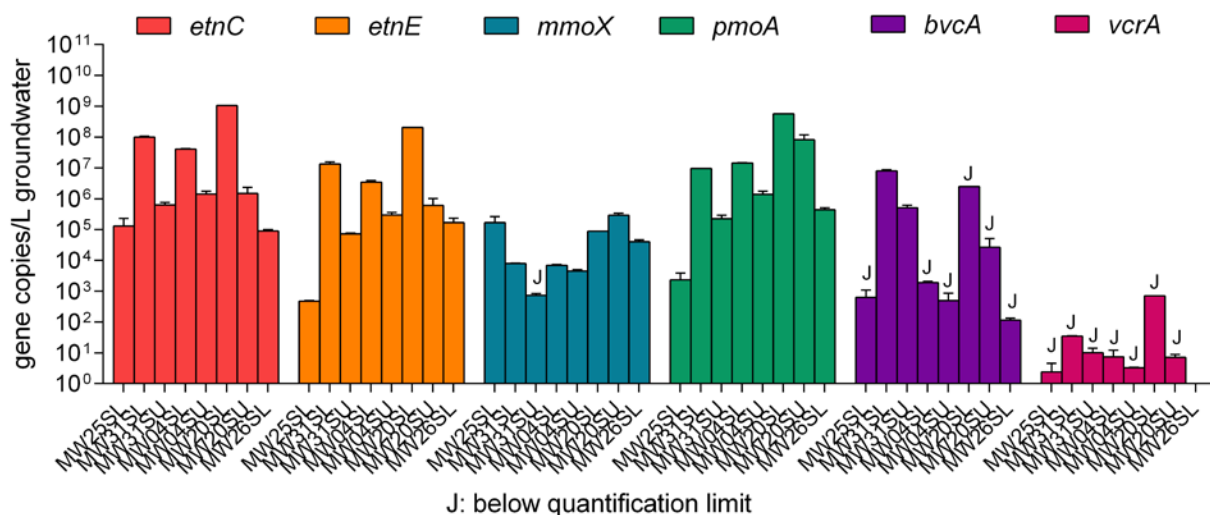
Figure 56. Abundance of *etnC, etnE, mmoX, pmoA, bvcA*, and *vcrA* in the Southern VC Plume Wells Located in Both the Upper (SU) and Lower (SL) Surficial Aquifers at Parris Island Site 45.

Groundwater was sampled in October 2015 by University of Iowa personnel. The wells sampled include several of the multi-levels wells in the source zone as well as monitoring wells out along the plume. Data points labeled with "J" indicate estimated values as amplification was detected but the result was below our qPCR quantification limits
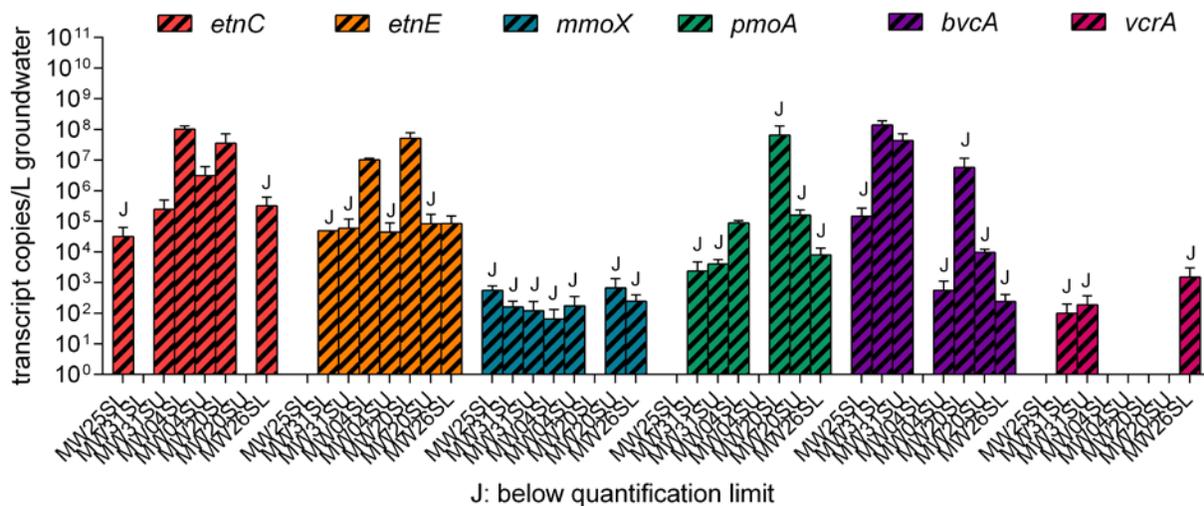
Figure 57. Abundance of *etnC, etnE, mmoX, pmoA, bvcA,* and *vcrA* Transcripts in the Southern VC Plume Wells Located in Both the Upper and Lower Surficial Aquifers at Parris Island Site 45.

Groundwater was sampled in October 2015 by University of Iowa personnel. The wells sampled include several of the multi-levels wells in the source zone as well as monitoring wells out along the plume. Data points labeled with "J" indicate estimated values as amplification was detected but the result was below our qPCR quantification limits

93

2016 sampling event - MW25SL is close to the source zone of the southern plume and displayed decreases in PCE, TCE and increases in cis-DCE and VC. However, the DNA and RNA extraction of MW25SL was not successful, probably because of the interference of magnesium oxide precipitates originating from permanganate (which was injected into this well in a previous EPA pilot study).
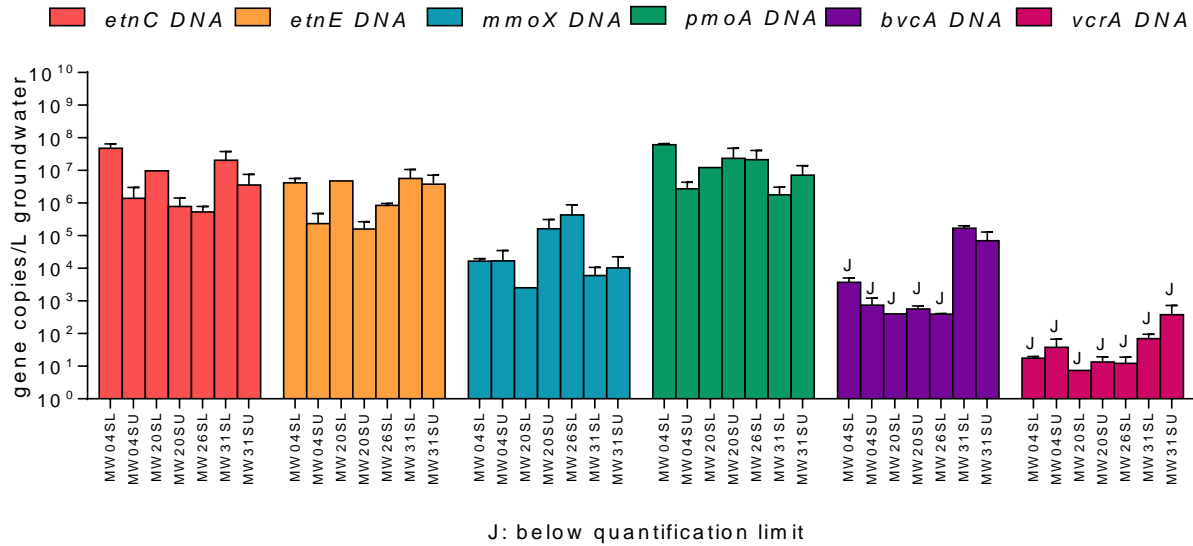
Figure 58.   Abundance of *etnC, etnE, mmoX, pmoA, bvcA,* and *vcrA* in the Southern VC Plume Wells Located in Both the Upper and Lower Surficial Aquifers at Parris Island site 45.

Groundwater was sampled in June 2016 by University of Iowa personnel. The wells sampled include several of the multi-levels wells in the source zone as well as monitoring wells out along the plume. Data points labeled with "J" indicate estimated values as amplification was detected but the result was below our qPCR quantification limits.
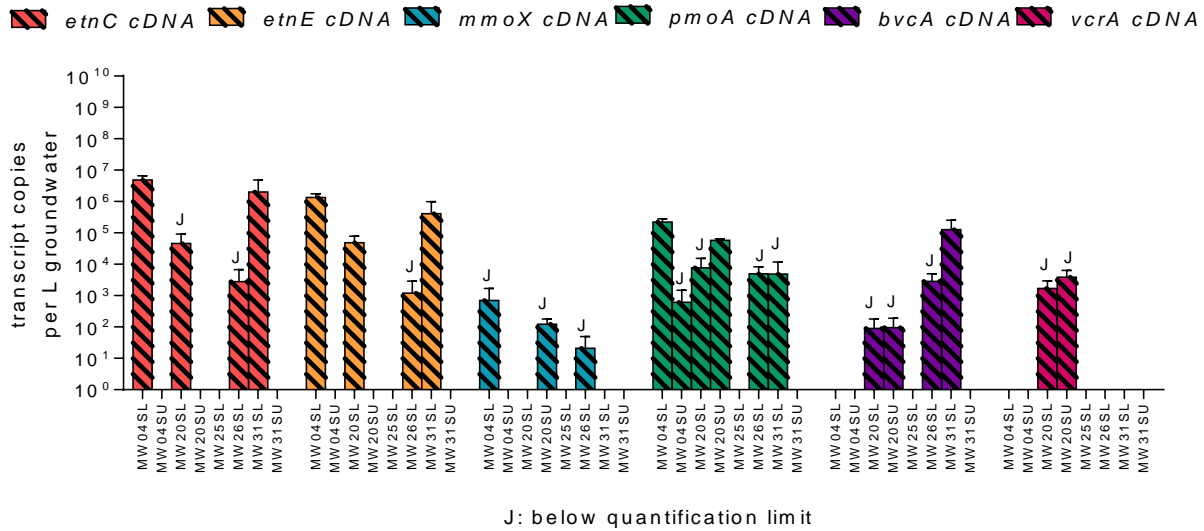
Figure 59. Abundance of *etnC, etnE, mmoX, pmoA, bvcA*, and *vcrA* Transcripts in the Southern VC Plume Wells Located in Both the Upper and Lower Surficial Aquifers at Parris Island Site 45.

Groundwater was sampled in June 2016 by University of Iowa personnel. The wells sampled include several of the multi-levels wells in the source zone as well as monitoring wells out along the plume. Data points labeled with "J" indicate estimated values as amplification was detected but the result was below our qPCR quantification limits.

5.6.8.2 Cryo-core aquifer sediment sampling results

Spatial patterns of VC biodegradation gene abundance and geochemical parameters with depth in sediment samples

Although the simultaneous presence and expression of genes from etheneotrophs and anaerobic VC-dechlorinators in groundwater samples is a novel and important observation that has implications for bioremediation of VC, whether or not aerobic and anaerobic VC0degrading bacteria actually co-occur remains inconclusive. It could be that aquifer material within the influence of monitoring wells contains aerobic and anaerobic microenvironments in close proximity to each other or that mixing of aerobic and anaerobic groundwater zones occurred during sampling. Analysis of aquifer sediment samples was therefore conducted to provide more precise spatial proximity and distribution of aerobic and anaerobic VC-degrading populations. Aquifer sediments were collected from four borehole locations in the northern VC plume at Parris Island site 45 with the cryo-coring technique (**Figure 12**). The surficial aquifer at Parris Island site 45 has an upper unit composed of silt and a lower unit composed of silty sand. These are termed the upper surficial aquifer and the lower surficial aquifer (a diagram of the two hydrogeologic units is shown in **Figure 60**)

Initial geochemical results (cDCE, VC, ethene and methane concentrations) for core 1, located near the PCE source zone, are shown in **Figure 60**. Inspection of **Figure 60** reveals that dissolved chlorinated ethenes are migrating in both the upper and lower surficial aquifers, and that reductive dechlorination of VC to ethene is also occurring in both units.
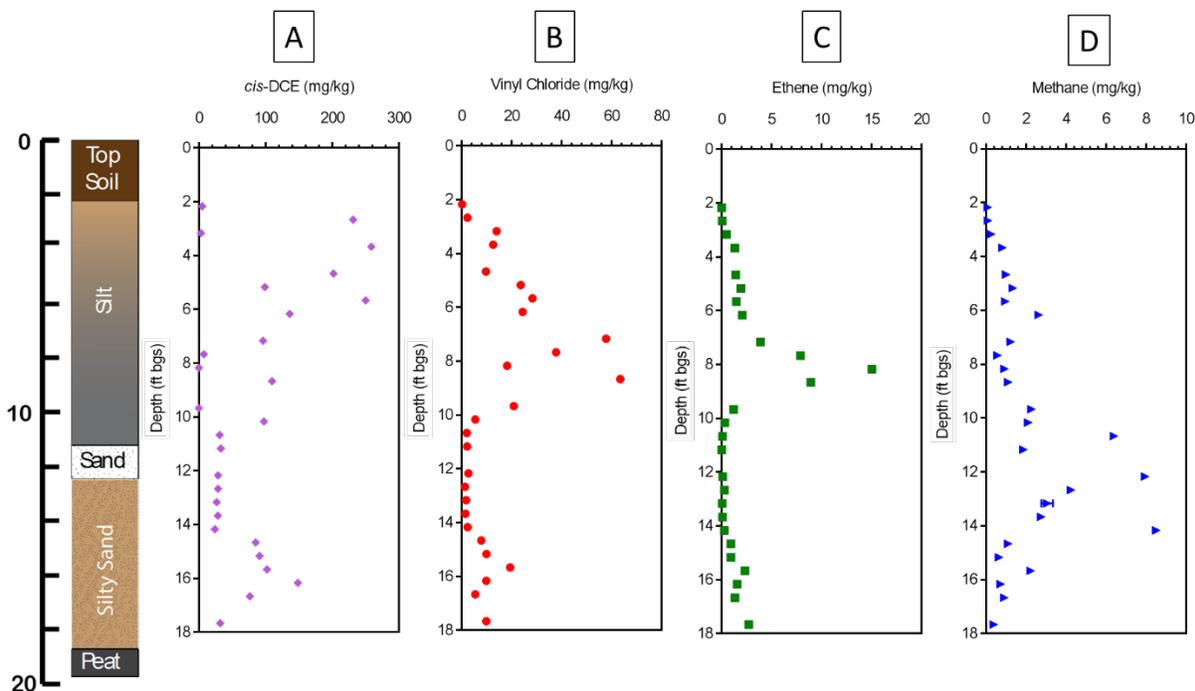
Figure 60. Spatial Resolution of A) cDCE, B) VC, C) Ethene, and D) Methane in Sediment Core 1, Frozen in Place with Liquid Nitrogen, Obtained from Parris Island Site 45.

The graphic on the left shows the soil characteristics of the upper (silt) and lower (silty sand) surficial aquifers.

DNA was extracted from relatively small aquifer sediment samples (~0.25 g) (also within the same 1" cryo-core sections) with the DNeasy PowerSoil kit (Qiagen, Germantown, MD) according to manufacturer's instructions, and qPCR was performed for six functional genes (*etnC*, *etnE*, *mmoX*, *pmoA*, *bvcA*, and *vcrA*), as well as total 16S rRNA genes. The results of this analysis for core 1, is shown in **Figure 61** below.
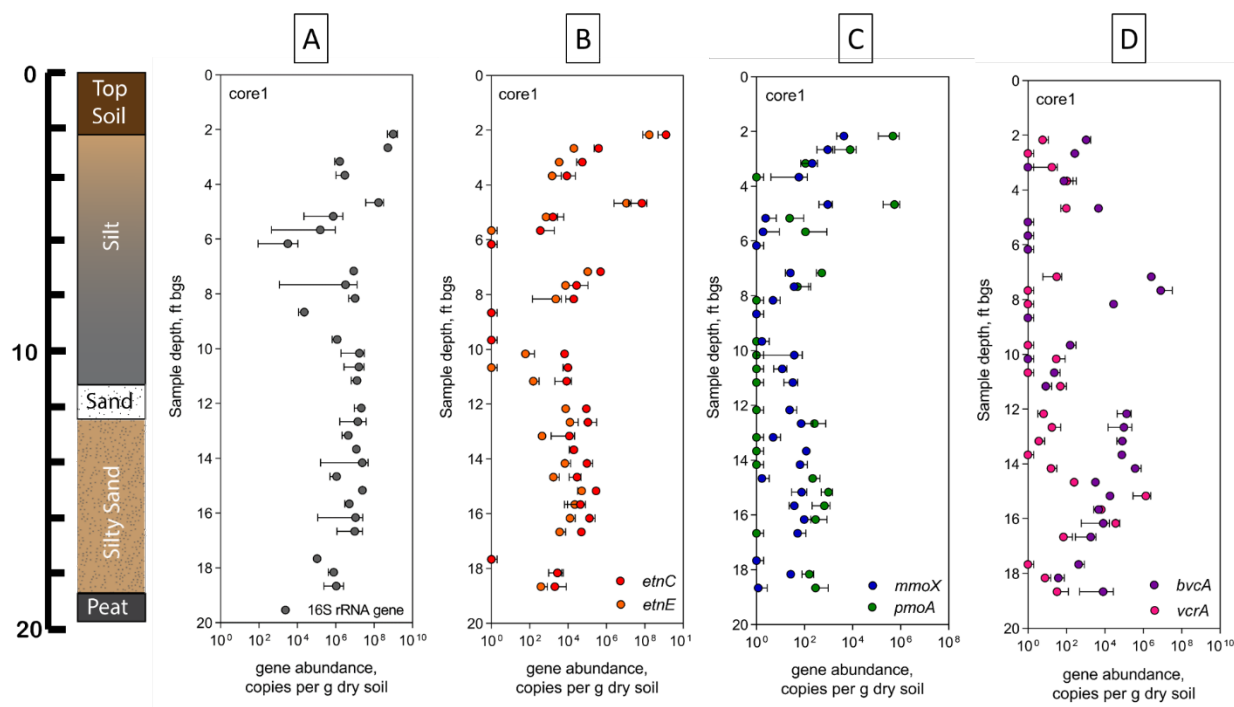
Figure 61. Spatial Resolution of A) Total 16S rRNA Genes, B) etnC and etnE (Etheneotroph Functional Genes), C) mmoX and pmoA (Methanotroph Functional Genes), and D) bvcA and vcrA (VC Reductive Dehalogenase genes) in an Aquifer Sediment Core, Frozen in Place with Liquid Nitrogen, Obtained from Parris Island Site 45.

The graphic on the left shows the soil characteristics of the upper (silt) and lower (silty sand) surficial aquifers.

The qPCR analysis shows that indeed, functional genes from etheneotrophs and anaerobic VC-dechlorinators coexist within small (~0.25 g) sediment samples as deep as 18 feet below ground surface in this particular sediment core. ***This suggests that there is the potential for essentially simultaneous aerobic and anaerobic VC biodegradation at this site, even at a substantial depth.*** The source of DO at depth is currently unknown and poorly understood. However, as expected, the abundance of etheneotroph and methanotroph functional genes are highest closer to the ground surface, presumably because there is the strongest oxygen gradient here near the shallow groundwater table (~2-3 feet bgs).

More detailed graphs showing chemical and biomarker analysis of all 4 boreholes and some additional discussion are provided below.

Variations in chlorinated ethene concentrations among boreholes
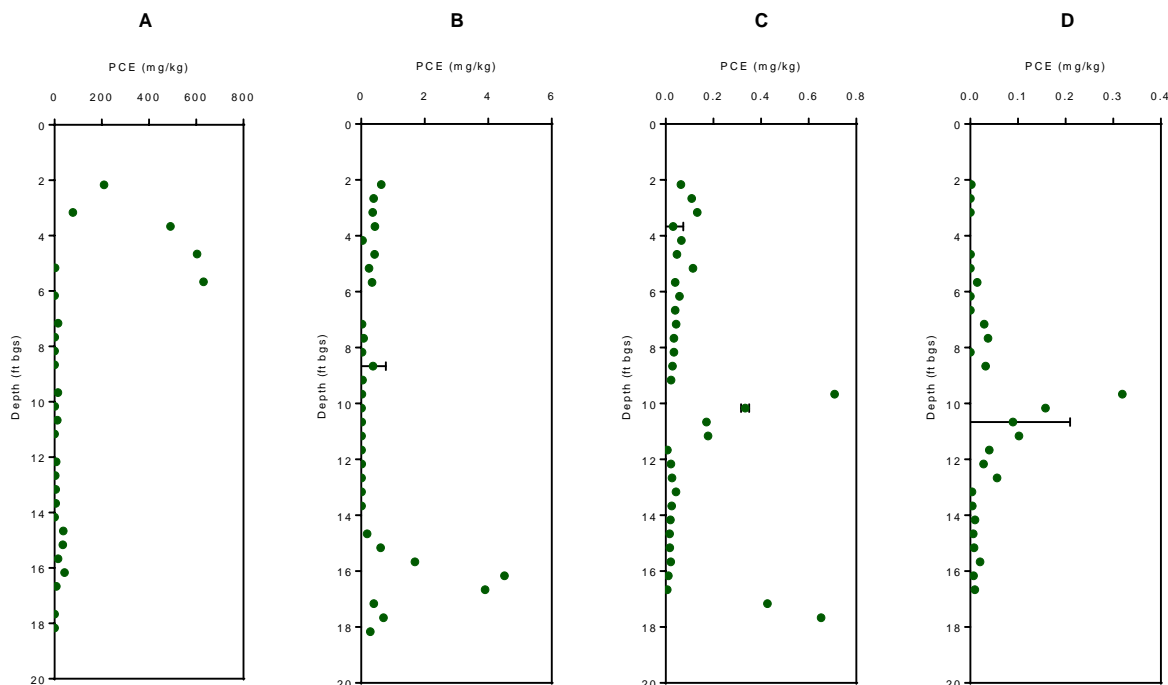
Figure 62. PCE Concentration with Depth in Boreholes 1-4 (panels A-D, respectively).

Concentrations are expressed in mg PCE/kg sediment dry weight. Error bars show ±1 standard deviation of analytic duplicates (10% of total samples).

Cryo-coring was successful in capturing trends in geochemical data that revel steep gradients in chlorinated ethene concentrations. The highest concentrations of chlorinated ethenes were found in borehole 1. PCE concentrations up to 700 mg/kg were found in a few of the shallow samples (<5 ft bgs) (**Figure 62**). With the exception of these few samples described above, the overall trend in PCE concentration was an increase in with depth to 5 ft bgs, then leveling off until 11 ft bgs. This is consistent with the location of the DNAPL source zone nearby borehole 1 and suggests that a significant amount of DNAPL still exists in the part of the aquifer.PCE concentrations then proceed to drop off with increasing depth, until rising sharply at 14-16 ft bgs to approximately 40 mg/kg. PCE concentrations in borehole 2 were much lower than in borehole 1, but showed a similar trend (**Figure 62**). The majority of the PCR detected was present in a narrow vertical band at 15-17 ft bgs, suggesting that some DNAPL had reach this depth upgradient and dissolved in the groundwater. Only low concentrations of PCE (<1 mg/kg) were found in either borehole 3 or 4, both of which had small spikes in PCE at 10-11 and 17-18 ft bgs. This is likely because the PCE is subjected to anaerobic reductive dechlorination as it moves downgradient, as can be seen in the following figures.

TCE concentrations in borehole 1 were much lower than PCE concentrations, but followed the same distribution pattern (**Figure 63**). This suggests that PCE in the upper surficial aquifer is being dechlorinated to TCE. Low concentrations of TCE (4 mg/kg) were seen throughout the upper surficial aquifer in the remaining boreholes. TCE concentrations decrease with depth until the bottom of the sand unit at 15-17 ft bgs. TCE concentrations at the bottom of the borehole 1 were only about 10% of the PCE concentrations in the same location. In boreholes 2-4, the TCE concentration in the silt unit decreased to very low levels (< 10 μg/kg). TCE concentrations at the bottom of the sand unit in borehole 2 were nearly identical to those in borehole 1. TCE concentrations in the bottom of the sand unit more than doubled between boreholes 2 and 3 from 3 to 6.6 mg/kg, then decreased approximately 35% to 4.3 mg/kg between boreholes 3 and 4. These observations are clear indicators of reductive dechlorination of PCE to TCE as the plume moves downgradient. We seem to have successfully sampled an appropriate plume transect with the 4 borehole locations.
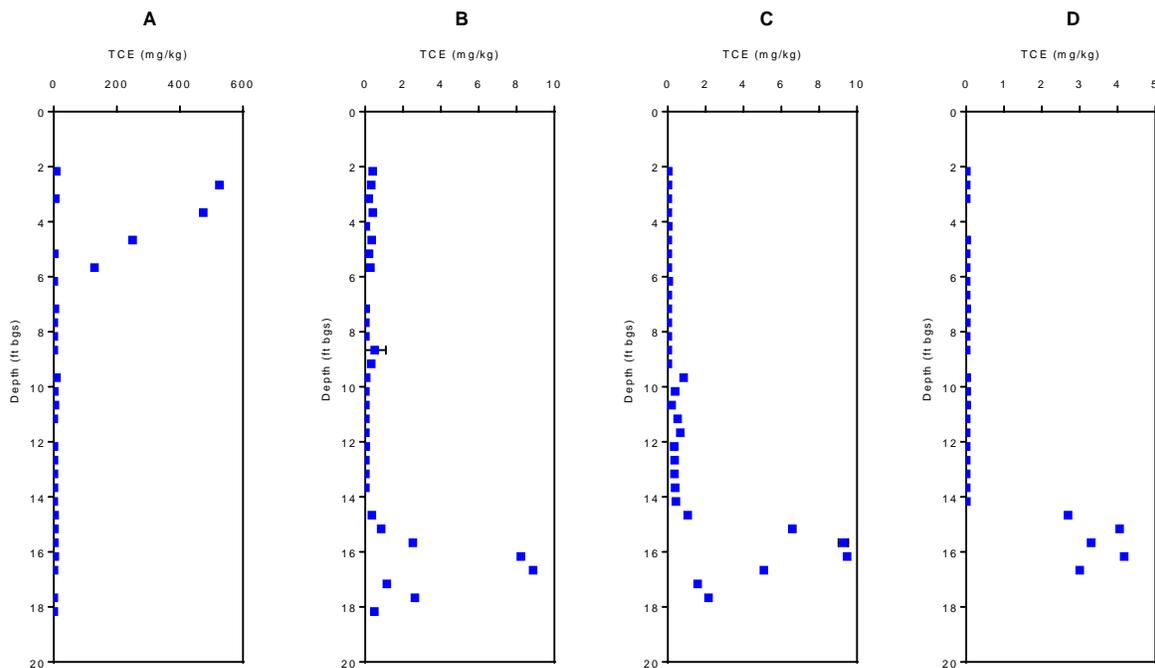
Figure 63. TCE Concentration with Depth in Boreholes 1-4 (a-d, Respectively).

Concentrations are expressed in mg TCE/ g sediment dry weight. Error bars show ±1 standard deviation of analytic duplicates (10% of total samples).

Concentrations *cis*-DCE were very high in the upper surficial aquifer in borehole 1, ranging from 100-300 mg/kg (**Figure 64**). This is in the same order of magnitude as the highest concentration PCE samples, and more than 100x the highest measured TCE concentrations. This is further evidence of reductive dechlorination of TCE to cis-DCE. In the lower surficial aquifer of borehole 1, *cis*-DCE concentrations have the same pattern as seen for PCE and TCE, with lower concentrations at the top of the unit and a rise in concentration at the bottom of the unit. The maximum *cis*-DCE concentration in the lower aquifer of borehole 1 was only about 30% of that seen in the upper aquifer. In boreholes 2-4, there is essentially no *cis*-DCE present in the upper aquifer. The *cis*-DCE in the lower aquifer of borehole 1 shows a bimodal distribution with a broad peak between 9-12 ft bgs, then a sharp spike between 15-16 ft bgs. The *cis*-DCE concentrations in boreholes 3 and 4 are much lower, but retain this distribution. Concentrations of *trans*-DCE and 1,1-DCE were below method detection limits in virtually all samples.
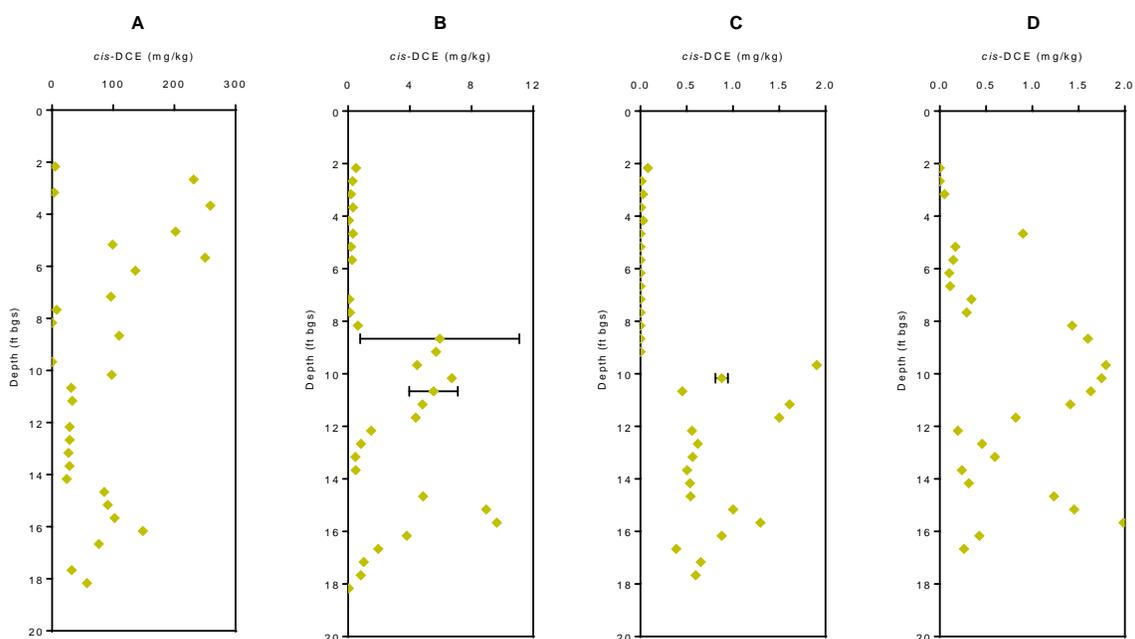
Figure 64. cis-DCE Concentration with Depth in Boreholes 1-4 (A-D, Respectively).

Concentrations are expressed in mg cis-DCE / g sediment dry weight. Error bars show ±1 standard deviation of analytic duplicates (10% of total samples).

There was a significant amount of VC in the upper aquifer portion of borehole 1 (**Figure 65**). This is consistent with reductive dechlorination of cis-DCE to VC. The rise in VC occurred at a greater depth than observed for TCE or *cis*-DCE, starting at 5 ft bgs, then peaking at 7 ft bgs. There was only a modest increase in VC bgs. VC concentrations rapidly dropped off between boreholes 1 and 2, and continued to decrease to much lower concentrations in boreholes 3 and 4 (<100 µg/kg at all depths). The VC concentrations in the upper aquifer of borehole 2 were similar to the *cis*-DCE concentrations. In the lower aquifer of borehole 2, VC showed a nearly linear increase with depth from 7-11 ft bgs, before rapidly dropping off. The elevated concentrations in VC overlapped with *cis*-DCE, but shifted to an even shallower depth. A similar increase with depth was seen in borehole 4, but further offset with the increase occurring between 12-14 ft bgs. The VC concentration in borehole 3 was lower than either borehole 2 or 4.
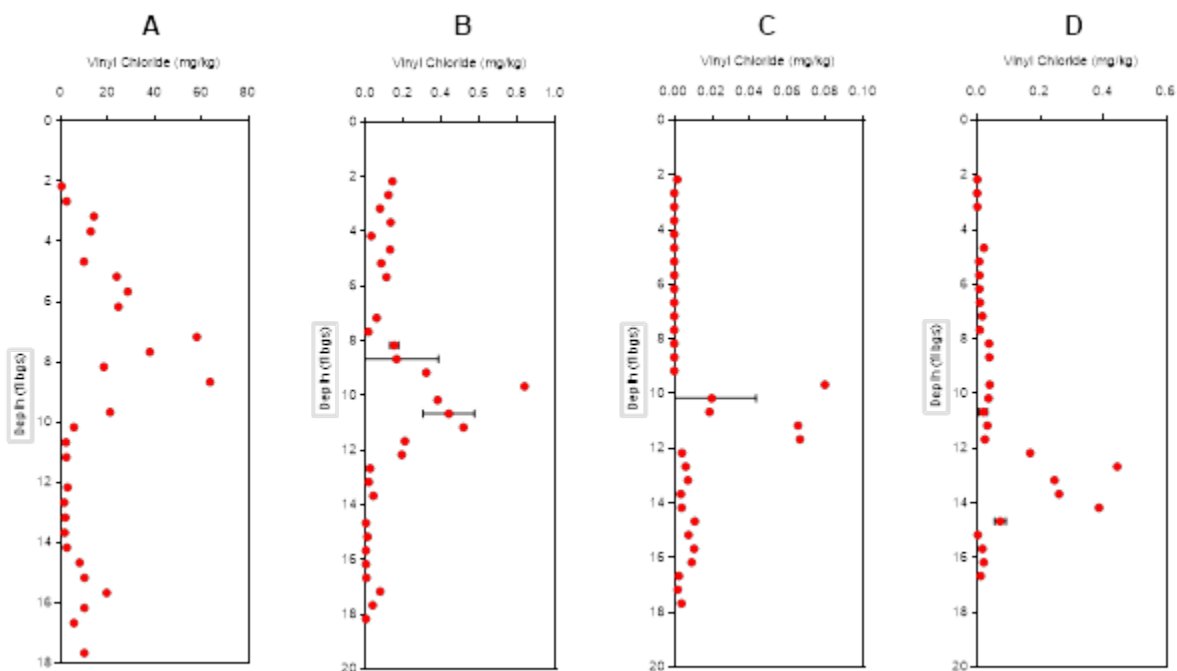
Figure 65. VC Concentration with Depth in Boreholes 1-4 (Panels A-D, Respectively).

Concentrations are expressed in mg VC/ g sediment dry weight. Error bars show ±1 standard deviation of analytic duplicates (10% of total samples).

Dissolved gases

Ethene was present in borehole 1 with a large spike in concentration occurring between 7-10 ft bgs (**Figure 66).** Below this depth, ethene concentrations were very low. The vertical distribution of ethene in borehole 1 was similar to vinyl chloride, except that the spike at 7-10 ft bgs was much sharper than with vinyl chloride. Ethene concentrations drop nearly two orders of magnitude between borehole 1 and 2. Ethene distribution is similar in Borehole 2 to Borehole 1, but with more scatter. Borehole 3 has a narrow spike in ethene between 3-5 ft bgs, but otherwise resembles borehole 2. No ethene was detected in borehole 4. Trace levels of ethane or acetylene were detected in several samples.
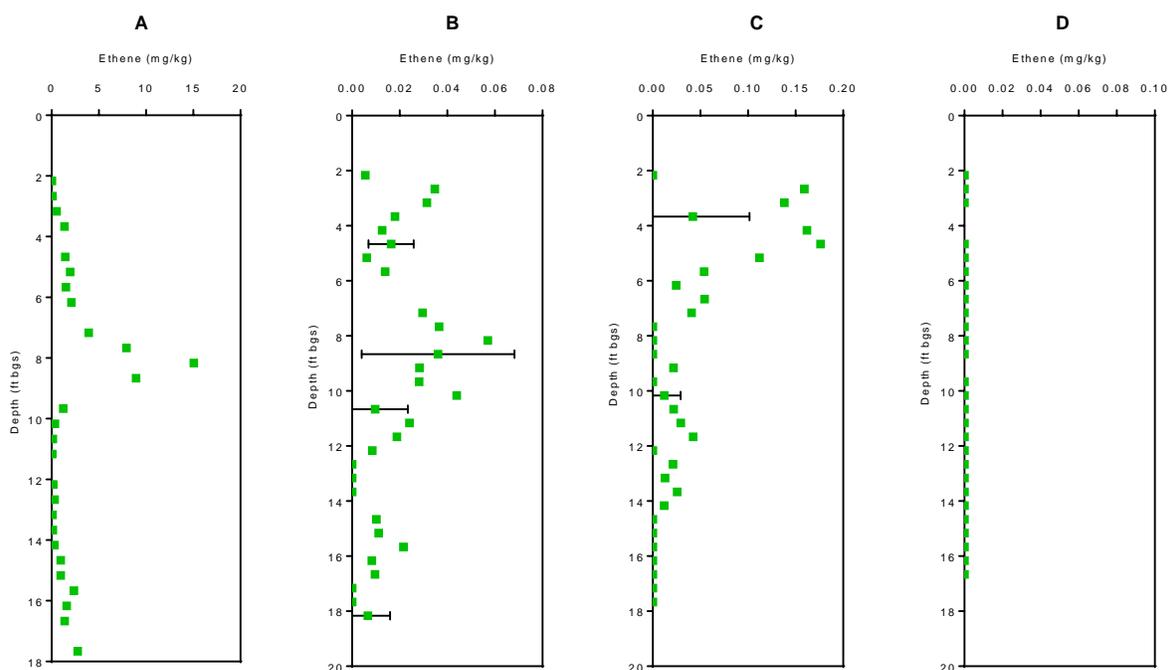
Figure 66. Ethene Concentration with Depth in Boreholes 1-4 (Panels A-D, Respectively).

Concentrations are expressed in mg ethene/ g sediment dry weight. Error bars show ±1 standard deviation of analytic duplicates (10% of total samples).

No dissolved oxygen was detected in any of the samples - significant levels of background oxygen introduced when processing the samples prevented us from confidently determining if low levels of DO could have been present.

Methane concentrations increased with depth in boreholes 1, 2, and 4 down to 12-14 ft bgs, before decreasing (**Figure 67**). The highest methane concentrations were seen in borehole 1, which was probably experience the most highly reducing conditions compared to the other boreholes. Methane concentrations were an order of magnitude lower in Borehole 3 than in the other Boreholes.
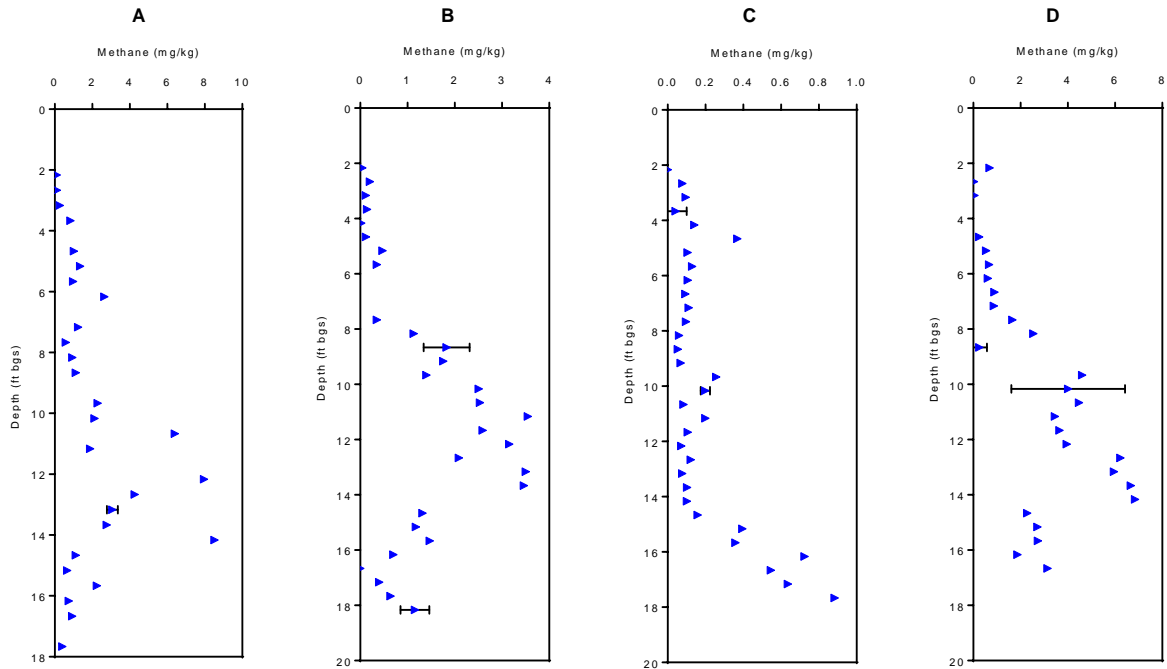
Figure 67. Methane Concentration with Depth in Boreholes 1-4 (Panels A-D, Respectively).

Concentrations are expressed in mg methane/ g sediment dry weight. Error bars show ±1 standard deviation of analytic duplicates (10% of total samples).

Chloride concentrations

In Borehole 1, chloride concentrations were very high (150-300 mg/kg) throughout the upper aquifer. Based on this data and the profiles of the chlorinated ethenes showing reductive dechlorination, the high chloride levels are likely the result of reductive dechlorination processes.

Concentrations were much lower (<50 mg/kg) in the top half of the lower aquifer (11-14 ft bgs), but spiked to 200-550 mg/kg. Boreholes 2 and 4 had a similar trend with a large chloride spike of up to 200 mg/kg occurring in the upper aquifer (6-10 and 2-6 ft bgs, respectively) and a smaller chloride spike occurring near the bottom of the lower aquifer (50 and 100 mg/kg, respectively). This supports the chlorinated ethene data, and indicates that reductive dechlorination was occurring in the lower surficial aquifer as well. Borehole 3 had much lower chloride concentrations than the others, with a maximum concentration of <50 mg/kg occurring at the bottom of the upper aquifer. This is consistent with the pattern of reductive dechlorination observed in the lower surficial aquifer.
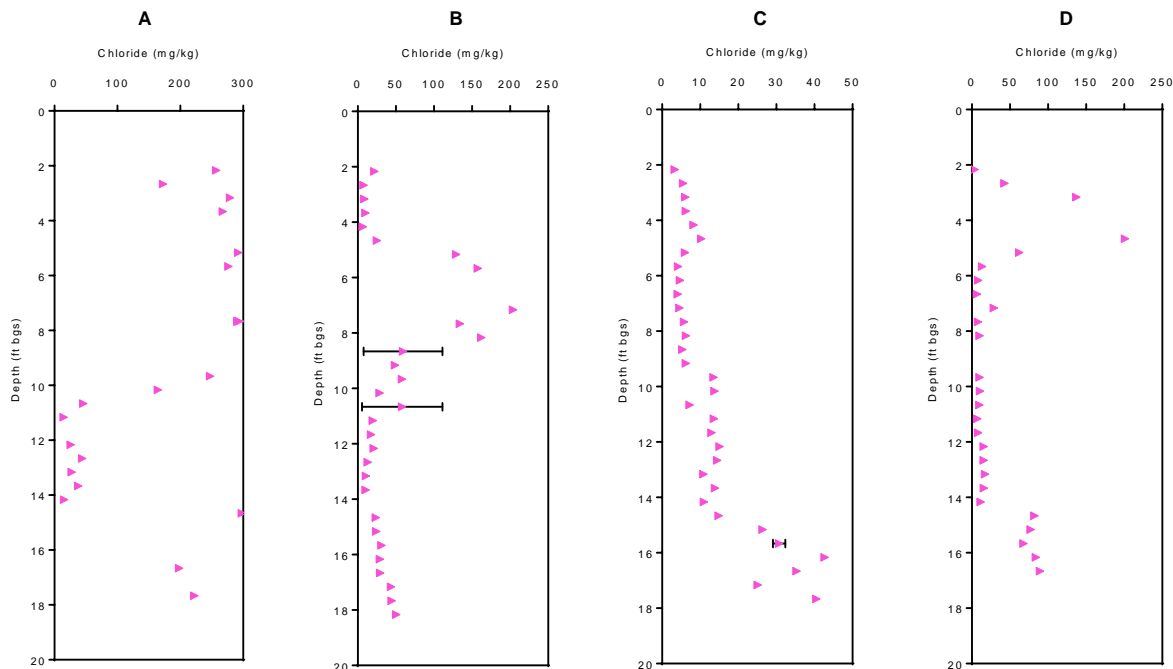
Figure 68. Chloride Concentration with Depth in Boreholes 1-4 (Panels A-D, Respectively).

Concentrations are expressed in mg Cl-/ g sediment dry weight. Error bars show ±1 standard deviation of analytic duplicates (10% of total samples).

Terminal electron accepting conditions in aquifer sediments

Nitrate was below detection in all of the samples. Presumably it had been depleted by microbial respiration under the reducing conditions encountered in the aquifer.

Ferrous Iron

In Borehole 1, ferrous iron was first detected at a depth of 3 ft bgs. The concentration remained stable at 23-34 mg/kg between 4-8 ft bgs, then spiked to 73 mg/kg between 8-9 ft bgs (**Figure 69**). This pattern indicates the development of iron-reducing conditions in the upper surficial aquifer. Interestingly, ferrous iron concentrations dropped to near-zero below this depth. In Borehole 2, ferrous iron concentrations did not become significant until a depth of 7 ft bgs, and formed a narrow vertical spike to 17 mg/kg between 7-9 ft bgs. Only very low amounts of ferrous iron were seen in Boreholes 3 and 4, with peak concentrations of 0.21 and 0.89 mg/kg, respectively, occurring at approximately 9 ft bgs.
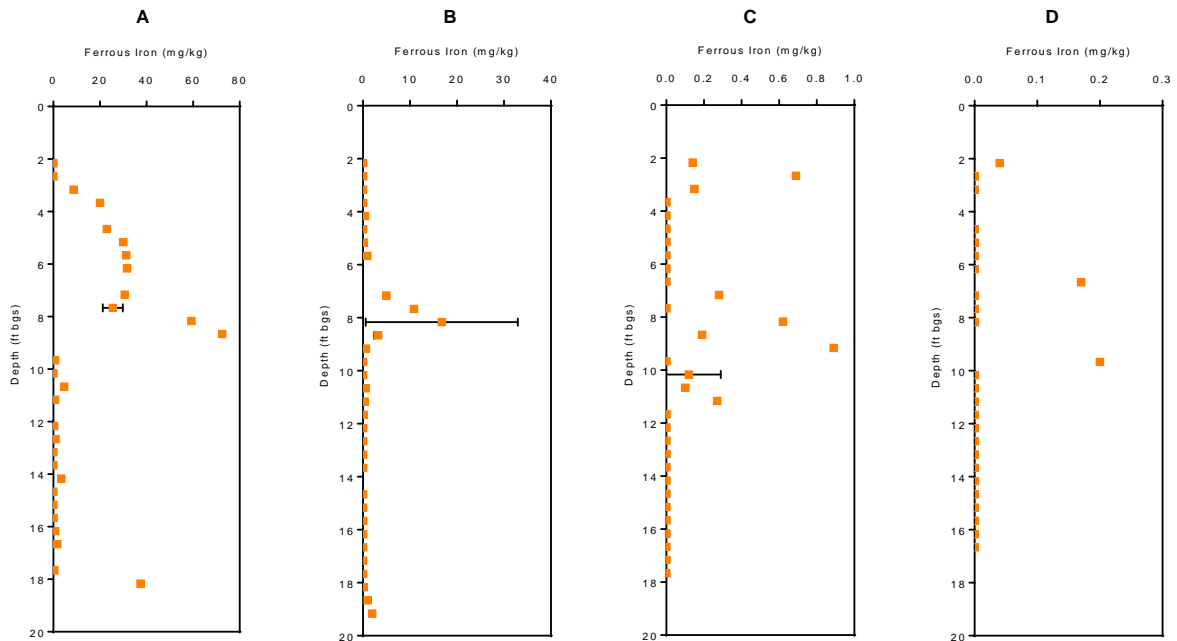
Figure 69. Ferrous Iron Concentration with Depth in Boreholes 1-4 (a-d, Respectively).

Concentrations are expressed in mg Fe^{2+}/ g sediment dry weight. Error bars show ±1 standard deviation of analytic duplicates (10% of total samples).

Sulfate concentrations

In Borehole 1, the sulfate concentration was 53 mg/kg at the top of the upper aquifer (2 ft bgs), and decreased to below detection by 4 ft bgs (**Figure** 70). Sulfate remained below detection throughout the remainder of the upper and into the lower aquifers. Interpreting this data along with the methane data (**Figure 67**) suggests that methanogenic conditions were present over much of this depth – conditions that are conducive to reductive dechlorination of chlorinated ethenes.

Sulfate began to increase at 12 ft bgs, and reached a maximum of 80 mg/kg at 15 ft bgs, before dropping below detection again at 18 ft bgs. This suggests that the lower surficial aquifer was experiencing less reducing conditions than the upper surficial aquifer. In boreholes 2-4, sulfate concentration generally decreased with depth from 5-11 ft bgs. Sulfate concentrations in boreholes 3 and 4 where lower overall than in borehole 1, likely a result of the reduced flux of sulfate to these locations.
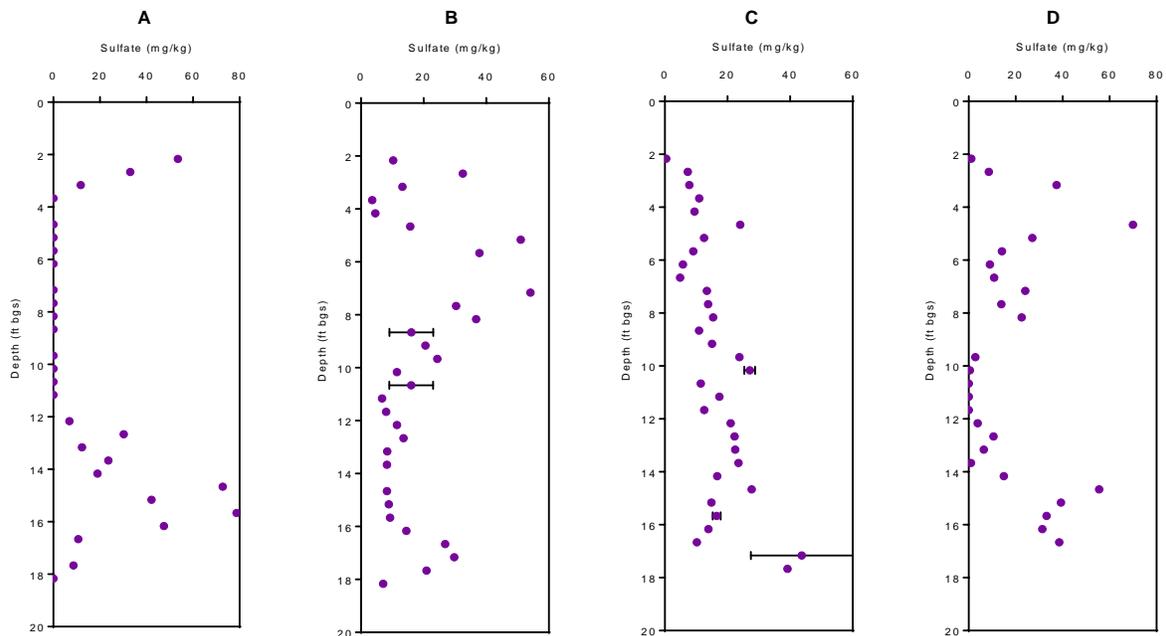
Figure 70. Sulfate Concentration with Depth in Boreholes 1-4 (a-d, Respectively).

Concentrations are expressed in mg sulfate/ g sediment dry weight. Error bars show ±1 standard deviation of analytic duplicates (10% of total samples).
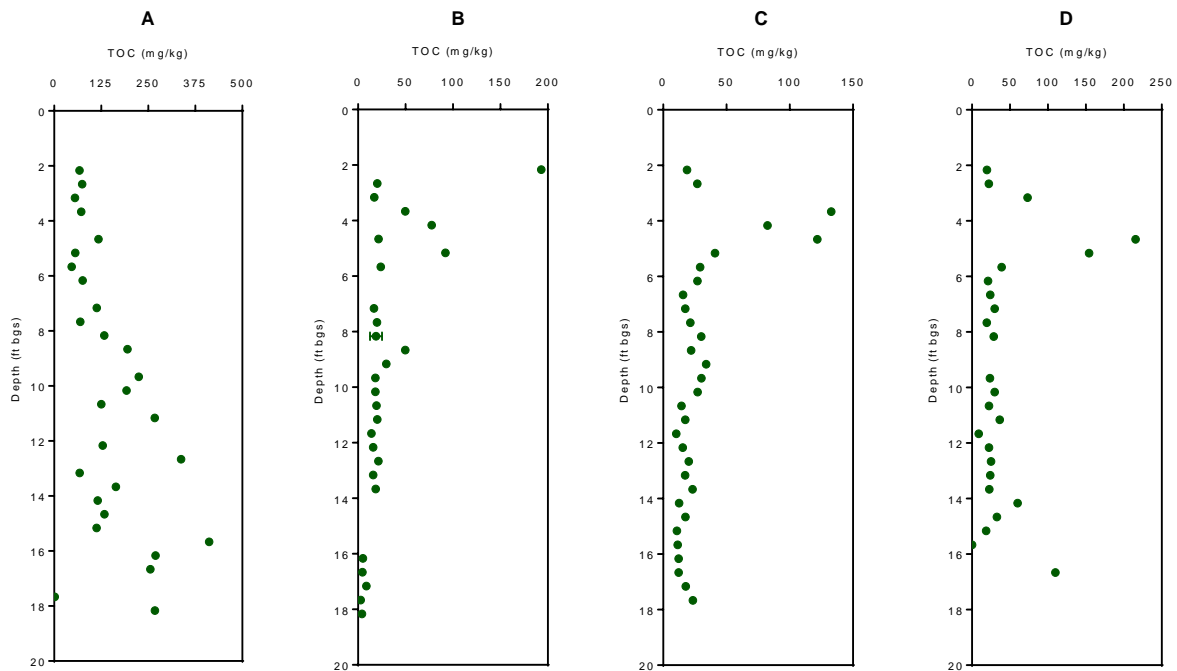
Figure 71. TOC Concentration with Depth in Boreholes 1-4 (Panels A-D, Respectively).

Concentrations are expressed in mg carbon/ g sediment dry weight. Error bars show ±1 standard deviation of analytic duplicates (10% of total samples).

TOC

Very high TOC concentrations were found in borehole 1 between 8-18 ft bgs (**Figure** 71). This is likely derived from an emulsified vegetable oil (EVO) injection in 2014 during a pilot study that was intended to stimulate reductive dechlorination. The drastic drop in TOC between 14-15 ft bgs correlates with the reductive dechlorination activity occurring near the DNAPL. TOC concentrations in the other boreholes were much lower, and not likely influenced by the EVO injections. TOC in boreholes 2-4 were not likely high enough to support an appreciable amount of reductive dechlorination.
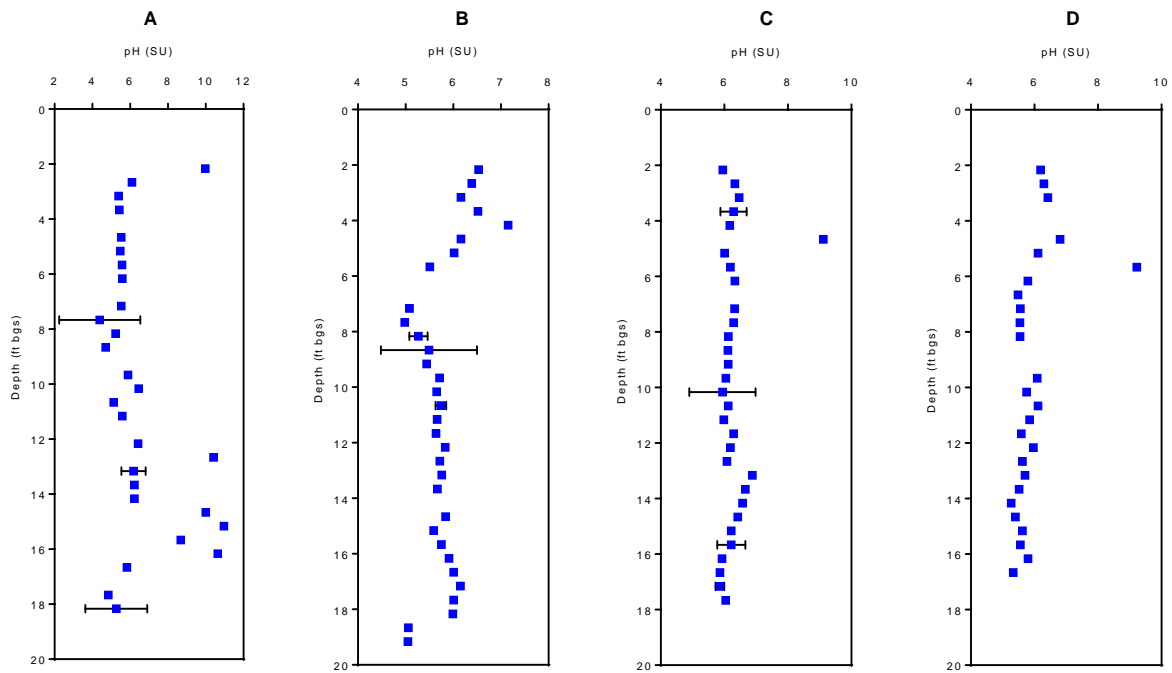
Figure 72. pH Values with Depth in Boreholes 1-4 (Panels A-D, Respectively).

Error bars show ±1 standard deviation of analytic duplicates (10% of total samples).

pH

pH ranged from 4.5-6.5 SU across most of the samples (**Figure 72**). This is notable as the pH values are lower than what is considered ideal for anaerobic reductive dechlorination of chlorinated ethenes. However much higher pH values (9-11 SU) were found in a few samples across all cores between 2-5 ft bgs, and in borehole 1 between 12-16 ft bgs.

Abundance of total bacterial 16S rRNA genes and functional gene biomarkers of VC, ethene and methane biodegradation in cryo-cores

The four cores had similar level of total bacterial abundances (as represented by total 16S rRNA gene abundances), with an average of 4.0×10^7 gene copies per g soil and ranging from 1.3×10^2 to 1.1×10^9 gene copies per g soil (**Figure 73**). Generally, the bacterial abundance at Parris Island Site 45 was relatively low compared to other soil samples, probably because of the sandy and silty soil texture.

The depth patterns of total bacterial 16S rRNA genes in the four cores were similar. Bacteria were the most abundant in topsoil and decreased until 5-6 ft bgs. After 5-6 ft bgs, bacterial abundances were either relatively stable (core 1) or gradually increased (core2, 3 and 4) until 20 ft depth. The depth pattern of total bacterial abundances could be influenced by several factors, including soil texture, organic carbon content, soil oxygen level, and the cVOC contamination.
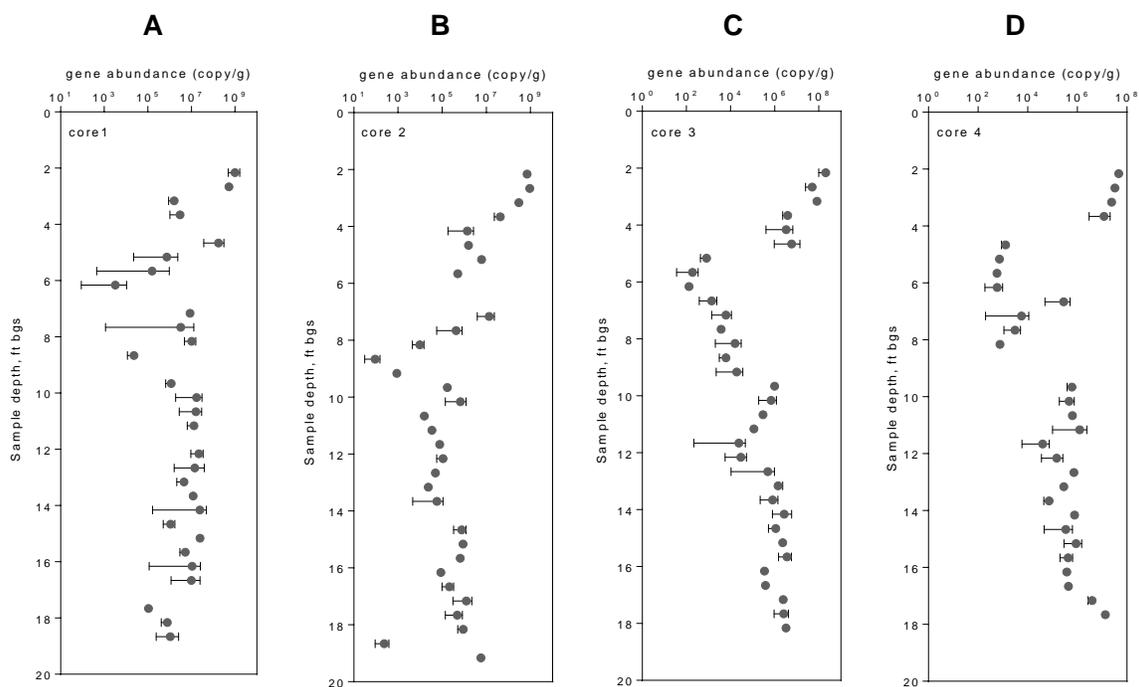
Figure 73. Total 16S rRNA Gene Abundance with Depth in Boreholes 1-4 (Panels A-D, Respectively).

Values are reported as gene copy/g dry sediment weight. Error bars represent the range of duplicate measurements.
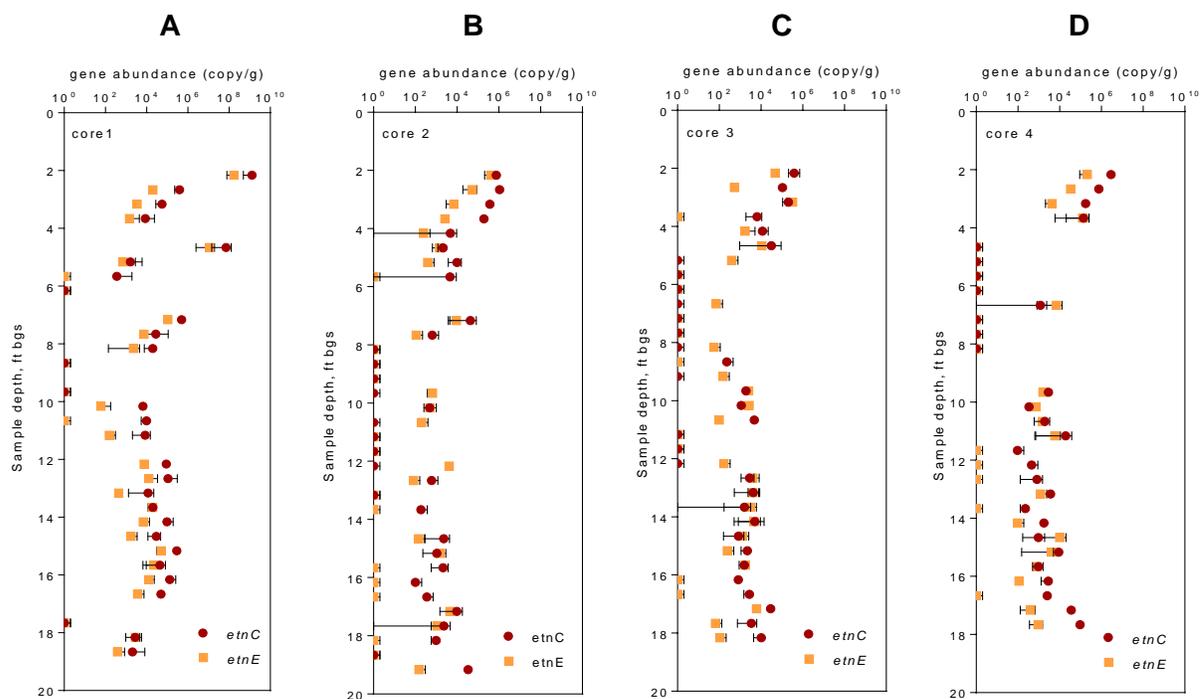
Figure 74. Etheneotroph Functional Gene (*etnC* and *etnE*) Abundance with Depth in Boreholes 1-4 (Panels A-D, Respectively).

Values are reported as gene copy/g dry sediment weight. Error bars represent the range of duplicate measurements.

Among the three possible VC-degrading bacterial guilds, etheneotrophs and VC-dechlorinating bacteria were more abundant than methanotrophs in the core samples. Different bacterial guilds had different depth distribution. Etheneotrophs and methanotrophs were more abundant in top soil and were correlated with total bacterial abundance (Spearman's correlation, p<0.001 except for *pmoA* in core 1). It is possible that etheneotrophs and methanotrophs were affected the same way the majority of microbial communities were affected. The abundances and distributions of etheneotrophs and methanotrophs were also similar in four cores.

110
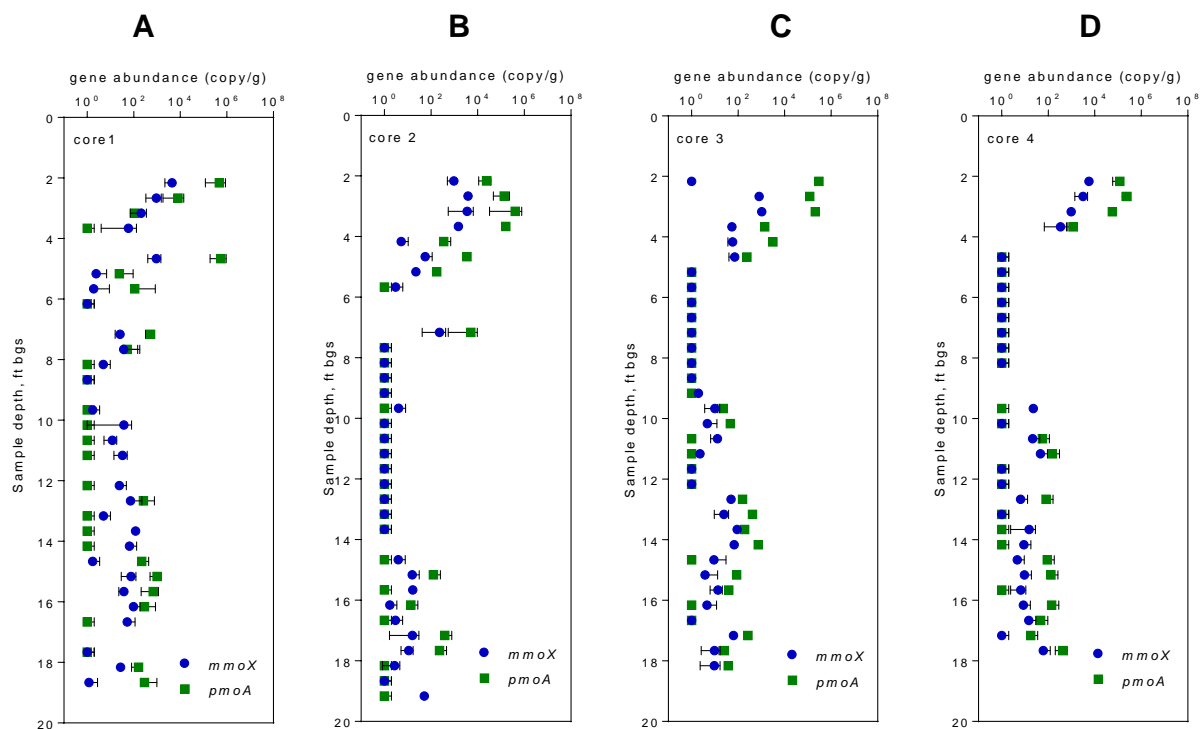
Figure 75. Methanotroph Functional Gene (*mmoX* and *pmoA*) Abundance with Depth in Boreholes 1-4 (Panels A-D, Respectively).

Values are reported as gene copy/g dry sediment weight. Error bars represent the range of duplicate measurements.
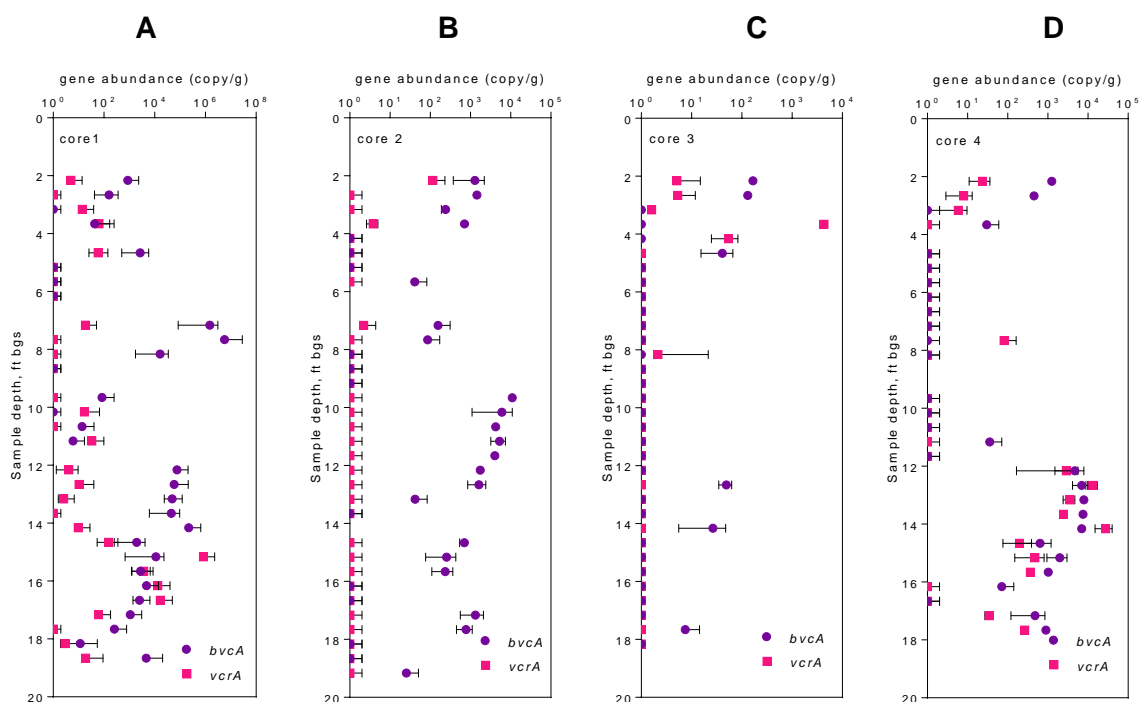
Figure 76. VC Reductive Dehalogenase Gene (*bvcA* and *vcrA*) Abundance with Depth in Boreholes 1-4 (Panels A-D, Respectively).

Values are reported as gene copy/g dry sediment weight. Error bars represent the range of duplicate measurements.

Unlike aerobic VC-degrading bacteria, anaerobic VC-dechlorinating bacteria were more abundant in deep soils. For example, in core1, *bvcA* was the most abundant at 7-8 ft below ground surface and reached 10^6 - 10^7 gene copies per g soil. In core4, *bvcA* reached 10^3-10^4 gene copies per g soil after 12 ft, much higher than in the shallower sections. A possible explanation is that the oxygen in surficial soils inhibited anaerobic VC-dechlorinating bacteria. The distributions of VC-dechlorinating bacteria were different among four cores. In the four cores, bvcA in core3 was much less than in other cores. Generally, *bvcA* was more abundant than *vcrA* at Parris Island Site 45.

Core 1 is located within the source zone and had the highest PCE, TCE, cis-DCE and VC contamination. In core1, we found significant positive correlation between VC-dechlorinating bacteria (the ratio of *bvcA* and *vcrA* to total 16S rRNA gene) with cis-DCE, VC, and ethene (Spearman's correlation, p<0.05). Etheneotrophs were not correlated to VC or ethene, probably because their growth was limited by the lack of oxygen in deeper soils, where VC concentrations were high. However, in soils deeper than 10 ft, etheneotrophs and VC-dechlorinating bacteria were at about the same level (10^3-10^4 gene copies per g soil), suggesting they may both contribute to *in situ* VC degradation.

112

5.6.9   Microcosms and enrichment cultures

We are interested in providing a link with the functional genes and transcripts we quantified with qPCR and the metabolic potential and activity of VC oxidizers in groundwater. We obtained unfiltered groundwater samples three of the six DoD sites studied in this project: NWS Seal Beach site 70 (well MW-14B), Joint Base Pearl Harbor-Hickam site LF05, and Paris Island Marine Corp Recruit Depot site 45 (well ML-2). We also obtained groundwater samples from four wells at Naval Air Station North Island (NAS NI) Site 9 in June 2017, in collaboration with Neal Durant at Geosyntec and Michael Pound at NAS NI. Microcosms were prepared by mixing groundwater with a defined minimal salts medium (MSM) (Coleman, *et al.*, 2002a) in serum bottles at a 1:1 ratio and then adding VC, ethene, or methane as the sole carbon/energy source. Bottles were incubated with shaking at room temperature in the dark and monitored for biodegradation with GC-FID. The results of these initial microcosm experiments are summarized below.

5.6.9.1   *Paris Island Marine Corp Recruit Depot site 45 (well ML-2) microcosms*

A 1-liter groundwater sample from well ML-2 was collected in June 2016 and stored in at 4C until March 2017, at which time VC, ethene- and methane-fed microcosms were prepared. These microcosms were monitored until mid-July 2017. No appreciable VC, ethene or methane biodegradation activity was noted and monitoring of the cultures was discontinued. It is possible that the long incubation time at 4C was responsible for the lack of activity in aerobic microcosms.

5.6.9.2   *NWS Seal Beach site 70 microcosms*

A 1-liter groundwater sample was obtained from well MW-14B at NWS Seal Beach in July 2017. We chose to sample from this well as previous qPCR results indicated that etheneotrophs were present and active when last sampled in December 2015. Both ethene and methane-fed microcosms showed biodegradation without a lag period, indicating that active methanotrophs and etheneotrophs were present in the groundwater sample. This activity was transferable to fresh bottles with MSM only. The VC fed microcosm, on the other hand, did not display VC biodegradation after extended incubation. However, an ethene-grown culture from derived from Seal Beach groundwater was fed VC and eventually adapted to growth on VC. The growth rate of this culture on VC is slower than the others described below, thus we did not use it for further experiments.

5.6.9.3   *Joint Base Pearl Harbor-Hickam site LF05 microcosms*

Groundwater from site LF05 was obtained in April 2017 and microcosms were prepared shortly thereafter. Microcosms (fed ethene, VC or methane separately) began degrading ethene after about 35 days incubation, VC after about 40 days incubation and methane after 60 days incubation. Aerobic VC biodegradation activity was transferable into MSM only, and was robust. The relatively short lag time for aerobic VC biodegradation to commence in these microcosms suggests that active VC-oxidizing bacteria are present at site LF05. These cultures were used in further experiments to characterize the VC biodegradation rate and relationship with etheneotroph biomarker abundance.

5.6.9.4   5.6.9.5. NAS North Island Site 9 microcosms

Four groundwater samples were collected from a chlorinated solvent plume at Naval Air Station-North Island by Geosyntec and sent to the University of Iowa in June 2017. The groundwater was analyzed for anion concentration and ethenotroph functional genes, and used to construct microcosm testing for aerobic vinyl chloride and ethene degradation. The samples listed in **Table 11** were received at the University of Iowa on 6/21/2017. A single 1 L poly bottle of each sample was included. All of the samples were received intact and cold. No temperature blank was included. Sample S9MW1-17Q2 had a significant amount of headspace, and the water was rust-colored. The other bottles had no significant headspace.

Table 11. Field Sample IDs, Well Numbers and Sampling Times and Dates for NAS North Island site 9 Samples

Sample ID	Well	Collection Date & Time
S9MW1-17Q2	MW-1	6/19/2017 17:20
S9MW19-17Q2	MW-19	6/19/2017 15:16
S9MW57-17Q2	MW-57	6/19/2017 11:45
S9MW60l-17Q2	MW-60	6/19/2017 17:10

Methods. Chloride and sulfate measured in each sample using EPA method 300.1. Aliquots of each sample were filtered using 0.45 μm pore-size filters and analyzed on a Dionex ICS-2100 using an IonPac AS-18 column.

Quantitative polymerase chain reaction (qPCR) analyses were performed on each of the field samples to quantify the abundance of the etheneotroph functional genes *etnC* and *etnE*. A 50 ml aliquot of each sample was filtered through a Sterivex filter. DNA was extracted from the filter and purified using a Qiagen PowerWater® Sterivex kit. The concentration of the purified DNA was measured using a Qubit double-stranded DNA high-sensitivity assay. Extraction and quantification were conducted per the manufacturers' instructions. qPCR assays use SYBR green chemistry and degenerate primers targeting each functional gene. This allows for the simultaneous quantification of these functional genes from multiple organisms. Standard curves were prepared using *Mycobacterium* JS60 DNA.

Microcosms were prepared using groundwater from each of the wells, as shown in **Table 12.** Only aerobic microcosms were prepared, with the goal of investigating ethene and vinyl chloride oxidation by etheneotrophs. The microcosms were prepared in 160 ml serum bottles. Each bottle received 36 ml of sterile minimal salts media, and an equal volume of groundwater. The MSM was supplemented with 3.5% (m/m) sodium chloride for the MW-19 and MW-57 bottles, to better simulate field conditions. The bottles were sealed with butyl rubber septa held in place with aluminum crimp seals. Filter-sterilized ethene or vinyl chloride was added through the septa using a syringe. The bottles were incubated inverted, at room temperature (approximately 21ºC), and in the dark. The headspace concentrations of ethene and vinyl chloride were periodically analyzed using a gas chromatograph with a flame ionization detector. Additional substrate was added as needed. Cultures were transferred (10% v/v inoculum) into fresh media when two doses of substrate had been consumed.

Table 12. Microcosm Setup for NAS North Island Groundwater Samples

Sample ID	Inoculum	Inoculum vol. (ml)	MSM vol (ml)	Substrate	Substrate added (μmol)
NI01-VC	MW-01	36	36	VC	8.3
NI19-VC	MW-19	36	36*	VC	8.3
NI57-VC	MW-57	36	36*	VC	8.3
NI60-VC	MW-60	36	36	VC	8.3
NI01-ETH	MW-01	36	36	Ethene	415
NI19-ETH	MW-19	36	36	Ethene	415
NI57-ETH	MW-57	36	36*	Ethene	415
NI60-ETH	MW-60	36	36*	Ethene	415

*MSM supplemented with 3.5% (m/m) sodium chloride

Anions. Chloride and sulfate concentrations are shown in **Table 13**. The concentration of both ions were much higher in wells MW-19 and MW-57 than in MW-1 or MW-60. The concentrations of these ions measured in MW-19 and MW-57 are similar to sea water. The concentrations in MW-1 and MW-60 are higher than typical freshwater, but are within the normal range of groundwater.

Table 13. Groundwater Anions in NAS North Island Groundwater Samples

Sample ID	Chloride (mg/L)	Sulfate (mg/L)
MW 1	3,200	BD
MW 19	20,000	2,500
MW 57	25,000	3,500
MW 60	1,700	740

Baseline qPCR. The ethenotroph functional genes *etnC* and *etnE* were found in low, but measurable concentrations for all of the samples. Several of the samples had gene copy numbers that were quantification limit base on the standard curve, but were significantly higher than the blanks, and are reported as estimated values. The highest concentrations were found in MW-60, where *etnE* was more than an order of magnitude more abundant than in the other wells (**Table 14**). There was no obvious difference between the wells with high or low chloride and sulfate concentrations.

Table 14. Baseline qPCR Results for NAS North Island Groundwater Samples.

J: estimated value. Detection was significantly higher than blanks, but below quantification limit base on the standard curves.

Well	gene copy/L	
	etnC	*etnE*
MW-1	1.3×10^4 J	1.4×10^4 J
MW-19	1.3×10^5	2.4×10^4 J
MW-57	2.9×10^3 J	6.7×10^3 J
MW-60	2.9×10^5	2.9×10^5

Microcosms. Data from the VC fed microcosms is shown in **Figure 77 (A-D).** All microcosms appeared to display some initial aerobic VC-degrading activity. VC degradation in NI-19 and NI-57 appears to have stopped or severely slowed after 20-30 days of incubation. NI-1 had higher initial activity, and the culture was fed additional VC after only 23 days. However, activity in this culture also seems to have stopped. NI-60 had approximately twice the initial VC concentration of the other microcosms. The groundwater samples were not analyzed for VC, but this sample was given the same initial dose (8 µmol) as the other microcosms, so the additional VC must have been from the groundwater. NI-60 appears to have had an extended lag time (>20 days) before VC degradation was measurable. It is likely that higher initial VC concentration made small changes difficult to detect. This culture has since demonstrated robust VC degradation by fully consuming repeated gas additions. The culture has been transferred, and is being giving increasing doses of VC; the rate of aerobic VC degradation appears to be increasing.
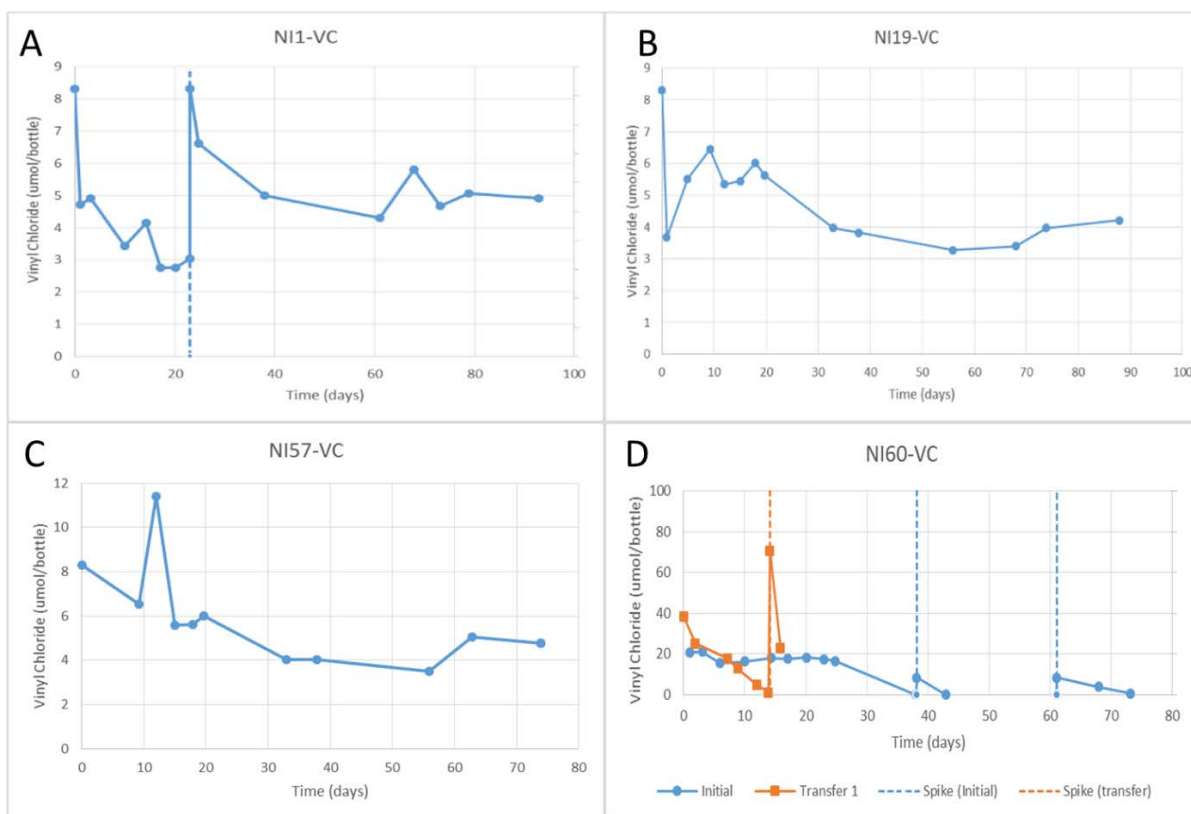
Figure 77. Microcosm VC Concentrations.

Dashed lines indicate substrate addition.

Data from the ethene microcosms is shown in **Figure 78 (A-D).** NI-1 and NI-57 have shown little or no aerobic ethene degradation after >90 days. NI-1 was inadvertently given a second dose of ethene at day 63. NI-19 had a lag time of about 70 days before rapid ethene degradation began. This culture has been re-fed and is continuing to show ethene degradation. NI-60 had a brief lag time of about 25 days before ethene degradation began; less than was observed in the vinyl chloride-fed culture. This culture has been transferred, and re-fed. Robust ethene degradation is continuing.
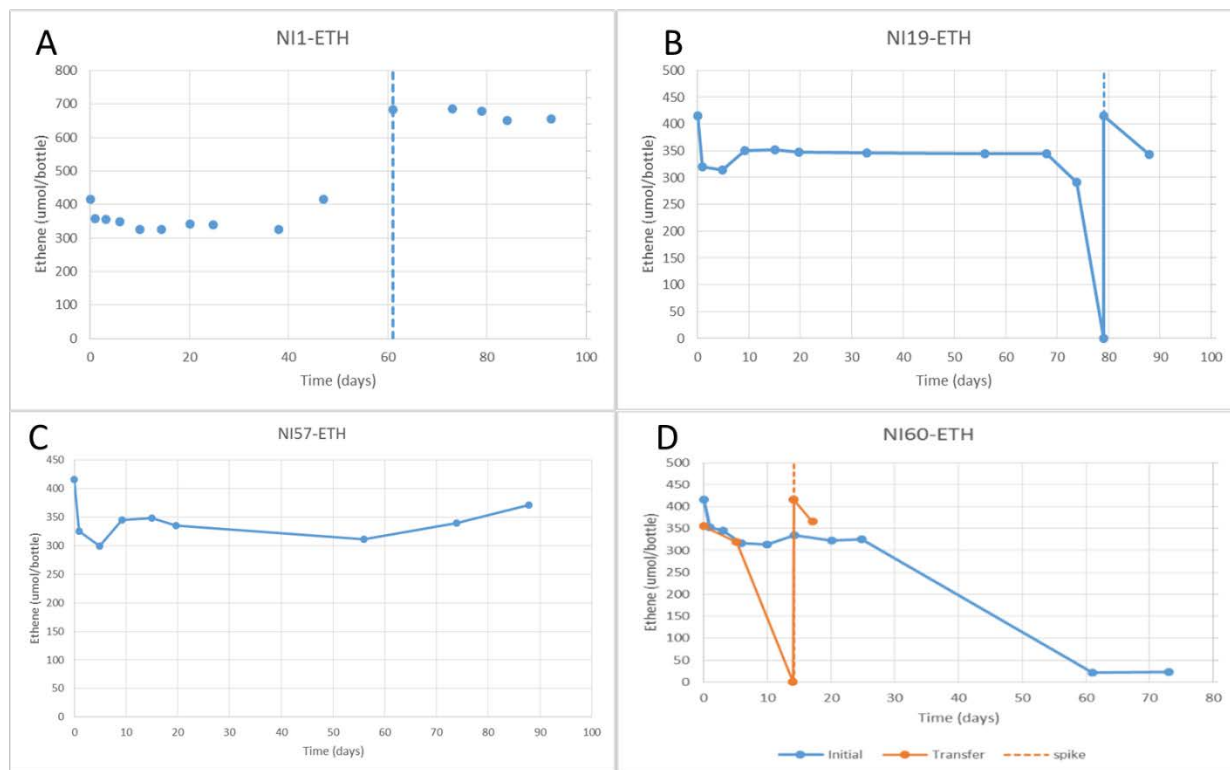
Figure 78. Microcosm Ethene Concentrations Using Groundwater Collected from NAS North Island.

Discussion

The anion data suggest that the groundwater from all of the wells shows some level of sea water influence, as may be expected at a coastal site. MW-1 and MW-60 anion concentrations were similar to typical fresh groundwater, while MW-19 and MW-57 have significantly elevated chloride and sulfate concentrations, similar to sea water. Ethenotrophs have previously been described in seawater, but to our knowledge their ability to degrade vinyl chloride has not been investigated.

The baseline qPCR results indicate that etheneotrophs are present in each of the wells, indicating that there is potential for aerobic ethene and vinyl chloride degradation. There was no clear difference between the concentrations of functional genes in the wells with higher anion concentrations and those having lower anion concentrations. MW-60 had the highest concentration of functional genes by at least an order of magnitude, and would be expected to have the greatest vinyl chloride and ethene-degrading potential. There was some discrepancy between our qPCR results, and those reported by the Löeffler group which may be a result of differing analytical methods.

The Löeffler group uses TaqMan probes for their qPCR analyses, which provided sensitive detection of organism-specific gene targets, while our assay uses SYBR Green chemistry and degenerate primers to capture multiple organisms expressing differing versions of the target genes. This difference can been seen in the MW-57 results where we found low levels of *etnC*, while the Löeffler did not detect *etnC*. However, the general trends in our finding are in agreement with the Löeffler group, notably that the etheneotroph functional genes were present at much higher concentrations in MW-60 than the other wells.

In the microcosms, initial aerobic vinyl chloride-degrading activity was seen in NI-1, NI-19, and NI-57; but in each case it seems to have slowed to a halt. This suggests that the observed degradation was due to co-metabolism. If growth had been occurring on vinyl chloride, the degradation rate should increase, as was seen in NI-60. The limited ethene degradation seen in most of the microcosms is surprising, as etheneotroph functional genes were measured in the initial ground water. It is possible that these organisms are undergoing an extended lag time, as seen in NI-19, due to the low initial etheneotroph concentrations. As would be expected, NI-60 has the most robust ethene degradation as well as vinyl chloride degradation. These findings agree with the much higher concentration of etheneotroph functional genes found in the MW-60 groundwater.

5.6.9.5 *Enrichment cultures used for rate experiments*

The most active VC-oxidizing cultures were obtained from Hawaii and NAS North Island (NI-60). These were selected for subsequent laboratory experiments to investigate normalized rates of VC oxidation (one of the performance objectives). These results of these experiments will be described in Section 6.0 Performance Assessment.

6.0   PERFORMANCE ASSESSMENT

6.1   QUALITATIVE PERFORMANCE OBJECTIVES

6.1.1   On-site sampling, handling and preservation protocols for RT-qPCR/qPCR methods are time-effective and easy to implement

Our sampling experiences so far in this project have shown that groundwater sampling with Sterivex filters fits well within typical groundwater sampling procedures for VOC analysis. After collecting groundwater in vials for VOC and other geochemical parameter analysis, Sterivex filters are attached to the end of silicon tubing to collect microorganisms in the groundwater. Usually four Sterivex filters are needed for one monitoring well (two for DNA samples and two for RNA samples). Each DNA sample requires 1 liter of groundwater and each RNA sample needs up to 3 liters of groundwater. Clogging is a common issue during groundwater sampling by Sterivex filters. If filter get clogged, sampling is stopped. For each monitoring well, extra 30-45 min may be needed for Sterivex filter collection.

For storage, Sterivex filters are kept on ice after sampling, the same way as for VOC sample storage. RNAlater is used to preserve RNA in Sterivex filters – this is easily added in the field. Overnight shipment to laboratory is required for Stervex filters.

Sterivex filters with sampling guidelines are shipped to field technicians before sampling event. With minimal training, a single field technician is able to perform the groundwater sampling with sterivex filters along with groundwater sampling for VOC and geochemical parameter analysis. An example of sampling guidelines is shown in Appendix C. The success criteria, which is that the sampling procedure should be streamlined and straightforward enough for a single field technician to accomplish, has been met.

6.1.2   RT-qPCR/qPCR technology is accepted by regulators

As indicated by SiREM, their commercialized *etnE* assay has so far only been used 7 times. We are not aware of any etheneotroph qPCR data that has been used to obtain approval for MNA at any sites at this time. Therefore, this objective could not be met due to lack of data. The qPCR technology must be more widely applied in practice before it may even come to the attention of regulators.

6.1.3   RT-qPCR/qPCR technology is useful.

Over the course of the project we have communicated our results with RPMs of several sites (including NAS Oceana, Parris Island site 45, site LF5 in Hawaii, and NWS Seal Beach). This culminated in publications in Environmental Science and Pollution Research (Liang*, et al.*, 2017a) and ES&T in 2017 (Liang*, et al.*, 2017b).   The ES&T publication in particular demonstrates the usefulness of the technology in uncovering the existence of genes for both aerobic and anaerobic VC biodegradation in the same groundwater samples. We have taken this further to show that these genes are co-located within the same sediment samples. In review comments on this report, the ESTCP Program Office has indicated that "the fact that VC oxidizers can be in close proximity to VC dechlorinators and can provide useful information and guidance."

The ESTCP Program Office was also interested in the relationships that could be uncovered between VC biodegradation genes and geochemical parameters, because these potential relationships could "provide valuable information to site owners, as it will enable site managers to use readily available data (biogeochemical indicators) as potentially infer whether their particular site is an amenable/ suitable environment for these oxidizers to be present".

In addition, we have successfully transferred the technology to SiREM, and there have been some initial sales of the service, which indicates that some of their clients find the technology potentially useful. Therefore, we can preliminarily conclude that this qualitative performance objective has been met.

6.2   QUANTITATIVE PERFORMANCE OBJECTIVES

6.2.1   RT-qPCR/qPCR technology is time efficient

The time required to process samples for RT-qPCR/qPCR, once the filters have been received in the lab, is estimated in **Table 15**. We typically collected 60 filters during one site visit. It usually takes about one week for DNA and RNA extraction, and another week to process RNA samples given the normal amount of filters collected. The RT-qPCR/qPCR experiments usually take another one to two weeks for the quantification of six functional genes and transcriptions (*etnC, etnE, mmoX, pmoA, bvcA*, and *vcrA*) and quantification of luciferase mRNA in RNA samples. In total, three to four weeks are needed to process samples from one sampling event from one site. Please note that this is the time required for one skilled worker to complete these tasks. The time required could be decreased with more labor devoted to these tasks. The balance of course is labor costs. Costs are discussed in the next performance objective. However, it is clear that the time required for RT-qPCR/qPCR is much less than that of conventional microcosm approaches, which usually take months. The success criteria that time requirements for RT-qPCR is less than that of conventional microcosm technique is met.

Table 15. Time Estimation for Various RT-qPCR/qPCR Procedures

Procedure	Time required
DNA extraction	3-4 hrs per batch (8 samples)
RNA extraction	3-4 hrs per batch (8 samples)
RNA reverse transcription	3 hrs per batch (4-6 samples)
RT-qPCR/qPCR set up	4 hrs per 384 well plate
RT-qPCR/qPCR running	2 hrs per plate
RT-qPCR/qPCR data analysis	2-3 hrs per plate

6.2.2   RT-qPCR/qPCR technology is cost effective

The sampling collection and preservation cost is summarized in Table 16. For each monitoring well, DNA and RNA samples are taken in replicate and cost about $345. The materials required for conventional qPCR with a 384 well plate include the Power SYBR green reagent mix, luciferase mRNA qPCR, and other miscellaneous consumables. There is also a $20 fee per plate

for running the qPCR instrument. We estimated the costs to run qPCR and RT-qPCR for samples from 17 monitoring wells. The reagents costs were $550 ($390 for SYBR green, $115 for luciferase, and $45 for miscellaneous). The instruments fees were $60. Thus, the cost per monitoring well for six gene qPCR/RT-qPCR analysis is $36 for conventional qPCR. In sum, RT-qPCR/qPCR technology costs in total about $380 for each monitoring well to analyze six functional genes/transcripts that involved in VC degradation. The success criterion that unit cost of RT-qPCR/qPCR technology is less than analogous microcosm tests is met.

Table 16. Material Cost Summary of DNA and RNA Sample Preparation Cost for Each Monitoring Well.

Workflow task	per sample cost	number of samples per monitoring well	per monitoring well cost
DNA - sterivex filter collection	$8.70	2	$17.40
DNA - extraction	$14	2	$28
RNA - sterivex filter collection and preservation	$12.40	2	$24.80
RNA - extraction	$12	2	$24
RNA - reverse transcription	$38.50	2	$77
RNA - lucifererase mRNA	$11.50	2	$23
DNA and RNA - overnight shipping			$150
Sum			$345

6.2.3   RT-qPCR/qPCR technology is accurate

The accuracy of RT-qPCR technology refers to the difference between the actual quantities and experimentally measured results. Although it is not possible to know the exact absolute quantity of genes and transcripts in an environmental sample, we aim to maximize via strict quality controls to ensure that the data generated is representative.

The following QA/QC approaches are employed to ensure the accuracy of the RT-qPCR/qPCR technique. First, duplicate DNA and RNA extractions were performed and results were reported as the average of duplicate extractions. Secondly, RNAlater was used to preserve Sterivex filters used for RNA extractions. Luciferase mRNA was used as an internal standard to evaluate the RNA loss during extraction and subsequent DNase treatment, reverse transcription. The luciferase mRNA recoveries of 63 samples averaged 2.71%, ranging from 0.03% to 17.8%. The recovery differences could be resulted from the differences in the groundwater geochemical characteristics, which may affect the extraction efficiency.

Strict quality control for qPCR experiments was employed. Each qPCR experiment contained a freshly prepared standard curve, which is a series of dilutions of known amounts of target gene. Standard curves were also used to evaluate amplification efficiency of each qPCR experiment. The slope, Y-intercept, R squared value, and PCR efficiency for each target gene assay were summarized in Table 17. For luciferase gene, *etnC, etnE, bvcA* and *vcrA*, the qPCR efficiencies were all between 90-110%. For *mmoX* and *pmoA*, seven qPCR experiments had relatively lower efficiency (87-90%).

No template control (NTC) was included on each qPCR plate, and no amplification of target gene was observed in NTC for all qPCR experiments. The specificity of qPCR amplification was checked by melting curve analysis. It is observed that for primer sets targeting *etnC* (RTC) and *mmoX* (mmoX536f/898r), melting curves sometimes displayed non-specific peaks when the target gene abundance was low in sample. The possible non-specific amplification was noted in qPCR results.

Table 17. Standard Curve Summary for Each Target Gene Assay.

target gene		luciferase gene	*etnC*	*etnE*	*mmoX*	*pmoA*	*bvcA*	*vcrA*
n		5	14	14	13	13	10	10
slope	average	-3.42	-3.37	-3.43	-3.58	-3.52	-3.33	-3.36
	min	-3.46	-3.46	-3.58	-3.67	-3.65	-3.42	-3.42
	max	-3.39	-3.25	-3.31	-3.49	-3.39	-3.23	-3.33
Y-intercept	average	35.5	41.2	39.0	36.0	39.3	34.1	33.9
	min	33.0	40.7	38.2	33.9	35.7	32.4	32.1
	max	37.6	41.7	40.1	41.4	43.1	37.2	37.1
PCR efficiency	average	96.1%	98.1%	95.8%	90.4%	92.6%	99.8%	98.3%
	min	94.6%	94.4%	90.4%	87.3%	87.8%	96.0%	96.2%
	max	97.2%	103.1%	100.6%	93.5%	97.2%	104.0%	99.5%
R^2	average	0.999	0.998	0.998	0.998	0.998	0.999	0.999
	min	0.999	0.995	0.998	0.995	0.993	0.996	0.997
	max	1.000	0.999	0.999	1.000	0.999	1.000	1.0

In summary, the success criteria that no target gene detected in the NTC is met. The success criteria that luciferase mRNA recovery is > 5% is not met. However, because all transcript abundance data was corrected with obtained luciferase mRNA recovery to account for mRNA loss during RNA extraction and subsequent procedures, we believe that we are accounting as best we can for the relatively low mRNA recovery. The relatively lower mRNA recovery may cause higher quantification limit for RNA samples. The success criteria that amplification efficiency ranges from 90-110% was met for 91% of the qPCR experiments.

We offer the following suggestions and lessons learned for other interested in developing ribust RNA extraction procedures:

- add RNAlater to samples to protect RNA.
- perform RNA extraction as soon as possible when the sample arrives at the lab.
- use RNase free gloves.
- clean bench and pipettes with RNase cleaning solution to remove RNase before experiment.
- add RNase OUT before RNA storage and before DNase I treatment.

- If DNA concentration in RNA extract is too high, split RNA extract into several parts and perform DNase treatment to each part individually, and then combine parts during the RNA purification step.
- do not frequently freeze and thaw RNA extracts.

6.2.4   RT-qPCR/qPCR technology is precise

The precision of RT-qPCR technology refers to the robustness of this technology. High precision of RT-qPCR is critical and reflects proper laboratory procedures.

For each qPCR experiment, triplicate qPCR was performed for standards and duplicate qPCR reaction was performed for samples. The standard deviation of Ct values for triplicate qPCR reaction and differences of Ct values for duplicate qPCR reactions are summarized in **Table 18**. More than 80% of the time, Ct standard deviations were less than 0.5 for all target genes.

The R^2 value for standard curves are also used to evaluate the precision of qPCR experiment. As summarized in **Table 17**, for all qPCR experiments, standard curves displayed R^2 value>99%, suggesting great linearity of standard curves.

In summary, the success criteria that Ct standard deviation of triplicate qPCR reactions is less than 0.5 is met for more than 90% of the standards and more than 80% of the samples. The success criteria that R^2 value of standard curve is higher than 0.99 is met for all qPCR experiments.

Table 18. Summary of Ct Standard Deviation of Triplicate qPCR Reactions or Ct Difference of Duplicate qPCR Reactions for Each Target Gene Assay.

gene	standard				sample			
	n	replicate	n (Ct std dev<0.5)	% Ct std dev<0.5	n	replicate	n (Ct difference <0.5)	% Ct difference <0.5
luciferase	40	3	40	100.0%	192	3	157	81.8%
etnC	89	3	82	92.1%	267	2	251	94.0%
etnE	86	3	83	96.5%	262	2	241	92.0%
mmox	73	3	74	101.4%	169	2	164	97.0%
pmoA	70	3	67	95.7%	174	2	169	97.1%
bvcA	65	3	60	92.3%	139	2	124	89.2%
vcrA	48	3	46	95.8%	163	2	150	92.0%

6.2.5   RT-qPCR/qPCR technology is reproducible

The differences in Ct values (duplicate samples) and the standard deviation of Ct values (triplicate samples) are summarized in **Table 18**. For all six functional genes, more than 90% of standards showed Ct standard deviation less than 0.5, while more than 80% of samples showed Ct difference less than 0.5 in duplicate qPCR reactions. Thus, the success criteria that the deviation of the cycle threshold (Ct) of duplicate/triplicate samples does not exceed 0.5 more than 25% of the time is met.

6.2.6   qPCR chemistries available in different labs provide comparable results

We have been working to transfer the technology for etheneotroph qPCR to SiREM. Initially, we sent PCR products and plasmids containing *etnC* and *etnE* gene from *Nocardioides* sp. strain JS614 to SiREM for qPCR method development. DNA samples were tested in our lab and at SiREM and the results were compared. For *etnC* qPCR, both labs noticed that samples sometimes generated different melting curves from standards (i.e. plasmids containing *etnC* from *Nocardioides* sp. strain JS614 or PCR product of *etnC* from *Nocardioides* sp. strain JS614). However, gel electrophoresis confirmed PCR products of expected size (~100bp). The variable melting curves of samples could be explained by primer dimer formation in samples with low template abundance. For *etnE* qPCR, the melting curves were more consistent, often only showing one peak.

Gene abundance results from the two labs were compared. For *etnC*, SiREM results were within an order of magnitude of Mattes lab results. The variabilities in qPCR results could be partly because of different DNA concentration measurements for the same DNA samples shared between the labs. SiREM used a nanodrop spectrophotometer to measure DNA and we used a Qubit fluorometer. DNA concentrations measured in our lab were usually lower than the measurements of SiREM **(Table 19)**. For *etnE*, results from SiREM were usually much lower abundance than our results. We saw a good correlation among *etnE* qPCR results from SiREM and Mattes lab, suggesting that some systematic error is introduced during the qPCR procedure.

In summary, SiREM was able to implement qPCR for *etnC* and *etnE* gene quantification. The success criteria that the qPCR results from two labs should be within an order of magnitude (i.e., with a 10-fold difference) is met for *etnC* qPCR. More than 10-fold variability between the two labs did occur for *etnE* qPCR in this set of samples **(Table 19).** This could be improved by continued standardization of qPCR laboratory practices between the two groups.

Table 19. qPCR Results Comparison Between SiREM and Mattes Lab.

Sample	DNA conc measurement (ng/ul)		etnC qPCR			etnE qPCR		
	SiREM (nanodrop)	Mattes lab (Qubit)	SiREM	Mattes lab	ratio (S:M)	SiREM	Mattes lab	ratio (S:M)
DNA 15227	15.98	4.78	1.4×10^7	5.0×10^6	2.86	5.5×10^5	8.3×10^6	0.07
DNA 15889	13.57	4.43	1.1×10^7	1.7×10^6	6.29	2.8×10^4	3.5×10^5	0.08
DNA 16632	19.08	5.84	4.7×10^6	4.4×10^5	10.57	9.7×10^4	1.6×10^6	0.06
DNA 16873	15.29	6.93	8.9×10^5	7.4×10^5	1.20	3.2×10^5	3.9×10^6	0.08
DNA 16874	8.81	0.24	6.6×10^4	2.6×10^5	0.25	3.0×10^3	7.4×10^5	0.00
DNA 17673	10.04	0.60	1.7×10^5	8.4×10^5	0.21	3.0×10^3	7.5×10^4	0.04
DNA 17674	14.49	5.65	4.4×10^5	1.2×10^6	0.36	3.4×10^3	5.5×10^4	0.06
DNA 17952	15.04	19.70	2.3×10^5	1.1×10^6	0.21	1.1×10^4	1.1×10^5	0.10
DNA 17954	5.16	5.80	1.4×10^6	2.2×10^5	6.18	3.0×10^4	1.5×10^5	0.20

6.2.7   RT-qPCR/qPCR technology is sensitive

We assessed the sensitivity of our RT-qPCR/qPCR technology by first evaluating the linear dynamic range of standard curves for each of the target genes. For all target genes, the lower end of the linear dynamic range was consistently about 30 gene copies per reaction. With 30 gene copies per reaction considered the lower quantification limit, and assuming 60 µl of DNA extract is generated per 1 L groundwater sample, the quantification limit for DNA samples is then 900 gene copies per L groundwater (assuming no DNA dilution was performed for qPCR). For RNA samples, assuming a 2.7% mRNA recovery (which was the average recovery in our experiments), the quantification limit is 10,000 transcript copies per L groundwater (10 transcript per ml). Melting curves were also used to assess the amplification specificity in samples, especially when the gene or transcript abundances were below the quantification limit (**Figure 79**). When a single peak that corresponds to the peak observed in the standard is seen, this usually indicates good amplification specificity (**Figure 79A, C**). Multiple peaks indicate possible unspecific amplification or formation of primer dimers (**Figure 79B, D**).

In summary, the quantification limit of 900 genes per liter groundwater for DNA samples is close to the original success criterion of 500 genes per liter groundwater. For RNA samples, we could not achieve a lower quantification limit of 1,000 transcripts per liter groundwater mainly because of relatively lower RNA recovery than expected. However, in both cases we feel that perhaps these success criteria were a bit ambitious, as these quantification limits are very reasonable for qPCR. Based on our experience, we can say that lower quantification limits of 1,000 genes per liter of groundwater and 10,000 transcripts per liter of groundwater is sufficient sensitivity for RT-qPCR/qPCR in groundwater samples. However, the following changes to the RNA extraction methodology could be implemented to decrease the lower limit of quantification.

1. Minimize RNA degradation by using RNase cleaning solution, RNase OUT. All buffers should be prepared with RNase free water.

2. Be familiar with the protocol and reduce the experiment time. This will also help minimize RNA degradation during the experiment.

3. Investigate ways to improve reverse transcription efficiency (e.g., experiment with different reverse transcriptase kits).
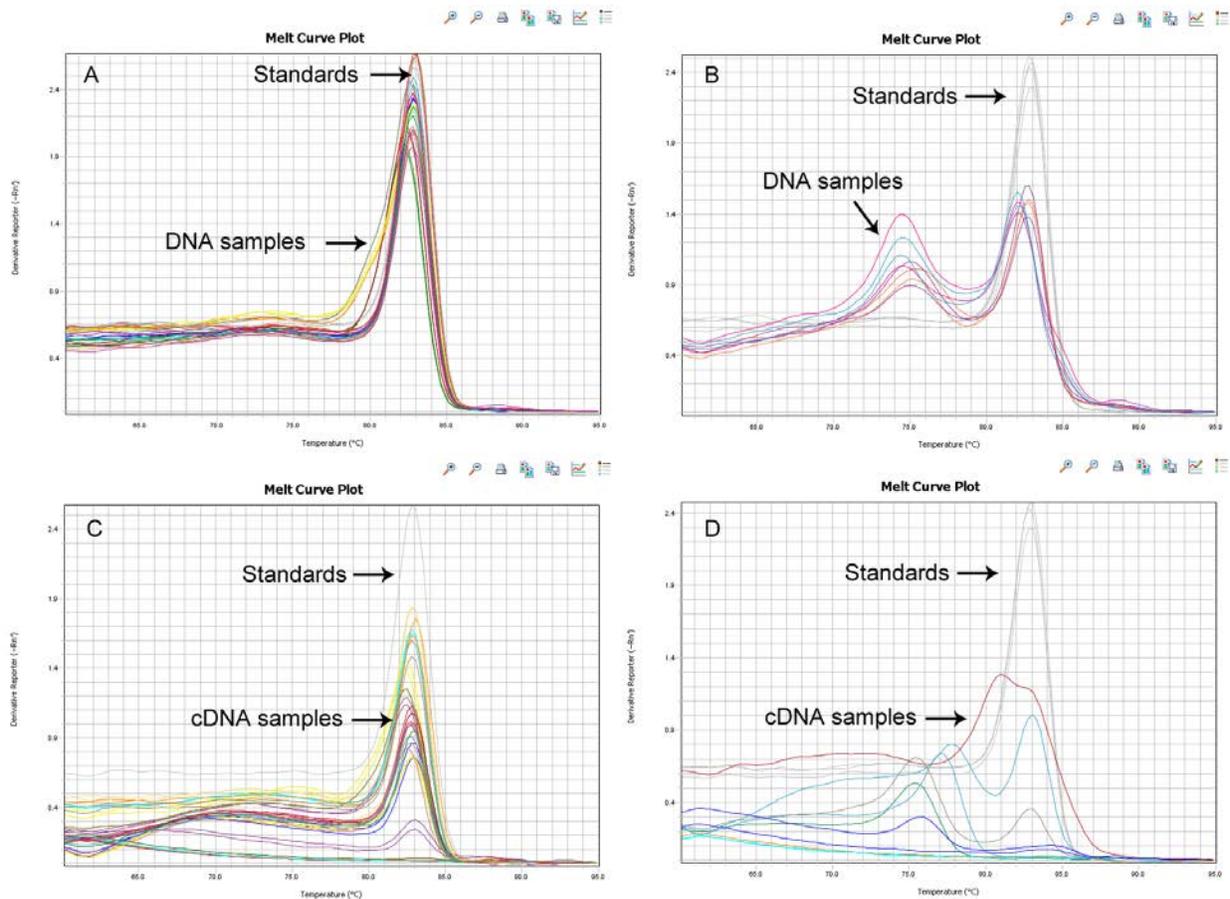
Figure 79. Melting Curve Examples with RTC Primers of A) Specific Amplification of DNA Samples, B) Possible Unspecific Amplification or Dimer Formation in DNA Samples, C) Specific Amplification of cDNA Samples, D) Possible Unspecific Amplification or Dimer Formation in cDNA Samples.

6.2.8 Determine how qPCR/RT-qPCR data correlates with temporal variation in VC concentration and other geochemical parameters

The temporal data we collected from NAS Oceana groundwater samples is the most extensive dataset collected to date. We used this data in the assessment of this performance objective, as we were not able to collect more than 2-3 timepoints for any of the other sites we obtained samples from during this project. The trends in VC concentration at NAS Oceana were generally downward in all three wells studied (**Figure 14**). However, these trends were not statistically significant according to a Mann-Kendall test (p=0.13) **(Table 20)**. This highlights the issues with dilute plumes in that VC attenuation rates can slow considerably as the concentration approaches the MCL.

126

DO was present at low levels (0 to 1.44 mg/L) and ORP values were consistently negative (-113 to -23 mV) in groundwater samples from MW05, MW25 and MW19, indicating the groundwater was slightly anoxic. Methane, an important growth substrate for aerobic cometabolic VC-oxidizers (methanotrophs), was relatively abundant (usually 1-9 mg/L). Ethene, an end product of reductive dechlorination of chloroethenes and growth substrate for etheneotrophs (also known aerobic VC-cometabolizers), was only detected once in MW25 in 2009 (0.008 mg/L), and was not analyzed in subsequent sampling events.

The presence of DO, ferrous iron, and methane in the groundwater suggests the co-occurrence of several terminal electron accepting processes. Temporal trends of functional these geochemical parameters were estimated by Mann-Kendall analysis **(Table 20)**. DO, ORP, pH, temperature, ferrous iron, and methane did not display any significant decreasing or increasing trends over the course of the study **(Table 20)**.

Temporal trends of functional gene abundances were also estimated by Mann-Kendall analysis **(Table 20)**. Only *mmo*X abundance (in all three monitoring wells) and *bvcA* abundance (in MW19) displayed significantly increasing trends from 2008 to 2014 ($p<0.1$). Abundance trends of *etnC*, *etnE*, and *pmoA* were relatively stable in the three monitoring wells.

We observed that transcript per gene ratios for *mmoX* in MW19 and *pmoA* in MW25 and MW19 in 2014 were higher than 2013 (**Table 9**). In MW05, transcript per gene ratios for *pmoA* were higher in 2013 and 2014 than in 2012. In MW19, the transcript per gene ratio for *bvcA* increased from 0.16 in 2012 to 2.90 in 2013 and to 30.7 in 2014. Trend analysis for transcript data was not performed because of limited temporal data and because some transcript abundance estimates were below the quantification limit and not appropriate for trend or correlation analysis.

Table 20. Temporal Trends of Functional Gene Abundances and Geochemical Parameters Assessed by Mann-Kendall test.

*: p<0.1, **: p<0.05. NA: not available

	MW05			MW25			MW19		
	n	tau	p value	n	tau	p value	n	tau	p value
log *etnC*	4	0.67	0.31	5	0.60	0.22	6	0.33	0.45
log *etnE*	4	-0.33	0.73	5	0.20	0.81	6	-0.20	0.71
log *mmoX*	4	1.00	0.09*	5	0.80	0.09*	6	0.87	0.02**
log *pmoA*	4	0.33	0.73	5	0.40	0.46	6	0.47	0.26
log *bvcA*	NA	NA	NA	NA	NA	NA	6	0.87	0.02**
DO	6	-0.33	0.45	6	-0.33	0.45	6	-0.33	0.45
ORP	6	0.33	0.45	6	0.20	0.71	6	-0.20	0.71
pH	6	0.07	1.00	6	-0.07	1.00	6	0.33	0.45
temp	6	0.60	0.13	6	0.20	0.71	6	0.60	0.13
VC	6	-0.60	0.13	6	-0.60	0.13	6	0.07	1.00
cis-DCE	6	0.20	0.71	6	-0.73	0.06*	6	-0.73	0.06*
ferrous	6	-0.20	0.71	6	0.28	0.57	6	0.47	0.26
methane	6	0.73	0.06*	6	0.47	0.26	6	0.07	1.00

Relationships between functional gene abundances and geochemical and contaminant parameters were explored with the Kendall rank correlation analysis during the 2008 – 2014 time period (**Figure 80**). The abundances of *mmoX* and *pmoA* were not correlated with methane, and showed mixed relationships with VC and *cis*-DCE concentrations. A significant negative correlation between *mmoX* abundances and VC and *cis*-DCE concentrations was observed in MW25 ($p<0.1$). DO and temperature were positively correlated with *pmoA* abundance in MW05 ($p<0.05$) and negative in MW25 ($p<0.1$). In MW05, *etnE* abundances were significantly correlated to *cis*-DCE concentrations but not to VC. In MW25, *etnC* and *etnE* abundances were negatively correlated with VC or *cis*-DCE, but not at a significant level. In MW19, *etnC* and *etnE* abundances were positively correlated to VC concentrations ($p<0.1$), and not significantly correlated to *cis*-DCE.

The qPCR analysis revealed that, compared to methanotrophs, etheneotrophs were less abundant and active at this site. The relatively low abundance of etheneotroph functional genes (i.e., *etnC* and *etnE*) and transcripts indicates low etheneotroph activity. This is consistent with the low levels of VC and ethene in the groundwater. Trend analysis supports this conclusion. Etheneotroph populations were relatively stable in NAS Oceana wells, as no significant decreasing or increasing temporal trend was observed for *etnC* and *etnE*. In MW19, the positive correlation between VC concentrations and *etnC* and *etnE* suggests that VC could be supporting some growth of etheneotrophs. We noted that there was not a strong significant correlation between *etnC* and *etnE* in our analyses, although these genes should be strongly correlated because both genes are present in etheneotrophs. We attribute this inconsistency with the tendency for qPCR to overestimate *etnC* abundance (caused by primer dimer formation with RTC primers at low target gene concentrations).

Overall, our performance assessment using data from NAS Oceana showed that establishing temporal relationships between VC degradation and functional gene abundance and activity is possible, but was difficult in the dilute VC plume scenario we encountered at NAS Oceana. VC attenuation rates in these wells were low, and the corresponding abundance and activity of VC-oxidizing bacteria was also low. Another issue is that it is difficult to obtain enough data points for statistical analysis due to the currently small size of our gene abundance database. Despite this we did observe a significant increase in *mmoX* abundance with time in all three wells. In the case of MW25, *mmoX* abundance was also negatively correlated with VC concentration, as would be expected if methanotrophs were controlling the rate of VC attenuation at this site.
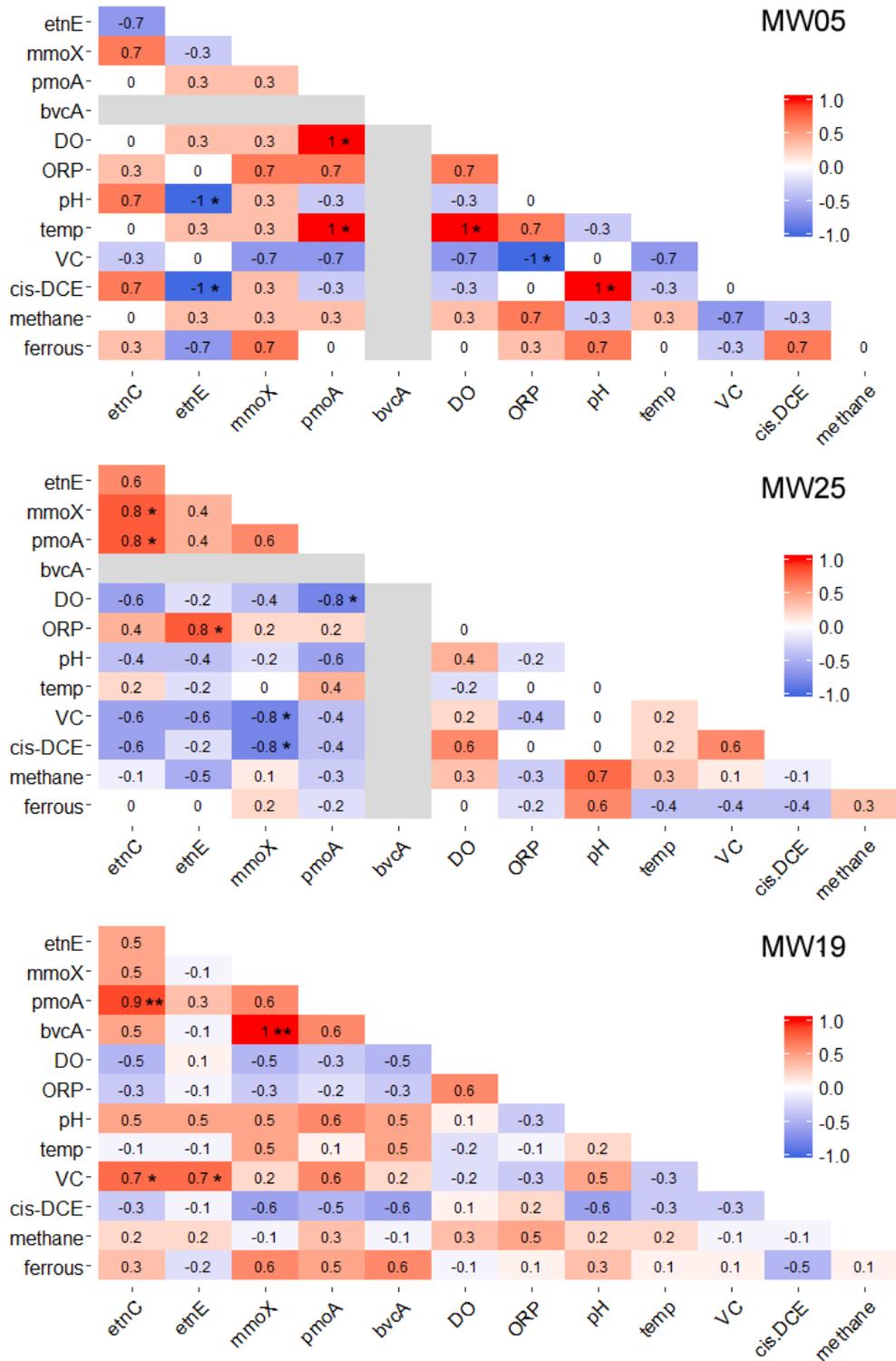
Figure 80. Correlation Heatmap of Kendall's Tau Coefficient Between Functional Genes and Geochemical Parameters in MW05, MW25 and MW19.

*: p<0.1, **: p<0.05. Gray boxes with no tau values indicates that correlation data is not available.*

6.2.9 Determine how qPCR/RT-qPCR data correlates with spatial variations in VC concentration and other geochemical parameters

Over the course of this project our efforts have resulted in an expanding database of functional gene sequences from etheneotrophs (VC-oxidizers) found in 7 different VC plumes and at several time points in some cases. So far, we have data from NAS Oceana (2013.11, 3 monitoring wells); NAS Oceana (2014.07, 3 monitoring wells); Kings Bay (2015.01, 4 monitoring wells); Altus AFB (2015.05, 3 monitoring wells); Seal Beach (2015.07, 10 monitoring wells); Seal Beach (2015.12, 13 monitoring wells); Parris Island North Plume (2015.10, 12 monitoring wells); Parris Island North Plume (2016.07, 12 monitoring wells); Parris Island South Plume (2015.10, 8 monitoring wells); Parris Island South Plume (2016.07, 8 monitoring wells);); LF05 Hawaii (2015.09, 4 monitoring wells); LF05 Hawaii (2015.12, 5 monitoring wells); LF05 Hawaii (2016.03, 6 monitoring wells); LF05 Hawaii (2016.09, 5 monitoring wells). We collected gene and transcript data for 6 different genes associated with VC degradation at these sites.

To begin assessing this performance objective we asked whether this qPCR dataset (genes and transcripts) shows any relationships with VC concentrations measured in the wells at the same time groundwater biomas was collection for qPCR analysis. We used different statistical methods, including Spearman's correlation, simple linear regression (slr), and multilevel regression (mlr) to assess the possible correlations between functional genes/transcripts and VC concentrations. The purpose of multilevel regression is to account for the effects of sample clustering (i.e. samples from the same sites and samples from the same monitoring wells collected on different dates). For simple linear regression and multilevel regression, log transformation was performed on gene and transcript abundance data, as well as VC concentration data as these log transformed values more closely fit a normal distribution. This subsequently allowed us to perform statistical analyses where the underlying assumption is that the data is normally distributed.

In **Table 21** we summarize the relationship between functional genes and transcripts and VC concentrations using mlr, slr, and Spearman's correlation. Mlr and slr results are also plotted in **Figure 81**. Mlr and slr model residuals are plotted in **Figure 82, Figure 83**, and **Figure 84**. Akaike's Information Criterion (AIC) scores were also calculated to facilitate a quantitative comparison, and are shown in **Table 21**. Lower AIC scores indicate a better fit of the statistical model with the data.

Mlr, slr, and Spearman's correlation analysis generated similar results in many cases, but discrepancies were noted. For example, slr and Spearman's correlations suggested a negative relationship between *pmoA* abundance and VC concentration, while mlr did not support their association. The discrepancies between the statistical analyses suggest that considering hierarchical data structure is important when inferring relationships between microbial data and geochemical parameters among sites.

Compared to slr, mlr usually yielded lower AIC scores, showing an overall improved fit to the dataset. Mlr also yielded more symmetrically distributed residual plots, while slr residual plots sometimes displayed patterns, suggesting non-ideal data fit (**Figure 82, Figure 83**, and **Figure 84).** Based on this analysis, mlr is considered the most appropriate model for inferring relationships among microbial and geochemical parameters.

Multilevel regression clearly indicates significant correlations (p values < 0.01) between gene and transcript abundances of *etnC, etnE, bvcA*, and *vcrA* and VC concentrations (except for *vcrA* transcript vs. VC). There was no significant correlation observed for VC concentrations and methanotroph functional genes or transcripts (*mmoX* and *pmoA*). The significant correlations between *etnC, etnE, bvcA, vcrA* and VC concentrations suggested that VC is an influential factor for the abundances and activities of etheneotrophs and anaerobic VC degraders, and VC is likely used as a growth substrate for etheneotrophs and anaerobic VC degraders on site. Methanotrophs can only degrade VC via co-metabolism. However, the lack of correlation between methanotrophs and VC concentrations does not mean that methanotrophs do not contribute to VC removal at these sites. They could be more relevant out at the plume fringes.

Table 21. Regression Analysis of Functional Gene and Transcript Abundances with VC Concentrations; p values < 0.05 are in bold.

VC vs gene	n	multilevel regression				simple linear regression				Spearman's correlation	
		Coef	p value	95% CI	AIC	Coef	p value	95% CI	AIC	Rho	p value
etnC	95	0.43	**<0.001**	0.28-0.58	272	0.46	**<0.001**	0.30-0.61	292	0.52	**<0.001**
etnE	95	0.45	**<0.001**	0.28-0.62	270	0.48	**<0.001**	0.33-0.64	290	0.55	**<0.001**
mmoX	95	-0.08	0.447	-0.31-0.15	288	-0.17	0.065	-0.35-0.01	320	-0.23	**0.028**
pmoA	95	0.08	0.499	-0.14-0.32	322	-0.27	**0.013**	-0.49--0.06	351	-0.25	**0.015**
bvcA	95	0.63	**<0.001**	0.31-0.98	361	0.38	**0.004**	0.13-0.63	381	0.26	**0.011**
vcrA	95	0.56	**0.006**	0.11-0.98	386	0.87	**<0.001**	0.59-1.15	402	0.52	**<0.001**
mmoX+pmoA	95	0.05	0.620	-0.17-0.29	309	-0.26	**0.010**	-0.47--0.06	339	-0.25	**0.013**
bvcA+vcrA	95	0.73	**<0.001**	0.39-1.08	371	0.67	**<0.001**	0.42-0.91	376	0.48	**<0.001**
VC vs. transcript	n	multilevel regression				simple linear regression				Spearman's correlation	
		Coef	p value	95% CI	AIC	Coef	p value	95% CI	AIC	Rho	p value
etnC	70	0.52	**<0.001**	0.24-0.78	256	0.49	**<0.001**	0.27-0.71	249	0.35	**<0.001**
etnE	71	0.42	**<0.001**	0.19-0.67	241	0.37	**<0.001**	0.16-0.57	240	0.36	**<0.001**
mmoX	61	0.06	0.597	-0.15-0.29	181	0.14	0.182	-0.07-0.34	188	-0.19	0.072
pmoA	80	0.05	0.721	-0.19-0.30	273	-0.14	0.201	-0.35-0.07	277	-0.24	**0.018**
bvcA	54	0.71	**0.002**	0.30-1.16	220	0.39	**0.036**	0.03-0.75	229	0.19	0.058
vcrA	51	0.20	0.407	-0.35-0.68	193	0.32	0.104	-0.07-0.71	200	0.48	**<0.001**
mmoX+pmoA	84	0.10	0.439	-0.17-0.36	288	-0.11	0.197	-0.32-0.10	296	-0.25	0.014
bvcA+vcrA	70	0.59	**0.004**	0.22-0.98	279	0.54	**<0.001**	0.23-0.84	281	0.46	**<0.001**

n: number of samples in the analysis

CI: confidence interval

Coef: regression coefficient

AIC: Akaike's Information Criterion. Lower AIC scores indicates improved fitting of the statistical model with the data
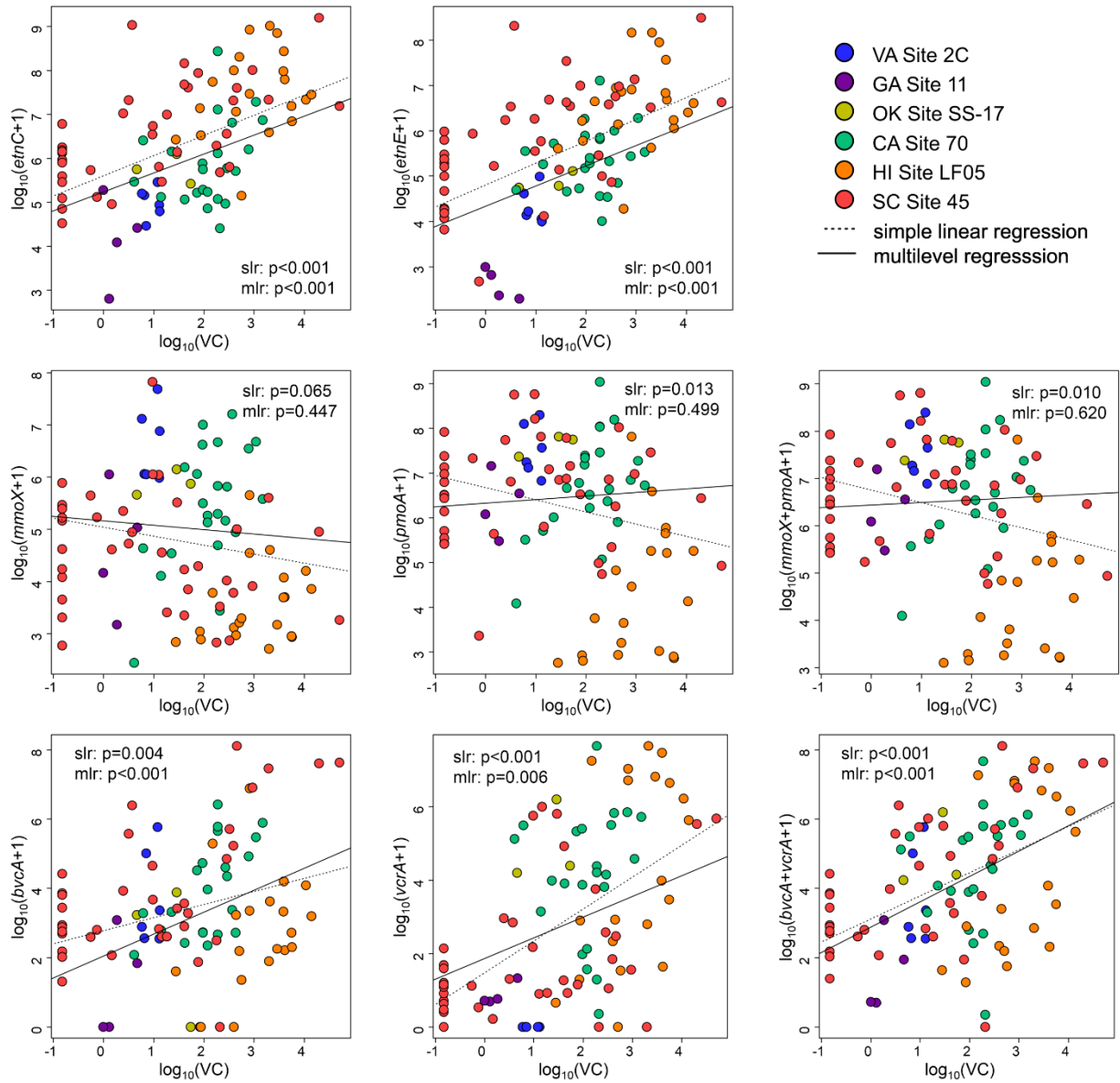
Figure 81. Relationships Among Functional Genes and VC Concentrations as Assessed by Multilevel Regression (mlr, Solid Line) and Simple Linear Regression (slr, Dotted Line).

p values for slr and mlr are indicated for each functional gene. Additional model parameters (regression coefficients, 95% CIs, and AIC scores) are listed in Table 21.
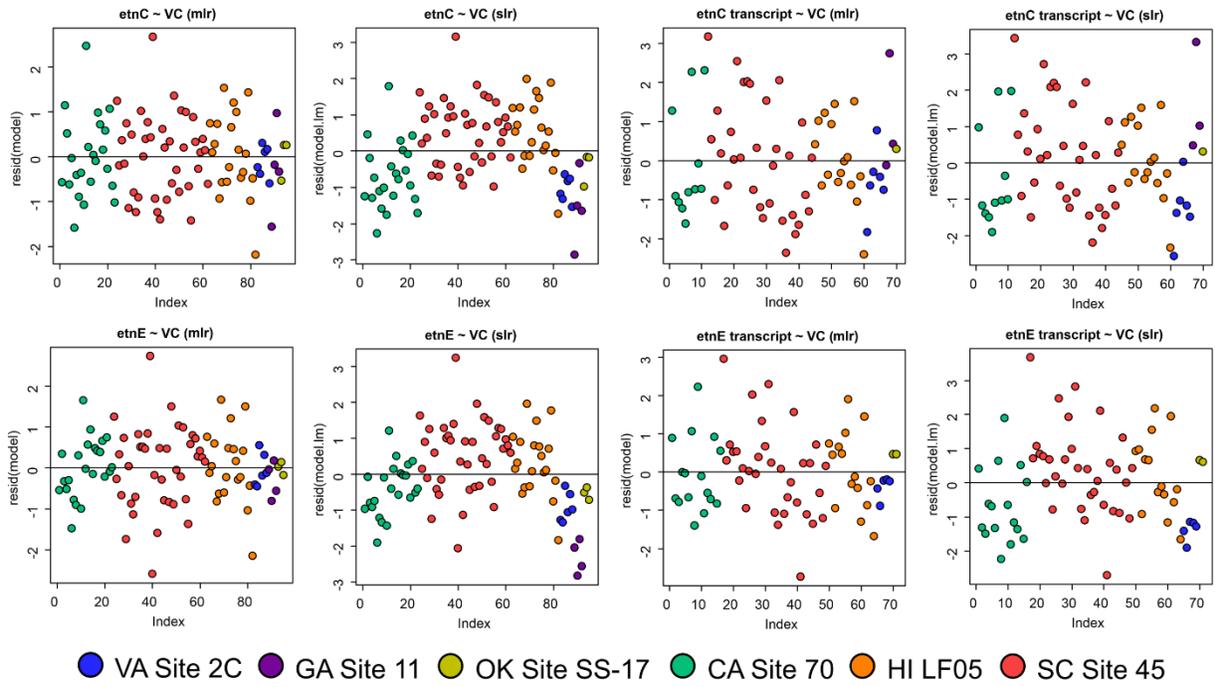
Figure 82. Residuals of Multilevel Regression (mlr) and Simple Linear Regression (slr) Analyses of VC Concentration vs. etnC and etnE Gene and Transcript Abundance.
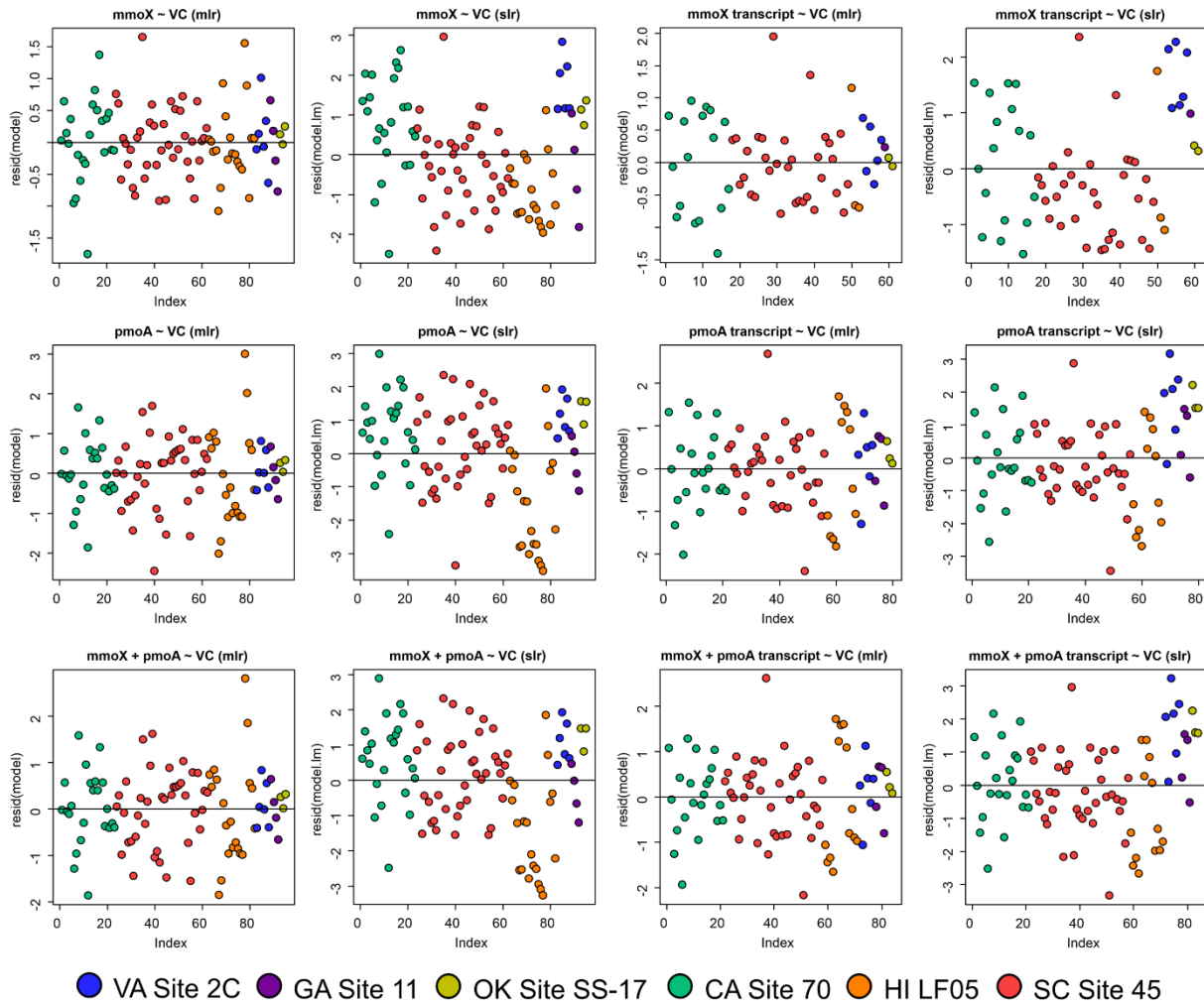
Figure 83. Residuals of Multilevel Regression (mlr) and Simple Linear Regression (slr) Analyses of VC Concentration vs. mmoX and pmoA Gene and Transcript Abundance.
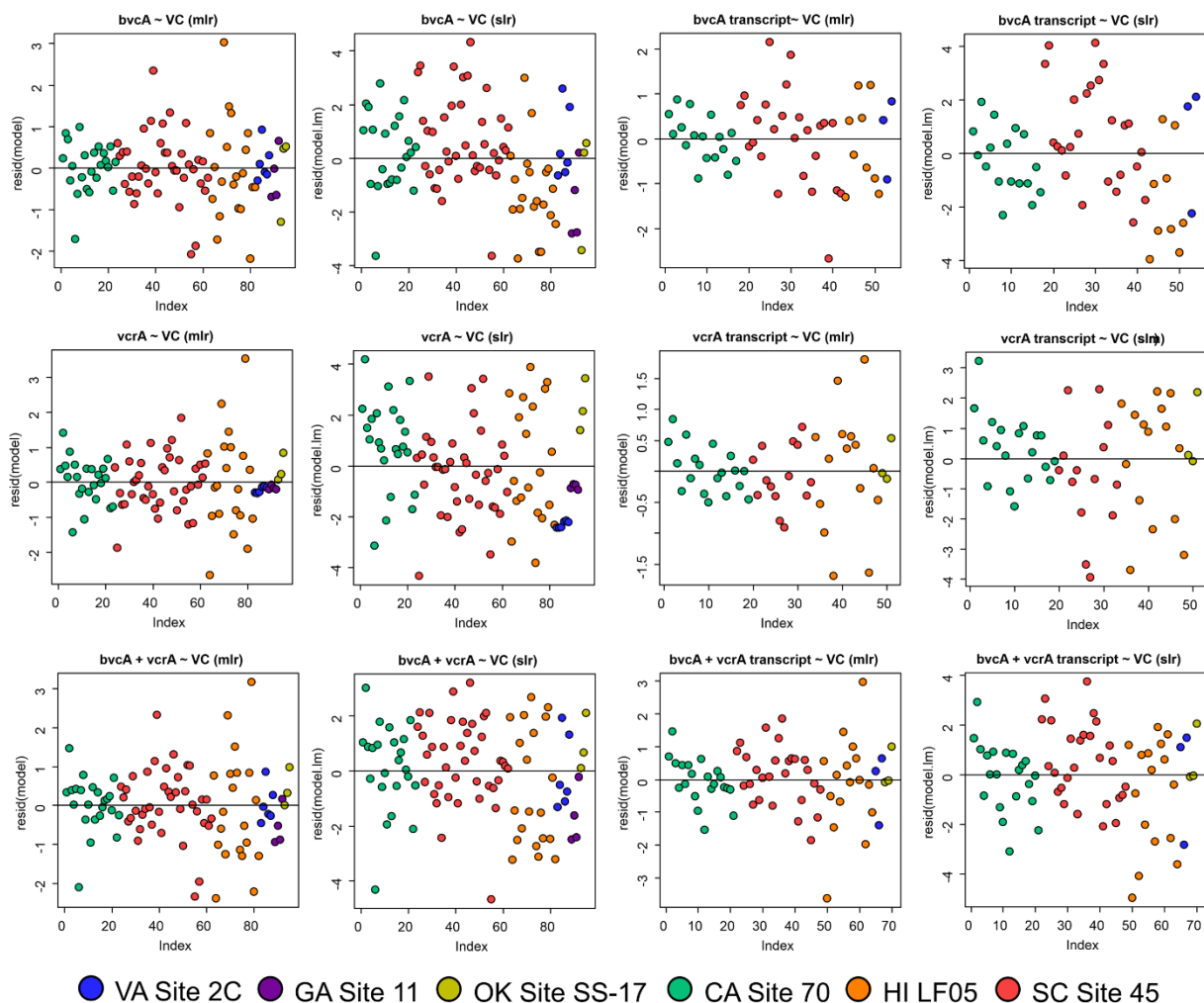
Figure 84. Residuals of Multilevel regression (mlr) and Simple Linear Regression (slr) Analyses of VC Concentration vs. bvcA and vcrA Gene and Transcript Abundance.

We also used multilevel modeling to perform correlation analysis between functional genes and transcripts and other geochemical parameters, including TCE, *cis*-DCE, *trans*-DCE, ethene, methane, and DO/ORP data. The results are summarized in **Table 22**, **Table 23,** and **Table 24**.

We investigated the relationships between those chlorinated ethenes and VC biodegradation functional genes and transcripts because TCE, *cis*-DCE and *trans*-DCE could be used as electron acceptors by anaerobic VC-dechlorinators and possibly induce expression of alkene monooxygenase genes. Etheneotroph functional genes and transcripts were positively associated with *cis*-DCE, *trans*-DCE and TCE concentrations, although etheneotrophs are only known to co-metabolize *cis*-DCE. The relationships between *etnC/etnE* abundances and other chlorinated ethenes could exist because VC is a dechlorination product of those compounds. TCE and the DCEs may also act as inducers of *etnC* and *etnE*, by analogy to the behavior of propene-oxidizing *Xanthobacter* strain Py2.

For VC reductive dehalogenase genes, *bvcA* and its transcripts were positively related to *cis*-DCE, *trans*-DCE, and TCE, while *vcrA* was positively related to *trans*-DCE and TCE. Positive associations with *cis*-DCE, *trans*-DCE and TCE concentrations and (*bvcA* + *vcrA*) genes were noted, but not with (*bvcA* +*vcrA*) transcripts. The VC reductive dehalogenases encoded by *bvcA* and *vcrA* also use DCEs as electron acceptors, which could explain their positive correlation with *cis*-DCE and *trans*-DCE. TCE is dechlorinated by the *vcrA* gene product, which could explain the relationship between these two parameters. The relationship between TCE and *bvcA* genes and transcripts (**Table 24**) might be explained by TCE being the parent compound of *cis*-DCE and *trans*-DCE. This is supported by strong correlations between TCE concentrations and DCE isomers.

Ethene concentrations were positively associated with the abundance of *etnC, etnE, bvcA, vcrA* and their transcripts (except for *vcrA* transcripts) (**Table 25**). Ethene could support the growth of etheneotrophs, which could explain their positive correlation. The observed correlation between VC reductive dehalogenase genes and transcripts with ethene could be because that ethene is the end product of reductive dechlorination.

Methanotroph functional gene and transcript abundances were associated with methane concentrations, but not ethene or other cVOCs (**Table 26**). Sites featuring dilute VC plumes and low ethene levels (e.g. VA Site 2C and GA Site 11) provide limited growth substrates for etheneotrophs and VC-dechlorinators. At those sites, methanotroph functional genes and transcripts were usually more abundant than those from etheneotrophs and anaerobic VC-dechlorinators suggesting co-metabolism by methanotrophs could be the prominent VC biodegradation pathway

No functional gene or transcript was related to field-measured DO concentrations ($p > 0.05$, data not shown). Etheneotroph functional genes were highly abundant and expressed in monitoring wells near or within source zones where DO was limited (<1 mg/L) and VC concentrations were high. DO levels<0.1 mg/L have been shown to sustain aerobic VC degradation under lab conditions. Oxygen flux may also exist to support aerobic VC degraders at locations with low DO concentrations. Macroscopic field DO measurements are not a reliable indicator for either aerobic or anaerobic VC degradation potential or activity likely because of the low resolution and quality of measurements at levels < 1 mg/L. We propose that functional gene and transcript data could instead be used to provide more accurate and reliable information about in situ VC biodegradation potential and activity.

For ORP, negative correlations were observed for functional gene *etnC, etnE*, and *pmoA*. However, the possible inaccuracy in field ORP measurements may introduce too much error to draw solid conclusions from the correlations. No significant relationships between transcripts and ORP were observed.

Overall the results of the assessment of this performance objective have met the success criteria. Application of qPCR technology to groundwater samples from several VC plumes have revealed a statistically significant correlation between etheneotroph functional genes and transcripts and VC concentrations. This relationship can be used to roughly predict that the higher the VC concentration in groundwater, the higher the etheneotroph abundance and activity will be.

On the other hand, no relationship or negative correlations were observed between etheneotroph abundance and DO and ORP measurements. These results are difficult to interpret but suggest that DO and ORP values do not hold any predictive value with respect to etheneotroph abundance or activity in the environment.

We saw the same general relationships between VC dehalogenase gene abundance and VC concentration, DO, and ORP in the same groundwater samples. This highlights the complexity of groundwater samples. Cryo-core samples, taken along a VC transect in the Parris Island site 45 northern VC plume, were collected and analyzed for cVOC contamination and VC-degrading bacterial guild abundances (as described in Section 5.6.8.2)

We used different statistical methods (censored regression, simple linear regression, and Spearman's correlation) to assess the relationships between functional genes and geochemical parameters in the cryo-core samples. Censored regression was performed to handle the censored structure of functional gene abundance datasets. Simple linear regression and Spearman's correlation was used for comparison with censored regression. The results of censored regression, simple linear regression, and Spearman's correlation were generally similar, yet differences were noted in some cases (**Table 27**).

Etheneotroph functional genes (*etnC* and *etnE*) were positively correlated with VC concentrations in the lower surficial aquifer (Spearman's correlation, $p<0.05$) but not in the upper surficial aquifer (Table 2). VC reductive dehalogenase functional genes (*bvcA* and *vcrA*) were strongly related to VC in the lower aquifer (cr and Spearman's correlation, $p<0.001$), but only *bvcA* was related to VC in the upper aquifer (cr, $p=0.002$). No significant association was observed between methanotroph functional genes (*mmoX* and *pmoA*) and VC concentrations in the upper or lower aquifer. Total bacterial 16S rRNA genes was positively associated with VC concentrations with depth in both the upper and lower aquifer samples (slr, $p=0.004$).

We also investigated the relationships between concentrations of other chlorinated ethenes (PCE, TCE, and cis-DCE) and VC biodegradation functional gene abundance. Etheneotroph functional genes were positively associated with PCE (**Table 28**) and TCE (**Table 29**) in the upper and lower aquifers, except for *etnE* and TCE, and were positively associated with cis-DCE in the lower surficial aquifer samples (**Table 30**). For VC reductive dehalogenase genes, *bvcA* was positively associated with PCE (**Table 28**) and cis-DCE (**Table 30**) along depth of both aquifers, while *vcrA* positively was associated with cis-DCE in lower surficial aquifer (**Table 30**). For methanotrophs, positive associations were observed for *mmoX* with PCE and TCE in both aquifers (**Table 28** and **Table 29**), and with cis-DCE in lower surficial aquifer (**Table 30**). PCE, TCE, and cis-DCE were positively associated with total bacterial 16S rRNA genes in both upper and lower surficial aquifers, while cis-DCE was related to total bacterial 16S rRNA gene only in the lower surficial aquifer.

Ethene concentrations were positively associated with *etnC, etnE, mmoX*, *bvcA*, and *vcrA* in the lower surficial aquifer (**Table 31**). Ethene was also positively correlated with *bvcA* in the upper aquifer (**Table 31**). Methane concentrations were negatively associated with *etnC, etnE*, *mmoX pmoA and vcrA* in the upper surficial aquifer (**Table 32**). Methane was also positively associated with *bvcA* through both aquifers and with *vcrA* in the lower aquifer (**Table 32**).

Table 22. Regression Analysis of Functional Gene and Transcript Abundances with cis-DCE in Groundwater Samples.

p values < 0.05 Are in bold

Gene vs *cis*-DCE	n	multilevel regression				simple linear regression				Spearman's correlation	
		Coef	p value	95% CI	AIC	Coef	p value	95% CI	AIC	Rho	p value
etnC	95	0.25	**0.002**	0.10-0.38	283	0.28	**0.001**	0.11-0.44	310	0.34	**0.001**
etnE	95	0.24	**0.002**	0.09-0.37	284	0.28	**0.001**	0.11-0.44	312	0.35	**<0.001**
mmoX	95	-0.13	0.146	-0.28-0.05	287	-0.19	**0.031**	-0.36--0.02	319	-0.23	**0.027**
pmoA	95	0.01	0.912	-0.15-0.22	323	-0.07	0.506	-0.28-0.14	357	-0.08	0.441
bvcA	95	0.36	**0.021**	0.07-0.63	367	0.34	**0.006**	0.10-0.58	382	0.25	**0.016**
vcrA	95	0.31	0.081	0.08-0.66	390	0.43	**0.005**	0.13-0.73	427	0.30	**0.003**
mmoX+pmoA	95	0.02	0.858	-0.16-0.18	310	-0.06	0.514	-0.26-0.13	345	-0.08	0.419
bvcA+vcrA	95	0.38	**0.024**	0.03-0.68	382	0.38	**0.003**	0.13-0.63	393	0.30	**0.003**
Transcript vs cis-DCE	**n**	**multilevel regression**				**simple linear regression**				**Spearman's correlation**	
		Coef	p value	95% CI	AIC	Coef	p value	95% CI	AIC	Rho	p value
etnC	70	0.38	**0.002**	0.16-0.62	259	0.40	**<0.001**	0.18-0.61	254	0.26	**0.010**
etnE	71	0.30	**0.003**	0.12-0.48	288	0.32	**0.001**	0.14-0.50	292	0.28	**0.006**
mmoX	61	-0.08	0.396	-0.27-0.10	181	-0.08	0.377	-0.27-0.10	189	-0.12	0.250
pmoA	80	0.05	0.616	-0.15-0.26	274	-0.03	0.791	-0.23-0.17	279	-0.09	0.378
bvcA	54	0.56	**0.003**	0.15-0.92	219	0.57	**0.001**	0.25-0.89	222	0.28	**0.007**
vcrA	51	-0.29	0.198	-0.77-0.15	192	-0.30	0.105	-0.66-0.06	200	0.24	**0.019**
mmoX+pmoA	84	0.04	0.707	-0.15-0.23	289	-0.05	0.648	-0.25-0.15	297	-0.09	0.367
bvcA+vcrA	70	0.35	0.054	-0.04-0.67	283	0.33	**0.027**	0.04-0.63	288	0.29	**0.004**

n: number of samples in the analysis

CI: confidence interval

Coef: regression coefficient

AIC: Akaike's Information Criterion. Lower AIC scores indicates improved fitting of the statistical model with the data

Table 23. Regression Analysis of Functional Gene and Transcript Abundances with Trans-DCE in Groundwater Samples.

p values < 0.05 are in bold

Gene vs *trans*-DCE	n	multilevel regression				simple linear regression				Spearman's correlation	
		Coef	p value	95% CI	AIC	Coef	p value	95% CI	AIC	Rho	p value
etnC	95	0.38	**0.01**	0.15-0.61	282	0.49	**<0.001**	0.29-0.70	300	0.43	**<0.001**
etnE	95	0.39	**0.001**	0.17-0.61	282	0.53	**<0.001**	0.33-0.74	298	0.47	**<0.001**
mmoX	95	-0.20	0.111	-0.46-0.06	285	-0.29	**0.012**	-0.52--0.07	317	-0.27	**0.009**
pmoA	95	0.03	0.828	-0.24-0.31	322	-0.29	**0.036**	-0.56--0.02	353	-0.20	**0.048**
bvcA	95	0.61	**0.004**	0.20-1.02	364	0.49	**0.003**	0.17-0.80	381	0.24	**0.021**
vcrA	95	0.64	**0.011**	0.14-1.15	387	0.87	**<0.001**	0.49-1.24	415	0.44	**<0.001**
mmoX+pmoA	95	0.03	0.829	-0.24-0.28	309	-0.28	**0.034**	-0.53--0.02	341	-0.21	**0.041**
bvcA+vcrA	95	0.71	**0.001**	0.34-1.08	375	0.69	**<0.001**	0.37-1.01	385	0.36	**<0.001**
Transcript vs *trans*-DCE	n	multilevel regression				simple linear regression				Spearman's correlation	
		Coef	p value	95% CI	AIC	Coef	p value	95% CI	AIC	Rho	p value
etnC	70	0.48	**0.005**	0.16-0.81	260	0.51	**0.001**	0.23-0.80	254	0.22	**0.033**
etnE	71	0.40	**0.009**	0.09-0.70	286	0.41	**0.002**	0.15-0.67	287	0.34	**0.001**
mmoX	61	-0.15	0.246	-0.43-0.11	179	-0.07	0.603	-0.32-0.19	190	-0.17	0.102
pmoA	80	0.00	0.980	-0.25-0.28	273	-0.17	0.211	-0.43-0.10	277	-0.25	**0.013**
bvcA	54	0.80	**0.003**	0.30-1.31	220	0.56	**0.012**	0.13-0.99	227	0.24	**0.017**
vcrA	51	0.06	0.835	-0.54-0.65	193	0.07	0.768	-0.44-0.57	203	0.38	**<0.001**
mmoX+pmoA	84	-0.04	0.806	-0.34-0.25	288	-0.21	0.118	-0.47-0.05	295	-0.25	**0.013**
bvcA+vcrA	70	0.44	0.061	0.00-0.91	283	0.48	**0.015**	0.10-0.87	287	0.37	**<0.001**

n: number of samples in the analysis

CI: confidence interval

Coef: regression coefficient

AIC: Akaike's Information Criterion. Lower AIC scores indicates improved fitting of the statistical model with the data

Table 24. Regression Analysis of Functional Gene and Transcript Abundances with TCE in Groundwater Samples.

p values < 0.05 are in bold

Gene vs TCE	n	multilevel regression				simple linear regression				Spearman's correlation	
		Coef	p value	95% CI	AIC	Coef	p value	95% CI	AIC	Rho	p value
etnC	95	0.21	**0.009**	0.07-0.38	287	0.33	**<0.001**	0.16-0.49	307	0.34	**0.001**
etnE	95	0.19	**0.017**	0.04-0.33	288	0.30	**0.001**	0.13-0.47	311	0.35	**0.001**
mmoX	95	-0.07	0.179	-0.24-0.11	288	-0.22	**0.015**	-0.40--0.04	318	-0.19	0.067
pmoA	95	0.03	0.725	-0.18-0.22	323	-0.18	0.109	-0.39-0.04	355	-0.11	0.279
bvcA	95	0.41	**0.005**	0.13-0.67	365	0.37	**0.004**	0.12-0.62	381	0.30	**0.003**
vcrA	95	0.35	**0.029**	0.03-0.67	389	0.54	**0.001**	0.23-0.85	423	0.36	**<0.001**
mmoX+pmoA	95	0.04	0.669	-0.14-0.21	310	-0.16	0.119	-0.36-0.04	343	-0.12	0.261
bvcA+vcrA	95	0.45	**0.004**	0.15-0.79	379	0.50	**<0.001**	0.24-0.76	388	0.38	**<0.001**
Transcript vs TCE	n	multilevel regression				simple linear regression				Spearman's correlation	
		Coef	p value	95% CI	AIC	Coef	p value	95% CI	AIC	Rho	p value
etnC	70	0.38	**0.003**	0.16-0.62	261	0.39	**0.001**	0.18-0.61	254	0.30	**0.003**
etnE	71	0.28	**0.011**	0.05-0.49	288	0.33	**0.001**	0.14-0.52	292	0.36	**<0.001**
mmoX	61	-0.14	0.179	-0.35-0.05	179	-0.10	0.312	-0.30-0.10	189	-0.15	0.155
pmoA	80	0.04	0.725	-0.17-0.26	273	-0.06	0.613	-0.29-0.17	278	-0.11	0.307
bvcA	54	0.76	**<0.001**	0.36-1.11	216	0.45	**0.009**	0.12-0.78	226	0.25	**0.016**
vcrA	51	0.02	0.921	-0.35-0.38	195	0.05	0.743	-0.24-0.34	203	0.28	**0.006**
mmoX+pmoA	84	-0.02	0.861	-0.23-0.21	289	-0.14	0.175	-0.35-0.07	296	-0.10	0.341
bvcA+vcrA	70	0.32	0.050	-0.02-0.66	284	0.35	**0.015**	0.07-0.63	287	0.34	**0.001**

n: number of samples in the analysis

CI: confidence interval

Coef: regression coefficient

AIC: Akaike's Information Criterion. Lower AIC scores indicates improved fitting of the statistical model with the data

Table 25. Regression Analysis of Functional Gene and Transcript Abundances with Ethene in Groundwater Samples.

p values < 0.05 are in bold

Gene vs ethene	n	multilevel regression				simple linear regression				Spearman's correlation	
		Coef	p value	95% CI	AIC	Coef	p value	95% CI	AIC	Rho	p value
etnC	65	0.53	**0.009**	0.13-0.92	190	0.59	**0.001**	0.24-0.94	188	0.35	**0.004**
etnE	65	0.46	**0.028**	0.04-0.85	194	0.53	**0.004**	0.17-0.88	190	0.28	**0.024**
mmoX	65	-0.05	0.813	-0.50-0.39	198	0.02	0.935	-0.40-0.43	209	-0.01	0.963
pmoA	65	-0.13	0.590	-0.61-0.35	205	-0.08	0.705	-0.47-0.32	204	0.02	0.871
bvcA	65	0.87	**0.014**	0.21-1.55	240	1.19	**<0.001**	0.62-1.75	250	0.37	**0.003**
vcrA	65	0.83	**0.020**	0.10-1.58	239	0.93	**0.010**	0.23-1.62	278	0.17	0.171
mmoX+pmoA	65	-0.14	0.512	-0.60-0.30	198	-0.09	0.620	-0.47-0.28	196	0.01	0.912
bvcA+vcrA	65	0.96	**0.007**	0.34-1.65	241	1.19	**<0.001**	0.62-1.76	252	0.39	**0.002**
Transcript vs ethene	n	multilevel regression				simple linear regression				Spearman's correlation	
		Coef	p value	95% CI	AIC	Coef	p value	95% CI	AIC	Rho	p value
etnC	45	0.85	**0.008**	0.30-1.37	173	0.86	**0.005**	0.28-1.44	167	0.32	**0.010**
etnE	51	0.63	**0.017**	0.13-1.11	178	0.63	**0.012**	0.15-1.11	172	0.24	0.055
mmoX	51	0.16	0.433	-0.26-0.57	148	0.25	0.236	-0.17-0.67	146	0.18	0.163
pmoA	59	-0.09	0.711	-0.58-0.39	191	-0.09	0.712	-0.56-0.38	189	0.05	0.691
bvcA	42	1.45	**<0.001**	0.77-2.10	165	1.53	**<0.001**	0.92-2.13	160	0.31	**0.012**
vcrA	36	0.44	0.163	-0.12-1.05	121	0.49	0.115	-0.13-1.10	135	0.22	0.077
mmoX+pmoA	61	-0.04	0.864	-0.56-0.41	199	-0.01	0.970	-0.49-0.47	199	0.04	0.756
bvcA+vcrA	51	1.39	**<0.001**	0.83-1.98	184	1.49	**<0.001**	0.97-2.00	181	0.38	**0.002**

n: number of samples in the analysis

CI: confidence interval

Coef: regression coefficient

AIC: Akaike's Information Criterion. Lower AIC scores indicates improved fitting of the statistical model with the data

Table 26. Regression Analysis of Functional Gene and Transcript Abundances with Methane in Groundwater Samples.

p values < 0.05 are in bold

Gene vs methane	n	multilevel regression				simple linear regression				Spearman's correlation	
		Coef	p value	95% CI	AIC	Coef	p value	95% CI	AIC	Rho	p value
etnC	74	0.30	0.087	-0.07-0.63	222	-0.01	0.966	-0.29-0.28	234	-0.09	0.449
etnE	74	0.30	0.09	-0.05-0.62	224	0.07	0.638	-0.22-0.35	231	-0.07	0.581
mmoX	74	0.52	**0.004**	-0.15-0.85	219	0.62	**<0.001**	-0.35-0.90	228	0.49	**<0.001**
pmoA	74	0.51	**0.007**	-0.12-0.86	232	0.46	**0.002**	-0.18-0.74	230	0.31	**0.007**
bvcA	74	0.43	0.118	-0.11-1.04	269	0.50	**0.020**	-0.08-0.93	291	0.33	**0.004**
vcrA	74	1.00	**0.001**	0.37-1.57	286	1.13	**<0.001**	0.64-1.61	311	0.48	**<0.001**
mmoX+pmoA	74	0.48	**0.006**	-0.14-0.79	224	0.44	**0.002**	-0.17-0.70	222	0.33	**0.005**
bvcA+vcrA	74	0.76	**0.005**	-0.23-1.31	283	0.79	**<0.001**	-0.37-1.20	290	0.46	**<0.001**
Transcript vs methane	n	multilevel regression				simple linear regression				Spearman's correlation	
		Coef	p value	95% CI	AIC	Coef	p value	95% CI	AIC	Rho	p value
etnC	54	0.36	0.204	-0.19-0.98	213	0.18	0.480	-0.32-0.67	213	-0.06	0.606
etnE	59	0.16	0.470	-0.31-0.66	211	-0.07	0.708	-0.47-0.32	214	-0.10	0.385
mmoX	57	0.36	**0.021**	-0.07-0.63	160	0.54	**<0.001**	-0.27-0.82	163	0.37	**0.001**
pmoA	68	0.51	**0.011**	-0.15-0.88	219	0.51	**0.003**	-0.17-0.85	226	0.30	**0.008**
bvcA	46	0.75	0.068	-0.08-1.53	192	0.52	0.126	-0.15-1.20	198	0.22	0.065
vcrA	38	1.37	**0.001**	-0.63-2.11	132	1.17	**<0.001**	-0.57-1.77	132	0.57	**<0.001**
mmoX+pmoA	70	0.58	**0.002**	-0.17-0.92	224	0.60	**<0.001**	-0.30-0.91	230	0.34	**0.004**
bvcA+vcrA	57	1.06	**0.011**	-0.25-1.93	229	1.17	**0.001**	-0.50-1.85	228	0.43	**<0.001**

n: number of samples in the analysis

CI: confidence interval

Coef: regression coefficient

AIC: Akaike's Information Criterion. Lower AIC scores indicates improved fitting of the statistical model with the data

Table 27. Regression Analysis of Gene Abundances and VC in Upper and Lower Aquifer.

Abbreviations: Coef: regression Coefficient, AIC: Akaike's Information Criterion, NA: not applicable.

upper surficial aquifer, n=68	censored regression				linear regression				Spearman's correlation	
	Coef	**p value**	**95% CI**	**AIC**	**Coef**	**p value**	**95% CI**	**AIC**	**Rho**	**p value**
16S rRNA gene	NA	NA	NA	NA	0.30	0.073	-0.03-0.63	280	0.19	0.112
etnC	0.41	0.236	-0.27-1.1	281	0.26	0.253	-0.19-0.7	320	0.11	0.373
etnE	0.16	0.578	-0.41-0.73	269	0.12	0.519	-0.25-0.5	298	0.07	0.582
mmoX	0.17	0.345	-0.19-0.54	216	0.03	0.801	-0.2-0.26	230	0.09	0.490
pmoA	-0.03	0.936	-0.83-0.77	226	-0.09	0.620	-0.47-0.28	297	-0.02	0.885
bvcA	1.05	**0.002**	0.4-1.7	197	0.54	**<0.001**	0.25-0.82	259	0.40	**<0.001**
vcrA	0.00	0.989	-0.43-0.42	132	0.02	0.794	-0.12-0.15	157	-0.06	0.633
lower surficial aquifer, n=49	censored regression				linear regression				Spearman's correlation	
	Coef	**p value**	**95% CI**	**AIC**	**Coef**	**p value**	**95% CI**	**AIC**	**Rho**	**p value**
16S rRNA gene	NA	NA	NA	NA	0.25	**0.004**	0.08-0.42	110	0.27	0.058
etnC	0.33	**0.046**	0.01-0.65	176	0.33	**0.035**	0.02-0.63	169	0.33	**0.019**
etnE	0.58	**0.024**	0.08-1.09	185	0.45	**0.019**	0.08-0.82	189	0.34	**0.017**
mmoX	0.14	0.151	-0.05-0.33	124	0.13	0.111	-0.03-0.29	106	0.19	0.187
pmoA	0.03	0.915	-0.53-0.59	146	0.04	0.766	-0.24-0.32	162	0.03	0.845
bvcA	1.22	**<0.001**	0.76-1.69	169	0.94	**<0.001**	0.61-1.27	177	0.66	**<0.001**
vcrA	1.83	**<0.001**	0.97-2.7	121	0.73	**<0.001**	0.41-1.06	175	0.64	**<0.001**

Table 28. Regression Analysis of Gene Abundances and PCE Along Depth of Both Aquifers.

Abbreviations: Coef: regression coefficient, CI: confidence interval, AIC: Akaike's Information Criterion, NA: not applicable.

upper surficial aquifer, n=68	censored regression				linear regression				Spearman's correlation	
	Coef	p value	95% CI	AIC	Coef	p value	95% CI	AIC	Rho	p value
16S rRNA gene	NA	NA	NA	NA	0.51	**<0.001**	0.22-0.8	272	0.40	**<0.001**
etnC	0.99	**<0.001**	0.41-1.58	271	0.67	**<0.001**	0.29-1.06	309	0.38	**0.001**
etnE	0.58	**0.023**	0.08-1.09	265	0.42	**0.015**	0.09-0.76	292	0.27	**0.029**
mmoX	0.46	**0.005**	0.13-0.78	209	0.24	**0.025**	0.03-0.44	225	0.37	**0.002**
pmoA	0.67	0.063	-0.04-1.38	222	0.28	0.108	-0.06-0.62	295	0.26	**0.033**
bvcA	0.55	0.083	-0.07-1.17	204	0.24	0.097	-0.05-0.53	270	0.12	0.324
vcrA	0.22	0.247	-0.15-0.59	131	0.08	0.195	-0.04-0.2	155	0.10	0.437
lower surficial aquifer, n=49	censored regression				linear regression				Spearman's correlation	
	Coef	p value	95% CI	AIC	Coef	p value	95% CI	AIC	Rho	p value
16S rRNA gene	NA	NA	NA	NA	0.38	**<0.001**	0.22-0.53	97	0.59	**<0.001**
etnC	0.58	**<0.001**	0.28-0.88	168	0.56	**<0.001**	0.27-0.84	160	0.51	**<0.001**
etnE	0.56	**0.036**	0.04-1.09	185	0.44	**0.028**	0.05-0.82	190	0.36	**0.012**
mmoX	0.29	**0.003**	0.1-0.48	118	0.22	**0.007**	0.06-0.38	101	0.44	**0.002**
pmoA	0.39	0.182	-0.18-0.96	144	0.20	0.158	-0.08-0.49	160	0.25	0.087
bvcA	0.75	**0.010**	0.18-1.31	185	0.56	**0.008**	0.15-0.97	196	0.31	**0.033**
vcrA	0.72	0.116	-0.18-1.61	141	0.26	0.183	-0.13-0.66	192	0.15	0.296

NA: not applicable.

Table 29. Regression Analysis of Gene Abundances and TCE Along Depth of Both Aquifers.

Abbreviations: Coef: regression coefficient, CI: confidence interval, AIC: Akaike's Information Criterion, NA: not applicable.

upper surficial aquifer, n=68	censored regression				linear regression				Spearman's correlation	
	Coef	**p value**	**95% CI**	**AIC**	**Coef**	**p value**	**95% CI**	**AIC**	**Rho**	**p value**
16S rRNA gene	NA	NA	NA	NA	0.53	**<0.001**	0.24-0.82	271	0.42	**<0.001**
etnC	1.00	**0.001**	0.4-1.6	272	0.66	**0.001**	0.27-1.05	310	0.36	**0.003**
etnE	0.52	**0.048**	0-1.04	266	0.37	**0.033**	0.03-0.72	294	0.24	0.051
mmoX	0.50	**0.003**	0.17-0.83	208	0.24	**0.021**	0.04-0.45	224	0.35	**0.003**
pmoA	0.73	0.052	-0.01-1.47	222	0.30	0.092	-0.05-0.64	295	0.25	**0.043**
bvcA	0.72	**0.029**	0.07-1.37	202	0.30	**0.039**	0.02-0.59	268	0.29	**0.015**
vcrA	0.24	0.224	-0.14-0.62	131	0.09	0.161	-0.04-0.21	155	0.12	0.331
lower surficial aquifer, n=49	censored regression				linear regression				Spearman's correlation	
	Coef	**p value**	**95% CI**	**AIC**	**Coef**	**p value**	**95% CI**	**AIC**	**Rho**	**p value**
16S rRNA gene	NA	NA	NA	NA	0.30	**0.003**	0.1-0.49	108	0.27	0.063
etnC	0.44	**0.019**	0.07-0.8	175	0.41	**0.021**	0.07-0.75	168	0.29	**0.047**
etnE	0.59	0.066	-0.04-1.22	186	0.39	0.076	-0.04-0.83	191	0.14	0.322
mmoX	0.33	**0.006**	0.1-0.56	119	0.20	**0.025**	0.03-0.38	103	0.18	0.228
pmoA	0.99	**0.009**	0.25-1.72	138	0.39	**0.013**	0.09-0.69	155	0.32	**0.026**
bvcA	-0.59	0.083	-1.26-0.08	189	-0.40	0.099	-0.88-0.08	200	-0.26	0.067
vcrA	-0.83	0.098	-1.82-0.15	141	-0.38	0.080	-0.81-0.05	190	-0.16	0.281

NA: not applicable.

Table 30. Regression Analysis of Gene Abundances and cis-DCE Along Depth of Both Aquifers.

Abbreviations: Coef: regression coefficient, CI: confidence interval, AIC: Akaike's Information Criterion, NA: not applicable.

upper surficial aquifer, n=68	censored regression				linear regression				Spearman's correlation	
	Coef	p value	95% CI	AIC	Coef	p value	95% CI	AIC	Rho	p value
16S rRNA gene	NA	NA	NA	NA	0.21	0.152	-0.08-0.5	281	0.10	0.436
etnC	0.28	0.368	-0.33-0.89	281	0.16	0.424	-0.23-0.54	320	0.02	0.860
etnE	0.06	0.829	-0.45-0.56	270	0.06	0.708	-0.27-0.39	298	0.01	0.927
mmoX	0.09	0.604	-0.24-0.41	217	-0.01	0.935	-0.21-0.19	230	0.02	0.851
pmoA	-0.14	0.699	-0.84-0.57	226	-0.12	0.460	-0.45-0.21	297	-0.10	0.435
bvcA	0.64	**0.043**	0.02-1.25	203	0.29	**0.032**	0.03-0.55	268	0.24	**0.046**
vcrA	-0.03	0.857	-0.41-0.34	132	0.01	0.809	-0.1-0.13	157	-0.05	0.664
lower surficial aquifer, n=49	censored regression				linear regression				Spearman's correlation	
	Coef	p value	95% CI	AIC	Coef	p value	95% CI	AIC	Rho	p value
16S rRNA gene	NA	NA	NA	NA	0.48	**<0.001**	0.26-0.69	102	0.46	**0.001**
etnC	0.62	**0.005**	0.18-1.05	173	0.60	**0.004**	0.2-1.01	165	0.45	**0.001**
etnE	1.09	**0.002**	0.41-1.77	180	0.83	**0.001**	0.33-1.32	184	0.49	**<0.001**
mmoX	0.33	**0.011**	0.08-0.59	120	0.28	**0.012**	0.06-0.49	102	0.32	**0.026**
pmoA	0.29	0.461	-0.49-1.08	146	0.16	0.399	-0.22-0.55	161	0.13	0.370
bvcA	1.38	**<0.001**	0.65-2.1	179	1.01	**<0.001**	0.49-1.53	189	0.37	**0.008**
vcrA	1.55	**0.015**	0.3-2.79	137	0.52	0.051	0-1.04	189	0.28	**0.049**

NA: not applicable.

Table 31. Regression Analysis of Gene Abundances and Ethene Along Depth of Both Aquifers.

Abbreviations: Coef: regression coefficient, CI: confidence nterval, AIC: Akaike's Information Criterion, NA: not applicable.

upper surficial aquifer, n=68	censored regression				linear regression				Spearman's correlation	
	Coef	**p value**	**95% CI**	**AIC**	**Coef**	**p value**	**95% CI**	**AIC**	**Rho**	**p value**
16S rRNA gene	NA	NA	NA	NA	0.26	0.198	-0.14-0.66	281	0.15	0.222
etnC	0.36	0.387	-0.45-1.17	281	0.22	0.400	-0.3-0.75	320	0.09	0.486
etnE	0.15	0.674	-0.53-0.82	270	0.08	0.709	-0.37-0.53	298	0.00	0.999
mmoX	0.24	0.282	-0.2-0.68	216	0.05	0.704	-0.22-0.32	230	0.12	0.323
pmoA	0.08	0.875	-0.88-1.03	226	-0.03	0.882	-0.48-0.41	298	0.01	0.909
bvcA	0.92	**0.024**	0.12-1.72	202	0.49	**0.008**	0.13-0.84	265	0.19	0.122
vcrA	0.17	0.506	-0.33-0.68	132	0.07	0.372	-0.09-0.23	156	0.08	0.503
lower surficial aquifer, n=49	censored regression				linear regression				Spearman's correlation	
	Coef	**p value**	**95% CI**	**AIC**	**Coef**	**p value**	**95% CI**	**AIC**	**Rho**	**p value**
16S rRNA gene	NA	NA	NA	NA	0.33	**<0.001**	0.15-0.51	106	0.48	**<0.001**
etnC	0.38	**0.036**	0.03-0.74	176	0.38	**0.026**	0.05-0.72	169	0.45	**0.001**
etnE	0.67	**0.017**	0.12-1.23	184	0.54	**0.011**	0.13-0.95	188	0.39	**0.006**
mmoX	0.29	**0.006**	0.08-0.49	119	0.24	**0.006**	0.07-0.41	101	0.49	**<0.001**
pmoA	0.30	0.341	-0.31-0.9	145	0.18	0.255	-0.13-0.49	160	0.15	0.307
bvcA	0.85	**0.006**	0.24-1.45	185	0.62	**0.007**	0.18-1.06	195	0.31	**0.031**
vcrA	1.04	**0.035**	0.07-2	139	0.35	0.097	-0.07-0.77	191	0.23	0.110

NA: not applicable.

Table 32. Regression Analysis of Gene Abundances and Methane Along Depth of Both Aquifers.

Abbreviations: Coef: regression coefficient, CI: confidence interval, AIC: Akaike's Information Criterion, NA: not applicable.

upper surficial aquifer, n=68	censored regression				linear regression				Spearman's correlation	
	Coef	p value	95% CI	AIC	Coef	p value	95% CI	AIC	Rho	p value
16S rRNA gene	NA	NA	NA	NA	-0.66	0.056	-1.33-0.02	279	-0.25	**0.039**
etnC	-1.48	**0.033**	-2.83--0.12	278	-1.04	**0.021**	-1.92--0.16	315	-0.29	**0.015**
etnE	-1.27	**0.027**	-2.4-0.14	265	-0.82	**0.031**	-1.57--0.08	293	-0.25	**0.038**
mmoX	-0.88	**0.015**	-1.59--0.17	212	-0.61	**0.007**	-1.06--0.17	222	-0.28	**0.019**
pmoA	-2.97	**<0.001**	-4.5--1.44	211	-1.50	**<0.001**	-2.17--0.82	280	-0.43	**<0.001**
bvcA	0.59	0.420	-0.84-2.03	206	0.33	0.311	-0.31-0.96	272	0.11	0.385
vcrA	-1.00	**0.040**	-1.96--0.05	127	-0.19	0.165	-0.46-0.08	155	-0.29	**0.018**
lower surficial aquifer, n=49	censored regression				linear regression				Spearman's correlation	
	Coef	p value	95% CI	AIC	Coef	p value	95% CI	AIC	Rho	p value
16S rRNA gene	NA	NA	NA	NA	0.10	0.593	-0.28-0.48	117	-0.02	0.889
etnC	0.47	0.180	-0.22-1.16	178	0.41	0.204	-0.23-1.06	172	0.06	0.694
etnE	-0.24	0.671	-1.35-0.87	189	-0.17	0.673	-0.98-0.64	194	-0.05	0.714
mmoX	-0.12	0.583	-0.53-0.3	126	-0.09	0.580	-0.43-0.24	108	-0.10	0.482
pmoA	-1.02	0.084	-2.18-0.14	143	-0.51	0.076	-1.07-0.06	158	-0.34	**0.017**
bvcA	2.71	**<0.001**	1.62-3.81	169	1.83	**<0.001**	1.13-2.53	180	0.63	**<0.001**
vcrA	4.29	**0.002**	1.62-6.95	127	1.12	**0.004**	0.38-1.85	184	0.52	**<0.001**

NA: not applicable

148

Etheneotroph functional genes were only correlated to VC concentrations in the lower surficial aquifer in Site 45 cryo-cores. Etheneotrophs can oxidize VC via co-metabolism with ethene as the primary growth substrate (Freedman & Herz, 1996), and some etheneotrophs use VC as sole carbon source under laboratory conditions.(Jin & Mattes, 2008) VC and ethene concentrations both showed positive relationships with *etnC* and *etnE* abundances in the lower surficial aquifer. This further supports similar relationships noted in groundwater samples (Liang, *et al.*, 2017b) and suggests that both VC and ethene supported the growth of etheneotrophs in portions of the lower surficial aquifer.

The positive relationship between VC concentrations and VC reductive dehalogenase gene abundances in the lower surficial aquifer could be explained by anaerobic VC dechlorinators using VC as electron acceptor.(He, *et al.*, 2003) Among the two VC reductive dehalogenase genes, *bvcA* was generally more abundant than *vcrA*. This observation is consistent with previous studies where both genes were tracked in microcosms and at a contaminated site.(Lee, *et al.*, 2008, Atashgahi, *et al.*, 2013) Only *bvcA* was correlated to VC concentrations in the upper surficial aquifer samples, which suggests that anaerobic VC dechlorinators employ BvcA for growth VC in less reducing conditions. (van der Zaan, *et al.*, 2010)

VC-oxidizing bacteria and their functional genes have previously been observed in in oxygen-limited subsurface environments.(Gossett, 2010, Fullerton, *et al.*, 2014, Liang, *et al.*, 2017b) Extensive searches have failed to reveal any organism capable of VC oxidation with an electron acceptor other than oxygen(Freedman, *et al.*, 2013). Several VC oxidizing isolates display very low oxygen half-velocity constants (0.07-0.3 mg/L)(Coleman, *et al.*, 2002b), and thus the ability to scavenge oxygen under very low DO conditions. It has been suggested that the systems where anaerobic VC oxidation was reported were not truly anaerobic, but experienced a cryptic low-level oxygen flux.(Gossett, 2010, Freedman, *et al.*, 2013) Indeed, sustained VC oxidation at DO levels below 0.02 mg/L have has been demonstrated in microcosms provided with a low-level DO flux.(Gossett, 2010) The possibility that similar low level DO fluxes can occur at depth in contaminated aquifers and sustain aerobic bacterial populations warrants further study.

In contrast to functional genes from etheneotrophs and anaerobic VC dechlorinators, methanotroph functional genes were not correlated with VC concentrations in either the upper or lower surficial aquifer samples. This is consistent with previously reported groundwater data,(Chang & Alvarez-Cohen, 1996) and we suspect this is related to the fact that methanotrophs only co-metabolize VC. Overall, methanotrophs were not very abundant at Site 45, suggesting that VC co-metabolism by methanotrophs was not a major pathway for VC attenuation.

Associations between cis-DCE concentrations and VC biodegradation functional genes were similar to those seen with VC concentrations. These positive associations could be present because cis-DCE is the parent compound of VC and that cis-DCE is used as electron acceptor by VC dechlorinators carrying *bvcA* and/or *vcrA*.(Löffler, *et al.*, 2013)

The associations between PCE and TCE concentrations and VC biodegradation functional genes differed from those seen with cis-DCE and VC concentrations (i.e., they were associated with etheneotroph functional genes in both the upper and lower surficial aquifers). Similar relationships were observed previously with groundwater samples(Liang, *et al.*, 2017b).

In summary, cryogenic coring has been an effective technique for capturing high spatial resolution trends in biomarker and geochemical data with depth in aquifer soil samples. We have demonstrated that functional genes from aerobic VC-degrading bacteria (both etheneotrophs and methanotrophs) are present and widely distributed in an apparently anaerobic aquifer. We have also shown a significant overlap between the occurrence of functional genes from aerobic etheneotrophs and anaerobic VC-reducing bacteria within this aquifer, and that etheneotroph functional genes are often more abundant despite prevailing anaerobic conditions. The lack of ethene as an anaerobic dechlorination product, along with the wide distribution and relatively high abundance of etheneotroph functional genes and the detection of *etnC* and *etnE* transcripts in nearby groundwater samples suggests that they play a significant role in VC removal at this site. Improved methods for isolating RNA from environmental samples are necessary in order to quantify the biological activity in the subsurface at a comparable spatial resolution. An improved understanding of aerobic VC degradation under low DO concentrations and low oxygen flux conditions would be useful in designing and implementing natural attenuation or aerobic bioremediation strategies for site cleanup.
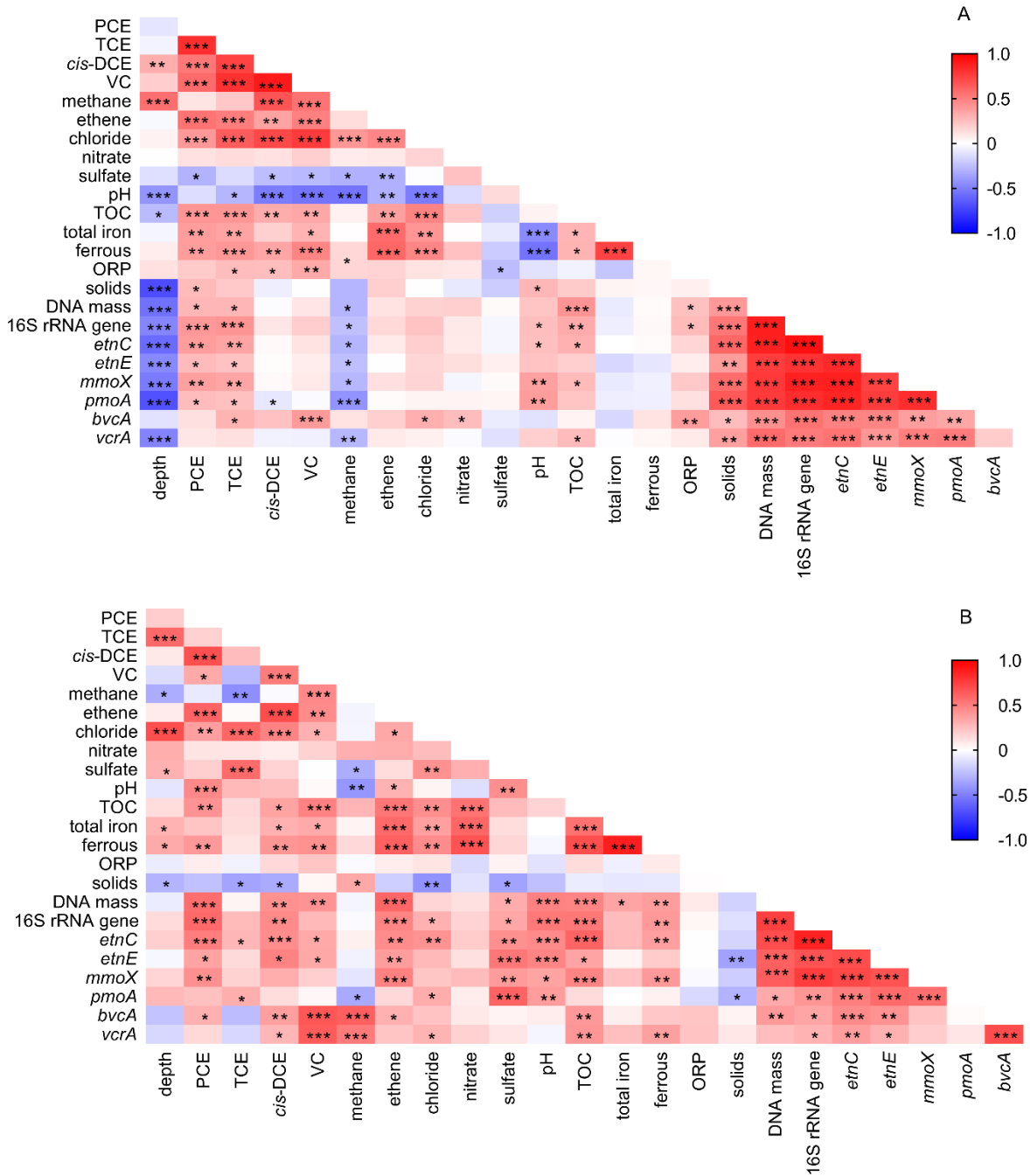
Figure 85. Heatmap of Spearman's Correlations Among Microbial Data and Geochemical Data in Upper Surficial Aquifer (A) and Lower Surficial Aquifer (B)

(*: p<0.05, **: p<0.01, ***: p<0.001).

6.2.10 Determine relationships between qPCR/RT-qPCR data and estimated VC degradation rates

The positive relationship between VC concentration and etheneotrophs noted in the previous performance objective assessment suggests that there will also be a relationship between etheneotroph and activity and VC degradation rates, as estimated over a plume transect. This is because as the VC plume moves further from the source it will be subject to attenuation processes, such as biodegradation.

Using site data (site maps and monitoring well data) we developed plume transects and plotted VC concentration vs. distance according to the direction of groundwater flow (see section 5). Using reported hydrogeological data (hydraulic gradient, porosity, hydraulic conductivity) we estimated seepage velocities for the transects so that VC concentration vs. distance plots were expressed as VC concentration vs. travel time (**Figure 86**). Bulk VC attenuation rates could be estimated from these plots by linear regression. These results of this analysis are shown in **Table 33**.

Legend:
- NAS Oceana - 2013.11
- NAS Oceana - 2014.07
- Kings Bay Site 11 - 2015.01
- Seal Beach Site 70 - 2015.07
- Seal Beach Site 70 - 2015.12
- Altus AFB - 201505
- Parris Island Site 45 northern plume lower aquifer - 2015.10
- Parris Island Site 45 northern plume upper aquifer - 2015.10
- Parris Island Site 45 southern plume lower aquifer - 2015.10
- Site LF05, Hawaii - 2015.04
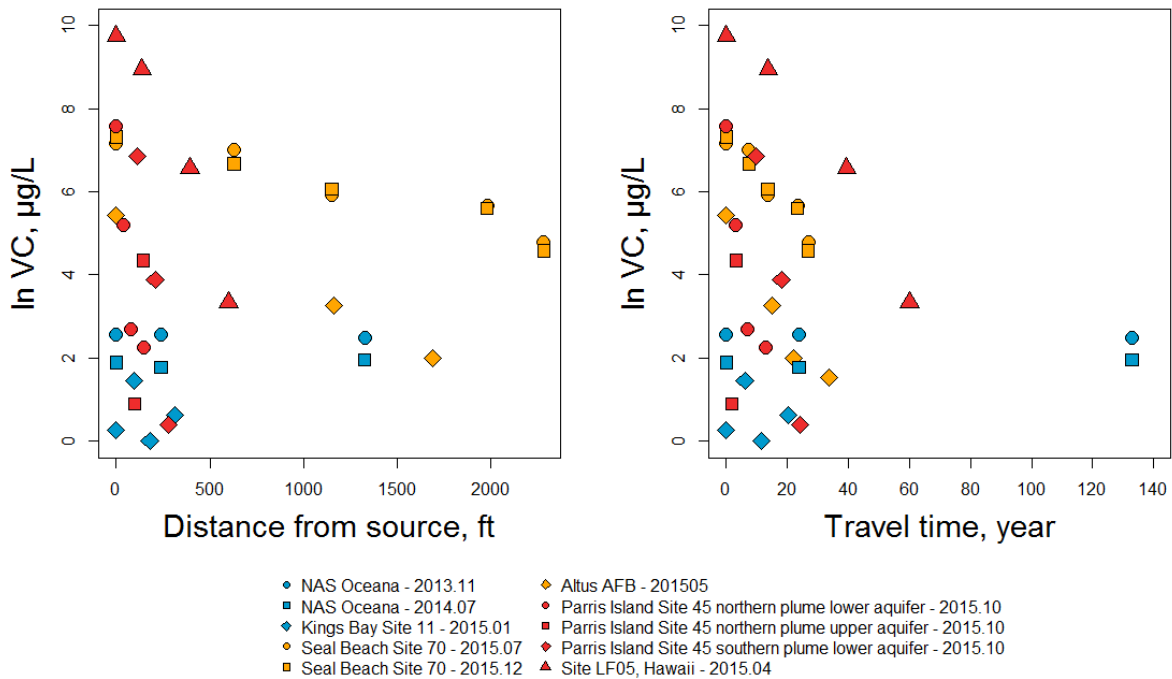
Figure 86. Plot depicting VC vs. distance (left panel) and VC vs. travel time (right panel) in six different VC plumes some of which have multiple time points.

Table 33. Bulk VC Attenuation Rate Estimate and Rate Categories.

p values < 0.05 are in bold. Low rate: bulk VC attenuation rates < 0.005 per year. High rates: bulk VC attenuation rate >0.08 per year.

Site	Remediation approach	Time	Bulk VC attenuation rate, yr^{-1}	R^2	p Value	Rate Category
VA Site 2C	Oxygen releasing compound injection	2013.11	0.0006	0.972	0.518	Low
		2014.07	-0.0009	0.472	0.108	Low
GA Site 11	Pump and treat; in situ chemical oxidation	2015.01	0.0037	0.003	0.950	Low
CA Site 70	Enhanced anaerobic bioremediation with biobarriers	2015.07	0.0849	0.909	0.012	High
		2015.12	0.0958	0.891	0.006	High
OK Site SS-17	Mulch biowalls	2015.05	0.1210	0.942	0.030	High
HI Site LF05	Enhanced anaerobic bioremediation - bioreactor	2015.04	0.1057	0.969	0.016	High
SC Site 45* (north plume lower aquifer)	Enhanced anaerobic bioremediation – emulsified vegetable oil injection	2015.10	0.4350	0.932	0.008	High
		2016.07	0.3752	0.879	0.019	High
SC Site 45* (north plume upper aquifer)		2016.07	1.0858	0.344	0.299	High
		2015.10	1.0409	0.23	0.414	High
SC Site 45* (south plume lower aquifer)	In situ chemical oxidation	2015.10	0.5182	0.764	0.126	High
		2016.07	0.2836	0.840	0.028	High

*At SC site 45, a northern and southern VC plume exist within a surficial aquifer which has upper and lower hydrogeologic units. Bulk VC attenuation rates were estimated in each of these cases.

The qPCR data for each of the six functional genes we measured (and their transcripts) in samples from each of the different VC plumes are displayed at boxplots in the following figures. A legend for the boxplots themselves is shown in **Figure 87.** The boxplots provide an illustration of how much variability is seen in the qPCR data among and within sites. The boxplots are also arranged in the order of low attenuation rate on the left-hand side to high attenuation rate on the right hand side. Abundance and expression data for each functional gene is also shown side-by-side for comparison. This provides a qualitative comparison of the relationship between bulk VC attenuation rate and different functional gene/transcript abundance. For instance, *pmoA* abundance does not appear to have a relationship with bulk VC attenuation rate while *pmoA* transcript, *mmoX* abundance, and *mmoX* transcript abundance all appear to decrease with increasing bulk VC attenuation rates (**Figure 88** and **Figure 89**). This suggests that the higher the VC attenuation rate, the less that methanotrophs actually contribute to the attenuation rate. The same pattern is seen with *vcrA*(**Figure 90**). Conversely, with *bvcA* there appears to be a positive relationship between bulk VC attenuation rate and *bvcA* abundance and expression (**Figure 91**).

Apparently positive relationships between bulk VC attenuation rate and *etnC* abundance (**Figure 92**) as well as with expression and *etnE* abundance and expression were observed (**Figure 93**). These will be explored in more detail below.
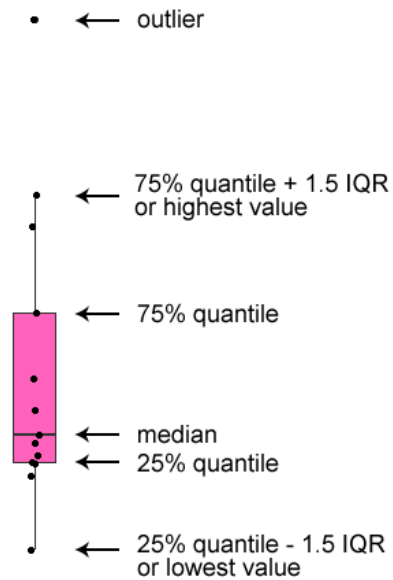
IQR: inter-quartile range, i.e. distance between the 25% and 75% quartiles

Figure 87. Legend that Explains the Data Presentation in the Boxplots That Are Presented in This Report.
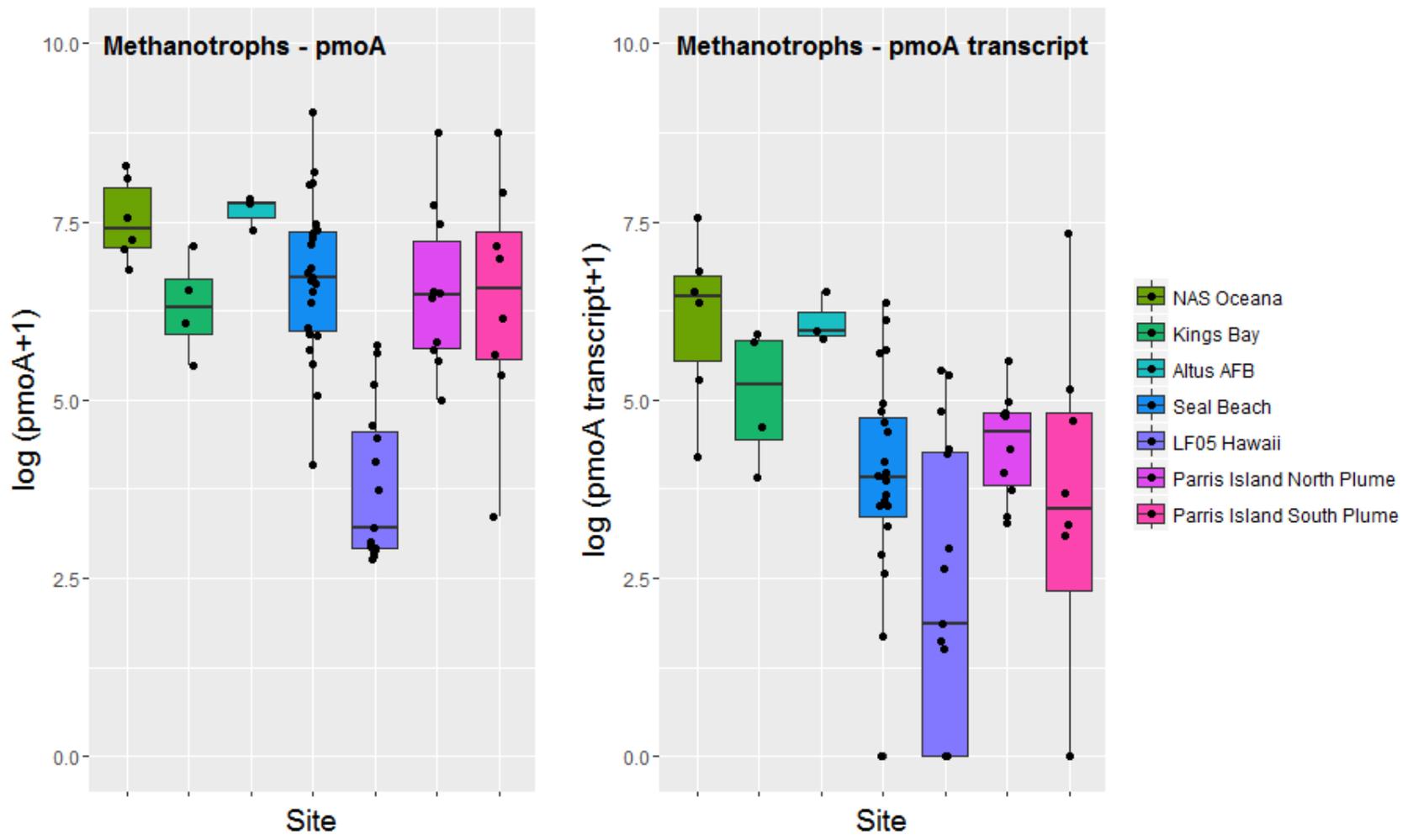
Figure 88. Variability in the Abundance and Expression of Methanotroph Functional Gene pmoA in Several VC Plumes.

The sites are arranged in order of low bulk VC attenuation rate (NAS Oceana, Kings Bay) to high relative bulk VC attenuation rate (Parris Island, Hawaii).
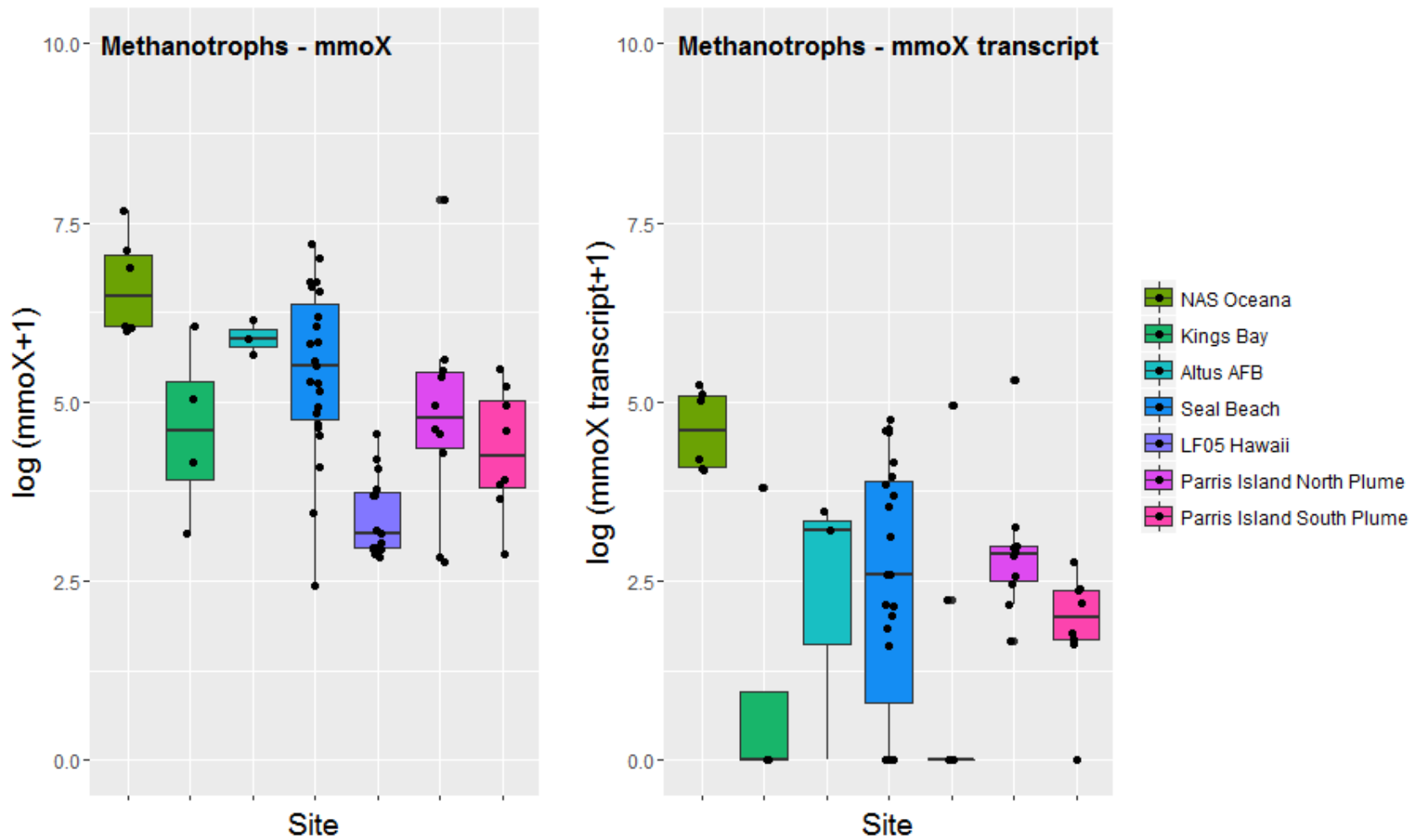
Figure 89. Variability in the Abundance and Expression of Methanotroph Functional Gene mmoX in Several VC Plumes.

The sites are arranged in order of low bulk VC attenuation rate (NAS Oceana, Kings Bay) to high relative bulk VC attenuation rate (Parris Island, Hawaii).
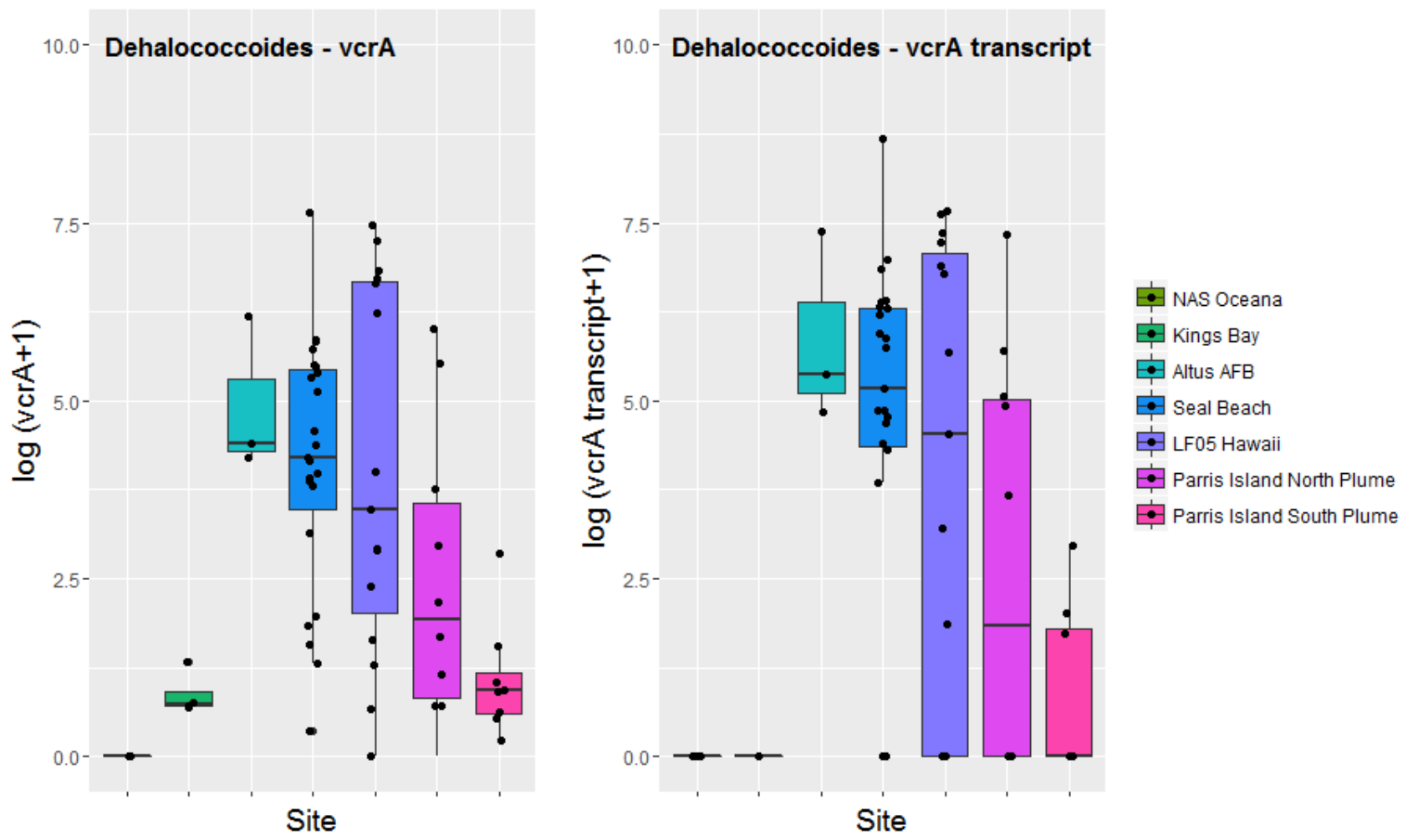
Figure 90. Variability in the Abundance and Expression of VC Dechlorinator Functional Gene vcrA in Several VC Plumes.

The sites are arranged in order of low bulk VC attenuation rate (NAS Oceana, Kings Bay) to high relative bulk VC attenuation rate (Parris Island, Hawaii).
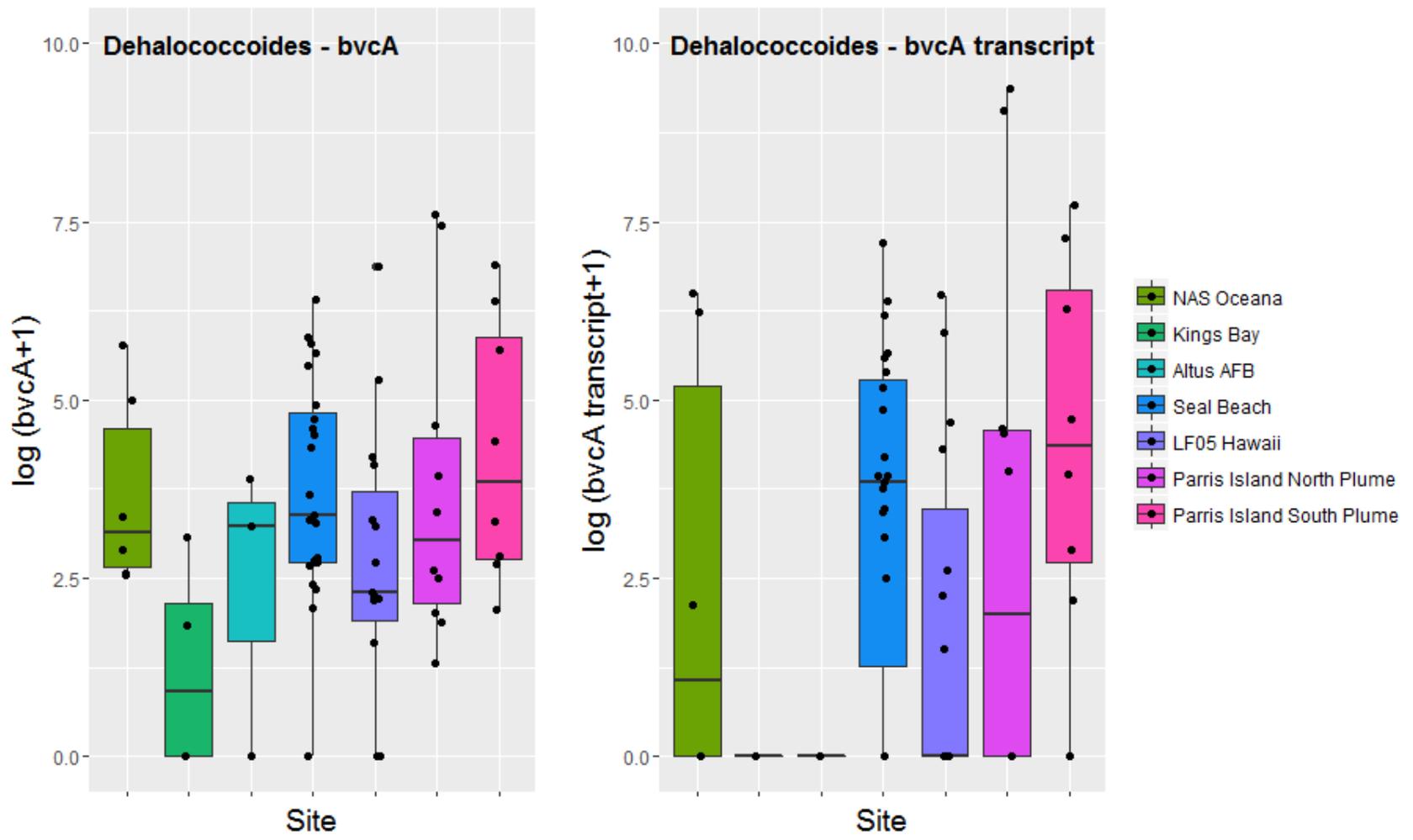
Figure 91. Variability in the Abundance and Expression of VC Dechlorinator Functional Gene bvcA in Several VC Plumes.

The sites are arranged in order of low bulk VC attenuation rate (NAS Oceana, Kings Bay) to high relative bulk VC attenuation rate (Parris Island, Hawaii).
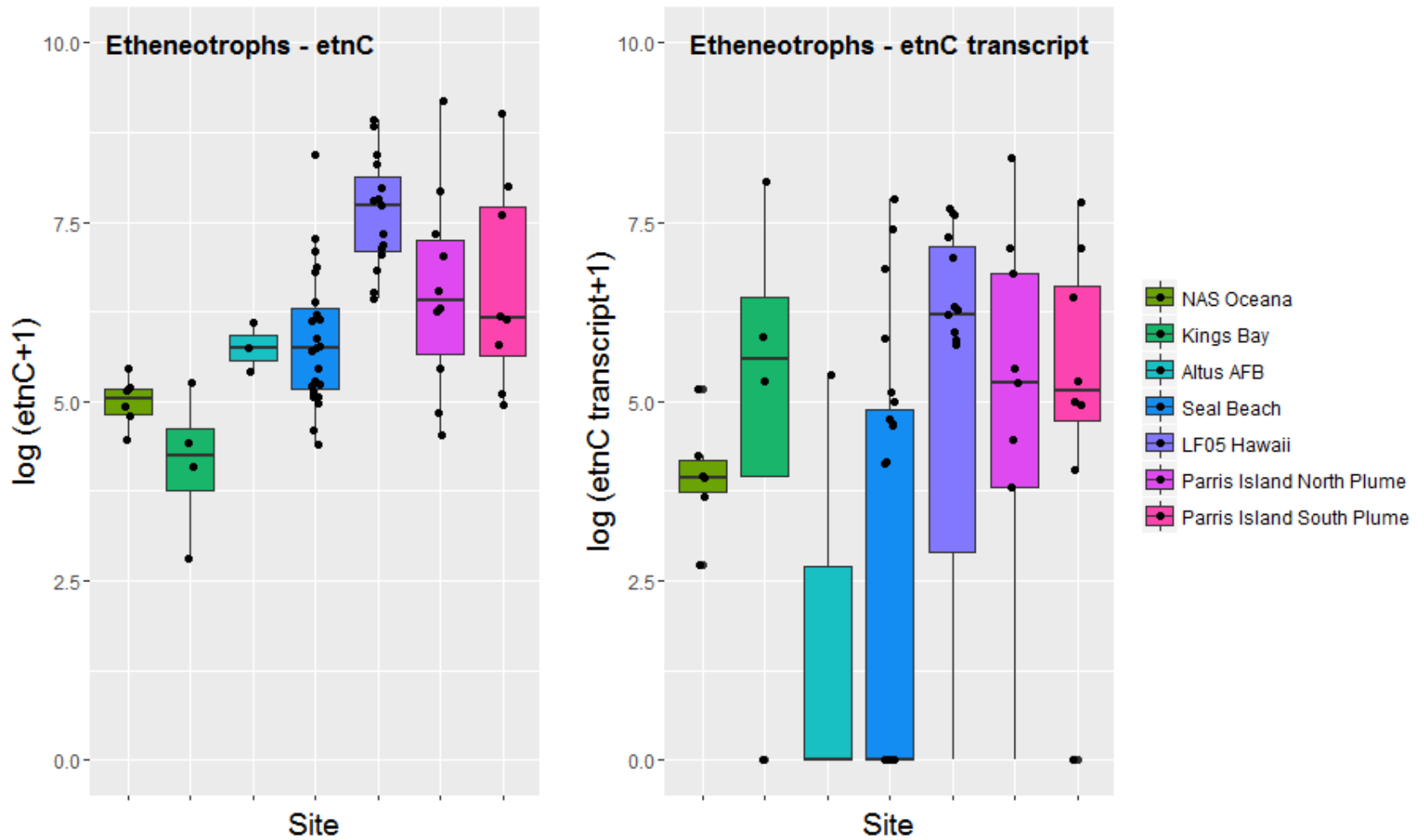
Figure 92. Variability in the Abundance and Expression of Etheneotroph Functional Gene etnC in Several VC Plumes.

The sites are arranged in order of low bulk VC attenuation rate (NAS Oceana, Kings Bay) to high relative bulk VC attenuation rate (Parris Island, Hawaii).
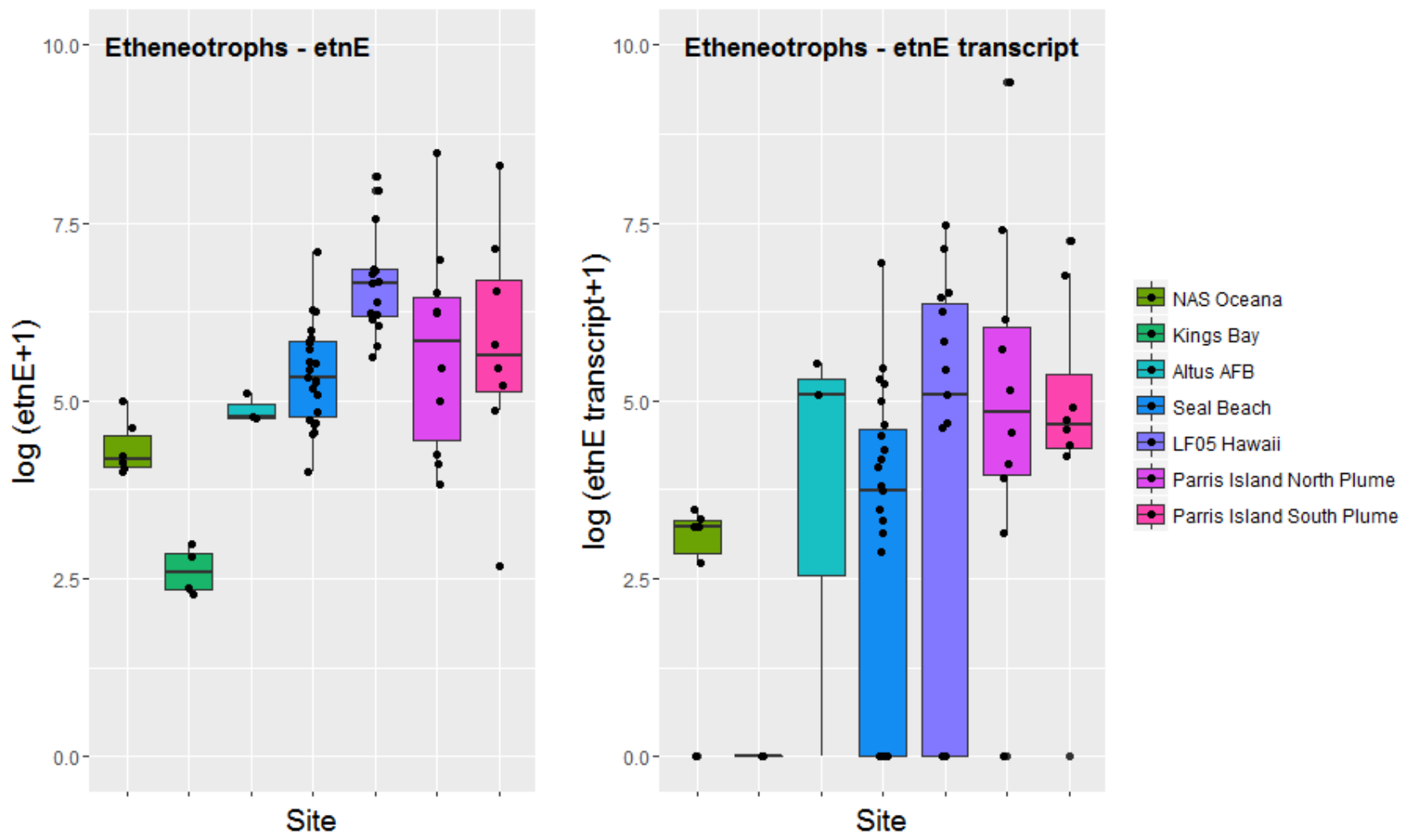
Figure 93. Variability in the Abundance and Expression of Etheneotroph Functional Gene etnE in Several VC Plumes.

The sites are arranged in order of low bulk VC attenuation rate (NAS Oceana, Kings Bay) to high relative bulk VC attenuation rate (Parris Island, Hawaii).

In order to validate these apparent relationships and assess whether we have achieved success in this performance objective we need to provide statistical support. Estimating accurate bulk VC attenuation rates is complicated by uncertainties in estimating the field hydraulic parameters. For example, seepage velocity is a crucial parameter in determining bulk VC attenuation rate. At different parts of the site and different time points, seepage velocity could vary substantially. In some cases, the calculated bulk VC attenuation rate is not statistically significant (i.e. p value > 0.05). This can result from a lack of data (not enough wells), a very low rate to begin with, or variability in the data leading to poor linear relationships. Additionally, attempting to develop quantitative relationship between a bulk (site-wide) VC attenuation rate and a functional gene requires that the functional gene abundance and expression also be averaged site-wide. However, inspection of the previous figures shows that there can be substantial variability in gene abundance and expression within a site. Yet another issue to consider is that the database of sites where functional gene abundance and expression has been measured is still relatively small.

All these factors described above conspire against applying a linear regression approach to validate quantitative relationships between bulk VC attenuation rates and functional gene/transcript abundances. Therefore, to determine the relationship between functional genes/transcripts and bulk VC attenuation rates, we used a categorical regression approach. Following estimation of the bulk VC attenuation rate over a transect at a site, each site was assigned to one of two categorical rate groups: high rate or low rate. Sites in the low attenuation group include NSB Kings Bay site 11 and NAS Oceana SWMU 2C, Altus AFB biowalls and Seal Beach Site 70. Sites included in the high attenuation group included Parris Island site 45 (northern and southern plumes) and Joint Base Pearl Harbor Hickam site LF05.

For the categorical regression analysis, a multilevel modeling approach was also used to take into account the effect of intercorrelations between samples from the same sites and the same monitoring wells sampled on different dates. Regression analysis was performed to test the hypothesis that functional gene or transcript abundances are different among the different rate groupings (null hypothesis is that there is no difference).

Compared to linear regression analysis, categorical regression analysis has the following advantages:

1. By dividing the sites into categorical degradation groups, we avoid using the bulk VC attenuation rate directly. Instead, several factors, including the calculated bulk VC attenuation rates, are taken into consideration to determine which rate group the site will be assigned to. The categorical regression analysis thus avoids the inaccuracy resulted from the uncertainties in bulk VC attenuation rate estimation.

2. For the categorical regression analysis, we do not take the average of the gene and transcript abundances along transects. Instead we used the gene or transcript abundance from each monitoring well as individual data points and incorporate the abundance variabilities among different monitoring wells into the analysis.

3. We use a multilevel regression model to analyze the dataset. This model takes into consideration the correlation of gene or transcript abundances of the same monitoring well at different sampling times.

We found that log transformed etheneotroph functional gene (*etnC* and *etnE*) abundances in high rate group were significantly higher than those in the low rate group, while no significant difference was found for methanotroph functional genes among different groups **Table 34**. For reference, log transformed functional gene abundances indicating anaerobic VC degradation (the sum of *bvcA* and *vcrA*) were significantly higher the high rate group as compared to the low rate group.

The significantly higher abundances of etheneotroph functional genes and anaerobic VC reductive dehalogenase genes in the high rate group (as compared to the low rate group) suggests that VC degradation was categorically faster when there were higher abundances of etheneotrophs and anaerobic VC-degraders together in the same groundwater sample. It is possible that under field conditions, VC may support the growth of etheneotrophs and anaerobic VC degraders, and etheneotrophs and anaerobic VC dechlorinators both contributed significantly to VC degradation in the contaminated groundwater.

For transcripts, significant differences were observed between *etnC, etnE* transcript abundances of the high rate group and slow rate group, suggesting that etheneotrophs were more active at sites where more rapid VC attenuation was observed. The sum of *bvcA* and *vcrA* in the high rate group was also significantly higher than the low degradation group.

In summary, the results of correlation analysis between functional gene/transcript abundances and VC degradation rates suggest that etheneotrophs and anaerobic VC degraders were more abundant and active at sites with faster bulk VC degradation rate, and they could be both important factors contributing to VC degradation in groundwater. Therefore, we believe that the results of this performance assessment indicate a success. Although we did not end up using the statistical tests we planned initially, the categorical regression analysis provides evidence of a statistically significant relationship between VC-oxidizers and bulk VC attenuation rates.

Table 34. Average Gene and Transcript Abundances within Slow and High Rate Group Categories as Assessed by Categorical Multilevel Regression.

p values <0.05, which indicate a statistically significant difference between two groups, are in bold.

	Rate category	gene		transcript	
		$\log_{10}(x+1)$	p value	$\log_{10}(x+1)$	p value
etnC	low rate	4.58		4.39	
	high rate	6.49	**0.040**	3.91	0.743
etnE	low rate	3.49		1.35	
	high rate	5.73	**0.036**	3.80	**0.026**
mmoX	low rate	5.61		2.79	
	high rate	4.79	0.454	1.81	0.474
pmoA	low rate	6.93		5.62	
	high rate	6.23	0.593	3.76	0.202
bvcA	low rate	2.41		1.21	
	high rate	3.28	0.389	2.62	0.349
vcrA	low rate	0.45		0.00	
	high rate	3.54	**0.030**	3.96	**0.035**
mmoX+pmoA	low rate	6.96		5.66	
	high rate	6.32	0.605	3.91	0.206
bvcA+vcrA	low rate	2.60		1.12	
	high rate	4.36	**0.024**	4.66	**0.002**

6.2.11 Determine relationships between etheneotroph functional genes and the VC biodegradation rate in VC-oxidizing laboratory enrichment cultures

To begin testing this performance objective we first developed a non-linear regression model in Aquasim for determining "raw" VC substrate utilization rates (i.e., not normalized to biomass concentration) in liquid laboratory enrichment cultures according to the Michaelis-Menton enzyme kinetics model. An example of the output of this model is shown in Figure 93. A typical substrate depletion curve for the HI culture is shown on the left, and the Aquasim model output is on the right. This shows that the model accurately describes the VC depletion data (as measured in the headspace). The difference between aqueous (Ca) and headspace (Cg) models is the Henry's constant for VC (0.908 at 20C). The model output parameters are raw maximum substrate depletion rate (qmax) and half-velocity constant (Ks). In this example, qmax = 146.9 uM/day and Ks = 0.0019 µM.
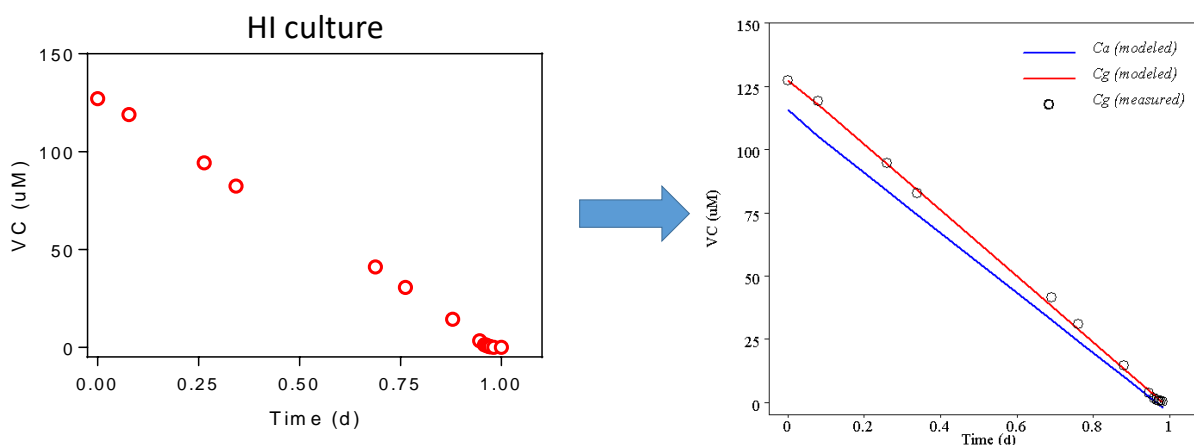
Figure 94. Modeling of VC Depletion Data in Microcosms Shows That the Data Fits Michaelis-Menten Kinetics.

The raw utilization (or biodegradation) rate is typically normalized by some measure of active biomass to generate a specific substrate utilization rate. In the literature, biomass is often measured as volatile suspended solids or protein. Here we wanted to demonstrate that qPCR for the *etnE* gene can be used as a specific surrogate for active etheneotroph biomass in the enrichment cultures, and that the abundance of *etnE* is correlated to the rate of VC biodegradation. This is most easily demonstrated with a pure culture of VC-assimilating *Nocardioides* strain JS614, grown on VC in MSM at pH7 and a temperature of 20C. In this experiment, we varied the initial JS614 biomass and then estimated the raw VC biodegradation rate from measured VC depletion curves as described above (**Figure 94**). This yielded cultures exhibiting different raw VC biodegradation rates. We also extracted DNA from the cultures after the end of the experiment and measured *etnE* abundance with qPCR. The relationship between the VC biodegradation rate and *etnE* abundance is shown in **Figure 95**. We observed a strong linear relationship (R^2=0.98) between the biomass concentration (as *etnE*) and the q_{max} for VC biodegradation by strain JS614. This data supports the idea that the rate of VC oxidation in these cultures is proportional to etheneotroph functional gene concentration, and that VC oxidation rates can be adequately described by Michaelis-Menton enzyme kinetics when functional gene concentrations are used as the biomass concentration.

Thus the success criteria for performance objective "Determine relationships between etheneotroph functional genes and the VC biodegradation rate in VC-oxidizing laboratory enrichment cultures" appears to be met, at least on a preliminary basis.

We hypothesize that if etheneotrophs are contributing significantly to the rate of VC oxidation in enrichment cultures that we will observe a similar linear relationship between the raw VC biodegradation rate and *etnE* abundance.

Figure 95. Raw VC Depletion Rate vs etnE Concentration in VC-grown Nocardioides sp. Strain JS614 (Black Circles) as Compared to VC-oxidizing Enrichment Cultures from Pearl Harbor (PH; Red Squares) and Naval Air Station North Island (NI; Blue Triangles).

For the JS614 experiments, six microcosms were prepared with varying amounts of active JS614 biomass. Substrate depletion curves were fit to the Michaelis-Menton kinetic model and q_{max} was estimated. DNA was extracted from the microcosms at the end of the experiment, and etnE was quantified by qPCR.

Subsequently we compared measured aerobic VC-biodegradation rates in VC-oxidizing enrichment cultures from PH and NI (in duplicate) under the same pH and temperature conditions as the JS614 experiments. These data points are included in **Figure 95**. The data indicate that relationships between *etnE* gene abundance and VC biodegradation rate in enrichment cultures are different than that for a pure culture of JS614 even at the same pH and temperature. A possible explanation for the observed differences is active etheneotroph biomass. In other words, there may have been lower active etheneotroph biomass in the PH culture and higher active biomass in the NI culture, as compared to the JS614 culture. Because we only measured DNA in this experiment, we do not know the expression level of *etnE* or the activity of the EtnE product in this case. We also know that the activity of EtnE is variable even among different pure cultures of etheneotrophs (Coleman & Spain, 2003a, Mattes*, et al.*, 2005). Further study of the relationship between *etnE* expression (or transcript per gene ratio) as well as the correlation of *etnC* gene and transcript abundance and VC biodegradation rates is warranted.

Further kinetic testing was performed to evaluate the influence of environmental parameters on VC-degradation rates. The environmental parameters tested were temperature, pH, and dissolved oxygen concentrations. Kinetics were evaluated at three temperatures: 10, 15, and 20⁰C (**Figure 96**). As expected, both PH and NI showed decreasing rates at lower temperatures. Culture NI had a higher rate at 20⁰C, but showed a steeper decline with at lower temperatures. The culture NI VC degradation rate dropped 90% between 20⁰C and 10⁰C, while the PH culture rate only decreased by 53%.
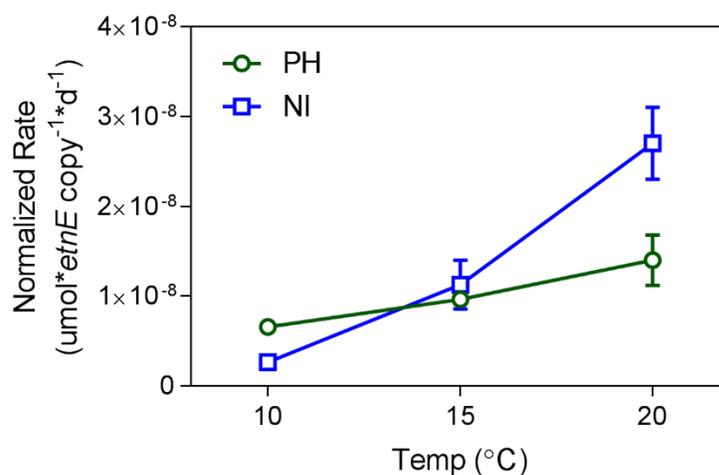
Figure 96. Normalized Rate vs Temperature.

Error bars show the range of duplicate bottles.

Cultures PH and NI retained activity between pH 5-7 (**Figure 97**). The culture NI VC depletion rate decreased approximately 44% between pH 7 and pH 6. Culture PH had a lower rate at pH 7, but showed a smaller decrease between pH 7 and pH 6 (30%).
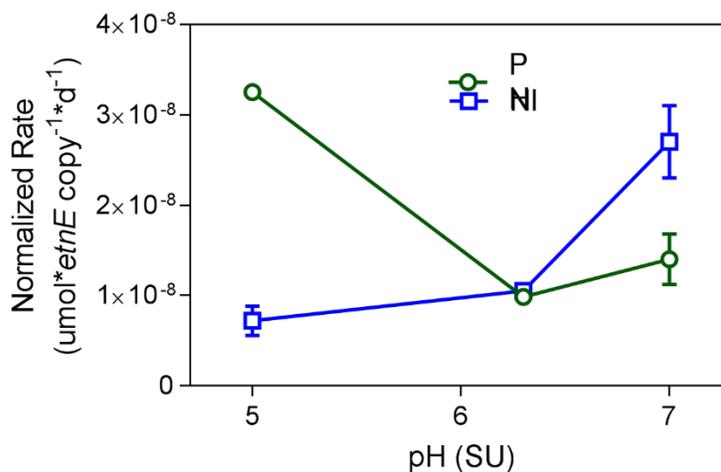
Figure 97. Normalized Rate vs pH.

Error bars show the range of duplicate bottles.

165

Oxygen depletion experiments were conducted with excess VC to determine the effect of oxygen limitation **(Figure 98)**. The oxygen depletion curve for the PH culture demonstrated Monod kinetics. The NI culture did not have Monod kinetics for oxygen depletion, but appeared to have approximately first order kinetics with respect to oxygen concentration in the range tested.
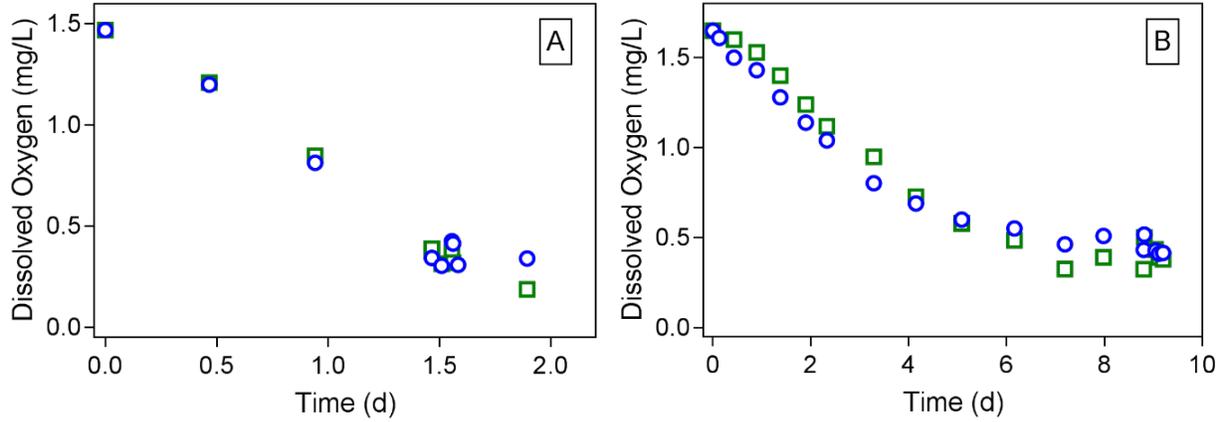
Figure 98. Oxygen Depletion Curves for (a) PH and (b) NI Enrichment Cultures.

Data was collected from duplicate microcosms.

7.0 COST ASSESSMENT

7.1 COST MODEL

There are two major elements of the cost model for implementing the qPCR technology into existing monitoring plans (**Table 35**).

7.1.1 Sampling cost

Ideally, groundwater samples for most DoD sites will be taken by field technicians during routine site sampling events. Thus, it can be argued that not much extra labor is needed for groundwater sample collection. For some sites, groundwater sampling was carried out by Mattes lab personnel. This provided some insight into how much time sampling efforts will take so that costs can be estimated as necessary.

7.1.2 qPCR and RT-qPCR cost

The qPCR and RT-qPCR analyses were performed in the Mattes laboratory. The costs include labor, consumables and reagents, and analytical fees associated with running the qPCR instrument. Labor was tracked according to the personnel required and their associated labor hours. The material purchases and analytical fees were also tracked. The basic cost model is shown in **Table 35.**

Table 35. Two Major Elements of the Cost Model for This Demonstration Are Sampling Cots and qPCR/RT-qPCR Costs

Cost Element	Data to be tracked
Sampling cost	Personnel required and associated labor Equipment rental cost Consumables and reagent cost Sample shipment cost
qPCR and RT-qPCR cost	Personnel required and associated labor Consumables and reagent cost

7.2 COST DRIVERS

The only cost drivers that should be considered is number of samples and replicates required as this will impact the total cost of implementing the technology as part of a long-term monitoring strategy. Typically, we take duplicate samples for DNA and RNA to assess sampling variability.

7.3 COST ANALYSIS

The time required to process samples for RT-qPCR/qPCR, once the filters have been received in the lab, is estimated in **Table 36**. We typically collected 60 filters during one site visit. It usually takes about one week for DNA and RNA extraction, and another week to process RNA samples given the normal number of filters collected. The RT-qPCR/qPCR experiments usually take another one to two weeks for the quantification of six functional genes and transcriptions (*etnC, etnE, mmoX, pmoA, bvcA*, and *vcrA*) and quantification of luciferase mRNA in RNA samples.

In total, three to four weeks are needed to process samples from one sampling event from one site (i.e., per 60 filter samples). If we consider this in terms of labor required to process samples from one monitoring well (4 filters, 2 each for DNA and RNA), we estimate 1 hr for DNA extraction, 1 hr for RNA extraction, 1 hr for reverse transcription, 6 hours for 384 plate set-up and running, and 3 hours per plate for analysis. We estimate that 3 plates were needed to complete analysis of six functional genes. This yields a total of 30 hours of labor to complete analysis of 4 samples per monitoring well for RNA and DNA. However, it should be noted that we were able to analyze 17 different monitoring wells per plate, which should be accounted for. This suggests that the labor to process (3 hr) and analyze (27 hr/17 wells = 1.6 hr) is about 5 hrs. Labor costs in the Mattes lab were approximately $30 per hour for a total of $150 per monitoring well.

Table 36. Time Estimation for Various RT-qPCR/qPCR Procedures

Procedure	Time required
DNA extraction	3-4 hrs per batch (8 samples)
RNA extraction	3-4 hrs per batch (8 samples)
RNA reverse transcription	3 hrs per batch (4-6 samples)
RT-qPCR/qPCR set up	4 hrs per 384 well plate
RT-qPCR/qPCR running	2 hrs per plate
RT-qPCR/qPCR data analysis	2-3 hrs per plate

The sampling collection and preservation cost is summarized in **Table 37Table** 16. For each monitoring well, DNA and RNA samples are taken in replicate and cost about $345. The materials required for conventional qPCR with a 384 well plate include the Power SYBR green reagent mix, luciferase mRNA qPCR, and other miscellaneous consumables. There is also a $20 fee per plate for running the qPCR instrument. We estimated the costs to run qPCR and RT-qPCR for samples from 17 monitoring wells. The reagents costs were $550 ($390 for SYBR green, $115 for luciferase, and $45 for miscellaneous). The instruments fees were $60. Thus, the cost per monitoring well for six gene qPCR/RT-qPCR analysis is $36 for conventional qPCR. In sum, RT-qPCR/qPCR technology costs in total about $380 for each monitoring well to analyze six functional genes/transcripts that involved in VC degradation.

Table 37. Material Cost Summary of DNA and RNA Sample Preparation Cost for Each Monitoring Well.

Workflow task	per sample cost	number of samples per monitoring well	per monitoring well cost
DNA - Sterivex filter collection	$8.70	2	$17.40
DNA - extraction	$14	2	$28
RNA - Sterivex filter collection and preservation	$12.40	2	$24.80
RNA - extraction	$12	2	$24
RNA - reverse transcription	$38.50	2	$77
RNA - luciferase mRNA	$11.50	2	$23
DNA and RNA - overnight shipping			$150
Sum			$345

Overall, our analysis indicates that labor and materials costs for qPCR/RT-qPCR were $530 per monitoring well. This does not include the sampling costs in the field. We estimate that the time required to set-up and take two 1 L filter samples for DNA and two 3L filter samples for RNA was about 2 hours per monitoring well, on average. Although one person could sample wells alone, it was often helpful to have another helping at times. So, to be conservative – 3 hours per well ($90). This brings the total costs per monitoring well to $620.

We do not include the costs for flights, hotel, food, rental car, equipment rental in this analysis. When we were sampling groundwater at Parris Island Site 45, there were additional costs for disposal of investigation derived wastes (IDW) incurred that perhaps should be taken into account as part of the overall cost per monitoring well. The groundwater IDW collection, storage, analysis, and disposal costs for one sampling event in 2015 were $2,800 for 17 monitoring wells (or ~ $165 per monitoring well). However, we were not charged for IDW costs for obtaining samples for any of the other sites when working alongside a contractor. This leads us to conclude that the extra groundwater filtered for qPCR analysis would not likely contribute very much extra to the overall IDW costs that we were forced to incur separately at Parris Island.

Page Intentionally Left Blank

8.0   IMPLEMENTATION ISSUES

8.1   COST OBSERVATIONS

The $620 cost per monitoring well to perform qPCR and RT-qPCR for six functional genes is probably conservative as qPCR is frequently employed during long term monitoring at chlorinated ethene contaminated sites. There are potential cost savings with increasing scale of application to save on shipping costs, and per plate analysis costs.

8.2   PERFORMANCE OBSERVATIONS

When using DNA for qPCR, the performance of the technology is strong, particularly for *etnE* (RTE primers). We did observe that the *etnC* primers (RTC) did not perform as well (i.e., primer dimer formation potential was higher) when the template concentration in the groundwater sample was low (near the quantification limit). It may be a worthwhile exercise to revisit the RTC primer design. Periodic evaluation and revision of qPCR primers is warranted in general, as the database of *etnC* and *etnE* genes continues to grow with further application of qPCR at contaminated sites.

When using RNA, the performance of the technology is dependent on the efficiency of RNA extraction. When extracting RNA the more groundwater that can be filtered the better. We aimed to collect 3L of groundwater per filter. However, in the field this may not always be possible as groundwater quality is variable and filters may clog quickly. Sampling variability undoubtedly contributed to the variability we noted in RNA extraction efficiency.

Although we thought that the cryo-cores would be an ideal approach to obtaining RNA from sediment, this turned out not to be the case. We also encountered difficulties extracting DNA from the frozen sediments, which was surprising to us.

RNA is not typically used in qPCR practice, as obtaining DNA is much more feasible and cost effective. The benefits of RNA are also not well recognized. We believe that the value of RNA may be found when attempting to correlate biodegradation rates with biomarkers. It may be possible to obtain meaningful relationships between rates and qPCR data obtained with DNA. But DNA is not necessarily a reliable indicator of active biomass. We believe that RT-qPCR may yield better correlations with rates that qPCR.

8.3   TECHNOLOGY TRANSFER OBSERVATIONS

We have transferred the qPCR technology for etheneotrophs to SiREM (*etnE* gene only so far). SiREM has developed a commercial genetic test called "Gene-Trac® etn". The following efforts have been made to raise awareness of the test availability:

- Web Site http://www.siremlab.com/gene-trac-testing-2
- Listing on SiREM cutsheet of available tests
- Listing under SiREMNA our natural attenuation line of testing
- I presented a SiREM Webinar on this topic in 2017
    - http://www.siremlab.com/webinar-series-next-webinar-june-8th-2017/

- SiREM has sold the test commercially (7 samples) and has ran another approximately 50 tests for R&D purposes and QA/QC

According to SiREM, development of bioaugmentation cultures for these aerobic pathways would, greatly enhance their ability to sell associated molecular tests (baseline and post-bioaugmentation analyses) this is a big part of their business model for selling *Dehalococcoides* qPCR tests. of which they sell 200-300 per month. This is an idea that warrants further consideration.

8.4   LESSONS LEARNED

The following are offered as lessons learned from the controlled evaluation:

1. The RT-qPCR/qPCR technology for etheneotrophs is an innovative and rapid means of revealing information about the potential for in situ microbial aerobic VC oxidation at contaminated sites.

2. Of the 95 samples analyzed during this effort, functional genes from etheneotrophs and methanotrophs and anaerobic VC-dechlorinators were frequently present (99%) and expressed (59%) in the same groundwater samples the majority of which featured low DO and ORP levels.

3. Although confident quantitative relationships between bulk VC attenuation rates and functional gene abundance and expression could not be made, data analysis shown in Table 5, revealed that both etheneotroph functional gene (*etnC* and *etnE)* abundances are significantly correlated with categorical bulk VC attenuation rate. This relationship was also seen for VC reductive dehalogenase gene *vcrA* and the sum of VC reductive dehalogenase genes *bvcA* and *vcrA*. In contrast, methanotroph functional genes *pmoA* and *mmoX* were not correlated with categorical bulk VC attenuation rates.

4. Strong positive relationships using both Spearman's correlation analysis (Liang et al., 2017b) and multilevel modeling were observed between VC concentrations and the abundance and expression of functional genes from etheneotrophs and anaerobic VC-dechlorinators. However, this relationship with VC concentration was not observed with methanotroph functional genes. This is an important observation with respect to etheneotrophs, and indicates the abundance of etheneotrophs is greater when VC concentrations are greater irrespective of the dissolved oxygen concentration. Functional gene abundance for etheneotrophs will be proportional to VC concentration irrespective of measured DO concentrations in the groundwater.

5. During the project, we also found a high level of co-occurrence of etheneotroph functional genes and VC reductive dehalogenase genes in groundwater samples. Therefore, we concluded from this analysis that etheneotrophs have a strong potential to contribute to VC biodegradation in groundwater when VC concentrations are high and in areas of the aquifer that may be considered anaerobic. Therefore, it is recommended that qPCR analyses for aerobic VC oxidizers always be conducted concurrently with those for anaerobic VC dechlorinators during long term groundwater monitoring, irrespective of DO concentrations, so as to build lines of evidence for natural attenuation of VC for the entire site.

The spatial resolution of A) total 16S rRNA genes, B) *etnC* and *etnE* (etheneotroph functional genes), C) *mmoX* and *pmoA* (methanotroph functional genes), and D) *bvcA* and *vcrA* (VC reductive dehalogenase genes) in an aquifer sediment core, frozen in place with liquid nitrogen, obtained from Parris Island Site 45 showed that indeed, functional genes from etheneotrophs and anaerobic VC-dechlorinators coexist within small (~0.25 g) sediment samples as deep as 18 feet below ground surface in this particular sediment core. This suggests that there is the potential for essentially simultaneous aerobic and anaerobic VC biodegradation at this site, even at a substantial depth.

6. We found that the qPCR technology has the potential to be correlated with rates of VC oxidation. These relationships should be investigated in future studies particularly under low DO conditions.

7. With regards to groundwater sampling, we discovered in certain wells that after low flow purging and sampling for geochemical parameters that the process of switching to filtration of groundwater allowed a little bit of groundwater to fall back into the well from the sampling tube. Presumably just enough oxygen dissolved into the groundwater during pumping that when it entered the well it caused rapid precipitation of iron oxides. Subsequently trying to filter groundwater at that point would lead to rapid clogging. We learned to pump for about 30 seconds to clear the well and the line of the precipitates before filtering. Filtration of biomass from groundwater can then proceed without rapid clogging incidents.

8.4.1 Statistical analyses

We recommend that when performing statistical analyses of multiple groundwater samples from different sites and different time points from single monitoring wells that a multi-level modeling approach be used to account for the hierarchy in the data. We found that this improved the accuracy of the resulting linear regression analyses (Liang*, et al.*, 2017b). To perform multi-level modeling we used a statistical program called R (Ihaka & Gentleman, 1996). The function lmer() in the lme4 package was used, considering a monitoring well as the first hierarchical level and site as the second hierarchical level (Snijders, 2011). For regression analysis, functional gene/transcript values and chlorinated ethene concentrations were log transformed to more closely follow a normal distribution than raw values.

Non-detects in geochemical and microbial datasets could introduce bias into regression analyses. Data points with non-detectable transcript abundances were removed from the analysis to minimize their influence on regression models. Non-detects for geochemical parameters (i.e. VC) were replaced by $0.5 \times$ the detection limit to facilitate log transformations and minimize the impact of censored data on regression analyses. Model residuals were plotted and Akaike's Information Criterion (AIC) scores (Akaike, 1992) were calculated to facilitate a quantitative comparison between multilevel regression and simple linear regression models.

Page Intentionally Left Blank

9.0 REFERENCES

Akaike H (1992) Information theory and an extension of the maximum likelihood principle. *Breakthroughs in Statistics: Foundations and Basic Theory,*(Kotz S & Johnson NL, ed.^eds.), p.^pp. 610-624. Springer New York, New York, NY.

Atashgahi S, Maphosa F, Doğan E, Smidt H, Springael D & Dejonghe W (2013) Small-scale oxygen distribution determines the vinyl chloride biodegradation pathway in surficial sediments of riverbed hyporheic zones. *FEMS Microbiol Ecol* **84**: 133-142.

Begley JF, Czarnecki M, Kemen S, Verardo A, Robb AK, Fogel S & Begley GS (2012) Oxygen and Ethene Biostimulation for a Persistent Dilute Vinyl Chloride Plume. *Ground Water Monit Remediat* **32**: 99-105.

Biggerstaff JP, Le Puil M, Weidow BL, Leblanc-Gridley J, Jennings E, Busch-Harris J, Sublette KL, White DC & Alberte RS (2007) A novel and in situ technique for the quantitative detection of MTBE and benzene degrading bacteria in contaminated matrices. *Journal of Microbiological Methods* **68**: 437-441.

Bustin SA, Benes V, Garson JA, Hellemans J, Huggett J, Kubista M, Mueller R, Nolan T, Pfaffl MW, Shipley GL, Vandesompele J & Wittwer CT (2009) The MIQE guidelines: minimum information for publication of quantitative real-time PCR experiments. *Clin Chem* **55**: 611-622.

Chang HL & Alvarez-Cohen L (1996) Biodegradation of individual and multiple chlorinated aliphatic hydrocarbons by methane-oxidizing cultures. *Appl Environ Microbiol* **62**: 3371-3377.

Churchill P (2013) Summary of the May 2013 Storm Water System Investigation at the former Morale, Welfare, and Recreation (MWR) Dry Cleaning Facility (Site 45) located at the Marine Corps Recruit Depot (MCRD) Parris Island, South Carolina.

Coleman NV & Spain JC (2003a) Distribution of the Coenzyme M Pathway of Epoxide Metabolism among Ethene- and Vinyl Chloride-Degrading Mycobacterium Strains. *Applied and Environmental Microbiology* **69**: 6041.

Coleman NV & Spain JC (2003b) Epoxyalkane:Coenzyme M transferase in the ethene and vinyl chloride biodegradation pathways of *Mycobacterium* strain JS60. *J. Bacteriol.* **185**: 5536-5545.

Coleman NV, Bui NB & Holmes AJ (2006) Soluble di-iron monooxygenase gene diversity in soils, sediments and ethene enrichments. *Environ. Microbiol.* **8**: 1228-1239.

Coleman NV, Mattes TE, Gossett JM & Spain JC (2002a) Biodegradation of *cis*-dichloroethene as the sole carbon source by a beta-proteobacterium. *Appl Environ Microbiol* **68**: 2726-2730.

Coleman NV, Mattes TE, Gossett JM & Spain JC (2002b) Phylogenetic and kinetic diversity of aerobic vinyl chloride-assimilating bacteria from contaminated sites. *Appl. Environ. Microbiol.* **68**: 6162-6171.

Cupples AM (2008) Real-time PCR quantification of *Dehalococcoides* populations: Methods and applications. *J. Microbiol. Methods* **72**: 1-11.

Dobson ML (2011) Assessment of methanotroph presence and activity in dilute vinyl chloride contaminated groundwater. Thesis, University of Iowa.

Freedman D, High J, Reid A, Bakenne A, Leo L, Zinder S & Fullerton H (2013) SERDP Project ER-1556 Characterization of microbes capable of using vinyl chloride and ethene as sole carbon and energy sources by anaerobic oxidation. https://serdp-estcp.org/content/download/22364/229880/file/ER-1556-FR.pdf.

Freedman DL & Herz SD (1996) Use of ethylene and ethane as primary substrates for aerobic cometabolism of vinyl chloride. *Water Environ Res* **68**: 320-328.

Freedman DL, Danko AS & Verce MF (2001) Substrate interactions during aerobic biodegradation of methane, ethene, vinyl chloride and 1,2-dichloroethenes. *Water Sci. Technol.* **43**: 333-340.

Fullerton H, Rogers R, Freedman D & Zinder S (2014) Isolation of an aerobic vinyl chloride oxidizer from anaerobic groundwater. *Biodegradation* **25**: 893-901.

Fuse H, Ohta M, Takimura O, Murakami K, Inoue H, Yamaoka Y, Oclarit JM & Omori T (1998) Oxidation of trichloroethylene and dimethyl sulfide by a marine *Methylomicrobium* strain containing soluble methane monooxygenase. *Biosci Biotech Bioch* **62**: 1925-1931.

Gossett JM (2010) Sustained aerobic oxidation of vinyl chloride at low oxygen concentrations. *Environ. Sci. Technol.* **44**: 1405-1411.

He J, Ritalahti KM, Yang K-L, Koenigsberg SS & Loffler FE (2003) Detoxification of vinyl chloride to ethene coupled to growth of an anaerobic bacterium. *Nature* **424**: 62-65.

Holmes AJ, Costello A, Lidstrom ME & Murrell JC (1995) Evidence that participate methane monooxygenase and ammonia monooxygenase may be evolutionarily related. *FEMS Microbiol Lett* **132**: 203-208.

Hwang C, Wu W, Gentry TJ, Carley J, Corbin GA, Carroll SL, Watson DB, Jardine PM, Zhou J, Criddle CS & Fields MW (2008) Bacterial community succession during in situ uranium bioremediation: spatial similarities along controlled flow paths. *ISME J* **3**: 47-64.

Ihaka R & Gentleman R (1996) R: a language for data analysis and graphics. *J Comput Graph Stat* **5**: 299-314.

Jin YO & Mattes TE (2008) Adaptation of aerobic, ethene-assimilating *Mycobacterium* strains to vinyl chloride as a growth substrate. *Environ Sci Technol* **42**: 4784-4789.

Jin YO & Mattes TE (2010) A quantitative PCR assay for aerobic, vinyl chloride- and ethene-assimilating microorganisms in groundwater. *Environ. Sci. Technol.* **44**: 9036-9041.

Jin YO & Mattes TE (2011) Assessment and modification of degenerate qPCR primers that amplify functional genes from etheneotrophs and vinyl chloride-assimilators. *Lett. Appl. Microbiol.* **53**: 576-580.

Johnson DR, Lee PKH, Holmes VF & Alvarez-Cohen L (2005) An internal reference technique for accurately quantifying specific mRNAs by real-time PCR with a application to the *tce*A reductive dehalogenase gene. *Appl Environ Microbiol* **71**: 3866-3871.

Johnson RL, Brow CN, Johnson ROB & Simon HM (2013) Cryogenic Core Collection and Preservation of Subsurface Samples for Biomolecular Analysis. *Groundwater Monitoring & Remediation* **33**: 38-43.

Kiaalhosseini S, Johnson RL, Rogers RC, Renno MI, Lyverse M & Sale TC (2016) Cryogenic Core Collection (C3) from Unconsolidated Subsurface Media. *Groundwater Monitoring & Remediation* **36**: 41-49.

Kolb S, Knief C, Stubner S & Conrad R (2003) Quantitative detection of methanotrophs in soil by novel *pmo*A-targeted real-time PCR assays. *Appl Environ Microbiol* **69**: 2423-2429.

Krajmalnik-Brown R, Hölscher T, Thomson IN, Saunders FM, Ritalahti KM & Löffler FE (2004) Genetic identification of a putative vinyl chloride reductase in *Dehalococcoides* sp. strain BAV1. *Appl Environ Microbiol* **70**: 6347-6351.

Krug TOH, Suzanne; Watling, Mark; Quinn, Jacqueline (2010) Emulsified zero-valent nano-scale iron treatment of chlorinated solvent DNAPL source areas.

Lee PKH, Macbeth TW, Sorenson KS, Deeb RA & Alvarez-Cohen L (2008) Quantifying genes and transcripts to assess the *in situ* physiology of "*Dehalococcoides*" spp. in a trichloroethene-contaminated groundwater site. *Appl Environ Microbiol* **74**: 2728-2739.

Liang Y, Cook LJ & Mattes TE (2017a) Temporal abundance and activity trends of vinyl chloride (VC)-degrading bacteria in a dilute VC plume at Naval Air Station Oceana. *Environmental Science and Pollution Research* **24**: 13760-13774.

Liang Y, Meggo R, Hu D, Schnoor JL & Mattes TE (2014) Enhanced polychlorinated biphenyl removal in a switchgrass rhizosphere by bioaugmentation with Burkholderia xenovorans LB400. *Ecological Engineering* **71**: 215-222.

Liang Y, Liu X, Singletary MA, Wang K & Mattes TE (2017b) Relationships between the abundance and expression of functional genes from vinyl chloride (VC)-degrading bacteria and geochemical parameters at VC-contaminated sites. *Environ Sci Technol* **51**: 12164-12174.

Löffler FE, Yan J, Ritalahti KM, Adrian L, Edwards EA, Konstantinidis KT, Müller JA, Fullerton H, Zinder SH & Spormann AM (2013) *Dehalococcoides mccartyi* gen. nov., sp. nov., obligately organohalide-respiring anaerobic bacteria relevant to halogen cycling and bioremediation, belong to a novel bacterial class, *Dehalococcoidia* classis nov., order *Dehalococcoidales* ord. nov. and family *Dehalococcoidaceae* fam. nov., within the phylum *Chloroflexi*. *Int J Syst Evol Micr* **63**: 625-635.

Lyew D & Guiot S (2003) Effects of aeration and organic loading rates on degradation of trichloroethylene in a methanogenic-methanotrophic coupled reactor. *Appl Microbiol Biotechnol* **61**: 206-213.

Mattes TE, Alexander AK & Coleman NV (2010) Aerobic biodegradation of the chloroethenes: pathways, enzymes, ecology, and evolution. *FEMS Microbiol. Rev.* **34**: 435-475.

Mattes TE, Coleman NV, Gossett JM & Spain JC (2005) Physiological and molecular genetic analyses of vinyl chloride and ethene biodegradation in *Nocardioides* sp. strain JS614. *Arch. Microbiol.* **183**: 95-106.

Mattes TE, Jin YO, Livermore J, Pearl M & Liu X (2015) Abundance and activity of vinyl chloride (VC)-oxidizing bacteria in a dilute groundwater VC plume biostimulated with oxygen and ethene. *Submitted*.

McDonald IR, Kenna EM & Murrell JC (1995) Detection of methanotrophic bacteria in environmental samples with the PCR. *Appl Environ Microbiol* **61**: 116-121.

McDonald IR, Bodrossy L, Chen Y & Murrell JC (2008) Molecular ecology techniques for the study of aerobic methanotrophs. *Appl Environ Microbiol* **74**: 1305-1315.

Müller JA, Rosner BM, von Abendroth G, Meshulam-Simon G, McCarty PL & Spormann AM (2004) Molecular identification of the catabolic vinyl chloride reductase from *Dehalococcoides* sp. strain VS and its environmental distribution. *Appl Environ Microbiol* **70**: 4880-4888.

Patterson BM, Aravena R, Davis GB, Furness AJ, Bastow TP & Bouchard D (2013) Multiple lines of evidence to demonstrate vinyl chloride aerobic biodegradation in the vadose zone, and factors controlling rates. *J Contam Hydrol* **153**: 69-77.

Powell S, Ferguson S, Bowman J & Snape I (2006) Using real-time PCR to assess changes in the hydrocarbon-degrading microbial community in Antarctic soil during bioremediation. *Microb Ecol* **52**: 523-532.

Puls RW & Barcelona MJ (1996) *Low-flow (minimal drawdown) ground-water sampling procedures*. US Environmental Protection Agency, Office of Research and Development, Office of Solid Waste and Emergency Response.

Ritalahti KM, Amos BK, Sung Y, Wu Q, Koenigsberg SS & Loffler FE (2006) Quantitative PCR targeting 16S rRNA and reductive dehalogenase genes simultaneously monitors multiple *Dehalococcoides* strains. *Appl Environ Microbiol* **72**: 2765-2774.

Smith CJ & Osborn AM (2009) Advantages and limitations of quantitative PCR (Q-PCR)-based approaches in microbial ecology. *FEMS Microbiol Ecol* **67**: 6-20.

Snijders TAB (2011) Multilevel Analysis. *International Encyclopedia of Statistical Science*,(Lovric M, ed.^eds.), p.^pp. 879-882. Springer Berlin Heidelberg, Berlin, Heidelberg.

Sowers KR & May HD (2013) *In situ* treatment of PCBs by anaerobic microbial dechlorination in aquatic sediment: are we there yet? *Curr Opin Biotechnol* **24**: 482-488.

TetraTech (2012) Remedial investigation addendum for Site 45 - Former Morale, Welfare, and Recreation dry cleaning facility, revision 4.

USEPA (1996) Low flow (minimal drawdown) ground-water sampling procedures.

USEPA (2004) Field sampling guidance document #1220: Groundwater well sampling.

USEPA (2010) EPA review of the 2010 CERCLA second five-year review report, Marine Corps Recruit Depot (MCRD), Parris Island, South Carolina.

van der Zaan B, Hannes F, Hoekstra N, Rijnaarts H, de Vos WM, Smidt H & Gerritse J (2010) Correlation of *Dehalococcoides*; 16S rRNA and chloroethene-reductive dehalogenase genes with geochemical conditions in chloroethene-contaminated groundwater. *Appl Environ Microbiol* **76**: 843.

Van Hylckama VJ, De Koning W & Janssen DB (1997) Effect of chlorinated ethene conversion on viability and activity of *Methylosinus trichosporium* OB3b. *Appl Environ Microbiol* **63**: 4961-4964.

Vroblesky DA, Petkewich MD, Landmeyer JE & Lowery MA (2009) Source, Transport, and Fate of Groundwater Contamination at Site 45, Marine Corps Recruit Depot, Parris Island, South Carolina. *U.S. Geological Survey Scientific Investigations Report 2009–5161, 80 p.*

Vroblesky DAP, Matthew D.; Landmeyer, James E.; Lowery, Mark A. (2009) Source, transport, and fate of groundwater cotamination at Site 45, Marine Corps Recruit Depot, Parris Island, South Carolina.

Wang Y, Peng B, Yang Z, Chai L, Liao Q, Zhang Z & Li C (2015) Bacterial community dynamics during bioremediation of Cr(VI)-contaminated soil. *Applied Soil Ecology* **85**: 50-55.

Wiedemeier TH (1999) *Natural attenuation of fuels and chlorinated solvents in the subsurface*. John Wiley & Sons.

Wiedemeier THS, Matthew A.; Moutoux, David E.; Gordon, E. Kinzie; Wilson, John T. ; Wilson, Barbara H.; Kampbell, Donald H., Haas, Patrick E.; Miller, Ross N.; Hansen, Jerry E.; Hansen, Jerry E. ; Chapelle, Francis H. (1998) Technical protocol for evaluating natural attenuation of chlorinated solvents in groundwater.

Page Intentionally Left Blank

APPENDIX A   POINTS OF CONTACT

POINT OF CONTACT Name	ORGANIZATION Name Address	Phone Fax E-mail	Role in Project
Timothy Mattes	The University of Iowa 4105 Seamans Center Iowa City, IA 52242	319-335-5065 319-335-5660 (fax) tim-mattes@uiowa.edu	Principal Investigator
Yi Liang	The University of Iowa 4105 Seamans Center Iowa City, IA 52242	319-335-5065 319-335-5660 (fax) yi-liang@uiowa.edu	Postdoctoral Research Associate
Mike Singletary	NAVFAC Southeast EV3 Environmental Restoration P.O. Box 30, Bldg. 135 Naval Air Station Jacksonville, FL 32212	904.542.4204 michael.a.singletary@navy.mil	DoD collaborator/liaison – Navy, primary contact for Parris Island site 45 and NSB Kings Bay site 11
Amy Hawkins	NAVFAC EXWC EV32 1000 23rd Ave Port Hueneme, CA 93043	(805) 982-4890 amy.hawkins@navy.mil	Dod liaison - Navy
Dora Ogles	Microbial Insights, Inc. 10515 Research Drive Knoxville, TN 37932	865.573.8188 ext 107 dogles@microbe.com	QuantArray and Microbial Insights database
Nicole Cowand	Remedial Project Manager NE IPT, Code OPTE3	757-341-2009 nicole.cowand@navy.mil	RPM for Parris Island site 45
Richard Johnson	Oregon Health & Science University HRC3 3181 SW Sam Jackson Park Road Portland, OR 97239	johnsori@ohsu.edu	Cryo-coring at Parris Island Site 45
GEL Laboratories LLC	Charleston, SC 2040 Savage Road Charleston, SC 29407 P.O. Box 30712 Charleston, SC 29417	(843) 556-8171 info@gel.com	VOC analyses at Parris Island site 45
Hunter Anderson	Technical Support Branch (CZTE) Air Force Civil Engineer Center (AFCEC) Lackland AFB, TX	(210) 395-9289 richard.anderson.55@us.af.mil	DoD Liaison – Air Force
Jeff Dale	NAVFAC Mid-Atlantic 4911 South Broad Street Philadelphia, PA 19112	(215) 897-4914 jeffrey.m.dale@navy.mil	Navy POC for NCBC Davisville and NAWC Trenton
Arun Gavaskar	NAVFAC EXWC, Code EV31 1000 23rd Avenue Port Hueneme, CA 93043	(805) 982-1661 arun.gavaskar@navy.mil	NAVFAC Contact for Seal Beach Site 70
Andrea Leeson	Deputy Director & Environmental Restoration Program Manager Contracting Officer's Representative SERDP & ESTCP	(571) 372-6398 Andrea.Leeson.civ@mail.mil	Project Sponsor

Page Intentionally Left Blank

APPENDIX B   CRYOGENIC CORE COLLECTION PROTOCOL (FROM DR. RICK JOHNSON)

Introduction

The protocol outlined below describes the steps involved in collecting cryogenic cores using a CME hollow-stem auger. The tooling needed to accomplish core collection is described in the report on cryogenic core collection as part of SERDP ER-1740.

The protocol steps outlined below are designed to cover assembly of the core barrel, making connection between the liquid nitrogen (LN) tank, freezing of the core, removal of the core from the core barrel, and packing the core. A subsequent protocol has been developed for laboratory analysis of those cores and will not be discussed here.

At the conclusion of the protocol steps there is a brief section on troubleshooting. The primary function of this section is to deal with freezing of components of the system (e.g., cooling tubes, core barrel in auger, and core sleeve in core barrel). We believe that both the protocols and the troubleshooting tips will provide sufficient insight to allow an experienced driller to collect cryogenic cores.

1. Prepare the cooling system

    a. Place the tube retrieval rods into the core barrel.

        i. These are two 6-foot ¼" O.D. rods with Swagelok nuts on the ends.

        ii. They are fed through the holes in the core barrel top in order to pull the cooling coils/cylinder into the core barrel.

Tube retrieval rods

    b. Attach the tube retrieval rods to the cooling coils

        i. The rods feed through the core barrel and connect to the tops of the cooling coil tubes

c. Pull/push the cooling coil/cylinder into core barrel

d. Insert the core sleeve into the core barrel.

e. Screw the drive shoe onto the core barrel

f. connect sample tube to hex rod

g. connect LN riser tubes to the cooling coil tubes

h. attach the LN riser tubes to the hex rod

i. lower hex rod assembly 5 feet

j. repeat "g-i" until core barrel is at the sampling depth

k. add one length of hex rod above ground surface, as well as lengths of LN riser tube

l. attach an additional auger flight

m. Attach the auger string to the drill rig and advance the drill string 2 to 5 feet, depending on the length of core desired.

n. Disconnect auger from drill rig

o. connect one of the LN riser tubes to LN supply

p. attach the LN effluent pressure control assembly to the other LN riser tube

   i. The solenoid valve should be in the normally open position (not powered)

   ii. If a manual valve is used, it should be in the open position.

   iii. NOTE: it is important that the valve used in this application be designed for cryogenic service.

q. Turn on the LN at the tank

   i. LN should be discharged from the solenoid valve.

r. When the temperature at the vent reaches 0C, the valve should be closed and at that point all of the flow should be out of the orifice (1/8″)

s. After 5-7 minutest of cooling, the LN is turned off, the LN tank line and the pressure manifold are disconnected from the LN riser tubes and the core sample is recovered from the ground.

t. During core extraction to ground surface the LN riser tubes and the hex rod must be sequentially removed. (Note: depending on the depth, 20-foot sections of the hex rod and riser tubes may be taken off at a time to speed the process.)

u. Loosen and remove the drive shoe

v. Remove the core sleeve from the core barrel

    i. Note: the sleeve can become frozen in the core barrel. If necessary, hot water can be circulated through the cooling coils for <1 min to free the core sleeve from the core barrel.

w. Cut the core as desired

x. Pack core in dry ice for shipment to the lab.

y. Insert a new core sleeve in the core barrel and return to step "e"

Troubleshooting

a. Plugging of the LN lines and coil

   i. During the core recovery process it is possible to get water and other materials in the cooling pipes and coil. Generally this material will be blown out by nitrogen vapor at the beginning of cooling cycle. If not, water may freeze in the lines and plug the flow. In this case it will be necessary to warm the pipes until the water melts and the cooling process can be tried again.

b. Freezing of the core barrel in the auger

   i. This sometimes occurs with longer freezing times. In all cases the driller was able to unfreeze the barrel with a combination of downward pressure on the augers, upward pull on the hex rod with the wench, and on rare occasions hitting the hex rod with a large hammer.

c. Freezing of the core sleeve in the core barrel

   i. If freezing times are long, there is a greater risk of freezing the sample in the core barrel. The strategy we have used to free the sleeve is to flush hot water through the cooling coils just until the sleeve releases from the coils. In our experience, this did not result in appreciable thawing of the core sample

ii.   Following this process there is an increased chance that water remaining in the lines will freeze. So, care should be taken to remove water prior to the next freezing

cycle.

d. Freezing of the auger flights in the ground

i.   In some cases the augers can become frozen and are not readily retrieved. In all cases the drillers employed a combination of "tricks" to free the augers. Freezing of the augers is not common in our experience when LN delivery times are kept <~8 min. Breaking the augers free rarely required more than 5 minutes.

Page Intentionally Left Blank

APPENDIX C   GUIDELINES FOR GROUNDWATER SAMPLING WITH STERIVEX FILTERS

1. Take filter samples after enough water has been pumped out of the well for readings to "stabilize" (this is to ensure a representative sample and minimize filter clogging issues)

Hose

Clamp

Luer-Lock adapter
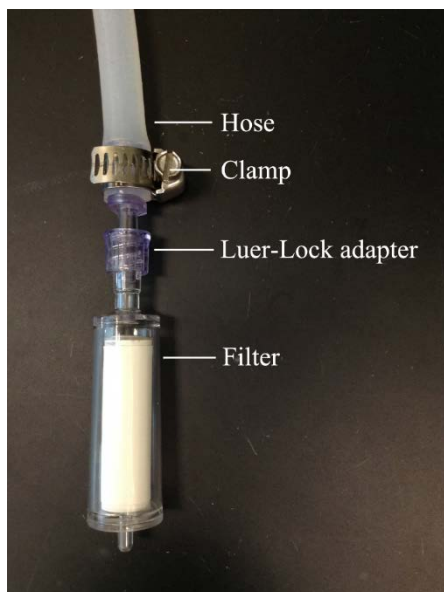
Filter

2. Attach filter to peristaltic pump (need a luerlock fitting and a clamp on the end of the tubing – the filters have a luer-lock fitting.) A diagram of this set-up is provided to the left. Please let me know if there are issues.

3. The inlet and outlet caps for the Sterivex filters are provided. Please attach the caps to the filters before placing them into the red-capped (Falcon) tube.

4. Please provide filter samples from the following **5** wells: **MW-01, MW-02, MW-13, MW-17 and MW-20.**

5. We have provided 21 tubes and filters (there is 1 extra). Please sample 4 filters per well– two for DNA analysis and two for RNA analysis. RNA filters require special treatment after sampling as described in 8 below.

6. Pump groundwater through the filter until enough volume (1L for DNA filters, 3L for RNA filters) has been filtered (or it clogs) – whichever comes first**. Note precisely how much volume passed through the filter (this is very important as it is needed for quantitation).**

7. Use 10 mL syringe to get rid of the residual groundwater in the filter (use a new syringe for each sample). Place each filter into red-capped (Falcon) tube, close and note sample description, the date, and how much water was filtered on the side of the tube using indelible marker. The water may be discarded afterwards.

8. Please treat 2 of the 4 filters from each well with RNAlater preservative ****immediately following collection**.** Use 10 ml syringe to remove residual groundwater in the filter first. Then load 3 mL syringe with 3 mL of preservative, attach the filter onto the end of the syringe, and inject. *Please take precautions to prevent cross-contamination of samples.* Only one syringe is to be used per sample (and discarded). Always remove preservative from the bottle provided with a sterile syringe. After injection immediately place the filter in a Falcon tube (labeled accordingly) into the cooler (or on ice as appropriate).

9. Place tubes (containing filters) and bottles with left over RNAlater in cooler with frozen ice packs (provided in thawed form) and FedEx **priority overnight** to Tim Mattes (319-335-5065; cell:319-541-3458), 4105 Seamans Center, Iowa City, IA, 52242. Return shipment instruction and label are included in the cooler. Please use **<u>FedEx number: 1467 6729 0</u>**

10. It is important to minimize hold time for these samples. We prefer that filters be shipped the day that they are sampled. If sampling will occur over several days, please coordinate with Tim Mattes (319-335-5065; cell: 319-541-3458) for daily shipping options.